

A survey of Phrurolithidae spiders from Jinggang Mountain National Nature Reserve, Jiangxi Province, China

Ke-Ke Liu¹, Hui-Pu Luo¹, Yuan-Hao Ying¹,
Yu-Xin Xiao¹, Xiang Xu², Yong-Hong Xiao¹

1 College of Life Science, Jinggangshan University, Ji'an 343009, Jiangxi, China **2** College of Life Science, Hunan Normal University, Changsha 410081, Hunan, China

Corresponding author: Yong-Hong Xiao (yonghongxiao01@126.com)

Academic editor: C. Haddad | Received 16 February 2020 | Accepted 12 May 2020 | Published 8 July 2020

<http://zoobank.org/A6378B16-EE56-4DB1-8DD1-C073CA10D366>

Citation: Liu K-K, Luo H-P, Ying Y-H, Xiao Y-X, Xu X, Xiao Y-H (2020) A survey of Phrurolithidae spiders from Jinggang Mountain National Nature Reserve, Jiangxi Province, China. ZooKeys 947: 1–37. <https://doi.org/10.3897/zookeys.947.51175>

Abstract

Phrurolithidae spiders were collected from Jinggang Mountain National Nature Reserve, Jiangxi Province, China, during the past six years. The new genus *Alboculus* Liu, **gen. nov.**, with the type species *Phrurolithus zhejiangensis* Song & Kim, 1991, is described, and its previously unknown male is described for the first time. Furthermore, seven new species of *Otacilia* are described: *O. acutangula* Liu, **sp. nov.** (♂♀), *O. bijiashanica* Liu, **sp. nov.** (♂♀), *O. longtanica* Liu, **sp. nov.** (♀), *O. ovoidea* Liu, **sp. nov.** (♂♀), *O. shenshanica* Liu, **sp. nov.** (♂♀), *O. subovoidea* Liu, **sp. nov.** (♂♀), and *O. xiaoxiica* Liu, **sp. nov.** (♀). All species are illustrated with photographs and their distributions are mapped.

Keywords

Taxonomy, new species, *Alboculus* gen. nov., *Otacilia*

Introduction

Otacilia was established by Thorell (1897), with the type species *O. armatissima* Thorell, 1897 from Myanmar (Burma). In the past ten years, the total number of spe-

cies in this genus has increased greatly, approximately tripling, with many new species being discovered particularly from China (WSC 2020). Recently, after 27 *Phrurolithus* C.L. Koch, 1839 species were transferred to *Otacilia* (Zamani and Marusik 2020), the genus became the most diverse group of the 14 phrurolithid genera, currently including 99 of the 231 described phrurolithid species (WSC 2020). To date, there are 74 *Otacilia* species reported from China (ca. 75% of the total; WSC 2020). However, there are still many poorly known Phrurolithidae species from southern China with unusual morphological characteristics.

Even in 2020, there is no clear way of differentiating between the genera *Otacilia* and *Phrurolithus*, although some taxonomists have tried to do so (e.g., Wang et al. 2015; Fu et al. 2016; Jin et al. 2016; Liu et al. 2019). Detailed morphological characteristics of the genus *Phrurolithus* were not revealed until the study of Zamani and Marusik (2020), wherein many previously undocumented characters on the palps and epigynes were described for the first time. Many species described in *Phrurolithus* were incorrectly attributed to this genus, including the Chinese species, which were all transferred to *Otacilia* recently (Zamani and Marusik 2020). Only a few taxonomic works were published in recent years, but *Otacilia* has not been subjected to a comprehensive revision yet.

While studying spiders from Jinggang Mountain National Nature Reserve, Jiangxi Province, China, we found several phrurolithid spiders belonging to unknown species or undescribed sexes in the past six years. The male of *Otacilia zhejiangensis* (Song & Kim, 1991) was firstly recognised as the undescribed conspecific sex of this species. *Alboculus* Liu gen. nov. is proposed here based on the male and female of *O. zhejiangensis*. Furthermore, seven new *Otacilia* species are described in the present study.

Materials and methods

Specimens were examined using a Zeiss Stereo Discovery V12 stereomicroscope with a Zoom Microscope System. Both male palps and female copulatory organs were detached and examined in 75% ethanol, using a Zeiss Axio Scope A1 compound microscope with a KUY NICE CCD. The epigynes were digested and cleared with pancreatin. Specimens including detached male palps and epigynes were stored in 80% ethanol after examination. All the specimens are deposited in Animal Specimen Museum, Life Science of College, Jinggangshan University (**ASM-JGSU**).

Somatic morphological measurements were taken with the ImageView CM2000 software and given in millimetres. The body length of all specimens excludes the chelicerae and spinnerets. Terminology of the male and female genitalia follows Jäger and Wunderlich (2012), Ramírez (2014), and Zamani and Marusik (2020). Promarginal and retromarginal teeth on the chelicerae are given as the first, second, third, etc., and measured from the base of the fang to the distal groove.

Leg measurements are given as total length (femur, patella, tibia, metatarsus, tarsus). Leg spines are documented by dividing each leg segment into two aspects, prolateral (p) and retrolateral (r), and indicating the ventral (v) spines as single (1) or paired (2), e.g., femur I pv1111; tibia I v2222.

The abbreviations used in the text are as follows:

Eyes

ALE anterior lateral eye;
AME anterior median eye;
MOA median ocular area;
PLE posterior lateral eye;
PME posterior median eye.

Chelicerae

PES promarginal escort seta;
PRS promarginal rake setae;
RES retromarginal escort seta;
SS slit sensillum;
WS whisker setae.

Legs

LO lyriform organ;
MTS metatarsal stopper;
TO tarsal organ.

Male palp

DTA dorsal tibial apophysis;
dTA distal tegular apophysis;
E embolus;
FA femoral apophysis;
RTA retrolateral tibial apophysis;
rTA retrolateral tegular apophysis;
SD sperm duct.

Epigyne

B bursa;
CD copulatory duct;
CO copulatory opening;
CT connecting tube;
FD fertilisation duct;
GA glandular appendage;
MS median septum;
SP spermathecae.

Taxonomy

Family Phrurolithidae Banks, 1892

Comments. Phrurolithidae spiders are mainly distributed in Asia, North America and Europe. Half of them are found from Asia. Four phrurolithid genera are Asian endemics, i.e., *Abdosetae* Fu, Zhang & MacDermott, 2010, *Bosselaerius* Zamani & Marusik, 2020, *Otacilia* Thorell, 1897 and *Plynnon* Deeleman-Reinhold, 2001. Only one genus, *Phrurolithus*, is widely distributed in Asia, America and Europe. Currently, more than 80 known species in the four former genera have been reported from China. The total number of known Phrurolithidae species from China will rapidly rise to 100 with the addition of seven new species described in the present paper and the future descriptions of additional new species from the country.

***Alboculus* Liu, gen. nov.**

<http://zoobank.org/3EF7496B-294B-4683-9887-C4367E06BA63>

Diagnosis. The new genus differs from other Phrurolithidae by the oval PME without a layer of black pigment around the eye cup (Figs 1A, D, 3A) (vs. with layer of black pigment around eye cup), posterior eye row slightly procurved (Figs 1A, D, 3A) (vs. straight to recurved), lacking distinct longitudinal and radial stripes on the dorsal carapace (Figs 1A, D, 3A) (vs. black longitudinal or radial stripes present), and lacking a chevron-shaped marking on the abdominal dorsum (Figs 1A, 3A) (vs. with at least two chevron-shaped markings). Males of this genus can be easily distinguished by the lack of a dorsal tibial apophysis on the palp (Figs 2A–C, 6A, B, D) (vs. palpal tibia with dorsal tibial apophysis) and the well-developed terminal apophysis of the bulb (Figs 2A–C, 6B–D) (vs. absent). The female of this genus has the glandular appendages slender (Fig. 3C, D) (vs. relatively short and thick) and the spermathecal tail of epigyne distinct (Fig. 3D, E) (vs. without a spermathecal tail).

Type species. *Otacilia zhejiangensis* (Song & Kim, 1991).

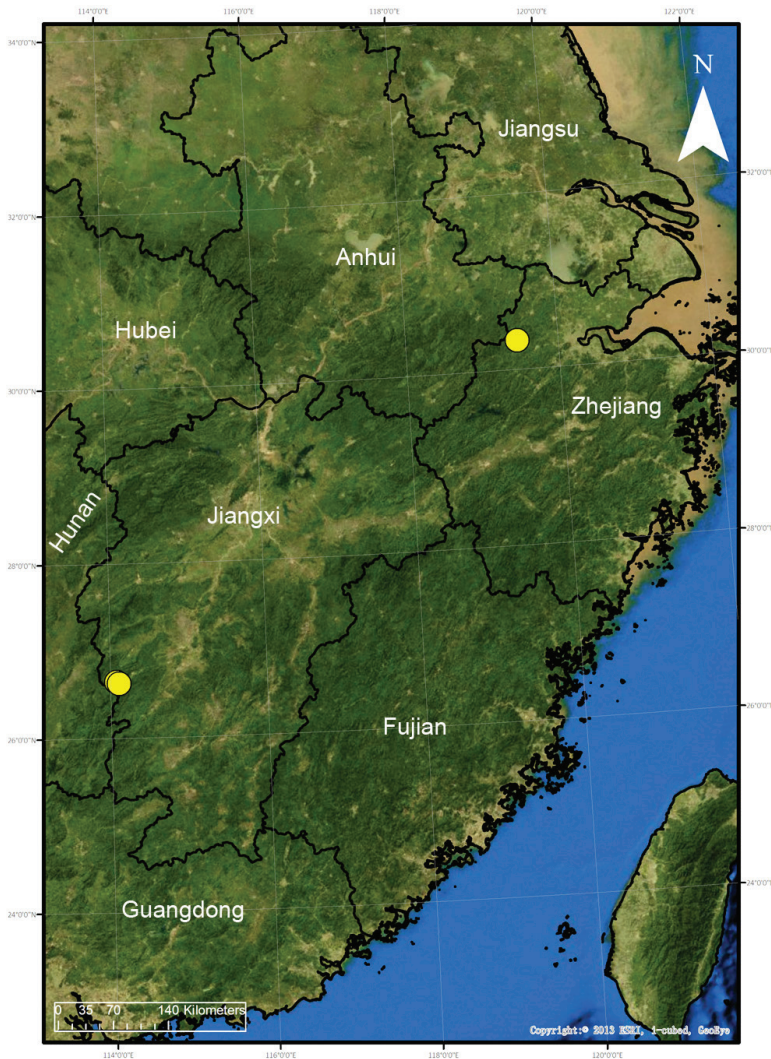
Etymology. The genus name is formed from two Latin words *albus* and *oculus*, alluding to the light-coloured posterior median eyes; the gender is masculine.

Remarks. The type species *O. zhejiangensis* was first described by Song and Kim (1991) as a new species of *Phrurolithus* based on a single female specimen from Tianmu Mountain, Zhejiang province, China. Recently, it was transferred to *Otacilia* by Zamani and Marusik (2020). It is interesting to compare the three specimens of this species, clearly recognised by differences in morphological characters with the type species of *Otacilia* and *Phrurolithus*. Males of this genus differ from *Phrurolithus festivus* (C.L. Koch, 1835) by lacking a layer of black pigment around the PME (Figs 1A, B, D, 3A) (vs. PME with black pigment), and having a single tibial apophysis (Figs 2A–C, 6A, B, D) (vs. present two tibial apophysis). Although the male of *Otacilia armatissima* is unknown, male *Alboculus* species differ from *Otacilia* males (e.g., Figs 7A, 9A, 13A, 15A, 18A) by the procurved posterior eye row (vs. recurved), and by the dorsal scutum covering the entire dorsal surface of the abdomen (Fig. 1A, C) as opposed to a narrow scutum only extending to approximately half the abdomen length in *Otacilia* (e.g., Figs 7A, 9A). The females clearly differ from these two type species (*O. armatissima* and *P. festivus*) by the slender glandular appendages (Fig. 3C, D) (vs. relatively short and thick [Figs 8D, 10D, 12D, 14D, 16D, 19D, 21D]) and the spermathecal tail of epigyne (Fig. 3C, D) (vs. without the spermathecal tail [Figs 8D, 10D, 12D, 14D, 16D, 19D, 21D]).

Description. Small, body length 1.8–2.8 mm. **Eyes:** AME rounded, PME oval, light-coloured, without black pigment, anterior eye row straight, posterior eye row procurved. Each chelicera with three promarginal and two retromarginal teeth. Femur I with two spines, tibia I with five pairs of ventral spines, metatarsus I with three pairs of ventral spines. Abdomen without dorsal scutum in females, covering entire dorsum in males.

Male palp: femur with large ventral extension; tibia with long, sharply-pointed retroventral tibial apophysis, without dorsal apophysis; bulb without median apophysis or conductor; sperm duct long, reaching middle part of the tegulum, narrowed near base of embolus; base of embolus slightly narrowed, embolus very small, hook-shaped, directed antero-prolaterally, embolus accompanied by thick, short distal terminal apophysis (TA) (larger than embolus). Epigyne with clear copulatory atrium medially; glandular appendages slender, located on anterior of connecting tubes; spermathecae rounded, with clavate-like tail.

Distribution. China (Map 1) (Zhejiang and Jiangxi Provinces)



Map 1. Distribution of *Alboculus zhejiangensis* (Song & Kim, 1991), comb. nov., in China.

***Alboculus zhejiangensis* (Song & Kim, 1991), comb. nov.**

Figures 1–6

Phrurolithus zhejiangensis Song & Kim, 1991: 23, figs 16–18 (♀); Song et al. 1999: 412, fig. 240E–F (♀).

Otacilia zhejiangensis Zamani & Marusik, 2020: 312.

Material examined. CHINA: Jiangxi Province, Ji'an City, Jinggangshan County Level City. 2♂, Dalong Town, Yuantou Village, 26°37'40.8"N, 114°6'21.6"E, 906 m, 5 April 2014, leg. Ke-Ke Liu et al.; 1♀, Longshi Town, Maoping, Shenshan Village, Shenshan, 26°38'49.2"N, 114°4'26.4"E, 798 m, 8 August 2015, leg. Ke-ke Liu et al.

Notes. These two collection localities of males and a female of this species are very close and located on both sides of Shenshan Mt. They are assigned in different two adjacent towns in Jinggang Mountain National Nature Reserve, Jiangxi Province, China. Meanwhile, one sub-adult male was also collected on 8 August 2015, which has the same habitus as the males collected on April 5 2014. These males are therefore recognised as corresponding to the conspecific female.

Diagnosis. This species is easily distinguished from other Phrurolithidae spiders by the following combination of morphological characteristics: (1) lacking a layer of black pigment around the PME (Figs 1A, D, 3A) (vs. PME with black pigment); (2) lacking distinct longitudinal and radial stripes on the dorsal carapace (Figs 1A, D, 3A) (vs. black longitudinal or radial stripes present); (3) lacking chevron-shaped marking on abdominal dorsum (Figs 1A, 3A) (vs. with at least two chevron-shaped markings); (4) male palpal tibia with a single retrolateral apophysis (Figs 2A–C, 6A, B, D) (vs. two tibial apophyses present); (5) female epigyne (Fig. 3C, D) with the glandular appendages slender (vs. relatively short and thick), and the spermathecal tail club-shaped (vs. without a spermathecal tail).

Description. Male. Habitus as in Fig. 1A–C. Total length 2.50, carapace 1.18 long, 0.90 wide. **Eye** sizes and interdistances: AME 0.06, ALE 0.07, PME 0.06, PLE 0.06; ALE–AME 0.02, AME–AME 0.04, PLE–PME 0.06, PME–PME 0.06, ALE–ALE 0.21, PLE–PLE 0.28, ALE–PLE 0.05, AME–PME 0.06, ALE–PME 0.11. MOA 0.17 long, front width 0.17, back width 0.19. Cervical groove distinct. Radial furrow and fovea indistinct. **Chelicerae** (Figs 2A, B, 4): with two frontal spines long and short, three promarginal (proximal largest, distal smallest) and two retromarginal teeth (distal larger); promargin with one escort seta, a row of rake setae, a row of whisker setae; retromargin with one escort seta; the other row of whisker setae present near the cheliceral base in retrolateral view; near base of fang with a prolateral and a retrolateral slit sensillum. Sternum with strongly rebordered margins (Fig. 1B). Leg measurements: I 3.21 (0.94, 0.39, 0.87, 0.62, 0.39); II 2.67 (0.81, 0.36, 0.66, 0.49, 0.35); III 2.48 (0.67, 0.31, 0.55, 0.57, 0.38); IV 3.59 (0.96, 0.37, 0.82, 0.92, 0.52). **Leg** setae: metatarsi I, II, and IV with a long trichobothrium, as long as tarsus; tarsi I–IV with 2–4 trichobothria each; tarsal claws with 5–12 pseudotenent setae each, superior tarsal claw with two teeth. Tarsal organ teardrop shaped (Fig. 5K). Tarsal slit sensillum present.

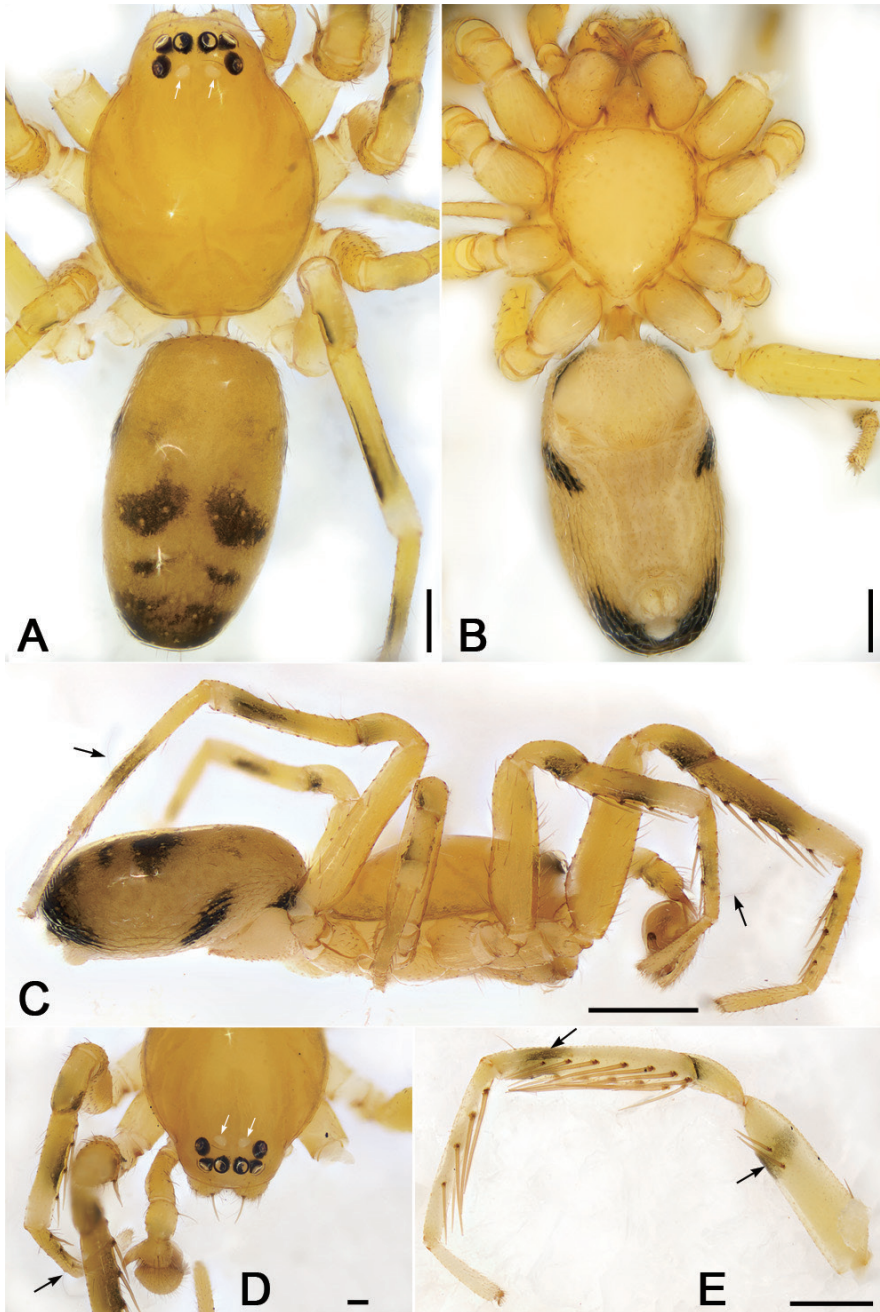


Figure 1. *Alboculus zhejiangensis* (Song & Kim, 1991) comb. nov., male **A** habitus, dorsal view, white arrows show the light-coloured, oval posterior median eyes **B** same, ventral view **C** same, lateral view, black arrows showing the long trichobothria on metatarsi II and IV **D** carapace, dorsal view, white arrows show the light-coloured, oval posterior median eyes, black arrow shows the long trichobothrium on metatarsus II **E** right leg I, prolateral view, black arrows showing the dark annulations. Scale bars: 0.2 mm (**A**, **B**), 0.5 mm (**C**, **E**), 0.1 mm (**D**).

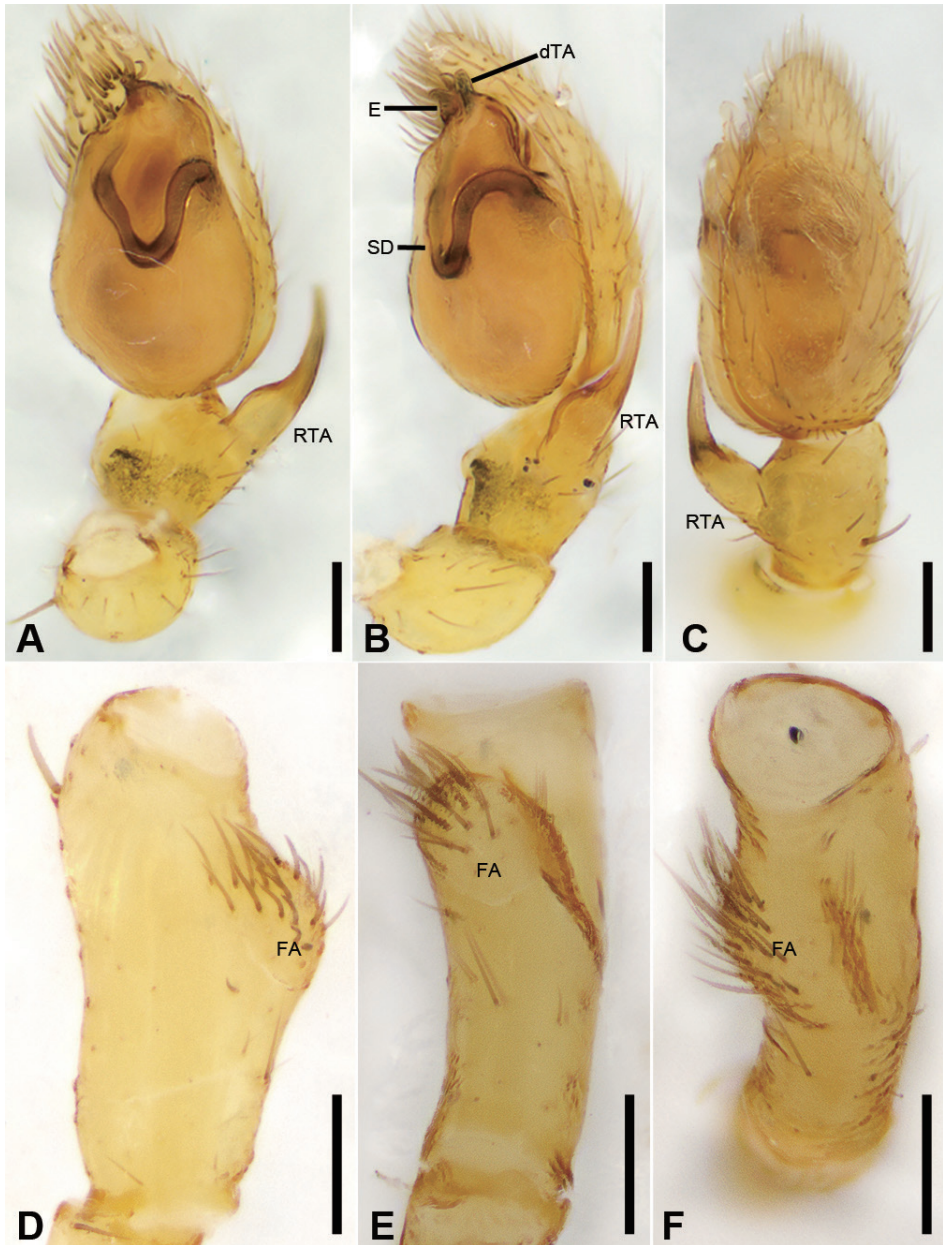


Figure 2. *Albulcus zhejiangensis* (Song & Kim, 1991) comb. nov., male palp **A** palp, proteral view **B** same, ventral view **C** same, retrolateral view **D** femur, proteral view **E** same, ventral view **F** same, retrolateral view. Scale bars: 0.2 mm (**A, B**), 0.1 mm (**C–F**). Abbreviations: dTA – distal tegular apophysis, E – embolus, FA – femoral apophysis, RTA – retrolateral tibial apophysis, SD – sperm duct.

Leg spination: femur I pv11; tibiae I v22222, II v222; metatarsi I pv1111, rv111, II pv111, rv11. Abdomen elongate elliptical in dorsal view (Fig. 1A–C), scutum covering entire dorsum, 1.24 long, 0.69 wide.

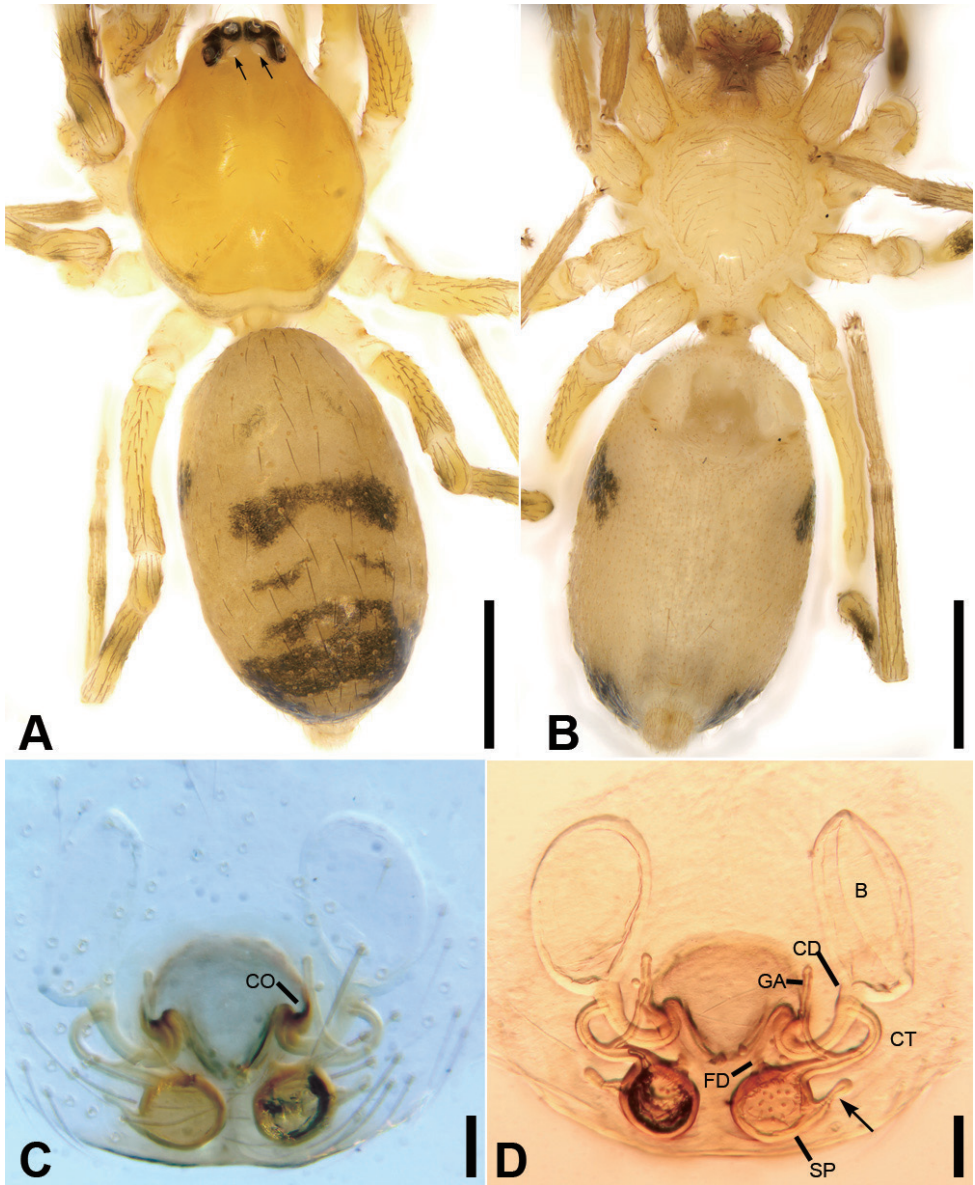


Figure 3. *Alboculus zhejiangensis* (Song & Kim, 1991) comb. nov., female **A** habitus, dorsal view, black arrows show the light-coloured, oval posterior median eyes **B** same, ventral view **C** epigyne, ventral view **D** same, dorsal view, black arrow shows the detail of spermathecal tail. Scale bars: 0.5 mm (**A, B**), 0.1 mm (**C, D**). Abbreviations: B – bursa, CD – copulatory duct, CO – copulatory opening, CT – connecting tube, FD – fertilisation ducts, GA – glandular appendage, SP – spermathecae.

Colouration (Fig. 1A–C). Carapace yellow, with indistinct radial stripes from median to marginal. Chelicerae, endites, labium, and sternum yellow. Legs yellow, with dark strips on patellae, tibiae and metatarsi I–IV (Figs 1, 5). Abdomen yellow, with

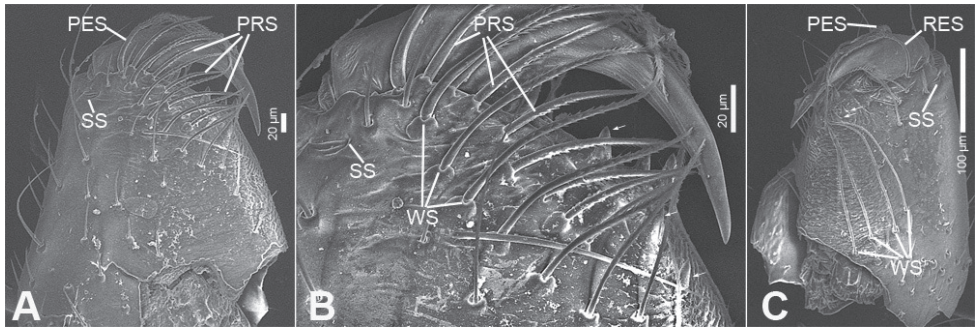


Figure 4. SEM micrographs of *Alboculus zhejiangensis* (Song & Kim, 1991) comb. nov., male chelicera **A** frontal view **B** detail of promargin, frontal view **C** posterior view, slightly retrolateral. Abbreviations: PES – promarginal escort seta, PRS – promarginal rake setae, RES – retromarginal escort seta, SS – slit sensillum, WS – whisker setae.

pair of large oval dark spots medially, pair of blade-shaped dark spots on sub-medial part, and semi-circular dark spot posteriorly.

Palp (Figs 2, 6). Femoral apophysis well-developed, width slightly less than half of length, with abundant short setae. Patella unmodified. Tibia with a large retrolateral apophysis, longer than tibia, with sharply pointed and broad base. Cymbium approximately two times longer than wide. Bulb oval, with long V-shaped sperm duct, apophyses absent. Embolus hook-shaped, small, with large base, accompanied by a small regular apophysis of embolic base, terminal apophysis slightly longer than embolus and surrounded by the embolic base.

Female. Habitus as in Fig. 3A, B. Total length 2.40, carapace (Fig. 3A) 1.01 long, 0.79 wide. **Eye** sizes and interdistances: AME 0.06, ALE 0.07, PME 0.05, PLE 0.05; ALE–AME 0.02, AME–AME 0.04, PLE–PME 0.03, PME–PME 0.04, ALE–ALE 0.17, PLE–PLE 0.20, ALE–PLE 0.06, AME–PME 0.06, ALE–PME 0.20. MOA 0.15 long, front width 0.14, back width 0.14. **Abdomen** (Fig. 3A), 1.08 long, 1.19 wide. **Leg** measurements: I 2.73 (0.76, 0.31, 0.71, 0.59, 0.36); II 2.15 (0.65, 0.27, 0.50, 0.49, 0.33); III 1.99 (0.58, 0.25, 0.37, 0.48, 0.31); IV 2.78 (0.79, 0.30, 0.60, 0.68, 0.41). Dorsal scutum absent on abdomen.

Epigyne (Fig. 3C, D). Anterior fovea separated by weakly sclerotised V-shaped margin, bilaterally with concaved copulatory openings. Copulatory ducts and gland appendages distinctly visible through integument in intact epigyne. Copulatory ducts slender, curved forward, connecting with the oval bursae. Connecting tubes slender, ear-shaped, located at the distal of copulatory ducts, curved backwards to spermathecae, posteriorly with slender glandular appendages. Glandular appendages as long as connecting tubes, extending forwards. Spermathecae globular, separated less than their diameter. Fertilisation duct short, located anteriorly on spermathecae. Spermathecal tails shorter than spermathecal diameter, club-shaped, ectally located.

Distribution. Known from Zhejiang and Jiangxi (Map 1).

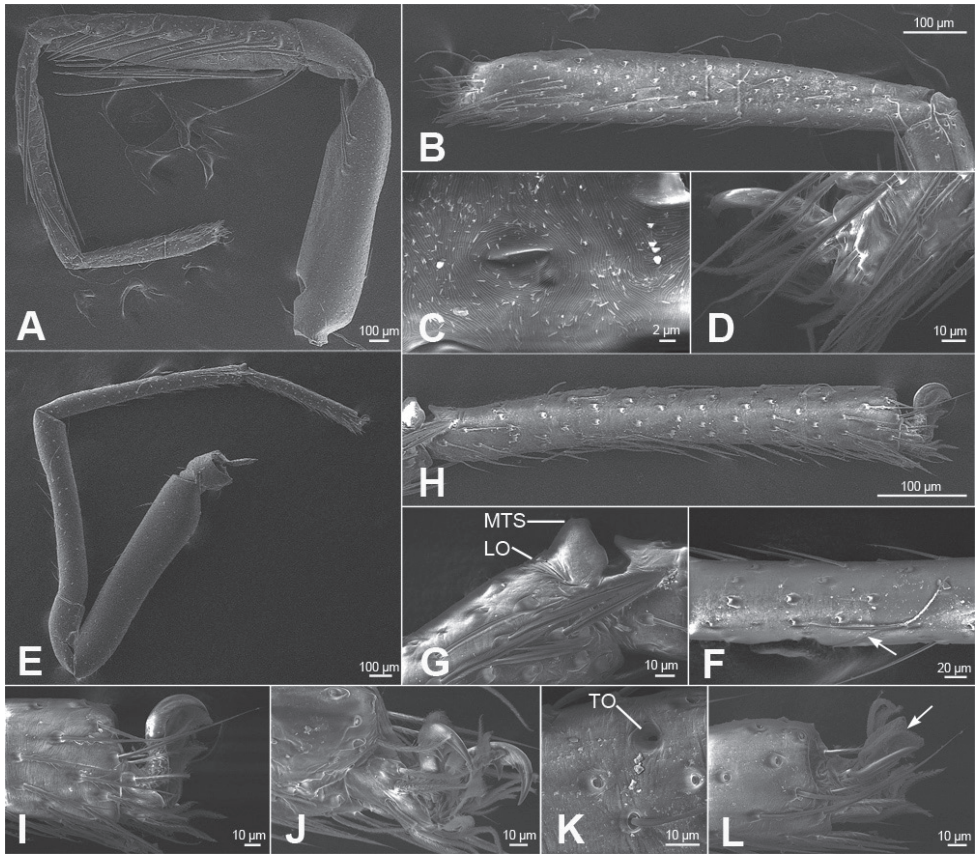


Figure 5. SEM micrographs of *Alboculus zhejiangensis* (Song & Kim, 1991) comb. nov., male legs **A** right leg I, prolateral view **B** same, tarsus, prolateral view **C** same, tarsal slit sensillum, prolateral view **D** same, tarsal claw and claw tuft setae, prolateral view **E** left leg IV, prolateral view **F** same, metatarsus, white arrow shows the long trichobothrium, prolateral view **G** same, metatarsus-tarsus joint, prolateral view **H** same, tarsus, prolateral view **I** same, tarsal claw and claw tuft setae, prolateral view **J** right tarsal claw I and claw tuft setae, retrolateral view **K** left tarsus IV, detail of tarsal organ, dorsal view **L** left tarsal claw IV and claw tuft setae, dorsal view. Abbreviations: LO – lyriform organ, MTS – metatarsal stopper, TO – tarsal organ.

Genus *Otacilia* Thorell, 1897

Notes. Currently, there are 99 species included in this genus, with 74 recorded from China. In the last five years, the total number of species from the country has increased considerably, due to the considerable attention paid to them by many arachnologists. They are widely distributed in southern China, such as Hainan (six species), Taiwan (two species), Zhejiang (four species), Yunnan (ten species), Guangxi (two species), Guizhou (five species), Sichuan (eight species), Chongqing (nine species), Hunan (19 species), Hubei (four species) and Jiangxi (seven species) provinces. Jin et al. (2016)

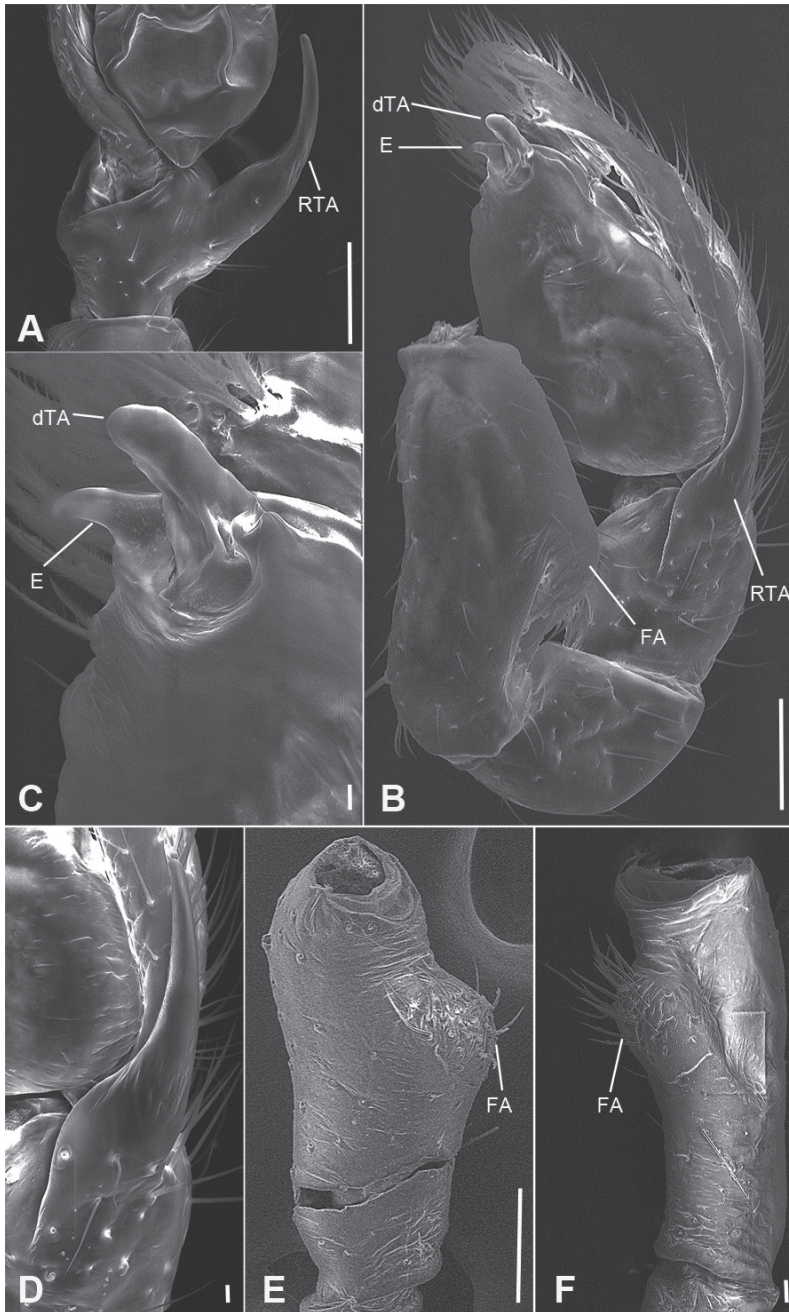


Figure 6. SEM micrographs of *Alboculus zhejiangensis* (Song & Kim, 1991) comb. nov., male palp **A** ventral view, showing detail of retrolateral tibial apophysis **B** same, ventro-retrolateral view **C** same, detail showing embolus and distal tegular apophysis **D** same, detail showing retrolateral tibial apophysis **E** palp femur, prolateral view **F** same, retrolateral view. Scale bars: 0.1 mm (**A, B, E**), 10 μ m (**C, D**), 20 μ m (**F**). Abbreviations: dTA – distal tegular apophysis, E – embolus, FA – femoral apophysis, RTA – retrolateral tibial apophysis.

divided *Otacilia* into five species groups, i.e., the *armatissima*-group, *ambon*-group, *longituba*-group, *pseudostella*-group, and a fifth unnamed group containing the remaining species (i.e., species known from a single sex, or with poor original descriptions and figures or peculiar structures). These seven new species most likely belong to the *armatissima*-group. Only one new species, *O. bijiashanica* Liu, sp. nov., has two tibial apophyses, while the others only have one.

***Otacilia acutangula* Liu, sp. nov.**

<http://zoobank.org/B8364C5E-8AE3-4E18-BA7B-EF9D2D11454D>

Figures 7, 8

Type material. *Holotype*: ♂, CHINA: Jiangxi Province, Ji'an City, Jinggangshan County Level City, Ciping Town, Dajing Village, Jingzhushan Scenic Spot, 26°31'33.37"N, 114°06'30.34"E, 786 m, 1 October 2018, leg. Ke-Ke Liu et al. *Paratypes*: 2♀, with same data as holotype; 1♂, 1♀, same locality, Lingxiufeng Scenic Spot, 26°34'16.72"N, 114°07'00.56"E, 971 m, 1 October 2018, leg. Ke-Ke Liu et al.; 1♂, same locality, Xiaojing Village, Longtan Scenic Spot, 26°35'33.08"N, 114°08'18.50"E, 909 m, 1 October 2018, leg. Ke-Ke Liu et al.; 1♂, same locality, Bijiashan Scenic Spot, Hongjun Road, 26°36'25.88"N, 114°11'43.07"E, 549 m, 3 October 2018, leg. Ke-Ke Liu et al.

Etymology. The specific name is derived from the Latin adjective *acutangulus*, referring to the bent retrolateral tibial apophysis that forms an angle of ca. 45° with its transverse base; adjective.

Differential diagnosis. The new species differs from *O. dawuishan* Liu, Xu, Xiao, Yin & Peng, 2019 by an oval distal tegular apophysis (Fig. 7C–F) (vs. teardrop shaped), the bent RTA forming an angle of ca. 45° (Fig. 7D, E) (vs. ca. 60°), and the strongly sclerotised ridges in the epigyne (Fig. 8C) (vs. weakly sclerotised).

Description. Male (Holotype). Habitus as in Fig. 7A, B. Total length 3.10, carapace 1.45 long, 1.31 wide. *Eye* sizes and interdistances: AME 0.08, ALE 0.10, PME 0.07, PLE 0.11; ALE–AME 0.02, AME–AME 0.06, PLE–PME 0.07, PME–PME 0.12, ALE–ALE 0.25, PLE–PLE 0.39, ALE–PLE 0.10, AME–PME 0.10, ALE–PME 0.10. MOA 0.25 long, front width 0.20, back width 0.27. *Chelicerae* (Fig. 7A, B) with three promarginal (middle largest, distal smallest) and five retromarginal teeth (distal largest, proximal smallest). *Sternum* (Fig. 7B), posteriorly pointed. *Abdomen* (Fig. 7A) 1.43 long, 0.91 wide. *Leg* measurements: I 6.64 (1.73, 0.57, 1.98, 1.48, 0.88); II 5.42 (1.38, 0.50, 1.52, 1.26, 0.76); III 4.57 (1.16, 0.50, 1.07, 1.15, 0.69); IV 7.15 (1.96, 0.55, 1.73, 1.95, 0.96). Leg spination: femora I–IV with one dorsal spine each; femora I pv1111, II pv11; tibiae I v22222222, II v2222222; metatarsi I v2222, II pv1222.

Colouration (Fig. 7A, B). Carapace yellow-brown. Chelicerae yellow-brown. Endites yellow. Labium and sternum yellow-brown. Legs yellow. Abdomen yellowish brown, with pair of small oval large triangular yellowish spots medially, large irregular yellowish spots medially also on the posterior dorsal scutum, three light chevron-

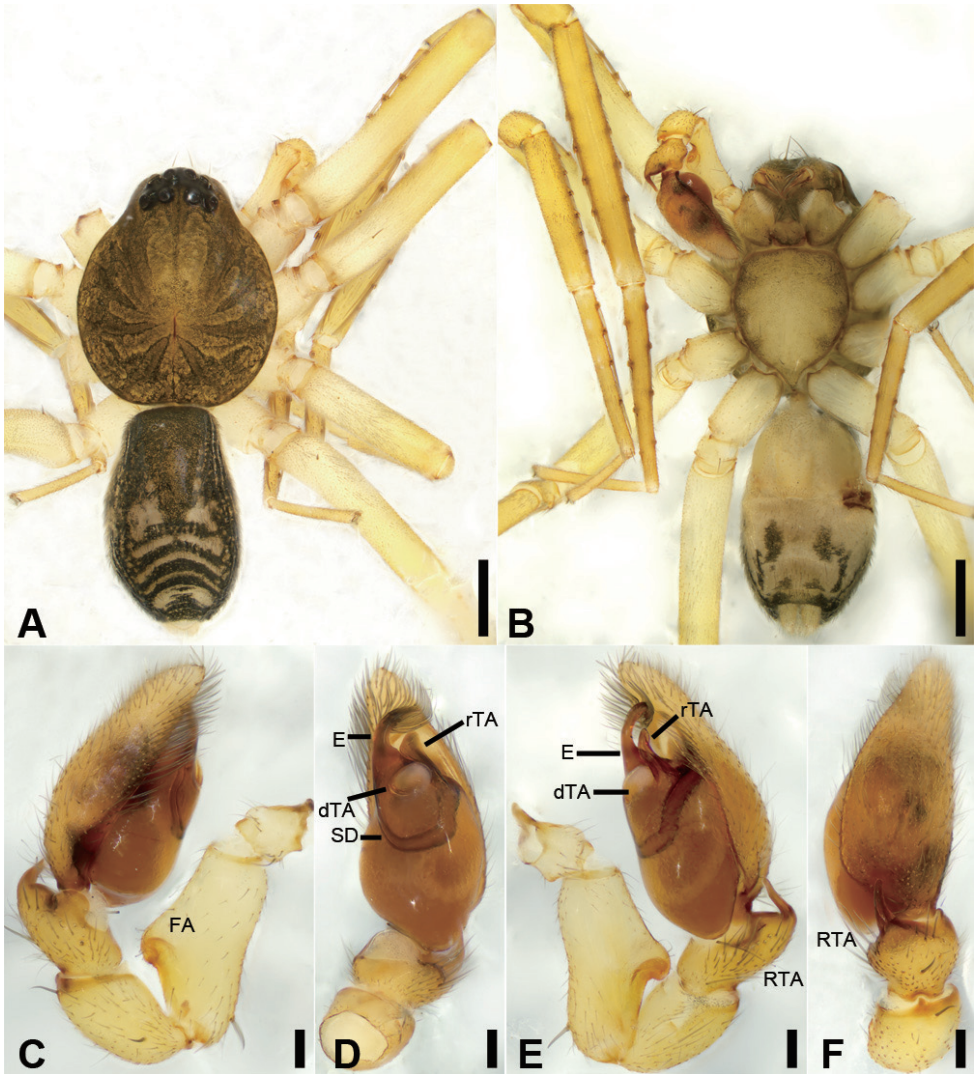


Figure 7. *Otacilia acutangula* sp. nov., male holotype **A** habitus, dorsal view **B** same, ventral view **C** palp, prolateral view **D** same, ventral view **E** same, retrolateral view **F** same, dorsal view. Scale bars: 0.5 mm (**A, B**), 0.1 mm (**C–F**). Abbreviations: dTA – distal tegular apophysis, E – embolus, FA – femoral apophysis, RTA – retrolateral tibial apophysis, rTA –retrolateral tegular apophysis, SD – sperm duct.

shaped stripes on sub-medial part, and yellowish arc-shaped stripe posteriorly; weak dorsal scutum in anterior half, extending slightly past the midpoint.

Palp (Fig. 7C–F). Femoral apophysis well-developed, width longer than half of length. Patella unmodified. Tibia with short retrolateral apophysis, less than tibial length, tapering-pointed, bending inwards to base of cymbium, forming an acute angle of ca. 45° with its transverse base in retrolateral view. Cymbium more than two times longer than wide. Bulb oval, with long U-shaped sperm duct, apophyses absent. Em-

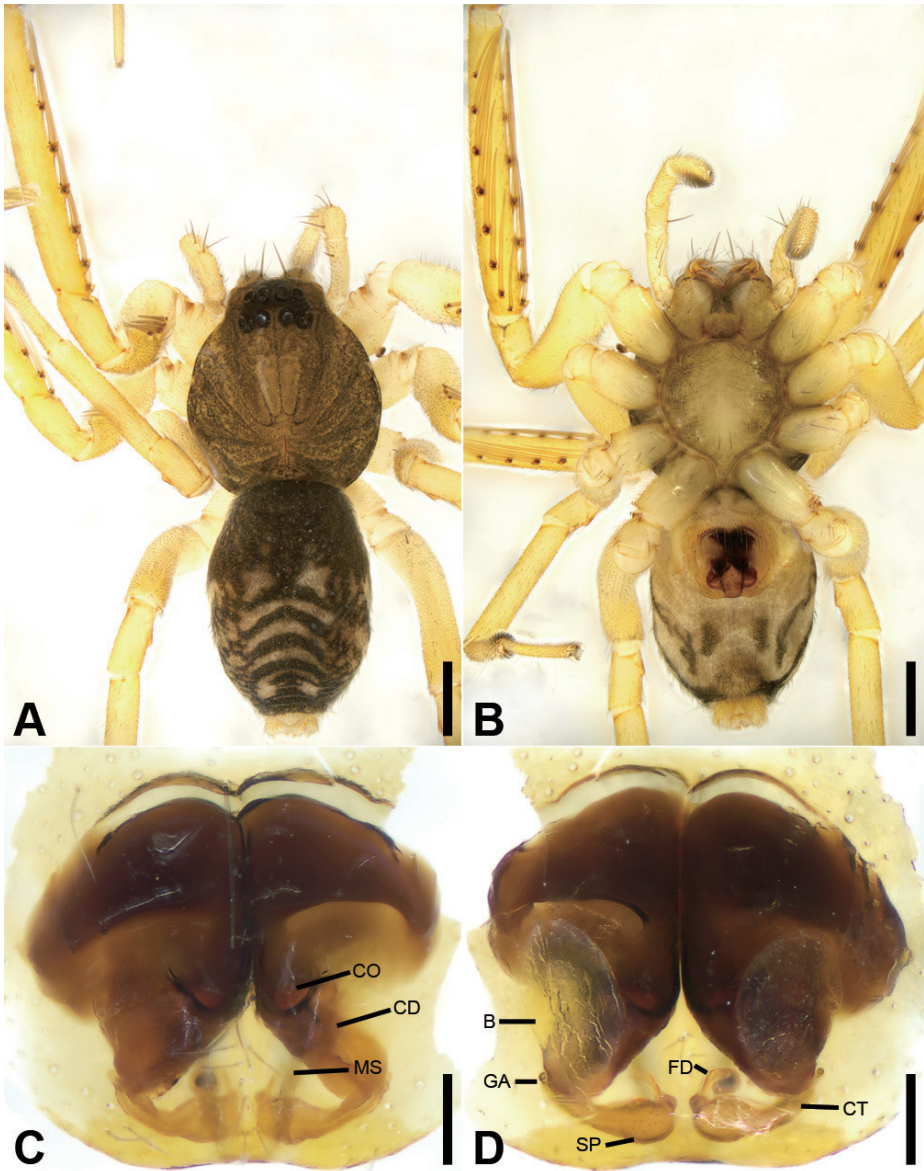


Figure 8. *Otacilia acutangula* sp. nov., female paratype **A** habitus, dorsal view **B** same, ventral view **C** epigyne, ventral view **D** epigyne, dorsal view. Scale bars: 0.5 mm (**A**, **B**), 0.1 mm (**C**, **D**). Abbreviations: B – bursa, CD – copulatory duct, CO – copulatory opening, CT – connecting tube, FD – fertilisation ducts, GA – glandular appendage, MS – median septum, SP – spermathecae.

bolus hook-shaped, thick, with broad triangular base, apart from distal and retrolateral regular apophyses. Retrolateral regular apophysis straight, thickened, finger-shaped, submedial part covered by oval distal regular apophysis.

Female. Habitus as in Fig. 8A, B. Lighter than male. Total length 2.87, carapace 1.42 long, 1.20 wide. **Eye** diameters: AME 0.09, ALE 0.09, PME 0.07, PLE 0.09; ALE–AME 0.01, AME–AME 0.04, PLE–PME 0.06, PME–PME 0.11, ALE–ALE 0.23, PLE–PLE 0.35, ALE–PLE 0.08, AME–PME 0.09, ALE–PME 0.10. MOA 0.23 long, front width 0.21, back width 0.24. **Abdomen** (Fig. 8A) 1.37 long, 0.86 wide. **Leg** measurements: I 6.41 (1.62, 0.49, 2.00, 1.58, 0.72); II 5.27 (1.35, 0.53, 1.45, 1.22, 0.72); III 4.36 (1.15, 0.42, 1.00, 1.15, 0.64); IV 7.07 (1.88, 0.55, 1.75, 1.95, 0.94). Leg spination: femora I–IV with one dorsal spine each; tibiae I v2222222, II v222222.

Epigyne (Fig. 8C, D). Epigynal plate mushroom-like, posterior with a triangular median septum, copulatory ducts, glandular appendages, connecting tubes and spermathecae distinctly visible through integument in intact epigyne. Anterior fovea separated by strongly sclerotised M-shaped margin, medially with concaved, large copulatory openings. Copulatory ducts broad, declivitous, posteriorly with pair of kidney-shaped transparent bursae medially. Glandular appendages short, anterior part covered by bursae, located on anterior of connecting tubes. Connecting tubes short, located between glandular appendages and spermathecae. Spermathecae slightly swollen, slightly separated. Fertilisation duct short, located apically on spermathecae.

Distribution. Known only from the type locality in Jiangxi Province, China (Map 2).

***Otacilia bijiashanica* Liu, sp. nov.**

<http://zoobank.org/467DE20C-2700-49F0-A52D-B98B136164AE>

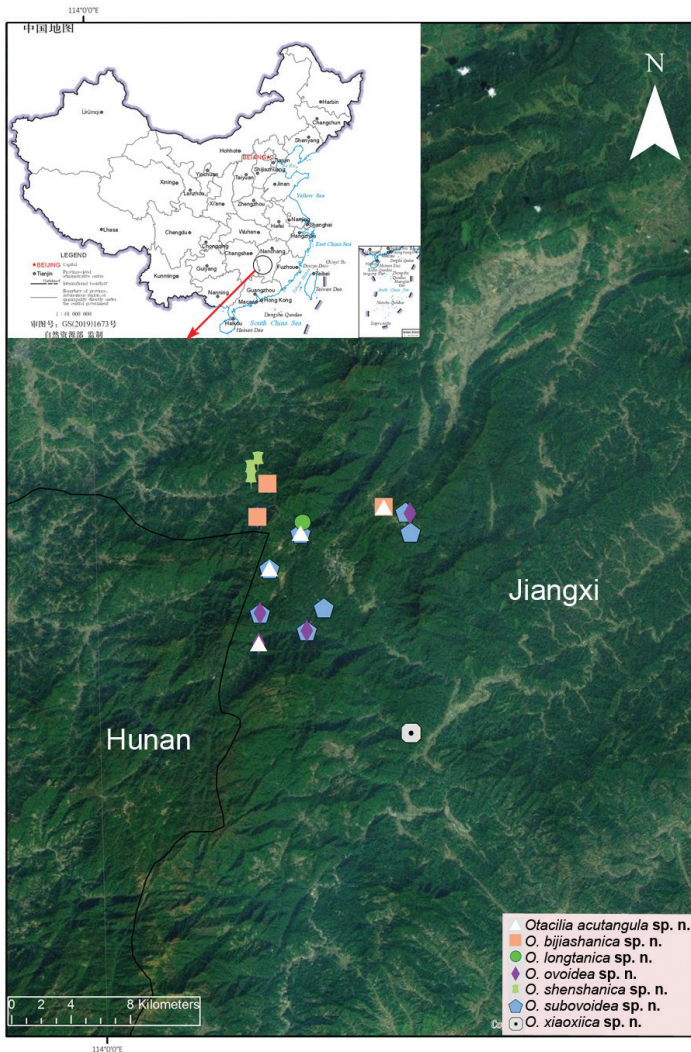
Figures 9–11

Type material. **Holotype:** ♂, CHINA: Jiangxi Province, Ji'an City, Jinggangshan County Level City, Ciping Town, Bijiashan Scenic Spot, Hongjun Road, 26°36'25.88"N, 114°11'43.07"E, 549 m, 3 October 2018, leg. Ke-Ke Liu et al. **Paratypes:** 3♂, 1♀, same locality as holotype, Luofu Town, Xiangzhou Village, Fengshuping Group, 26°36'10.31"N, 114°06'34.69"E, 364 m, 5 October 2018, leg. Ke-Ke Liu and Hui-Pu Luo; 1♂, Ciping Town, Huangyangjie Scenic Spot, 26°37'22.8"N, 114°7'1.2"E, 1055 m, 5 April 2014, leg. Ke-Ke Liu et al.

Etymology. The specific name refers to the type locality, Bijiashan; adjective.

Differential diagnosis. The new species differs from *O. fabiformis* Liu, Xu, Xiao, Yin & Peng, 2019 and *O. hippocampa* Jin, Fu, Yin & Zhang, 2016 by the short hook-shaped embolus (Figs 9D, 11A, B) (vs. spine-like in *O. fabiformis* and *O. hippocampa*), and the C-shaped spermathecae (Fig. 10D) (vs. peanut-like in *O. fabiformis* and globular in *O. hippocampa*).

Description. Male (holotype). Habitus as in Fig. 9A, B. Total length 2.56, carapace 1.24 long, 1.07 wide. **Eye** sizes and interdistances: AME 0.06, ALE 0.08, PME 0.08, PLE 0.08; ALE–AME 0.01, AME–AME 0.04, PLE–PME 0.04, PME–PME 0.07, ALE–ALE 0.17, PLE–PLE 0.30, ALE–PLE 0.07, AME–PME 0.07, ALE–PME 0.07. MOA 0.21 long, front width 0.15, back width 0.22. **Chelicerae** (Fig. 9B) three promarginal (proximal largest, distal smallest) and two retromarginal teeth (distal larger



Map 2. Map of China, enlargement showing records of *Otacilia acutangula* sp. nov., *O. bijiashanica* sp. nov., *O. longtanica* sp. nov., *O. ovoidea* sp. nov., *O. shenshanica* sp. nov., *Otacilia subovoidea* sp. nov. and *O. xiaoxiica* sp. nov. in Jinggang Mountain National Nature Reserve, Jiangxi.

Sternum, posteriorly pointed. **Abdomen** (Fig. 9A, B), 1.42 long, 0.97 wide. Leg measurements: I 4.64 (1.21, 0.50, 1.35, 1.08, 0.50); II 4.00 (1.10, 0.48, 1.05, 0.95, 0.42); III 3.49 (0.90, 0.41, 0.74, 0.93, 0.51); IV 4.95 (1.30, 0.46, 1.10, 1.38, 0.71). **Leg** spination: femur I with two dorsal spines, femora II–IV with one dorsal spine each; femora I pv11, II pv11; tibiae I v2222222, II v222222; metatarsi I v2222, II v1222.

Colouration (Fig. 9A, B). Carapace yellow, with radial, irregular dark stripes submarginally and arc-shaped dark stripes around margin. Chelicerae yellow brown. Endites, labium and sternum yellow. Legs yellow, with distinct annulations on tibiae and

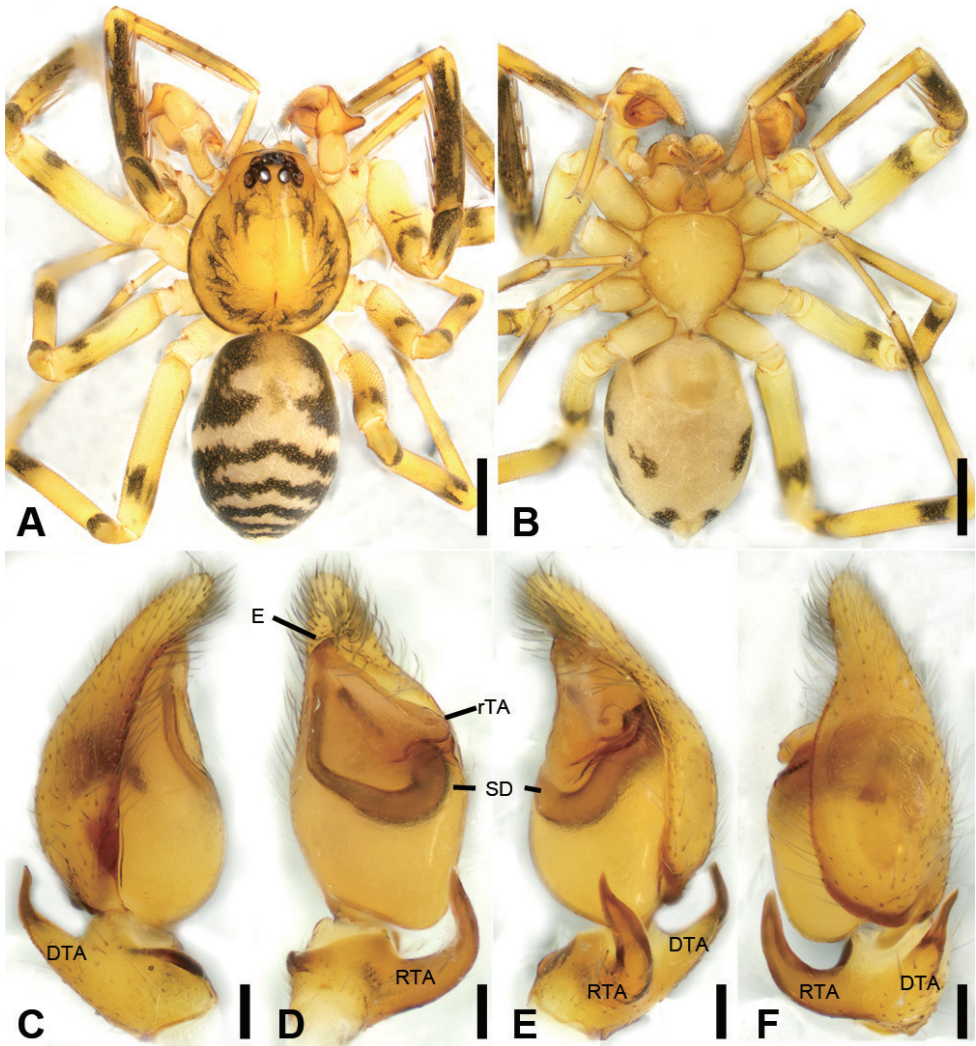


Figure 9. *Oracilia bijiashanica* sp. nov., male holotype **A** habitus, dorsal view **B** same, ventral view **C** palp, prolateral view **D** same, ventral view **E** same, retrolateral view **F** same, dorsal view, slightly retrolateral. Scale bars: 0.5 mm (**A**, **B**), 0.1 mm (**C**–**F**). Abbreviations: DTA – dorsal tibial apophysis, E – embolus, rTA – retrolateral tegular apophysis, RTA – retrolateral tibial apophysis, SD – sperm duct.

distal part of femora, patellae and metatarsi. Abdomen yellowish, with two large C-shaped stripes on the two sides of dorsal scutum and four light chevron-shaped stripes in submedial part, and single yellowish transverse stripe posteriorly.

Palp (Figs 9C–F, 11). Femoral apophysis well-developed, width longer than half of length. Patella unmodified. Retrolateral tibial apophysis large, longer than tibia, horn-shaped, with a sharp apex in retrolateral view. Dorsal tibial apophysis large, slightly shorter than tibia, with sharp narrowed sub-medial part and a spine-like apex in dorsal

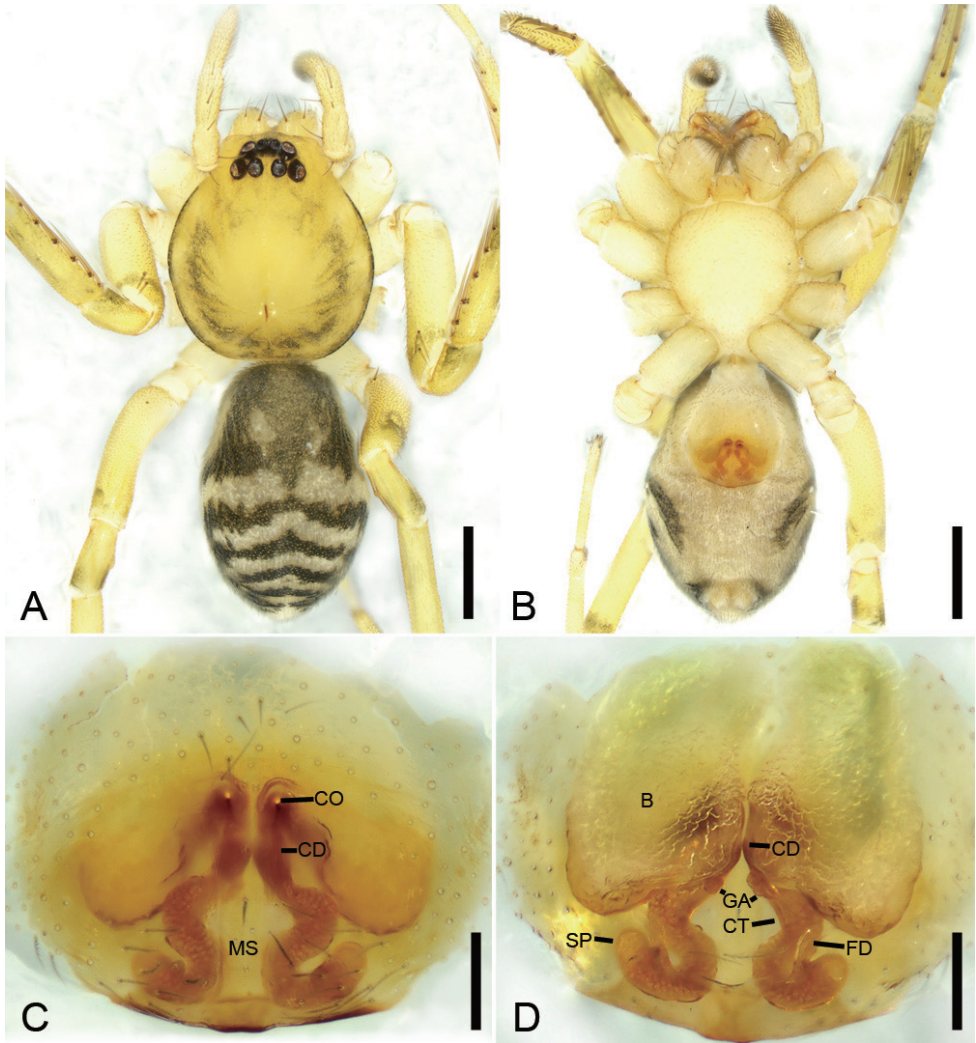


Figure 10. *Otacilia bijiashanica* sp. nov., female paratype **A** habitus, dorsal view **B** same, ventral view **C** epigyne, ventral view **D** epigyne, dorsal view. Scale bars: 0.5 mm (**A, B**), 0.1 mm (**C, D**). Abbreviations: B – bursa, CD – copulatory duct, CO – copulatory opening, CT – connecting tube, FD – fertilisation ducts, GA – glandular appendage, MS – median septum, SP – spermathecae.

view. Sperm duct strongly sclerotised, hook-shaped in ventral view, anterior part thick, gradually narrowed in posterior part. Retrolateral tegular apophysis extruding laterally, in front of anterior part of sperm duct. Embolus short and hook-shaped.

Female. Habitus as in Fig. 10A, B. Lighter than males. Total length 2.62, carapace length 1.26, width 1.10. *Eye* diameters: AME 0.06, ALE 0.08, PME 0.07, PLE 0.08; interdistances: ALE–AME 0.01, AME–AME 0.03, PLE–PME 0.05, PME–PME 0.07, ALE–ALE 0.14, PLE–PLE 0.31, ALE–PLE 0.08, AME–PME 0.08, ALE–PME 0.09.

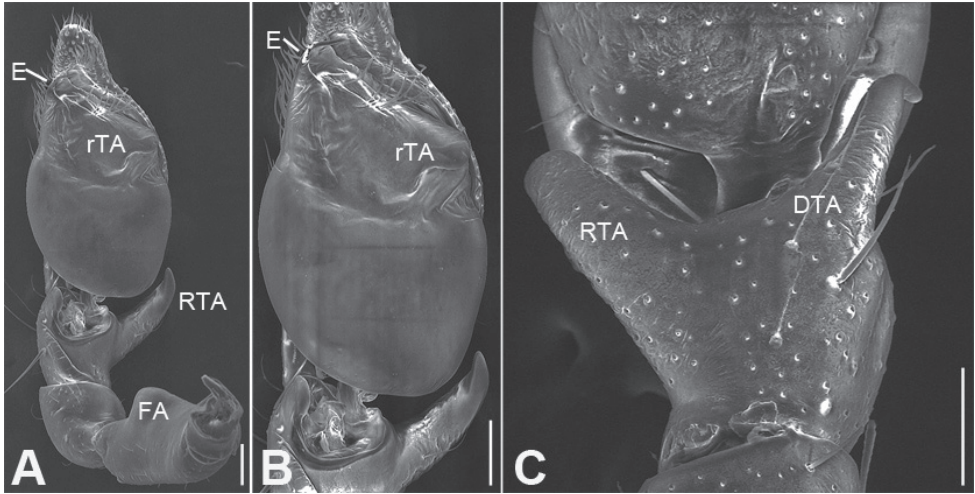


Figure 11. SEM micrographs of *Otacilia bijiashanica* sp. nov., palp of male paratype **A** ventral view **B** same, detail of bulb **C** dorsal view, detail of tibia apophysis. Scale bars: 0.1 mm. Abbreviations: DTA – dorsal tibial apophysis, E – embolus, FA – femoral apophysis, RTA – retrolateral tibial apophysis, rTA – retrolateral tegular apophysis.

MOA 0.20 long, front width 0.12, back width 0.21. Sternum, posterior end proper blunt. **Abdomen** (Fig. 10A, B) length 1.42, width 0.89. Leg measurements: I broken; II 3.93 (1.05, 0.45, 1.06, 0.94, 0.43); III broken; IV 4.92 (1.31, 0.44, 1.17, 1.35, 0.65). **Leg** spination: femur I with two dorsal spines, femora II–IV with one dorsal spine each; femur II pv11.

Colouration (Fig. 10A, B). Legs without distinct annulations on femora, patellae, tibiae and metatarsi. Abdomen, antero-medially with longitudinal grey-brown stripe connecting with paired yellowish spots in dorsal view.

Epigyne (Fig. 10C, D). Epigynal plate snake-like, with a narrowed median septum, copulatory ducts, connecting tubes and spermathecae distinctly visible through integument in intact epigyne. Anteromedially with small round copulatory openings. Copulatory ducts short, proper broad, almost parallel, medially located between copulatory openings and glandular appendage. Connecting tubes short, C-shaped, shorter than connecting tubes. Spermathecae, C-shaped. Fertilisation ducts extending anteriorly.

Distribution. Known only from the type locality in Jiangxi Province, China (Map 2).

***Otacilia longtanica* Liu, sp. nov.**

<http://zoobank.org/3E6CC983-C836-4156-8D66-571ABBC64FAD>

Figure 12

Type material. Holotype: ♀, CHINA: Jiangxi Province, Ji'an City, Jinggangshan County Level City, Ciping Town, Xiaojing Village, Longtan Scenic Spot, 26°35'56.4"N, 114°8'24.0"E, 838 m, 31 May 2014, leg. Ke-Ke Liu et al.

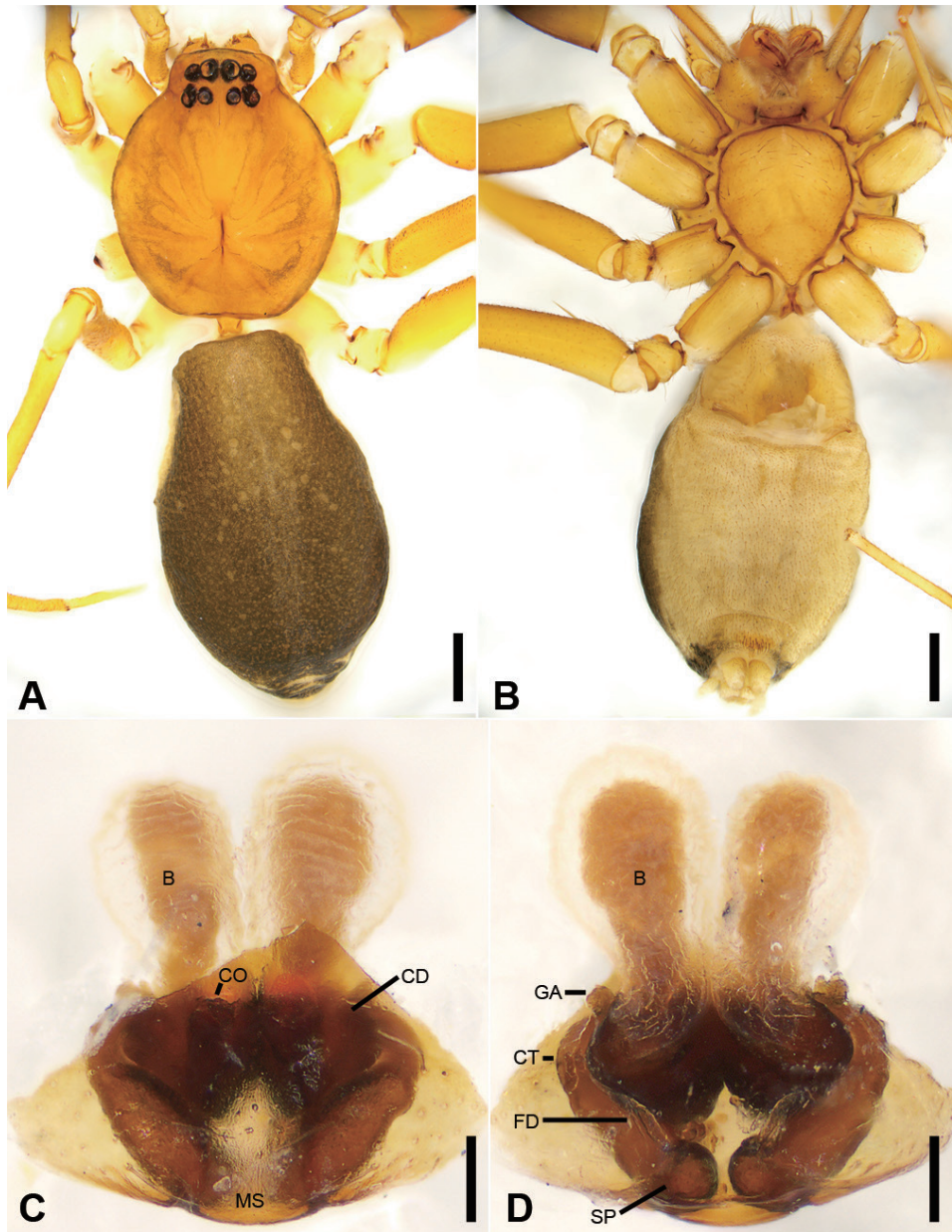


Figure 12. *Otacilia longtanica* sp. nov., female holotype **A** habitus, dorsal view **B** same, ventral view **C** epigyne, ventral view **D** same, dorsal view. Scale bars: 0.5 mm (**A, B**), 0.1 mm (**C, D**). Abbreviations: B – bursa, CD – copulatory duct, CO – copulatory opening, CT – connecting tube, FD – fertilisation ducts, GA – glandular appendage, MS – median septum, SP – spermathecae.

Etymology. The specific name refers to the type locality, Longtan; adjective.

Differential diagnosis. The female of this species is similar to that of *O. fujiana* Fu, Jin & Zhang, 2014 but differs by the chelicerae having two retromarginal teeth

(Fig. 12B) (vs. five retromarginal teeth) and the oval spermathecae (vs. with clavate shafts). Male unknown.

Description. Female. Habitus as in Fig. 12A, B. Total length 4.81, carapace 1.69 long, 1.01 wide. **Eye** sizes and interdistances: AME 0.11, ALE 0.11, PME 0.09, PLE 0.10; ALE–AME 0.04, AME–AME 0.08, PLE–PME 0.08, PME–PME 0.13, ALE–ALE 0.34, PLE–PLE 0.45, ALE–PLE 0.13, AME–PME 0.11, ALE–PME 0.18. MOA 0.32 long, front width 0.30, back width 0.32. **Chelicerae** (Fig. 12A) with three pro-marginal (middle largest, distal smallest) and two retromarginal teeth (distal larger). **Sternum** (Fig. 12B), with distinct precoxal triangles, posterior pointed. **Abdomen** (Fig. 12A) 2.70 long, 1.66 wide. **Leg** measurements: I 9.66 (2.41, 0.71, 3.17, 1.89, 1.48); II 7.91 (1.99, 0.62, 2.32, 1.68, 1.30); III 6.20 (1.50, 0.58, 1.56, 1.57, 0.99); IV 9.81 (2.45, 0.69, 2.51, 2.71, 1.45). Leg spination: femora I–IV with one dorsal spine each; femora I pv111111, II pv111; tibiae I v2222222222, II v22222222; metatarsi I v2222, II v1222.

Colouration (Fig. 12A, B). Carapace yellow to yellow-brown, with radial, irregular dark stripes mediolaterally and arch-shaped dark stripes around margin. Chelicerae yellow. Endites yellow. Labium yellow-brown. Sternum yellow, with yellow-brown margin. Legs yellow, without annulations on tibiae and distal part of femora, patellae and metatarsi (Fig. 12A, B). Abdomen dark brown, with abundant yellowish spots in dorsal view.

Epigyne (Fig. 12C, D). Epigynal plate trapezoid, antero-medially with pair of slit-like copulatory openings, with a narrowed median septum, copulatory ducts, glandular appendage, connecting tubes and spermathecae distinctly visible through integument in intact epigyne. Copulatory ducts very short, relative broad, between copulatory openings and glandular appendage, with pair of elongated transparent bursae anteriorly. Glandular appendages short, proper thick, located on the anterior of connecting tubes. Connecting tubes short, as long as copulatory duct, broad, located between glandular appendages and spermathecae. Spermathecae elongated, oval, slightly separated at their apex. Fertilisation duct short, located apically on spermathecae.

Distribution. Known only from the type locality in Jiangxi Province, China (Map 2).

***Otacilia ovoidea* Liu, sp. nov.**

<http://zoobank.org/1F47C8A6-95FB-4B9A-9994-4E78949142A6>

Figures 13, 14

Type material. Holotype: ♂, CHINA: Jiangxi Province, Ji'an City, Jinggangshan County Level City, Ciping Town, Dajing Village, Jingzhushan Scenic Spot, 26°32'39.69"N, 114°06'34.96"E, 1130 m, 1 October 2018, leg. Ke-Ke Liu et al. **Paratypes:** 7♂, 1♀, with same data as holotype; 1♂, 26°31'33.37"N, 114°06'30.34"E, 786 m, other data as holotype; 2♂, 26°32'39.69"N, 114°06'34.96"E, 1130 m, other data as holotype; 9♂, Ciping Town, Wuzhifeng Scenic Spot, 26°31'59.07"N, 114°08'28.47"E, 735 m, 2 October 2018, leg. Ke-Ke Liu et al.; 9♂, Ciping Town, Liping Village, around the Shiyan

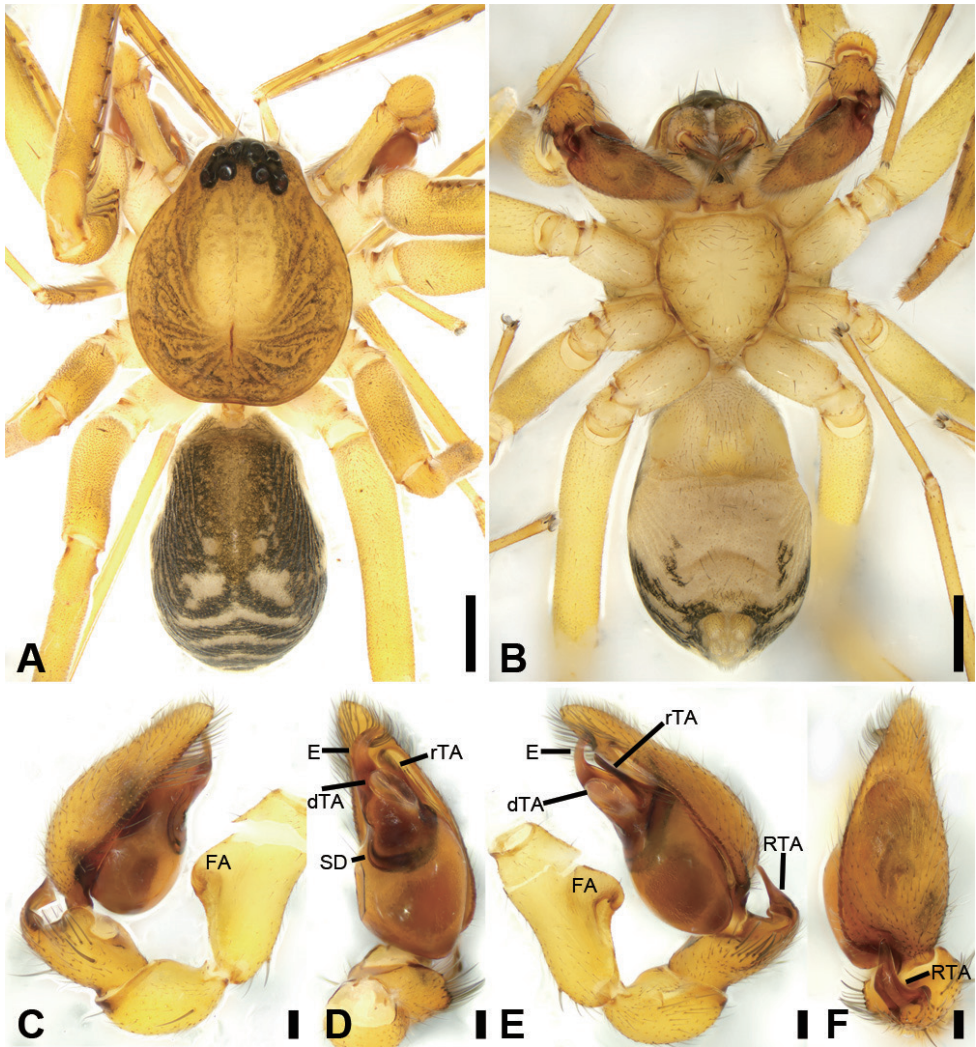


Figure 13. *Otacilia ovoidea* sp. nov., male holotype **A** habitus, dorsal view **B** same, ventral view **C** palp, prolateral view **D** same, ventral view **E** same, retrolateral view **F** same, dorsal view. Scale bars: 0.5 mm (**A, B**), 0.1 mm (**C–F**). Abbreviations: dTA – distal tegular apophysis, E – embolus, FA – femoral apophysis, rTA – retrolateral tegular apophysis, RTA – retrolateral tibial apophysis, SD – sperm duct.

Cave, 26°36'10.43"N, 114°12'46.35"E, 955 m, 6 October 2018, leg. Ke-Ke Liu and Hui-Pu Luo; 1♂, Luofu Town, Xiangzhou Village, Fengshuping Group, 26°36'10.31"N, 114°06'34.69"E, 364 m, 5 October 2018, leg. Ke-Ke Liu and Hui-Pu Luo.

Etymology. The specific name is derived from the Latin word *ovoideus*, referring to the ovoid terminal apophysis of the male palp; adjective.

Diagnosis. This species can be easily recognised by the palp (Fig. 13C–F) with the clavate retrolateral tegular apophysis (vs. absent, triangular, finger-shaped, or otherwise)

and the ovoid membranous fan-shaped distal tegular apophysis (Fig. 13D, E) (vs. absent, ovoid, triangular, finger-shaped, or otherwise). Females are distinguished by the epigyne (Fig. 14C, D) with a weakly sclerotised transversal margin (vs. absent, M-shaped, arc-shaped, or otherwise), the funnel-shaped median septum (vs. rectangular, triangular, others), and the touching globular spermathecae (vs. widely or slightly separated).

Description. Male (holotype). Habitus as in Fig. 13A, B. Total length 3.55, carapace 1.65 long, 1.42 wide. **Eye** sizes and interdistances: AME 0.10, ALE 0.10, PME 0.09, PLE 0.10; ALE–AME 0.01, AME–AME 0.05, PLE–PME 0.07, PME–PME 0.11, ALE–ALE 0.25, PLE–PLE 0.41, ALE–PLE 0.10, AME–PME 0.08, ALE–PME 0.17. MOA 0.25 long, front width 0.23, back width 0.29. **Chelicerae** (Fig. 13A, B) with three promarginal (middle largest, distal smallest) and six retromarginal teeth (distal largest, proximal smallest). Sternum (Fig. 13B) gradually pointed. **Abdomen** (Fig. 13A, B) 1.69 long, 1.01 wide. **Leg** measurements: I 7.10 (1.82, 0.65, 2.10, 1.71, 0.82); II 5.85 (1.53, 0.61, 1.61, 1.34, 0.76); III 4.82 (1.27, 0.49, 1.07, 1.28, 0.71); IV 7.47 (1.99, 0.66, 1.82, 2.16, 0.84). Leg spination: femur I with two dorsal spines, femora II–IV with one dorsal spine each; femora I pv1111 (right), pv11111, II pv111; tibiae I v22222222, II v2222222; metatarsi I v2222, II v2222.

Colouration (Fig. 13A, B). Prosoma yellow-brown, with radial, irregular dark brown mottled markings in the surface. Fovea distinct, black. Chelicerae yellow-brown. Endites, labium and sternum yellow. Legs yellow (Fig. 13A, B). Abdomen dark brown, with pair of round and Y-shaped spots located in the posterior dorsal scutum and three light chevron-shaped stripes on posterior part, with yellowish transversal stripe in front of the anal tubercle.

Palp (Fig. 13C–F). Femoral apophysis well-developed, width longer than half of length. Patella unmodified. Retrolateral tibial apophysis large, bending inward to the base of cymbium, triangular extruding in proximal part in retrolateral view, with a clear apophyses located at the base and a blunt apex in dorsal view. Sperm duct C-shaped, strongly sclerotised, around the base of retrolateral tegular apophysis, distal tegular apophysis and embolus; distal tegular apophysis club-shaped, longer than embolus. Conductor, ovoid, slightly shorter than embolus. Embolus, with proper broad base and a short, curved tip.

Female. Habitus as in Fig. 14A, B. Total length 3.73, carapace 1.77 long, 1.57 wide. **Eye** sizes and interdistances: AME 0.08, ALE 0.08, PME 0.08, PLE 0.10; ALE–AME 0.03, AME–AME 0.07, PLE–PME 0.08, PME–PME 0.15, ALE–ALE 0.28, PLE–PLE 0.46, ALE–PLE 0.12, AME–PME 0.10, ALE–PME 0.11. MOA 0.26 long, front width 0.23, back width 0.31. **Abdomen** (Fig. 14A, B) 1.90 long, 1.20 wide. **Leg** measurements: I 7.36 (1.80, 0.65, 2.30, 1.75, 0.86); II 5.85 (1.45, 0.62, 1.67, 1.29, 0.82); III 5.12 (1.38, 0.56, 1.12, 1.31, 0.75); IV 7.73 (2.12, 0.66, 1.79, 2.06, 1.10). Leg spination: femur I with two dorsal spines, femora II–IV with one dorsal spine each; femur I pv1111; tibiae I v22222222, II v2222222; metatarsus II v1222.

Epigyne (Fig. 14C, D). Epigynal plate bow-shaped, antero-medially with pair of concaved copulatory openings, with a funnel-shaped median septum, copulatory ducts, glandular appendage, connecting tubes and spermathecae distinctly visible

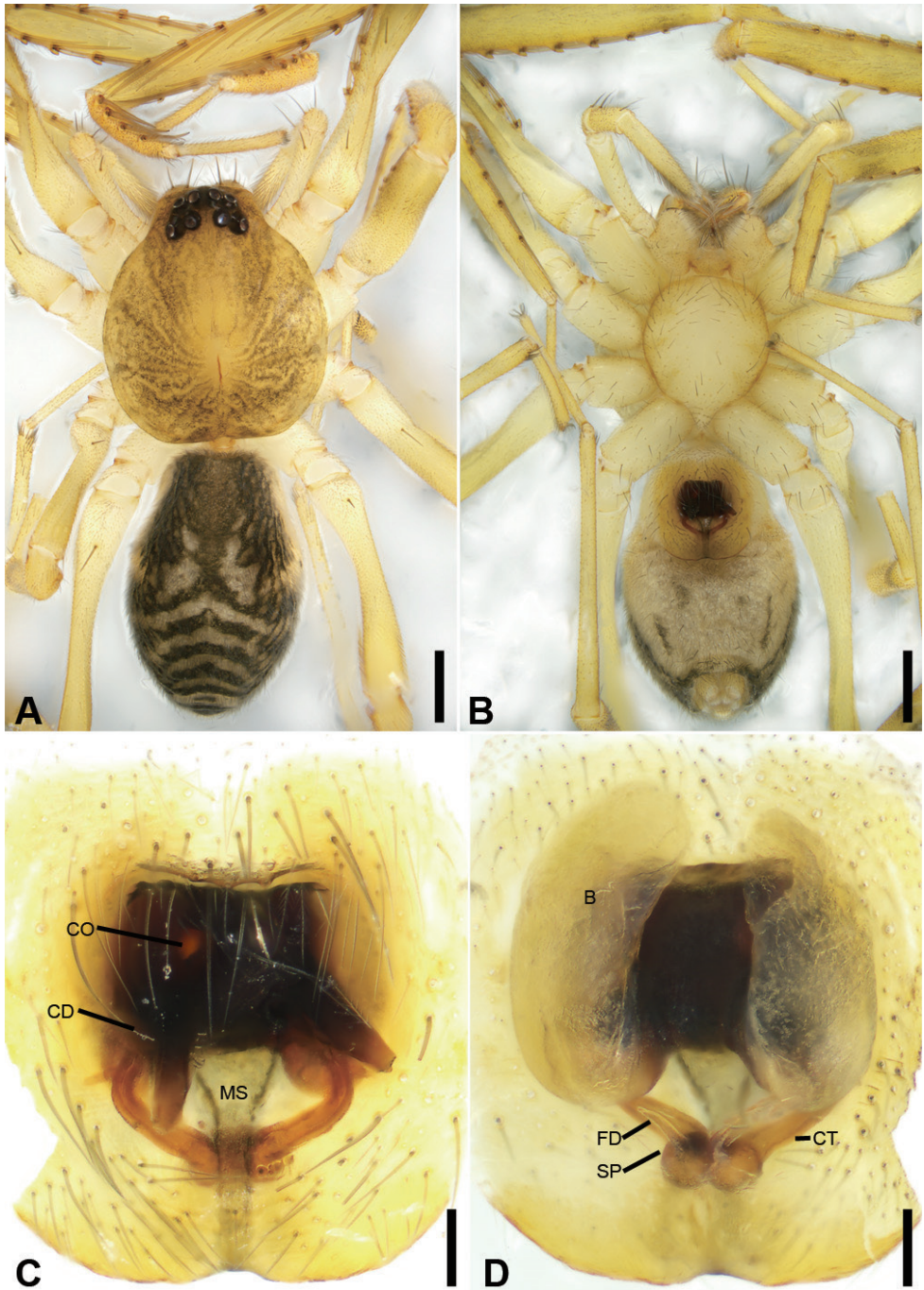


Figure 14. *Otacilia ovoidea* sp. nov., female paratype **A** habitus, dorsal view **B** same, ventral view **C** epigyne, ventral view **D** epigyne, dorsal view. Scale bars: 0.5 mm (**A**, **B**), 0.1 mm (**C**, **D**). Abbreviations: B – bursa, CD – copulatory duct, CO – copulatory opening, CT – connecting tube, FD – fertilisation ducts, GA – glandular appendage, MS – median septum, SP – spermathecae.

through integument in intact epigyne. Anterior fovea separated by weakly sclerotised transversal margin. Copulatory ducts broad, located between copulatory openings and glandular appendages, posteriorly with pair of large, oval, transparent bursae. Glandular appendages short, partly covered by bursae, located on the anterior of connecting tubes. Connecting tubes slightly shorter than copulatory ducts, located between glandular appendages and spermathecae. Spermathecae globular, directed medially. Fertilisation duct short, located apically on spermathecae.

Distribution. Known only from the type locality in Jiangxi Province, China (Map 2).

***Otacilia shenshanica* Liu, sp. nov.**

<http://zoobank.org/354A0C02-F10E-4B37-94AB-2FFDCA6F3EB2>

Figures 15–17

Type material. *Holotype*: ♂, CHINA: Jiangxi Province, Ji'an City, Jinggangshan County Level City, Dalong Town, Yuantou Village, 26°37'55.2"N, 114°06'21.6"E, 1029 m, 5 April 2014, leg. Ke-Ke Liu et al. *Paratypes*: ♀, with same data as holotype; 1♂, 2♀, 26°37'33.6"N, 114°06'21.6"E, 791 m, other data as holotype; 1♀, Longshi Town, Maoping, Shenshan Village, Shenshan, 26°38'13.2"N, 114°06'39.6"E, 1099 m, 6 April 2014, leg. Ke-Ke Liu et al.

Etymology. The specific name refers to the type locality, Shenshan; adjective.

Differential diagnosis. The new species differs from *O. hengshan* (Song, 1990) by the bend of the RTA with a strong basal apophysis (Figs 15C, E, F, 17C) (vs. the submedian part of the RTA with a strong apophysis) and the wider median septum located medially (Fig. 16C, D) (vs. narrowed).

Description. **Male** (holotype). Habitus as in Fig. 15A. Total length 3.87, carapace 1.72 long, 1.45 wide. *Eye* sizes and interdistances: AME 0.08, ALE 0.10, PME 0.08, PLE 0.09; ALE–AME 0.03, AME–AME 0.06, PLE–PME 0.07, PME–PME 0.14, ALE–ALE 0.27, PLE–PLE 0.41, ALE–PLE 0.11, AME–PME 0.10, ALE–PME 0.19. MOA 0.26 long, front width 0.21, back width 0.29. Cervical groove and fovea distinct. *Chelicerae* (Fig. 15A, B) with three promarginal (middle largest, distal smallest) and six retromarginal teeth (distal largest, proximal smallest). *Sternum* (Fig. 15B), posterior pointed. *Abdomen* (Fig. 15A, B) 1.98 long, 1.38 wide, weak dorsal scutum in anterior half. *Leg* measurements: I 7.21 (1.87, 0.70, 2.24, 1.77, 0.63); II 5.52 (1.52, 0.58, 1.45, 1.38, 0.59); III 4.86 (1.31, 0.54, 1.08, 1.33, 0.60); IV 7.77 (2.09, 0.63, 1.88, 2.15, 1.02). Leg spination: femur I with two dorsal spines, femora II–IV with one dorsal spine each; femora I pv1111 (right), pv11111, II pv111; tibiae I v22222222, II v222222; metatarsi I v2222, II v1222.

Colouration (Fig. 15A, B). Carapace yellow, with radial, irregular dark stripes medially and arch-shaped dark stripes around margin. Chelicerae yellow-brown. Endites yellow. Labium yellow-brown. Sternum yellow. Legs yellow, without annulations on tibiae and distal part of femora, patellae, and metatarsi. Abdomen dark brown, with pair of oval and pair of clavate yellowish spots on the posterior dorsal scutum, three

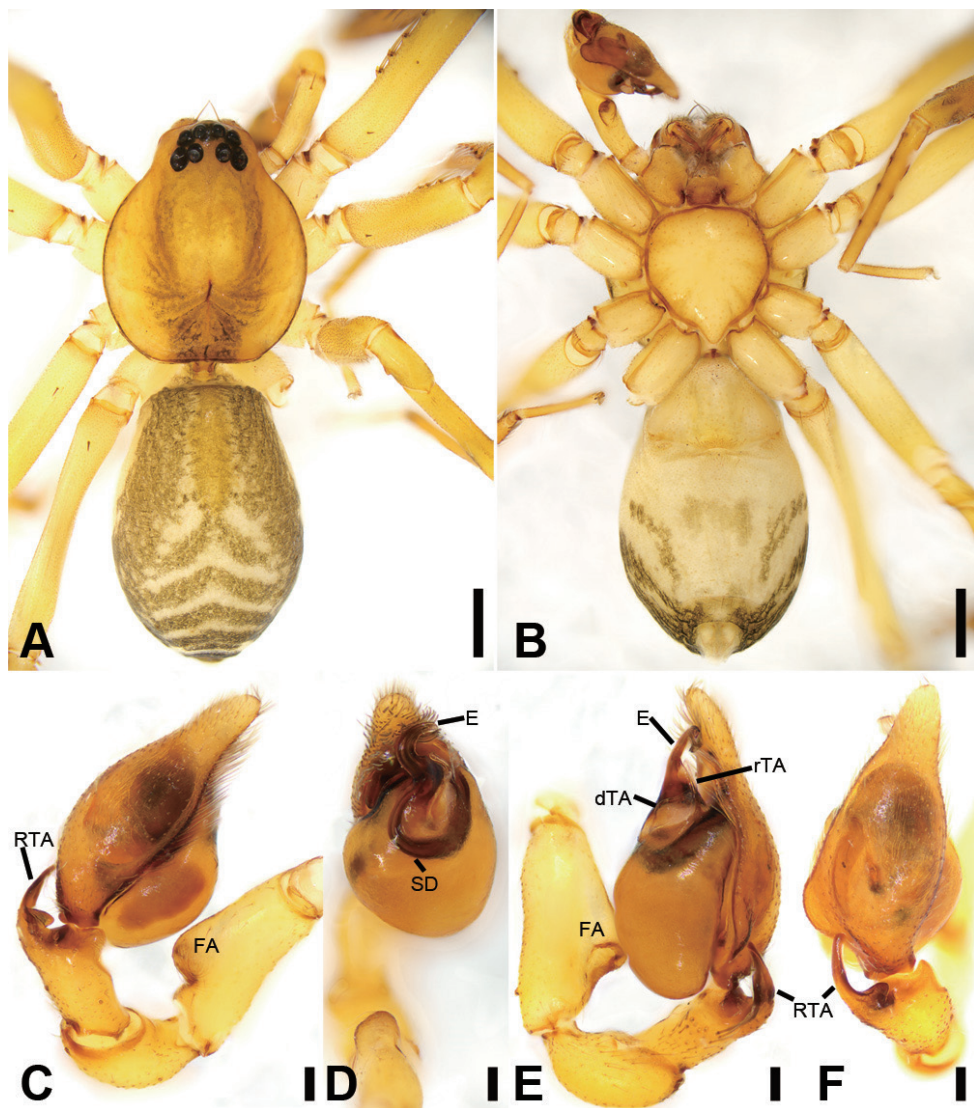


Figure 15. *Otacilia shenshanica* sp. nov., male holotype **A** habitus, dorsal view **B** same, ventral view **C** palp, proteral view **D** same, ventral-distal view **E** same, retrolateral view **F** same, dorsal view. Scale bars: 0.5 mm (**A, B**), 0.1 mm (**C–F**). Abbreviations: dTA – distal tegular apophysis, E – embolus, FA – femoral apophysis, RTA – retrolateral tibial apophysis, rTA – retrolateral tegular apophysis, SD – sperm duct.

light chevron-shaped stripes in posterior part, and yellowish arch-shaped stripe in front of the anal tubercle.

Palp (Figs 15C–F, 17). Femoral apophysis well developed, width less than half of length. Patella unmodified. Retrolateral tibial apophysis large, slightly less than tibia, finger-like, bending inwards towards base of cymbium, with strong basal apophysis and blunt tip. Sperm duct O-shaped, strongly sclerotised, around base of retrolateral

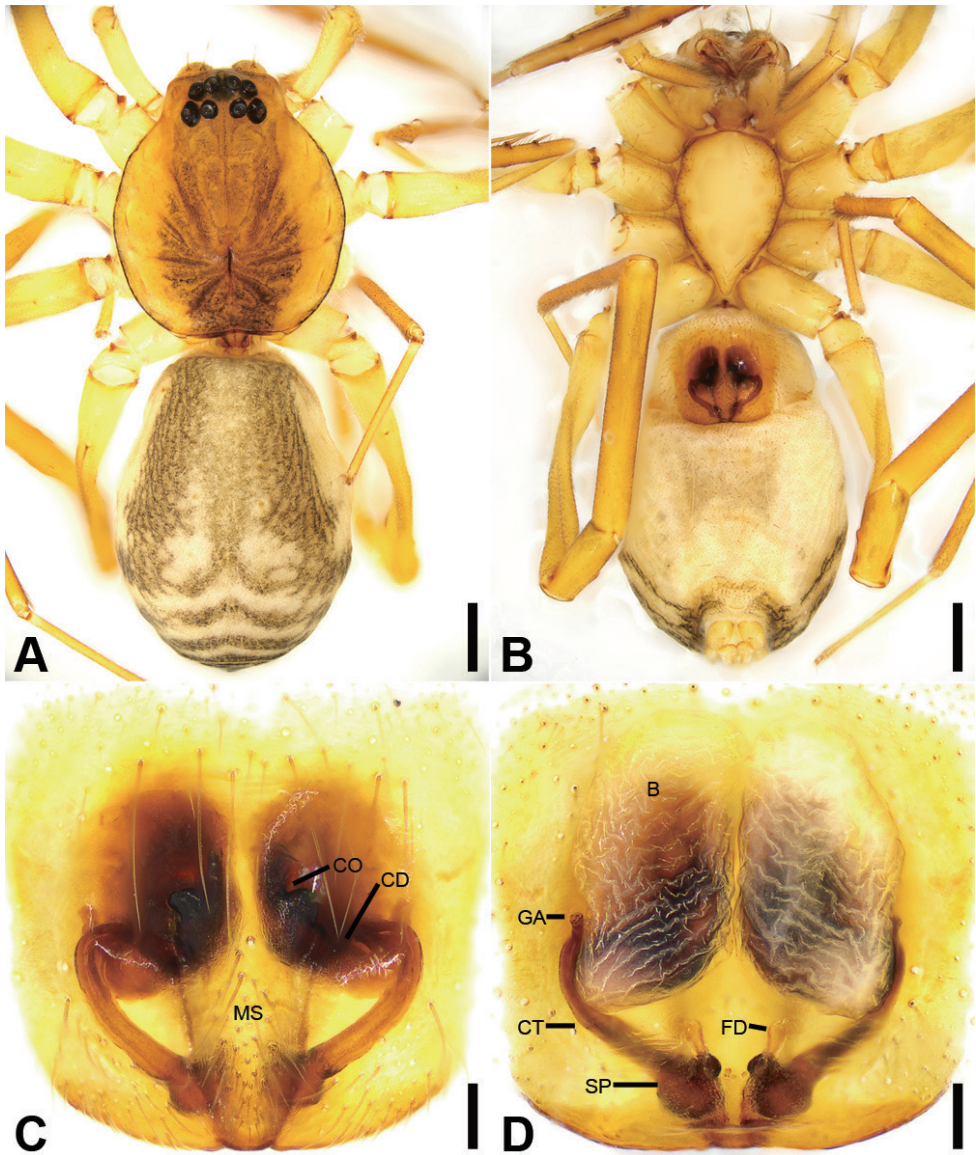


Figure 16. *Otacilia shenshanica* sp. nov., female paratype **A** habitus, dorsal view **B** same, ventral view **C** epigyne, ventral view **D** epigyne, dorsal view. Scale bars: 0.5 mm (**A**, **B**), 0.1 mm (**C**, **D**). Abbreviations: B – bursa, CD – copulatory duct, CO – copulatory opening, CT – connecting tube, FD – fertilisation ducts, GA – glandular appendage, MS – median septum, SP – spermathecae.

regular apophysis, distal tegular apophysis and embolus. Retrolateral tegular apophysis clavate, slightly shorter than embolus. Distal tegular apophysis triangular, accompanied by embolus and subterminal apophysis. Embolus, thick, hook-shaped, with broad base and blunt tip.

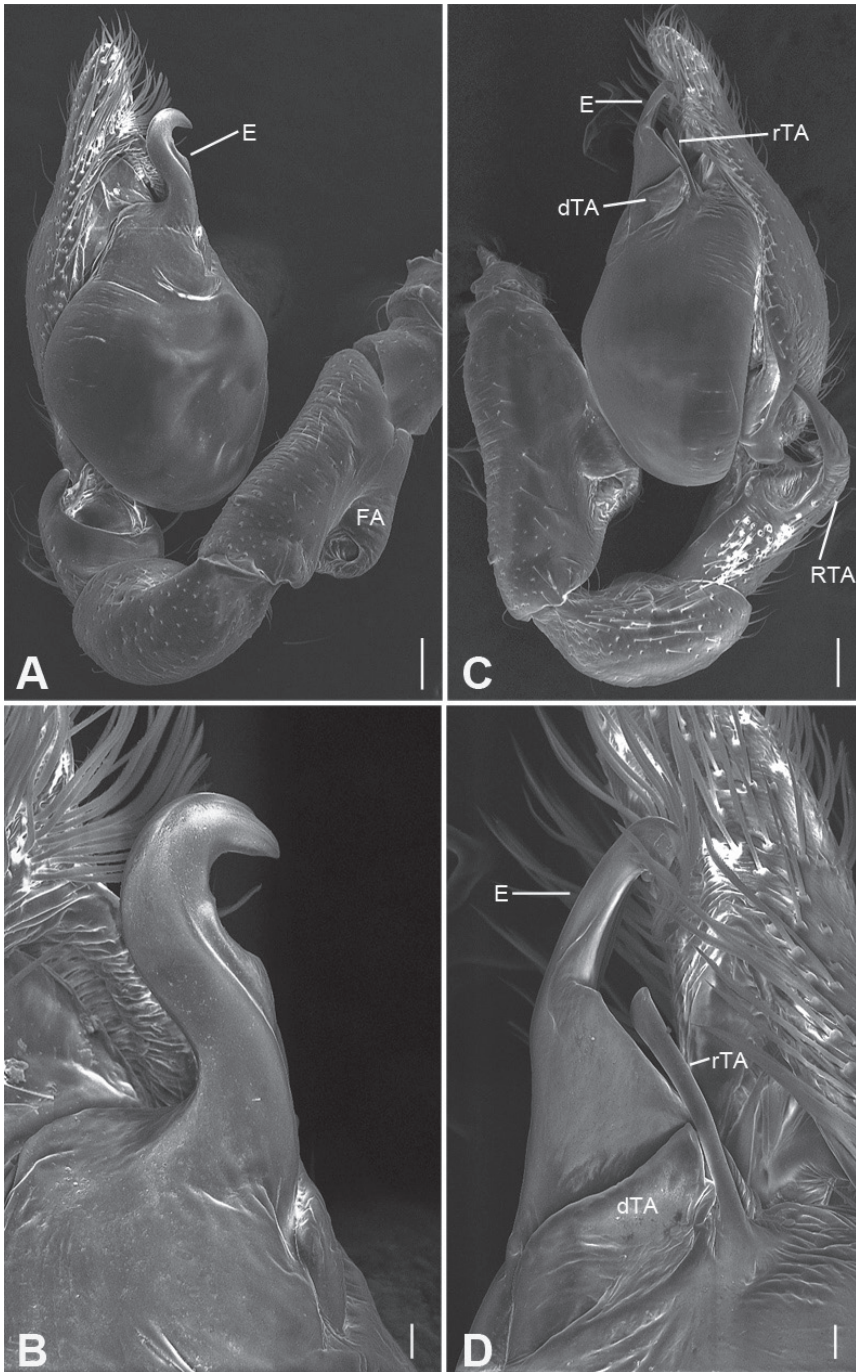


Figure 17. SEM micrographs of *Otacilia shenshanica* sp. nov., palp of male paratype **A** proventral view **B** same, detail showing embolus **C** retrolateral view **D** same, detail of conductor, embolus and tegular apophysis. Scale bars: 0.1 mm (**A, C**), 20 μ m (**B, D**). Abbreviations: dTA – distal tegular apophysis, E – embolus, FA – femoral apophysis, RTA – retrolateral tibial apophysis, rTA – retrolateral tegular apophysis.

Female. Habitus as in Fig. 16A, B. Darker than males. Total length 4.35, carapace 1.91 long, 1.67 wide. **Eye** sizes and interdistances: AME 0.10, ALE 0.11, PME 0.09, PLE 0.10; ALE–AME 0.02 AME–AME 0.07, PLE–PME 0.08, PME–PME 0.14, ALE–ALE 0.30, PLE–PLE 0.47, ALE–PLE 0.11, AME–PME 0.11, ALE–PME 0.11. MOA 0.28 long, front width 0.25, back width 0.33. **Abdomen** (Fig. 16A) 2.27 long, 1.73 wide. **Legs** (Fig. 13A) measurements: I 7.84 (2.03, 0.75, 2.39, 1.83, 0.84); II 6.61 (1.74, 0.66, 1.87, 1.51, 0.83); III 5.52 (1.43, 0.62, 1.34, 1.42, 0.71); IV 8.39 (2.23, 0.74, 2.01, 2.33, 1.08). Leg spination: femur I pv11111; tibia II v22222222.

Colouration (Fig. 16A, B). Abdomen with pair of irregular yellowish spots behind the first pair of oval spots.

Epigyne (Fig. 16C, D). Epigynal plate bow-shaped, antero-medially with pair of concaved copulatory openings, with triangular median septum, copulatory ducts, glandular appendage, connecting tubes and spermathecae distinctly visible through integument in intact epigyne. Copulatory ducts broad, slightly sloping, located between copulatory openings and glandular appendages, posteriorly with pair of large, bean-shaped, transparent bursae. Glandular appendages short, partly covered by bursae, located on anterior of connecting tubes. Connecting tubes, twice the length of copulatory ducts, located between glandular appendages and spermathecae. Spermathecae globular, slightly separated. Fertilisation duct short, located apically on spermathecae, extending anteriorly.

Distribution. Known only from the type locality in Jiangxi Province, China (Map 2).

Otacilia subovoidea Liu, sp. nov.

<http://zoobank.org/B862C4C7-C715-4DE1-B3A3-7A1C01B54518>

Figures 18–20

Type material. **Holotype:** ♂, CHINA: Jiangxi Province, Ji'an City, Jinggangshan County Level City, Ciping Town, Liping Village, Citic Sewage Treatment Plant, 26°35'28.93"N, 114°12'46.82"E, 810 m, 6 October 2018, leg. Ke-Ke Liu and Hui-Pu Luo. **Paratypes:** 6♂, 3♀, with same data as holotype; 4♂, 5♀, Liping Village, around the Shiyan Cave, 26°36'13.60"N, 114°12'35.91"E, 927 m, other data as holotype; 2♂, 2♀, Dajing Village, Lingxiufeng Scenic Spot, 26°34'16.72"N, 114°07'00.56"E, 971 m, 1 October 2018, leg. Ke-Ke Liu et al.; 5♂, Xiaojing Village, Longtan Scenic Spot, 26°35'33.08"N, 114°08'18.50"E, 909 m, 1 October 2018, leg. Ke-Ke Liu et al.; 2♂, 3♀, Wuzhifeng Scenic Spot, 26°31'59.07"N, 114°08'28.47"E, 735 m, 2 October 2018, leg. Ke-Ke Liu et al.; 3♀, Jingzhushan Scenic Spot, 26°32'39.69"N, 114°06'34.96"E, 1130 m, 1 October 2018, leg. Ke-Ke Liu et al.; 2♂, 3♀, Wuzhifeng Scenic Spot, 26°32'48.23"N, 114°09'10.61"E, 811 m, 2 October 2018, leg. Ke-Ke Liu et al.

Etymology. The specific name is derived from that of a similar species, *O. ovoidea* sp. nov.; adjective.

Diagnosis. The new species differs from *O. ovoidea* sp. nov. by the relatively longer spine-like tip of embolus (Figs 18D, 20) (vs. short, hook-shaped), the straight broad retrolateral regular apophysis (Figs 18D, 20) (vs. thin, clavate) and by the relatively broader



Figure 18. *Otacilia subovoidea* sp. nov., male holotype **A** habitus, dorsal view **B** same, ventral view **C** palp, prolateral view **D** same, ventral view **E** same, dorsal view. Scale bars: 0.5 mm (**A**, **B**), 0.1 mm (**C**–**E**). Abbreviations: dTA – distal tegular apophysis, E – embolus, FA – femoral apophysis, RTA – retrolateral tibial apophysis, rTA – retrolateral tegular apophysis, SD – sperm duct.

bar-shaped median septum (Fig. 19C) (vs. funnel-shaped, anteriorly broad, posteriorly thin), and the separated spermathecae (Fig. 19D) (vs. touching spermathecae).

Description. Male (holotype). Habitus as in Fig. 18A, B. Total length 3.44, carapace 1.69 long, width 1.44 wide. **Eye** sizes and interdistances: AME 0.10, ALE 0.10, PME 0.07, PLE 0.11; ALE–AME 0.02, AME–AME 0.06, PLE–PME 0.09, PME–PME 0.14, ALE–ALE 0.26, PLE–PLE 0.44, ALE–PLE 0.11, AME–PME 0.11,

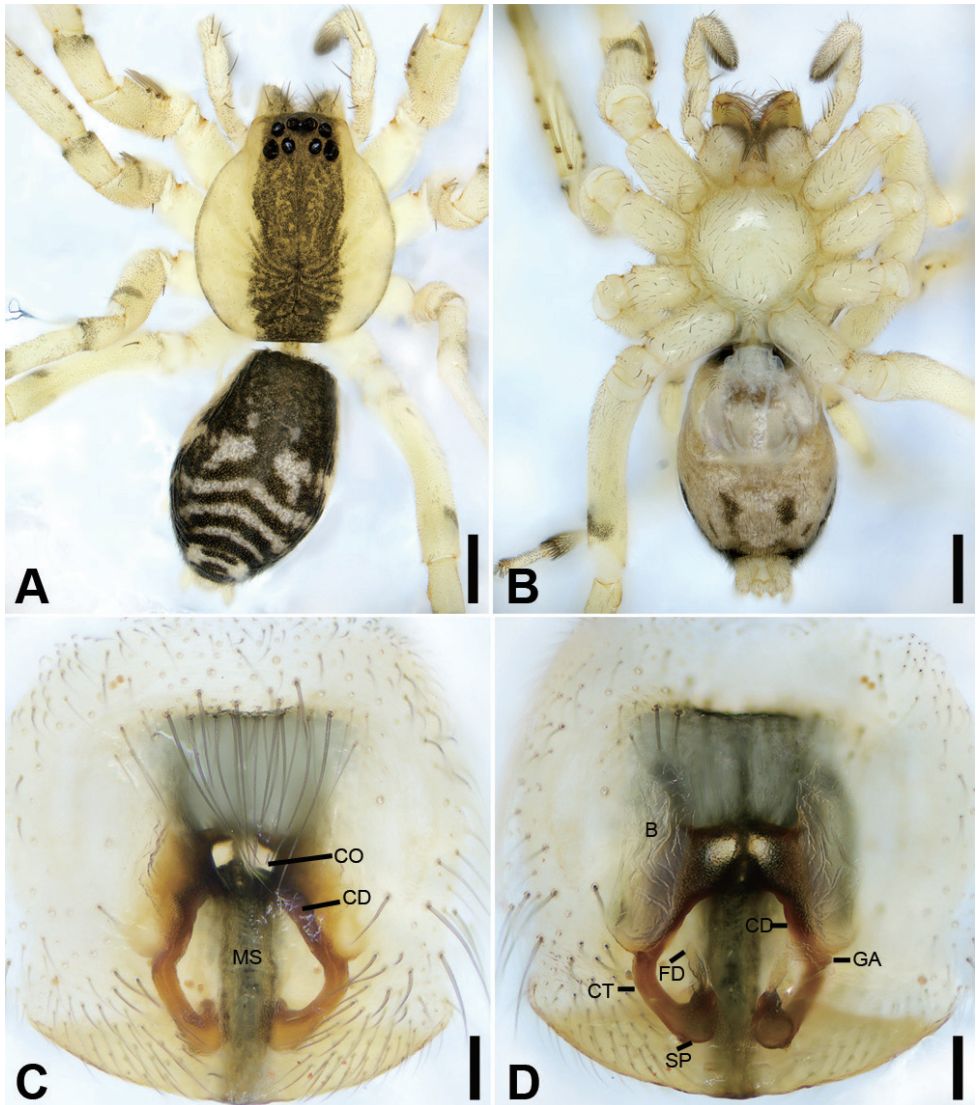


Figure 19. *Otacilia subovoidea* sp. nov., female paratype **A** habitus, dorsal view **B** same, ventral view **C** epigyne, ventral view **D** epigyne, dorsal view. Scale bars: 0.5 mm (**A**, **B**), 0.1 mm (**C**, **D**). Abbreviations: B – bursa, CD – copulatory duct, CO – copulatory opening, CT – connecting tube, FD – fertilisation ducts, GA – glandular appendage, MS – median septum, SP – spermathecae.

ALE-PME 0.19. MOA 0.25 long, front width 0.22, back width 0.29. **Chelicerae** (Fig. 18A, B) with three promarginal (proximal largest, distal smallest) and six retromarginal teeth (distal largest, proximal smallest). **Sternum** (Fig. 18B) longer than wide. **Abdomen** (Fig. 18A, B) 1.66 long, 1.01 wide. **Leg** measurements: I 7.00 (1.79, 0.63, 2.13, 1.69, 0.76); II 5.76 (1.50, 0.58, 1.60, 1.33, 0.75); III 4.30 (1.25, 0.53, 0.90, 1.03, 0.59); IV 7.48 (2.02, 0.60, 1.84, 2.10, 0.91). Leg spination: femur I with

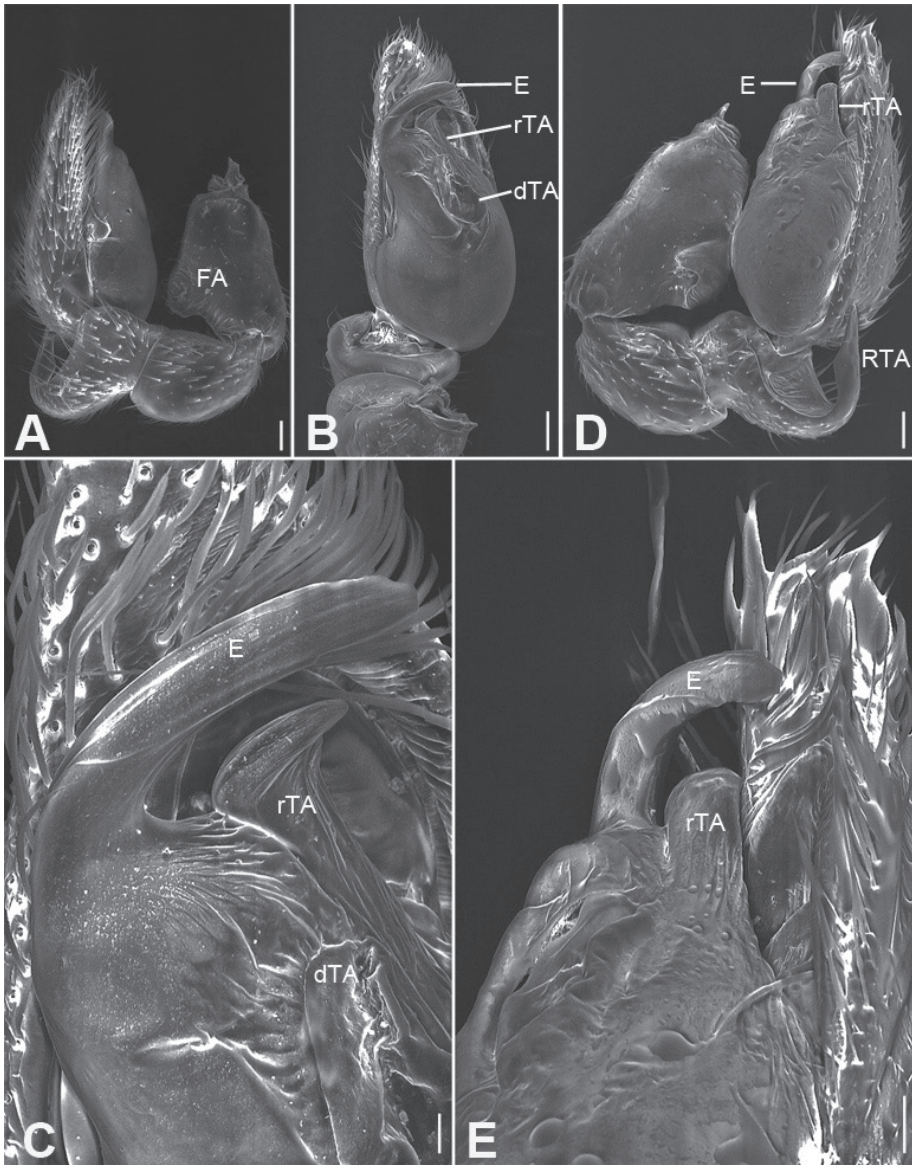


Figure 20. SEM micrographs of *Otacilia subovoidea* sp. nov., male paratype **A** palp, prolateral view **B** same, ventral view **C** same, ventral view, detail of conductor, embolus and tegular apophysis **D** same, retrolateral view **F** same, retrolateral view, detail of embolus and tegular apophysis. Scale bars: 0.1 mm (**A, B, D**), 20 μ m (**C**), 40 μ m (**E**). Abbreviations: dTA – distal tegular apophysis, E – embolus, FA – femoral apophysis, RTA – retrolateral tibial apophysis, rTA – retrolateral tegular apophysis.

two dorsal spines, femora II–IV with one dorsal spine each; femora I pv1111, II pv11; tibiae I v22222222, II v222222; metatarsi I v2222, II pv1222.

Colouration (Figs 18A, B). Carapace yellow, medially with broad dark brown mottled markings in the surface. Fovea distinct, black. Chelicerae, endites, labium and

sternum yellow brown. Legs yellow, without dark annulation. Abdomen dark brown, with pair of round and oval pale spots located in the posterior dorsal scutum and three light chevron-shaped stripes in posterior part, and one yellowish transversal stripe in front of the anal tubercle.

Palp (Figs 18C–E, 20). Femoral apophysis well-developed, width more than half of length. Patella unmodified. Retrolateral tibial apophysis large, longer than tibia, sword-like in ventral view, bending inward to the base of cymbium, medial part widened and slightly curved, with a strong spine-like tip. Sperm duct U-shaped, strongly sclerotised, around the base of subterminal apophysis, terminal apophysis and embolus. Subterminal apophysis, straight, broad, as long as embolus, anteriorly widened. Terminal apophysis, membranous, fan-shaped, extending to median bulb. Embolus, thick, hook-shaped, with a broad base and a blunt tip. Embolus relatively long, thick spine like, with broad base and a blunt apex.

Female. Habitus as in Fig. 19A, B. Lighter than males. Total length 3.57, carapace 1.66 long, 1.46 wide. **Eye** sizes and interdistances: AME 0.07, ALE 0.07, PME 0.07, PLE 0.09; ALE–AME 0.04, AME–AME 0.08, PLE–PME 0.09, PME–PME 0.14, ALE–ALE 0.28, PLE–PLE 0.43, ALE–PLE 0.12, AME–PME 0.13, AME–PLE 0.11. MOA 0.26 long, front width 0.21, back width 0.27. **Abdomen** (Fig. 19A, B) 1.80 long, 1.15 wide. **Leg** measurements: I 7.12 (1.81, 0.68, 2.21, 1.67, 0.75); II 5.76 (1.50, 0.58, 1.65, 1.29, 0.74); III 4.91 (1.31, 0.48, 1.14, 1.20, 0.78); IV 7.56 (2.10, 0.66, 1.85, 2.05, 0.90). Leg spination: tibia II v22222222.

Epigyne (Fig. 19C, D). Epigynal plate mask-like, anterior margin slightly sclerotised, transverse, medially with pair of touching hole-shaped copulatory openings, posteriorly with bar-shaped median septum, copulatory ducts, connecting tubes and spermathecae distinctly visible through integument in intact epigyne. Copulatory ducts between copulatory openings and glandular appendages, sloping laterally, proper broad, posteriorly with pair of large, oval, transparent bursae. Glandular appendages short, partly covered by bursae, located on anterior of connecting tubes. Connecting tubes slightly shorter than copulatory ducts, slightly curved backwards. Spermathecae sub-spherical, directed medially, separated by mark of median septum. Fertilisation duct short, with semi-ovoid base, directed forward.

Distribution. Known only from the type locality in Jiangxi Province, China (Map 2).

***Otacilia xiaoxiica* Liu, sp. nov.**

<http://zoobank.org/CFC851C2-2547-427C-9646-4ACD8B904229>

Figure 21

Type material. *Holotype*: ♂, CHINA: Jiangxi Province, Ji'an City, Jinggangshan County Level City, Huangao Town, Xiaoxi Forest Farm, 26°28'8.4"N, 114°12'36.0"E, 365 m, 30 May 2017, leg. Ke-Ke Liu et al.

Etymology. The specific name refers to the type locality, Xiaoxi Forest Farm; adjective.

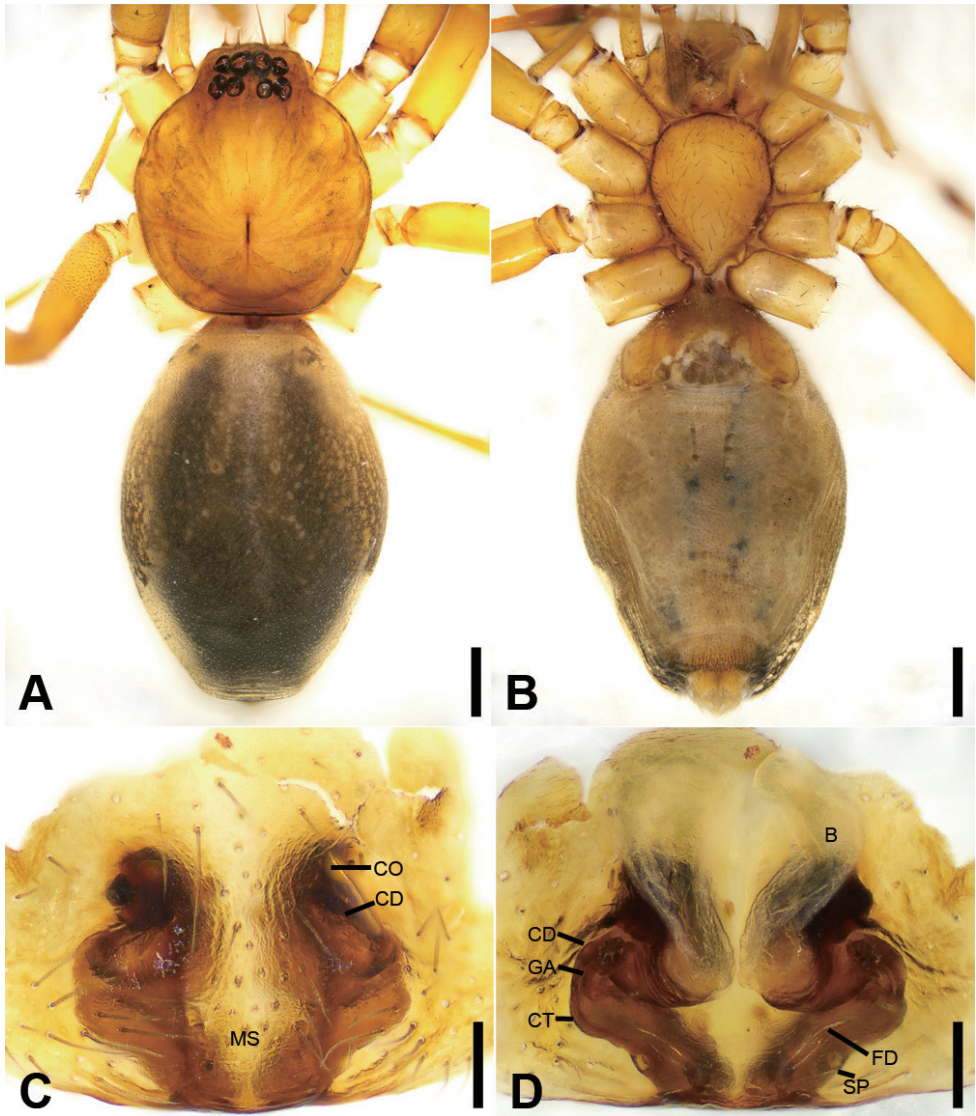


Figure 21. *Otacilia xiaoxiica* sp. nov., female holotype **A** habitus, dorsal view **B** same, ventral view **C** epigyne, ventral view **D** epigyne, dorsal view. Scale bars: 0.5 mm (**A**, **B**), 0.1 mm (**C**, **D**). Abbreviations: B – bursa, CD – copulatory duct, CO – copulatory opening, CT – connecting tube, FD – fertilisation ducts, GA – glandular appendage, MS – median septum, SP – spermathecae.

Differential diagnosis. The female of this species differs from these of *O. fujiana* and *O. taiwanica* (Hayashi & Yoshida, 1993) by the chelicerae with three retromarginal teeth (Fig. 21B) (vs. five in *O. fujiana* and two, three or four in *O. taiwanica*) and the broad spermathecae medially with indistinct curved (Fig. 21D) (vs. the thin

connecting tubes in *O. fujianana* and *O. taiwanica*, medially with distinct curve in *O. taiwanica*). Male unknown.

Description. Female. Habitus as in Fig. 21A, B. Total length 4.79, carapace 1.97 long, 1.68 wide. **Eye** sizes and interdistances: AME 0.12, ALE 0.12, PME 0.10, PLE 0.12; ALE–AME 0.03, AME–AME 0.06, PLE–PME 0.07, PME–PME 0.12, ALE–ALE 0.36, PLE–PLE 0.45, ALE–PLE 0.12, AME–PME 0.10, ALE–PME 0.15. MOA 0.31 long, front width 0.30, back width 0.32. **Chelicerae** (Fig. 21A, B) with three promarginal (middle largest, distal smallest) and three retromarginal teeth (distal largest, proximal smallest). **Sternum** (Fig. 21B), posteriorly proper blunt. **Abdomen** (Fig. 21A, B) 2.69 long, 1.91 wide. Sternum longer than wide. Leg measurements: I 10.15 (2.41, 0.71, 3.12, 2.22, 1.63); II 7.95 (2.05, 0.63, 2.43, 1.63, 1.21); III 6.70 (1.76, 0.61, 1.58, 1.73, 1.02); IV broken. **Leg** spination: femora I–IV with one dorsal spine each; femora I pv111111, II pv11111; patella I rv1; tibiae I v222222222, II v222222222; metatarsi I v2222, II pv1222.

Colouration (Fig. 21A, B). Carapace yellow, with radial, irregular dark stripes mediolaterally. Sternum yellow, with yellow-brown margin. Legs yellow, without annulations on tibiae and distal part of femora, patellae and metatarsi. Abdomen brown, with abundant yellowish spots in dorsal view.

Epigyne (Fig. 21C, D). Epigynal plate sub-square, anterolaterally with pair of crescent-shaped copulatory openings, medially with broad bar-shaped median septum, copulatory ducts and connecting tubes distinctly visible through integument in intact epigyne. Copulatory ducts broad, curved, posteriorly with pair of large, oval, transparent bursae. Glandular appendages relatively long, located on the anterior of connecting tubes. Connecting tube very short, posteriorly almost fused with spermathecae. Spermathecae broad, slightly separated at their apex. Fertilisation duct short, directed antero-laterally.

Distribution. Known only from the type locality in Jiangxi Province, China (Map 2).

Acknowledgements

This paper is greatly benefited from Charles R. Haddad (subject editor) (Bloemfontein, Republic of South Africa), Yuri Marusik (Magadan, Russia) and Alireza Zamani (Turku, Finland) for their helpful comments. We thank Zhan-Feng Wang, Zhi-Wu Chen, Ze-Yuan Meng, Xiao-Ping Huang, Yu-Bao Tang, Wen Sun, Wen-Jun Xie, Sha Wu, Ce Xu, Shi-Cong He, Yi-Fan Zhao (all from Jingtangshan University) and Wen Sun (Jingtangshan economic and trade school) for their assistance during the fieldwork. We also thank Nathalie Yonow and Ujjwal Malik for improving the English of the manuscript. This study was supported by the Natural Science Foundation of Jiangxi Province (20181BAB214008), the Science and Technology Innovation Project for College Students, the Science and Technology Foundation of Jiangxi Provincial Department of Education (GJJ160753), and the Natural Science Foundation of China (31560592/31772423).

References

- Deeleman-Reinhold CL (2001) Forest Spiders of South East Asia: with a Revision of the Sac and Ground Spiders (Araneae: Clubionidae, Corinnidae, Liocranidae, Gnaphosidae, Prodidomidae and Trochanterriidae [sic]). Brill, Leiden, 591 pp.
- Fu LN, Jin C, Zhang F (2014) Three new species of the genus *Otacilia* Thorell (Araneae: Phrurolithidae) from China. *Zootaxa* 3869(4): 483–492. <https://doi.org/10.11646/zootaxa.3869.4.10>
- Fu LN, Chen HM, Zhang F (2016a) New *Phrurolithus* species from China (Araneae, Phrurolithidae). *Ecologica Montenegrina* 7: 270–290.
- Fu LN, He JC, Zhang F (2015) Species of the genus *Otacilia* from Hainan Island, China (Araneae: Phrurolithidae). *Zoological Systematics* 40(4): 436–450.
- Fu LN, Zhang ZS, Zhang F (2016b) New *Otacilia* species from Southwest China (Araneae: Phrurolithidae). *Zootaxa* 4107(2): 197–221. <https://doi.org/10.11646/zootaxa.4107.2.4>
- Hu DS, Zhang F (2011) Description of a new *Otacilia* species from China, with transfer of two species from the genus *Phrurolithus* (Araneae: Corinnidae). *Zootaxa* 2993: 59–68. <https://doi.org/10.11646/zootaxa.2993.1.4>
- Jäger P, Wunderlich J (2012) Seven new species of the spider genus *Otacilia* Thorell 1897 (Araneae: Corinnidae) from China, Laos and Thailand. *Beiträge zur Araneologie* 7: 251–271, 352–357.
- Jin C, Fu L, Yin XC, Zhang F (2016) Four new species of the genus *Otacilia* Thorell, 1897 from Hunan Province, China (Araneae, Phrurolithidae). *ZooKeys* 620: 30–55. <https://doi.org/10.3897/zookeys.620.7982>
- Liu K, Xu X, Xiao YH, Yin HQ, Peng XJ (2019b) Six new species of *Otacilia* from southern China (Araneae: Phrurolithidae). *Zootaxa* 4585(3): 438–458. <https://doi.org/10.11646/zootaxa.4585.3.2>
- Ramírez MJ (2014) The morphology and phylogeny of dionychan spiders (Araneae: Araneomorphae). *Bulletin of the American Museum of Natural History* 390: 1–374. <https://doi.org/10.1206/821.1>
- Wang LY, Zhang F, Zhang ZS (2012) Ant-like sac spiders from Jinyun Mountain Natural Reserve of Chongqing, China (Araneae: Corinnidae). *Zootaxa* 3431(1): 37–53. <https://doi.org/10.11646/zootaxa.3431.1.3>
- World Spider Catalog (2020) World Spider Catalog. Natural History Museum Bern. Version 21.0. <https://wsc.nmbe.ch/> [accessed 19 February 2020]
- Zamani A, Marusik YM (2020) A survey of Phrurolithidae (Arachnida: Araneae) in southern Caucasus, Iran and Central Asia. *Zootaxa* 4758(2): 311–329. <https://doi.org/10.11646/zootaxa.4758.2.6>

Description of the supergiant isopod *Bathynomus raksasa* sp. nov. (Crustacea, Isopoda, Cirolanidae) from southern Java, the first record of the genus from Indonesia

Conni M. Sidabalok¹, Helen P.-S. Wong², Peter K. L. Ng³

1 Division of Zoology, Research Center for Biology, Indonesian Institute of Sciences (LIPI), Gedung Widiasat-waloka, Cibinong Science Center, Jl Raya Jakarta-Bogor Km 46, Cibinong 16911, Indonesia **2** St. John's Island National Marine Laboratory, Tropical Marine Science Institute, National University of Singapore (NUS), 18 Kent Ridge Road, 119227, Singapore **3** Lee Kong Chian Natural History Museum (LKCNHM), 2 Conservatory Drive, National University of Singapore, Singapore 117377, Singapore

Corresponding author: Conni M. Sidabalok (sidabalok_conni@yahoo.com)

Academic editor: Tammy Horton | Received 4 May 2020 | Accepted 28 May 2020 | Published 8 July 2020

<http://zoobank.org/1A80132D-D679-49C0-90D1-069770305473>

Citation: Sidabalok CM, Wong HP-S, Ng PKL (2020) Description of the supergiant isopod *Bathynomus raksasa* sp. nov. (Crustacea, Isopoda, Cirolanidae) from southern Java, the first record of the genus from Indonesia. ZooKeys 947: 39–52. <https://doi.org/10.3897/zookeys.947.53906>

Abstract

The giant isopod genus *Bathynomus* A. Milne-Edwards, 1879, is recorded for the first time in Indonesian waters, from deep waters off southern Java in the Indian Ocean. *Bathynomus raksasa* sp. nov. is described and notes on juvenile specimens of an unidentified species found in the same locality are also provided. *Bathynomus raksasa* sp. nov. is characterized by the large size (averaging at 330 mm), narrowly rounded clypeus apex, prominent longitudinal carina on the clypeus, convex lateral margins of the uropodal exopod and endopod, produced distolateral corners of the uropodal exopod and endopod which have acute ends, an uropodal exopod with a setal fringe of medium length (69%), a pleotelson 1.6 times wider than long with the posterior margin medially concave, and the large number (11–13) of spines on the pleotelson.

Keywords

Bathynomus, Cirolanidae, Indian Ocean, Indonesia, new species, South Java, taxonomy

Introduction

The genus *Bathynomus* A. Milne-Edwards, 1879 inhabits the deep sea in the Atlantic, Pacific and Indian Oceans, with some species reaching large sizes in excess of 30 cm length (Lowry and Dempsey 2006). Nineteen extant species are known in the genus (Bruce 1986, Magalhães and Young 2003, Lowry and Dempsey 2006, Boyko et al. 2008, Shipley et al. 2016, Kou et al. 2017).

Lowry and Dempsey (2006) revised the Indo-West Pacific taxa and recognized 16 species, of which seven were categorized as “supergiants”; species maturing above 150 mm and reaching 500 mm in length. Five “supergiant” species occur in the Indian and Pacific Oceans: *Bathynomus lowryi* Bruce & Bussarawit, 2004 (Andaman Sea), *B. crosnieri* Lowry & Dempsey, 2006 (Madagascar), *B. keablei* Lowry & Dempsey, 2006 (India, Sri Lanka, Burma), *B. kensleyi* Lowry & Dempsey, 2006 (Coral Sea, Philippines, South China Sea), and *B. richeri* Lowry & Dempsey, 2006 (New Caledonia) (Lowry and Dempsey 2006). Two other “supergiant” species are known from the western Atlantic: *B. giganteus* A. Milne-Edwards, 1879, and *B. miyarei* Lemos de Castro, 1978 (Boyko et al. 2008). The new species described here adds another “supergiant” *Bathynomus* from the Indian Ocean to this list, and is the first from Indonesia.

Material and methods

The material was collected by the 2018 South Java Deep Sea Survey (SJADES 2018), a joint project between NUS and LIPI, with localities mostly in southern Sumatra and Java (Fig. 1). The terminology used and description format follows Lowry and Dempsey (2006).

The following acronyms are used: AM – Australian Museum, Sydney; LIPI – Lembaga Ilmu Pengetahuan Indonesia (Indonesian Institute of Sciences); MZB – Museum Zoologicum Bogoriense, Indonesia; NUS – National University of Singapore; SJADES – South Java Deep Sea Expedition; ZRC – Zoological Reference Collection of the Lee Kong Chian Natural History Museum, National University of Singapore.

Taxonomy

Suborder Cymothoida Wägele, 1989

Family Cirolanidae Dana, 1852

Genus *Bathynomus* A. Milne-Edwards, 1879

Restricted synonymy. A. Milne-Edwards, 1879: 21.— Bruce 1986: 126.— Kensley and Schotte 1989: 129.— Lowry and Dempsey 2006: 168.

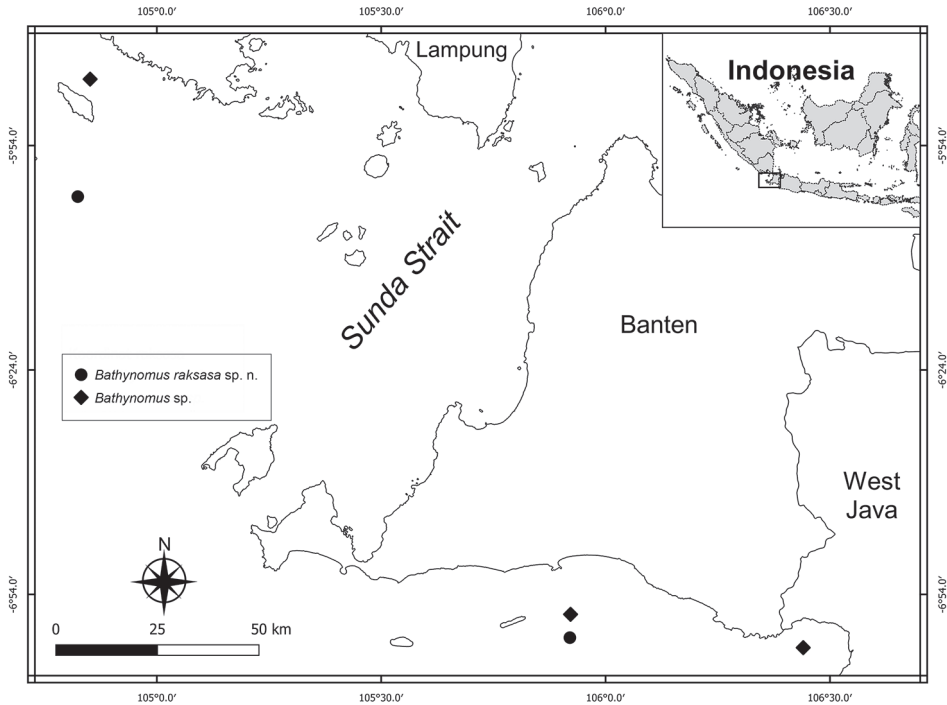


Figure 1. Distribution of *Bathynomus raksasa* sp. nov. and *Bathynomus* sp. in Indonesian waters.

Remarks. The taxonomy of *Bathynomus* has been reviewed by Bruce (1986), Magalhães and Young (2003), with most recently by Lowry and Dempsey (2006). Two new species were added by Shipley et al. (2016) and Kou et al. (2017). The most recent review on *Bathynomus* fossils was done by Hyžný et al. (2019).

Type species. *Bathynomus giganteus* A. Milne-Edwards 1879; by monotypy.

***Bathynomus raksasa* sp. nov.**

<http://zoobank.org/84D71359-90FB-4CC6-856F-B96402F23211>

Figs 2–5

Material examined. *Holotype*, male, 363 mm; Indonesia, Sunda Strait (between Sumatra and Java); 6°00.828'S, 104°49.428'E; 26 Mar. 2018; SJADES exped.; station CP 13, beam trawl 1259 m; MZB Cru.Iso 097. *Paratype*, female, 298 mm; Indonesia, Indian Ocean (East of Tinjil Island); 6°59.778'S, 105°55.224'E; 28 Mar. 2018; SJADES exped.; station CP 28, beam trawl 957 m; ZRC 2020.0015.

Comparative material. *Bathynomus giganteus* A. Milne-Edwards, 1879 – 1 male, 354 mm; U.S.A., Virginia, 100 miles off Virginia Beach; 36.483N, 74.8W; 30 May 1962; 73 m depth; ZRC 2014.0837. *Bathynomus doederleini* Ortmann, 1894 – 6 males,

100, 120, 120, 128, 136, 145 mm; 7 females, 88, 90, 94, 130, 130, 138, 145 mm; 3 juveniles; Taiwan; AM P68684. 1 male, 125 mm; 1 female, 85 mm; 4 juveniles; Taiwan, Tashi port; 1990s; P. K. L. Ng leg.; deep-water; ZRC 1998.417. *Bathynomus* sp. – 1 subadult, not sexually mature, pereopod 7 not fully developed, 107 mm; Indonesia, Indian Ocean (East of Tinjil Island); 6°56.664'S, 105°55.315'E; 28 Mar. 2018; SJADES exped.; station CP 26, beam trawl 517 m; MZB Cru.Iso 098. 1 juvenile; Indonesia, Sunda Strait (between Tabuan Island and Sumatra); 5°45.126'S, 104°51.080'E; 25 Mar. 2018; SJADES exped.; station CP 08, beam trawl 442 m; ZRC 2020.0016. 2 juveniles, 60, 63 mm; Indonesia, Indian Ocean (Pelabuhan Ratu Bay); 7°01.116'S, 106°26.421'E; 3 Apr. 2018; SJADES exped.; station CP 55, beam trawl 379 m; ZRC 2020.0017.

Type-locality. Indonesia, Sunda Strait: between Sumatra and Java, 06°00.828'S, 104°49.428'E.

Diagnosis. Narrowly rounded clypeus apex (Fig. 2C); prominent longitudinal carina on clypeus (Fig. 2C); convex lateral margins of uropodal exopod and endopod (Fig. 3D, E); produced distolateral corners of uropodal exopod and endopod with acute tips (Fig. 3D, E); uropodal exopod with medium-length setal fringe (69%) (Fig. 3D, E); pleotelson 1.6 times wider than long with posterior margin medially concave (Fig. 2D); 11–13 spines on pleotelson (Fig. 2D).

Description of holotype male. Body (Fig. 2A) 363 mm long, 155 mm wide at pereonite 5, length 2.3 times width. Head (Fig. 2B) with ridge above eyes discontinuous; clypeus (Fig. 2C) with prominent longitudinal carina, distal margins slightly concave, apex narrowly rounded.

Antenna 2 (Fig. 2A, E) flagellum extending to end of pleonite 2.

Pereopod 1 (Fig. 3A) ischium with 2 posteroproximal robust setae, 2 robust setae on posterodistal margin; merus with 4 short robust setae on anterodistal angle, posterior margin with 4 robust setae in proximal row and 2 robust setae in distal row; propodus length 2.3 times width, with 5 robust setae on posterior margin. Pereopod 2 (Fig. 3B, C) ischium with 3 robust setae on posterior margin and 2 robust setae on posterodistal margin; merus with 7 short robust setae on anterodistal angle, posteromedial margin with 3 robust setae in proximal row and 2 robust setae in distal row; propodus with 4 robust setae on posterior margin. Pereopod 7 coxa (Fig. 2F) distally attenuated, curved posteriorly.

Pleonite 3 (Fig. 2F) not extending beyond pleonite 5.

Uropod (Figs 2D, 3D, E) not extending beyond pleotelson; peduncle with 3 robust setae; exopod and endopod with smooth lateral and distal margins; exopodal lateral margin convex with 10 robust setae along margin, setal fringe medium to continuous in length (69%), medial margin straight, distomedial corner rounded, distal margin convex with 5 robust setae, distolateral corner slightly produced, acute; endopodal lateral margin convex, distally sinuate, with 4 robust setae; medial margin straight; distomedial corner rounded; distal margin straight with 11 robust setae; distolateral corner produced, acute.

Pleotelson (Fig. 2D) broader than long, 1.6 times as wide as length, posterior margin medially concave, smooth (minute pores), conspicuous longitudinal carina on

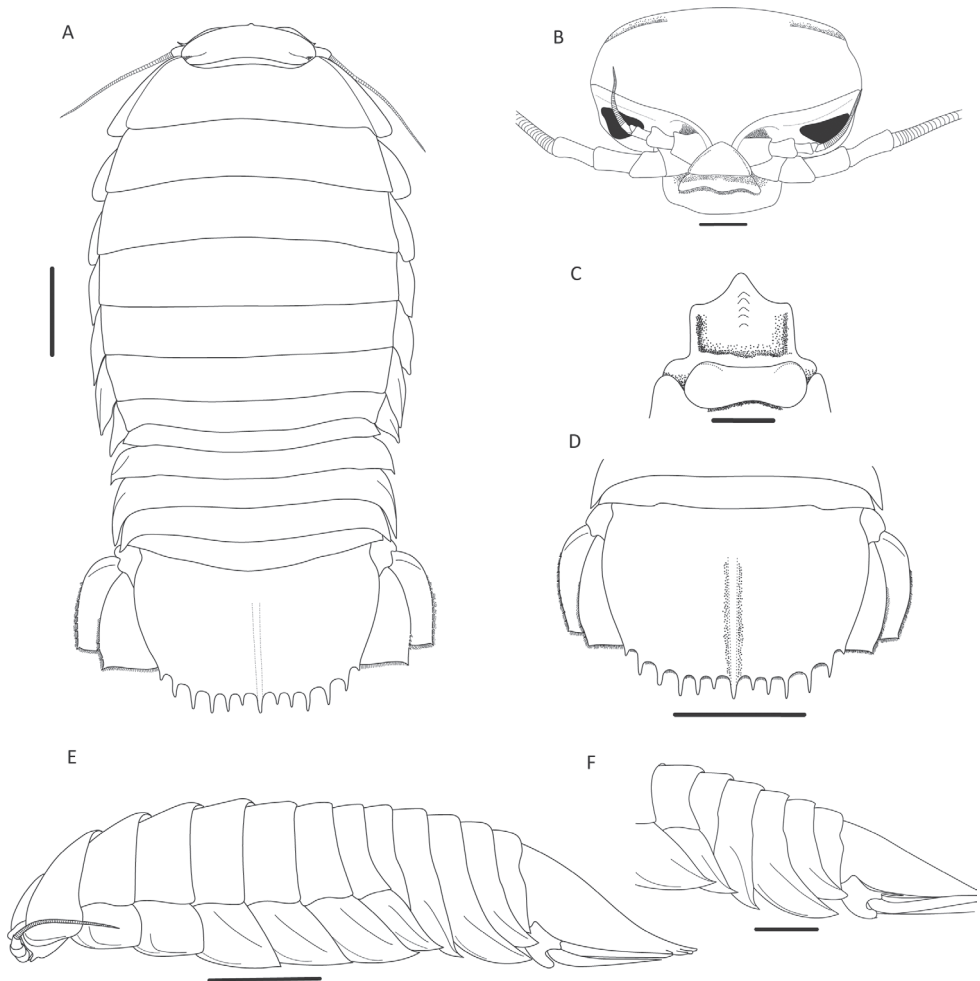


Figure 2. *Bathynomus raksasa* sp. nov., holotype male (363 mm) (MZB Cru.Iso 097), Indonesia **A** dorsal view **B** cephalon, anterior view **C** clypeal region **D** pleotelson **E** body, lateral view **F** pereon, lateral view. Scale bars: 5 cm (**A, D, E**); 1 cm (**B, C, F**).

dorsal surface, with 11 distal and 2 lateral straight acute prominent spines along distal margin, without setae between spines, central distal spine simple.

Female. Similar to male.

Variation. Robust setae count on female as follows: exopodal lateral margin with 7–10 robust setae, distal margin with 4 or 5, endopodal lateral margin with 3–5 and distal margin with 8–10; pleotelson with 9 distal and 2 lateral straight acute prominent spines along distal margin.

Etymology. The epithet is the Indonesian word “raksasa” for giant, alluding to its enormous size and the significance of the find. The name is used as a noun in apposition.

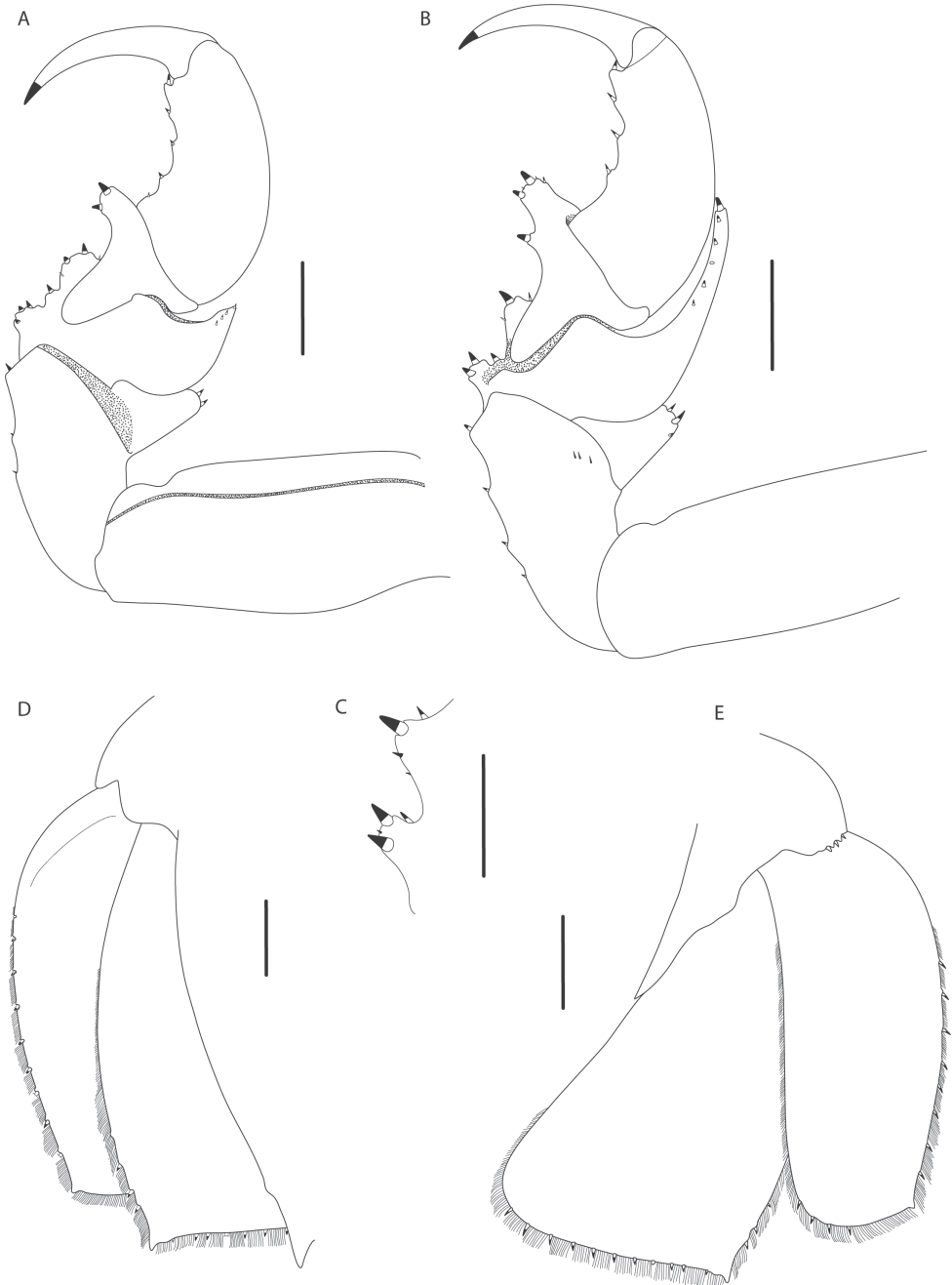


Figure 3. *Bathynomus raksasa* sp. nov., holotype male (363 mm) (MZB Cru.Iso 097), Indonesia **A** pereopod 1 **B** pereopod 2 **C** pereopod 2 merus, posterolateral margin **D** uropod, ventral view **E** uropod, dorsal view. Scale bars: 1 cm (**A, B, D, E**); 0.5 cm (**C**).

Remarks. *Bathynomus raksasa* sp. nov. can be readily identified by its large size (330 mm on average), narrowly rounded clypeus apex, produced and acute distolateral corners of uropodal rami, wider rather than long pleotelson with medially concave posterior margin and the presence of 11–13 pleotelson spines. *Bathynomus raksasa* sp. nov. is the sixth “supergiant” species from the Indo-West Pacific and is one of the largest known members of the genus.

In general appearance, *B. raksasa* sp. nov. is most similar to *B. giganteus* and *B. lowryi*. All three are large, averaging 300 mm in length, possess a prominent longitudinal carina on the dorsal surface of the pleotelson and have acute spines on the distal margin of the pleotelson. The new species is closest to *B. giganteus*, sharing the relatively medium length of antenna 2 (reaching to between the posterior of pereonite 2 and anterior of pereonite 3), lateral and posterior shape of the uropodal exopod and endopod, and the pleotelson spine count. *Bathynomus raksasa* sp. nov., however, differs markedly from *B. giganteus* by its more conspicuous longitudinal carina on the clypeus ventral surface (Fig. 4A) (vs. less conspicuous in *B. giganteus*; Fig. 4B), absence of a transverse carina on the anterior of the head (Fig. 4C) (vs. carina present in *B. giganteus*; Fig. 4D), the relatively shorter uropodal endopod (0.12 total body length, Fig. 4E) (vs. relatively longer, 0.15 body length in *B. giganteus*; Fig. 4F), the body surface, including that of the pleotelson, being covered with small low granules and smooth to the touch (Fig. 5A) (vs. granules more prominent and the surfaces distinctly rough in *B. giganteus*; Fig. 5B), the almost flat posterior ventral surface of the pleotelson (Fig. 5C) (vs. surface distinctly concave in *B. giganteus*; Fig. 5D), the straight spines of pleotelson (Fig. 5E) (vs. gently curved upwards in *B. giganteus*; Fig. 5F), the pleotelson is broader than long (Fig. 5A) (vs. as long as broad in *B. giganteus*, Fig. 5B), and the posterior margin of the pleotelson is broad and medially concave (Fig. 5A) (vs. broadly rounded in *B. giganteus*, Fig. 5B). *Bathynomus raksasa* sp. nov. can easily be distinguished from *B. lowryi* in possessing a relatively longer antenna 2 which reaches to the ends of pereonite 2 (vs. shorter antenna 2 which reaches only to the anterior part of pereonite 2 in *B. lowryi*), the narrowly rounded clypeus apex (vs. apex truncate in *B. lowryi*), straight pleotelson spines (vs. spines upwardly curved in *B. lowryi*) and the larger number (13) of robust setae on the pleotelson (vs. 9 in *B. lowryi*) (Bruce and Bussarawit 2004: figs 1, 6).

Bathynomus raksasa sp. nov. shares the same general uropodal exopod and endopod shape as *B. crosnieri*, *B. kensleyi* and *B. richeri* but can easily be distinguished from them in its possession of a conspicuous longitudinal carina on the dorsal surface of the pleotelson (Fig. 5A). Although the number of spines on the margin of the pleotelson (at least 11) is similar to those of *B. crosnieri* and *B. richeri*, the presence of the longitudinal ridge on the pleotelson easily separates *B. raksasa* sp. nov. from these species. *Bathynomus raksasa* sp. nov. also has the same number of spines on the margin of the pleotelson but can easily be distinguished from *B. keablei* in having the distolateral corners of the uropodal exopod and endopod distinctly produced (Fig. 3D, E) (vs. rounded and not produced in *B. keablei*; see Lowry and Dempsey 2006: fig. 17).

The appendix masculina is absent on the holotype male of *B. raksasa* sp. nov. (Fig. 5G) but this is almost certainly not a species-character. It is known to be sometimes

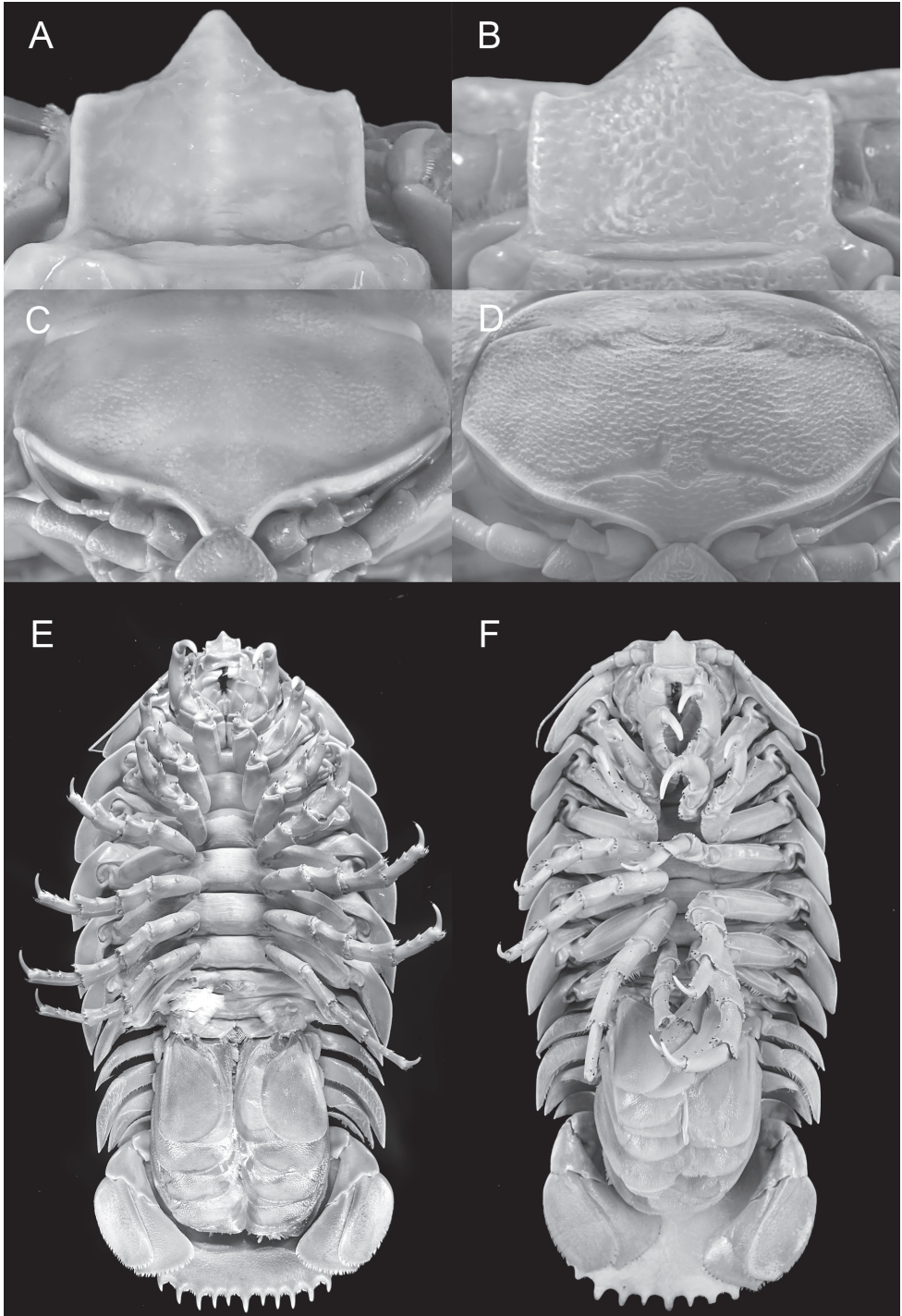


Figure 4. **A, C, E** *Bathynomus raksasa* sp. nov. holotype male (363 mm) (MZB Cru.Iso 097), Indonesia **B, D, F** *B. giganteus* male (354 mm) (ZRC 2014.0837), Caribbean **A, B** clypeus ventral surface **C, D** anterior of head **E, F** body, ventral view.

absent in *B. doederleini* from Taiwan (present study); with five out of seven males below the size of 130 mm lacking it. The largest males of *B. doederleini* (136–145 mm) possess appendix masculina. The absence or presence of appendix masculina has been previously used by Soong and Mok (1994) to determine the maturity of males of *Bathynomus doederleini*; “mature males” were males with appendix masculina and “maturing males” were those without appendix masculina and testes. Barradas-Ortiz et al. (2003) reported that some adult males of *B. giganteus* from Brazil (mostly smaller specimens below 290 mm) lacked appendix masculina, especially in summer. They suggested that these smaller males might have been less reproductively active in summer and/or the appendix masculina may be a non-permanent organ which is lost or regrown when the animals moult (Barradas-Ortiz et al. 2003). Barradas-Ortiz et al. (2003) also noted that larger male specimens of *B. giganteus* tend to keep the organ for longer periods than smaller ones, although even large individuals (310 mm) sometimes do not possess the structure. We cannot be certain that either of the patterns above apply to *B. raksasa* sp. nov. as only one male was collected. The appendix masculina (Fig. 5H) is present on the large male American specimen of *B. giganteus* (ZRC 2014.0837) examined here.

The SJADES cruise also obtained four juvenile and subadult specimens from southern Java (here identified as *Bathynomus* sp.) (Fig. 6) which we are unable to identify to the species level, especially as the diagnostic characters may not be developed. They are clearly not *Bathynomus raksasa* sp. nov. with a different pleotelson spination, shapes of pleotelson and uropodal rami. The largest specimen in the lot (107 mm) has an almost fully-developed pereopod 7 which indicates that the adult would not be too much larger in size. This, along with the presence of setae between the pleotelson spines, suggest that this species belongs to the “giant” group. The number of spines on the posterior margin of the pleotelson ranges between 5+2, 7+2 and 9+2. Soong and Mok (1994) used the development of pereopod 7 as one of the characters to classify the development stages of *Bathynomus doederleini*. According to Soong and Mok (1994), individuals with “small, white” pereopod 7 and lacking either oostegites or penes and/or appendix masculina were categorised as “subadult I” which equals to stage 2 of five development stages they proposed. However, we will not apply this approach to *Bathynomus* sp. because of the limited specimen number.

Bathynomus sp. superficially resembles the poorly known *Bathynomus affinis* Richardson, 1910, described from the Philippines from one specimen. There is, however, a problem with what has been identified as “*Bathynomus affinis*” by Lowry and Dempsey (2006: 169, figs 2, 3), who listed among their material, the type from the Philippines as well as two females from the Arafura Sea, providing figures of the latter. Bruce (1986: fig. 87A–E) had earlier figured the uropods, and pereopods 1 and 3 of the type specimen (sex not specified). The problem is that the distolateral corners of uropodal rami of the holotype from the Philippines is distinctly acute and curved (Bruce 1986: fig. 87A–C) whereas that of Lowry and Dempsey (2006: fig. 3D, E) from the Arafura Sea is distinctly wider and not produced. Significantly, Richardson’s (1910: fig. 1) figures of the uropods are the same as those by Bruce (1986). The material from Arafura Sea are thus unlikely to be *B. affinis* s. str.

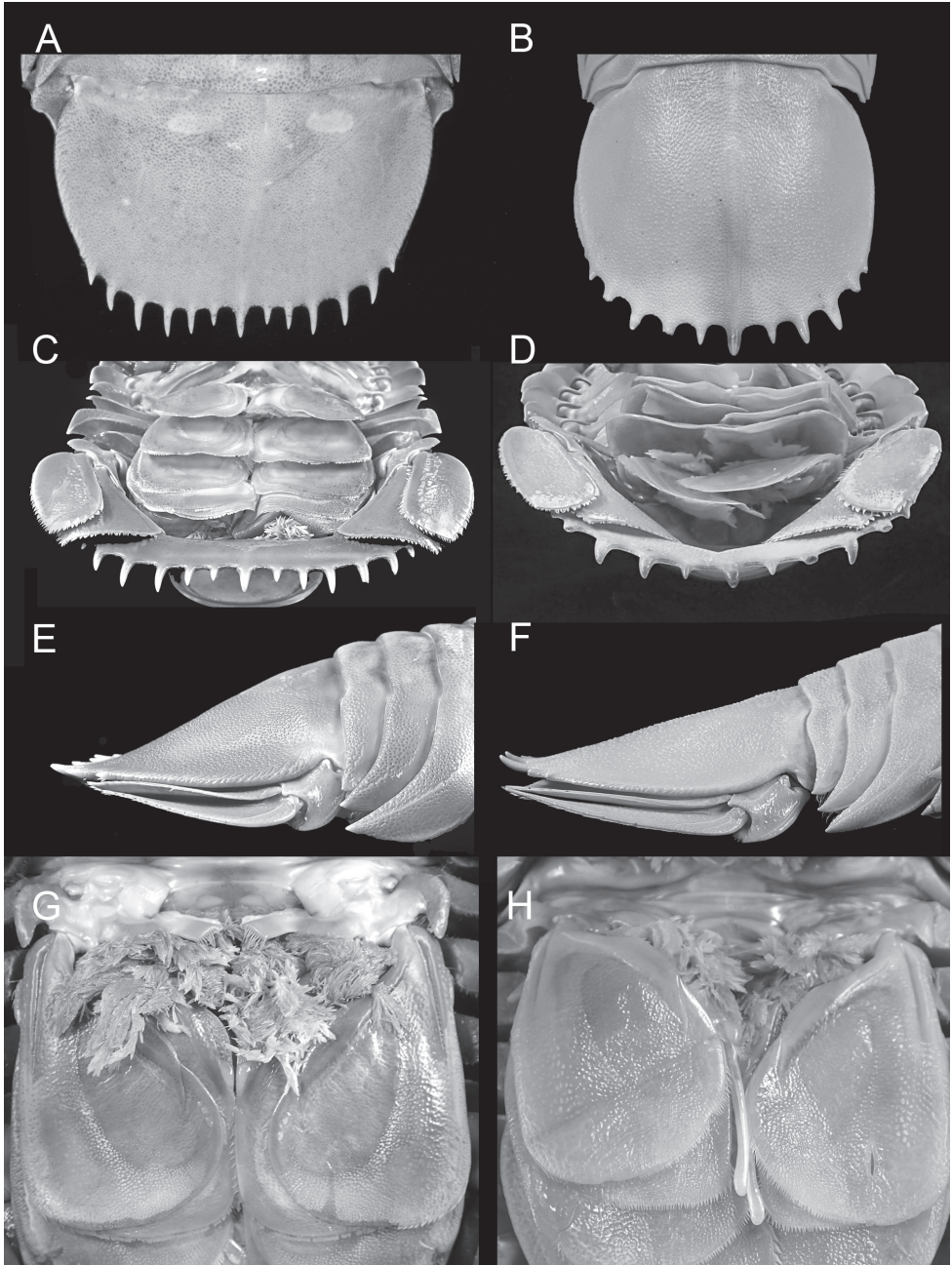


Figure 5. **A, C, E, G** *Bathynomus raksasa* sp. nov. holotype male (363 mm) (MZB Cru.Iso 097), Indonesia **B, D, F, H** *B. giganteus* male (354 mm) (ZRC 2014.0837), Caribbean **A, B** pleotelson dorsal view **C, D** pleotelson posterior view **E, F** pleotelson lateral view **G, H** pleopod 2.

Our material of *Bathynomus* sp. from Java resembles the “*B. affinis*” of Lowry and Dempsey (2006) in possessing the same relative length of antenna 2 (reaching between pereonites 3 and 4), straight clypeus distal margins, the setal fringe on the uropodal exopod is long and continuous ($\pm 90\%$), and similar pleotelson spine count (5+2, 7+2 and 9+2). The marked difference in the form of the uropodal endopod distolateral corner, however, indicates they are not conspecific. In addition, the uropod of *Bathynomus* sp. reaches to the end of the pleotelson (Fig. 6D) (vs. slightly extended beyond the pleotelson; Lowry and Dempsey 2006: fig. 2F) and the pleotelson central spine is weakly bifid (Fig. 6C) (vs. simple; Lowry and Dempsey 2006: fig. 2F). The uropods of our material from Java agree very well with the figures by Richardson (1910) and Bruce (1986), but until a complete redescription of the holotype of *B. affinis* is done and more character states are known, we are not certain if they are actually conspecific.

Bathynomus sp. differs from *B. pelor* Bruce, 1986 (from northwestern Australia) in having a longer antenna 2 that reaches to the middle of pereonite 4 (Fig. 6E) (vs. middle of pereonite 2; Bruce 1986: fig. 91A), weakly bifid pleotelson central spine (Fig. 6C) (vs. strongly bifid; Bruce 1986: fig. 91B), and the conspicuous longitudinal carina on the pleotelson (Fig. 6D) (vs. inconspicuous; Bruce 1986: fig. 91C). Both species share similar shape of uropodal rami with more acute and curved distolateral corner on the endopod of *Bathynomus* sp. (Fig. 6A, B) (vs. less acute and curved; Bruce 1986: fig. 91D). It differs from *B. immanis* Bruce, 1986, in the slightly concave lateral of uropodal exopod (Fig. 6A, B) (vs. strongly concave; Bruce 1986: fig. 90C, D), greater length of fringing setae ($\pm 80\%$) on the lateral uropod exopod (Fig. 6A, B) (vs. 66%; Bruce 1986: fig. 90C, D) and the weakly bifid pleotelson central spine (Fig. 6C) (vs. simple; Bruce 1986: fig. 89 D). The two species together with *B. doederleini* share similar uropodal endopod shapes (Fig. 6A, B).

Bathynomus sp. shares with *B. kapala* Griffin, 1975 (from Australia) a similar bifid central pleotelson spine but can easily be distinguished by its relatively longer antenna 2 (Fig. 6E) (middle of pereonite 4 vs. within pereonite 3; Lowry and Dempsey 2006: fig. 14 C), the straight head ridge (Fig. 6F) (vs. curved; Lowry and Dempsey 2006: fig. 14 D), a narrowly rounded clypeus apex (6G) (vs. broadly rounded; Lowry and Dempsey 2006: fig. 14 E), with only one row of fringing setae on the anterior margin of the basis of pereopod 7 (Fig. 6H) (vs. with two rows; Lowry and Dempsey 2006: fig. 23 F) and the uropodal endopod distolateral margin is subacute and only slightly produced (Fig. 6A, B) (vs. not produced; Lowry and Dempsey 2006: fig. 15 D, E).

Compared to *B. doederleini*, *Bathynomus* sp. has pereopod 7 coxa more slender (Fig. 6I) (vs. relatively broader; Lowry and Dempsey 2006: fig. 10B), there is one row of fringing setae on the anterior margin of the basis of pereopod 7 (Fig. 6H) (vs. with two rows; Lowry and Dempsey 2006: fig. 23D), and the lengths of the pleotelson spines are similarly sized (Fig. 6D) (vs. uneven; Lowry and Dempsey 2006: fig. 10F).

Distribution. Sunda Strait and Indian Ocean, South Java, Indonesia; at depths of 957–1259 m.

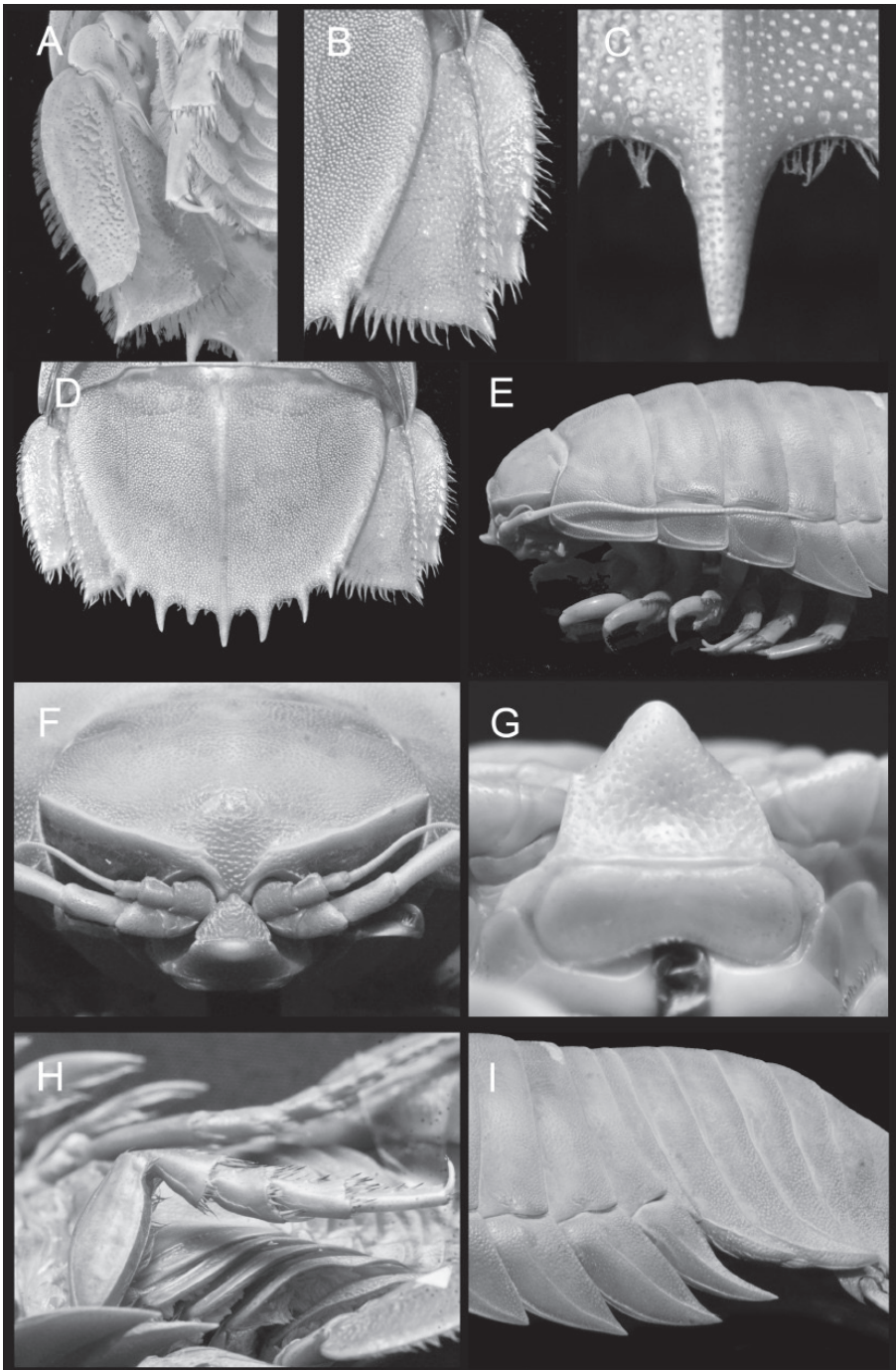


Figure 6. *Bathynomus* sp. (107 mm) (MZB Cru.Iso 098), Indonesia **A** uropod, ventral view **B** uropod, dorsal view **C** pleotelson central spine **D** pleotelson **E** length of antenna 2 **F** cephalon, anterior view **G** clypeal region **H** pereopod 7, ventral view **I** pereopod 7 coxa.

Acknowledgements

The SJADES cruise (chief scientists: Dwi Listyo Rahayu and Peter Ng) was a joint Indonesian-Singapore expedition to southern Java funded by the National University of Singapore and the Research Center for Oceanography, Indonesian Institute of Sciences (LIPI); and supported by their respective Ministries of Foreign Affairs under the RISING 50 program to promote bilateral co-operation. Thanks are also due to Bertrand Richer de Forges and Chan Tin-Yam for their invaluable help in the trawling work and other support. We thank Farid Rifaie and Arid of Research Center for Biology LIPI for the map and some of the photos, respectively. Rene Ong and Muhammad Dzaki Bin Safaruan of LKCNHM are also thanked for assisting us with the photography set up and visits to the collections in LKCNHM. We are also grateful to the reviewers for their constructive comments which significantly improved the quality of this paper.

References

- Barradas-Ortiz C, Briones-Fourzán P, Lozano-Álvarez E (2003) Seasonal reproduction and feeding ecology of giant isopods *Bathynomus giganteus* from the continental slope of the Yucatan peninsula. *Deep Sea Research Part I: Oceanographic Research Papers* 50: 495–513. [https://doi.org/10.1016/S0967-0637\(03\)00036-0](https://doi.org/10.1016/S0967-0637(03)00036-0)
- Boyko CB, Bruce NL, Hadfield KA, Merrin KL, Ota Y, Poore GCB, Taiti S, Schotte M, Wilson GDF (2008) World Marine, Freshwater and Terrestrial Isopod Crustaceans database. *Bathynomus* A. Milne-Edwards, 1879. <http://www.marinespecies.org/isopoda/aphia.php?p=taxdetails&cid=248508> [Accessed on 2020-03-08]
- Bruce NL (1986) Cirolanidae (Crustacea: Isopoda) of Australia. *Records of the Australian Museum, Supplement* 6: 1–239. <https://doi.org/10.3853/j.0812-7387.6.1986.98>
- Bruce NL, Bussarawit S (2004) *Bathynomus lowryi* sp. nov. (Crustacea: Isopoda: Cirolanidae), the first record of the ‘giant’ marine isopod genus from Thailand waters. *Phuket Marine Biological Center, Research Bulletin* 65: 1–8.
- Dana JD (1852) On the classification of the Crustacea Choristopoda or Tetracapoda. *American Journal of Sciences and Arts* 2: 297–316. <https://doi.org/10.5962/bhl.title.61409>
- Griffin DJG (1975) A new giant deep water isopod of the genus *Bathynomus* (Flabellifera: Cirolanidae). *Proceedings of the Linnean Society of New South Wales* 100: 103–109.
- Hyžný M, Pasini G, Garassino A (2019). Supergiants in Europe: on the cirolanid isopod *Bathynomus* A. Milne Edwards [*sic*], 1879 (Malacostraca, Peracarida) from the Plio-Pleistocene of Italy. *Neues Jahrbuch für Geologie und Paläontologie-Abhandlungen* 291(3): 283–298. <https://doi.org/10.1127/njgpa/2019/0802>
- Kensley B, Schotte M (1989) *Guide to the Marine Isopod Crustaceans of the Caribbean*. Smithsonian Institution Press, Washington, D.C. & London, 1–308 pp. <https://doi.org/10.5962/bhl.title.10375>

- Kou Q, Chen J, Li X, He L, Wang Y (2017) New species of the giant deep-sea isopod genus *Bathynomus* (Crustacea, Isopoda, Cirolanidae) from Hainan Island, South China Sea. *Integrative Zoology* 12: 283–291. <https://doi.org/10.1111/1749-4877.12256>
- Lemos de Castro A (1978) Descrição de uma espécie nova gigante do gênero *Bathynomus* Milne Edwards [*sic*] do litoral Brasileiro (Isopoda, Cirolanidae). *Revista Brasileira de Biologia* 38: 37–44.
- Lowry JK, Dempsey K (2006) The giant deep-sea scavenger genus *Bathynomus* (Crustacea, Isopoda, Cirolanidae) in the Indo-West Pacific. In: Richer De Forges B, Justine J-L (Eds) *Tropical Deep-Sea Benthos*, volume 24. *Mémoires du Muséum national d'Histoire naturelle* 193: 163–192.
- Magalhães N, Young PS (2003) *Bathynomus* A. Milne Edwards [*sic*], 1879 (Isopoda, Cirolanidae) from the Brazilian coast, with description of a new species. *Arquivos do Museu Nacional, Rio de Janeiro* 61: 221–239.
- Milne-Edwards A (1879) Sur un isopode gigantesque des grandes profondeurs de la mer. *Comptes Rendus de l'Académie des Sciences, Paris* 88: 21–23. <https://doi.org/10.3406/crai.1879.68524>
- Ortmann A (1894) A new species of the isopod-genus *Bathynomus*. *Proceedings of the National Academy of Science, Philadelphia* 1894: 191–193.
- Richardson H (1910) Marine isopods collected in the Philippines by the U.S. Fisheries steamer Albatross in 1907–08. *Bureau of Fisheries Document* 736: 1–44.
- Shiple ON, Bruce NL, Violich M, Baco A, Morgan N, Rawlins S, Brooks EJ (2016) A new species of *Bathynomus* Milne Edwards [*sic*], 1879 (Isopoda: Cirolanidae) from The Bahamas, Western Atlantic. *Zootaxa* 4147: 82–88. <https://doi.org/10.11646/zootaxa.4147.1.6>
- Soong K, Mok H-K (1994) Size and maturity stage observations of the deep-sea isopod *Bathynomus doederleini* Ortmann, 1894 (Flabellifera: Cirolanidae), in eastern Taiwan. *Journal of Crustacean Biology* 14: 72–79. <https://doi.org/10.2307/1549056>
- Wägele J-W (1989) Evolution und phylogenetisches System der Isopoda. *Stand der Forschung und neue Erkenntnisse. Zoologica* 140: 1–262.

First record of the family Colinauropodidae (Myriapoda, Pauropoda) in China, with the description of three new species

Yun Bu¹

¹ Natural History Research Center, Shanghai Natural History Museum, Shanghai Science & Technology Museum, Shanghai 200041, China

Corresponding author: Yun Bu (buy@sstm.org.cn)

Academic editor: Pavel Stoev | Received 28 April 2020 | Accepted 30 May 2020 | Published 8 July 2020

<http://zoobank.org/7E8524DC-A5E1-4F8A-BE1F-089CDFEE7F8>

Citation: Bu Y (2020) First record of the family Colinauropodidae (Myriapoda, Pauropoda) in China, with the description of three new species. *ZooKeys* 947: 53–70. <https://doi.org/10.3897/zookeys.947.53723>

Abstract

The pauropod family Colinauropodidae Scheller, 1985 is recorded from China for the first time. Three new species of the genus *Colinauropus* Remy, 1956 are described: *Colinauropus chinensis* **sp. nov.** and *C. chongzhoui* **sp. nov.** from Jiangsu Province, and *C. foliosus* **sp. nov.** from Sichuan Province. They can be easily separated from similar species by the number and the shape of sclerotized plates on the tergites, setae on the body and the anal plate. A key for all species of the genus is provided.

Keywords

anal plate, bothriotricha, pauropod, sclerotized plate, taxonomy

Introduction

The family Colinauropodidae Scheller, 1985 includes the single genus *Colinauropus* Remy, 1956 and contains three species in the world: *Colinauropus regis* Remy, 1956 from Réunion and Mauritius (Remy 1956, 1959), *C. schelleri* Hagino, 1991 from Japan (Hagino 1991, 2005), and *C. haginoi* Scheller, 2009 from Philippines (Scheller, 2009). Their most charming character lies in the tergites which split into several distinctly sclerotized plates of irregular shape (Scheller 2011).

In the original description, the genus *Colinauropus* was considered to be affiliated with species of the family Brachypauropodidae Silvestri, 1902 according to the fragmented tergites and the shape of anal plate (Remy 1956). Its taxonomic position was reconsidered and placed in the family Pauropodidae Lubbock 1867, under the new subfamily Colinauropodinae, which was supposed to be closely related to the subfamily Scleropauropodinae (Scheller 1985). In the latest classification system, the subfamily Colinauropodinae was upgraded to family Colinauropodidae (Scheller 2009, 2011).

The purposes of this study are 1) to record the occurrence of family Colinauropodidae Scheller, 1985 in China for the first time; 2) to describe three new species of the genus *Colinauropus* Remy, 1956 from China; 3) to give a key to the species of the genus.

Materials and methods

All pauropods were collected using a Tullgren's funnel. The specimens were sorted under a stereomicroscope and preserved in 80% alcohol. They were mounted on slides using Hoyer's solution and dried in an oven at 50 °C. Observations were performed under a phase contrast microscope (Leica DM 2500). Photos were taken using a digital camera (Leica DMC 4500). Line drawings were made using a drawing tube. All specimens were deposited in the collection maintained by the Shanghai Natural History Museum.

Abbreviations used in the descriptions follow Qian et al. (2018). Absolute lengths of all other body parts are given in mm and μm . Otherwise, the text refers to relative lengths. For the description of the new species, measurements and indices of paratypes are given in brackets.

Results

Taxonomy

Family Colinauropodidae Scheller, 1985

Genus *Colinauropus* Remy, 1956

Type species. *Colinauropus regis* Remy, 1956.

Diagnosis. Body fusiform; head and pygidium free; tergites divided into sclerotized coarse plates, partly of irregular shape; stalk of antennal globulus g shorter than globulus itself; adults with first and last pair of legs 5-segmented, remaining pairs 6-segmented; pygidial sternum with two pairs of setae b_1+b_2 (Scheller 2011).

Distribution. Ethiopian, Palearctic, and Oriental regions.

***Colinauropus chinensis* sp. nov.**

<http://zoobank.org/DFA53888-8023-4745-B84C-82E51BCB5E57>

Figures 1–3

Material examined. *Holotype*, female adult with 9 pairs of legs (slide no. JS-WX-PA2017033), China, Jiangsu Province, Wuxi City, Daji Mountain, extracted from soil samples in bamboo forest, elev. 5 m, 31°32'N, 120°12'E, 9-X-2017, coll. Y. Bu. *Paratypes*, 2 female adults with 9 pairs of legs (slides no. JS-WX-PA2017031, JS-WX-PA2017032), same data as holotype; 1 female adult with 9 pairs of legs (slide no. JS-WX-PA2018006), same locality as holotype, 9-X-2018, coll. Y. Bu.

Diagnosis. *Colinauropus chinensis* sp. nov. is characterized by the cylindrical, annulate setae on head, antennae and tergites; tergite I without distinct sclerotized plates; tergite II with 2 large and 4 small sclerotized plates; tergites III–V each with 4 large and 4 small plates; tergite VI with 2 large plates; seta *st* on tergum of pygidium cylindrical; bothriotrichum T_3 with thicker axis and dense tufted pubescence distally.

Description. Adult body length (0.88–) 0.96 (–0.98) mm ($N = 4$); body white-yellow in alcohol, sclerotized plates on tergites brown (Fig. 2A).

Head (Figs 1A, 2D). Dorsal setae cylindrical, annulate, first and second rows shorter than posterior rows. Relative lengths of setae, 1st row: $a_1 = 10$, $a_2 = 8$ (–9); 2nd row: $a_1 = 13$ (–14), $a_2 = 7$ (–9), $a_3 = 7$; 3rd row: $a_1 = (18–) 20$, $a_2 = (23–) 24$; 4th row: $a_1 = 16$ (–17), $a_2 = 16$ (–17), $a_3 = 22$ (–25), $a_4 = 14$ (–16); lateral group setae $l_1 = 21$ (–26), $l_2 = 26$ (–31), $l_3 = 29$ (–35); the ratio $a_1/a_1 - a_1$ in 1st row 0.7 (–0.9), 2nd row 0.5, 3rd row 1.2 and 4th row 0.7 (–0.8). Temporal organs oval in dorsal view, their length 0.8 of their shortest distance apart. Pistil present. Head cuticle faintly granular.

Antennae (Figs 1E, 2B, C). Antennal segments 1–3 with 2, 2, 3 short, cylindrical, annulate setae respectively, and 1 rudimentary setae present on segment 3. Antennal segment 4 with 4 cylindrical setae; relative lengths of setae: $p = 10$, $p' = 6$, $p'' = 5$, $r = 5$; tergal seta p (1.3–) 1.4 times as long as tergal branch t ; the latter cylindrical, 1.7 (–1.8) times as long as its greatest diameter and 0.8 of sternal branch s , which itself is 1.6 times as long as its greatest diameter. Seta q cylindrical, annulate, 0.9 of s . Relative lengths of flagella (base segments included) and base segments: $F_1 = 100$, $bs_1 = 8$ (–11); $F_2 = (41–) 49$, $bs_2 = (5–) 6$; $F_3 = (84–) 92$, $bs_3 = 9$ (–10). F_1 (6.6–) 7.2 times as long as t , F_2 and F_3 (2.3–) 2.7 and (4.8–) 5.1 times as long as s respectively. Distal calyces spherical; apex of flagella fusiform, with a short lateral flap. Globulus g 1.7 times as long as wide; about 12 bracts, capsule spherical; width of g (0.5–) 0.6 of the greatest diameter of t . Antennal cuticle granulated.

Trunk. Setae on collum segment cylindrical, annulate; sublateral setae length (20–) 22 μm , (1.9–) 2.0 times as long as submedian setae; sternite process triangular, furcate and granulated; appendages barrel shaped (Fig. 2E). Tergite I with 4+4 short, cylindrical setae (14–15 μm), posteriorly with two patches of thickened cuticles but not form distinct sclerotized plates (Fig. 2F); Tergite II with 6+6 setae (9–20 μm), 4 small anterior and 2 large posterior sclerotized plates (Figs 1B, 2G); Tergites III–V each with 6+6 setae (9–21 μm), 4 large and 4 small sclerotized plates (Fig. 2H–J); Ter-

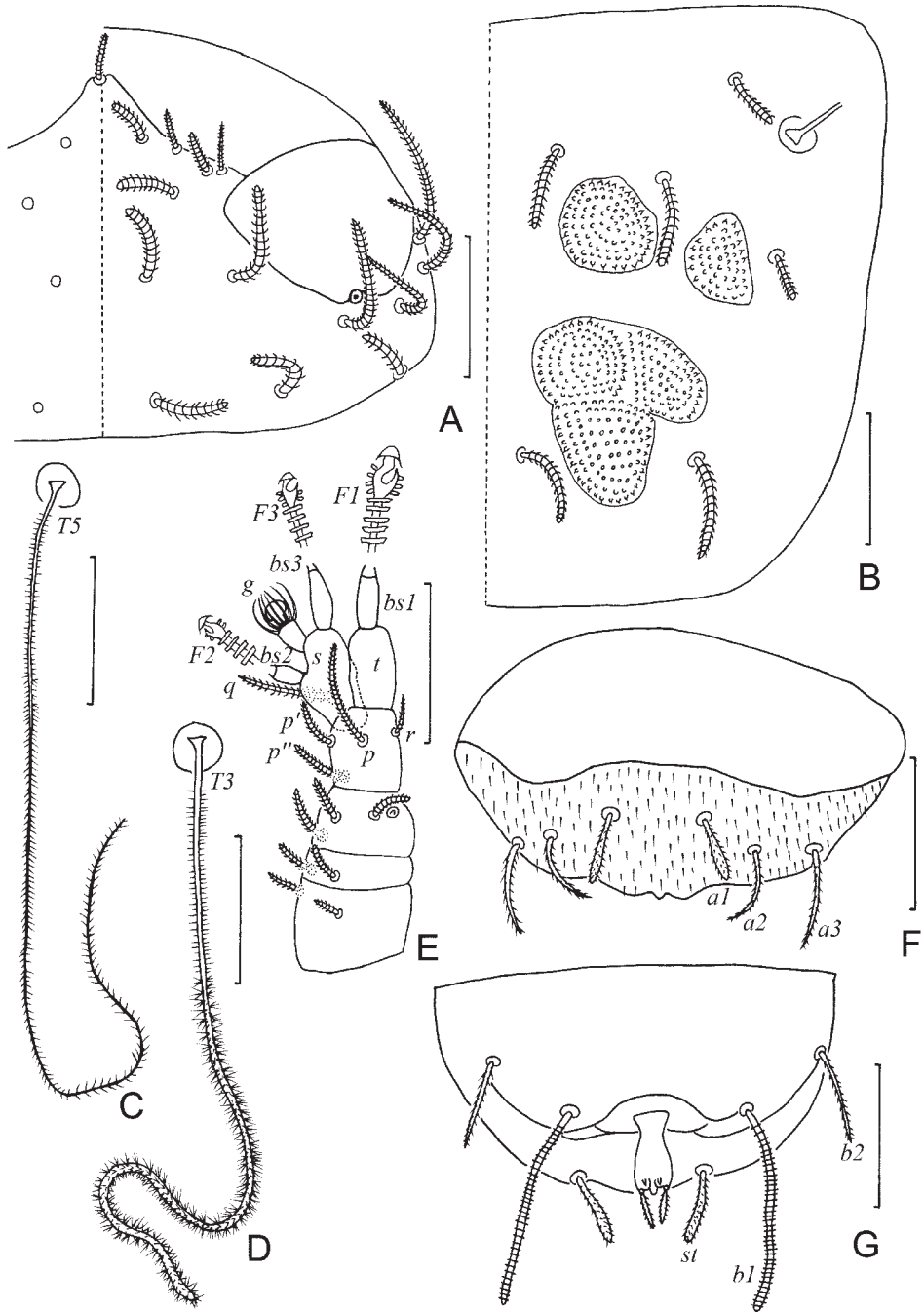


Figure 1. *Colinauropus chinensis* sp. nov. **A** head, dorsal view, right side **B** tergite II, right side **C** T_5 **D** T_3 **E** right antenna, tergal view **F** tergum of pygidium **G** sternum of pygidium and anal plate. Scale bars: 20 μm .

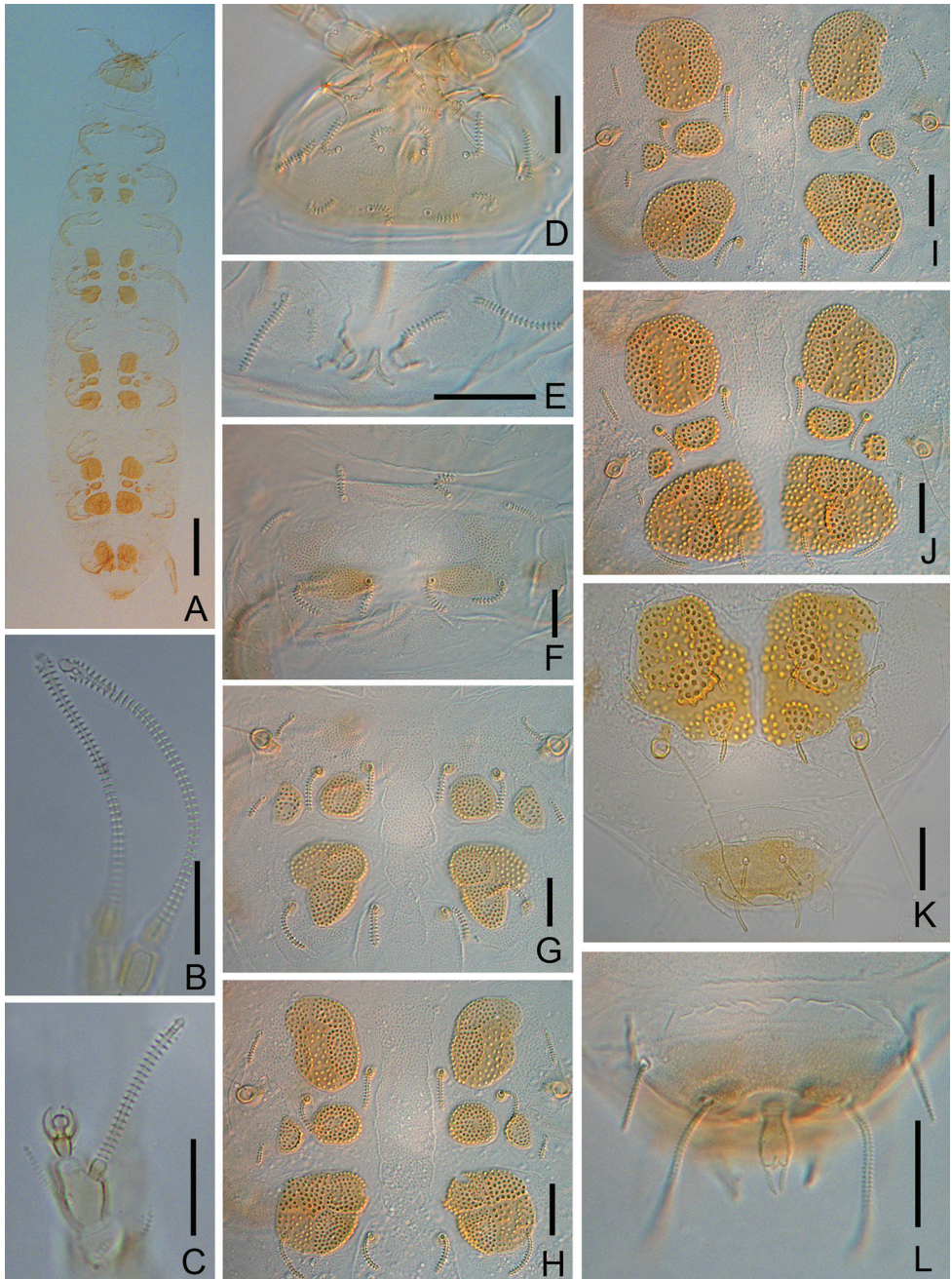


Figure 2. *Colinauropus chinensis* sp. nov. **A** habitus, tergal view **B** F_1 and F_3 of right antenna **C** globulus and F_2 of right antenna **D** head, dorsal view **E** collum segment, sternal view **F** tergite I **G** tergite II **H** tergite III **I** tergite IV **J** tergite V **K** tergite VI and tergum of pygidium **L** sternum of pygidium and anal plate. Scale bars: 100 μm (**A**); 20 μm (**B-L**).

gite VI with 4+2 setae and 2 large plates (Fig. 2K), posterior setae 10 (–11) μm long, their mutual distance 20 (–23) μm (Fig. 2K). Sclerotized plates with dense, brown granules, diameter 1.5–3.2 μm (Fig. 1B). Other areas of cuticle on tergites with pale and fine granules.

Bothriotricha. Relative lengths: $T_1 = 100$, $T_2 = (110\text{--}) 117$, $T_3 = (122\text{--}) 128$, $T_4 = 133(–140)$, $T_5 = (167\text{--}) 178$. T_1 , T_2 , T_4 and T_5 long, with short erect and oblique pubescence on axis (Fig. 1C). T_3 with thicker axis and dense tufted pubescence distally (Fig. 1D).

Legs. First and last pair of legs 5-segmented, others 6-segmented (Fig. 3A–C). Setae on coxa and trochanter of legs 1–8 cylindrical, annulate (Fig. 3A, C), length 13 (–14) μm and 18 (–20) μm respectively. Setae on coxa of leg 9 cylindrical, annulate, length (15–) 17 μm (Fig. 3B, D). Setae on trochanter of leg 9 furcate, with subcylindrical, annulate, blunt branches, shorter one about (0.6–) 0.7 of longer one (Fig. 3B, D). Tarsi 1–8 with short, annulate distal seta (6 μm) only (Fig. 3A, C). Tarsus of leg 9 tapering, 35 μm in length, 3.2 (–3.5) times as long as its greatest diameter (Fig. 3B), proximal seta slender, pointed, striate, 10 (–13) μm in length; distal seta cylindrical, annulate, 6 (–7) μm in length, about 0.2 of the tarsal length. Cuticle of tarsus pubescent.

Pygidium. Tergum. Posterior margin waved. Relative lengths of setae: $a_1 = 10$, $a_2 = 13$, $a_3 = 15$, $st = 10$ (–12). Setae distinctly differentiated, a_1 short, clavate, pubescent; a_2 and a_3 slender and pubescent (Figs 1F, 2K); st thick and pubescent (Figs 1G, 2K). Distance $a_1\text{--}a_1$ as same long as a_1 ; distance $a_1\text{--}a_2$ 2.0 (–2.5) times as long as $a_2\text{--}a_3$; distance $st\text{--}st$ (1.5–) 1.6 times as long as st and 1.6 (–1.8) times as long as distance $a_1\text{--}a_1$.

Sternum (Figs 1G, 2L). Posterior margin with a deep indentation between b_1 . Relative lengths of setae ($a_1=10$): $b_1 = 33(–35)$, $b_2 = 13$ (–15). Seta b_1 cylindrical, thick and annulate; b_2 slender and short, pubescent. Distance $b_1\text{--}b_1$ (0.7–) 0.8 of length of b_1 ; distance $b_1\text{--}b_2$ (0.7–) 0.9 of b_2 .

Anal plate linguiform, glabrous, 2.0 times longer than broad, lateral margins concave in anterior part, posterior margin with three small lobes; two pairs of appendages present: inner one tiny and conical; outer one cylindrical and longer, (0.4–) 0.5 of the length of plate and with short pubescence (Figs 1G, 2L).

Etymology. The species is named after China where the type specimens were collected.

Distribution. China (Jiangsu). Only known from the type locality.

Remarks. *Colinauropus chinensis* sp. nov. is most similar to *C. haginoi* Scheller, 2009 from Philippines in the similar shape of the anal plate and absence of sclerotized plates on tergite I. They can be easily distinguished by the number of sclerotized plates on tergites II and VI (6 and 2 in *C. chinensis* sp. nov., vs. 8 and 4 in *C. haginoi*), length of setae on collum segment (sublateral setae 1.9–2.0 times as long as submedian setae in *C. chinensis* sp. nov. vs. 3.2 times in *C. haginoi*), and the shape of T_3 (subcylindrical, not clavate in *C. chinensis* sp. nov. vs. proximal half distinctly clavate in *C. haginoi*).

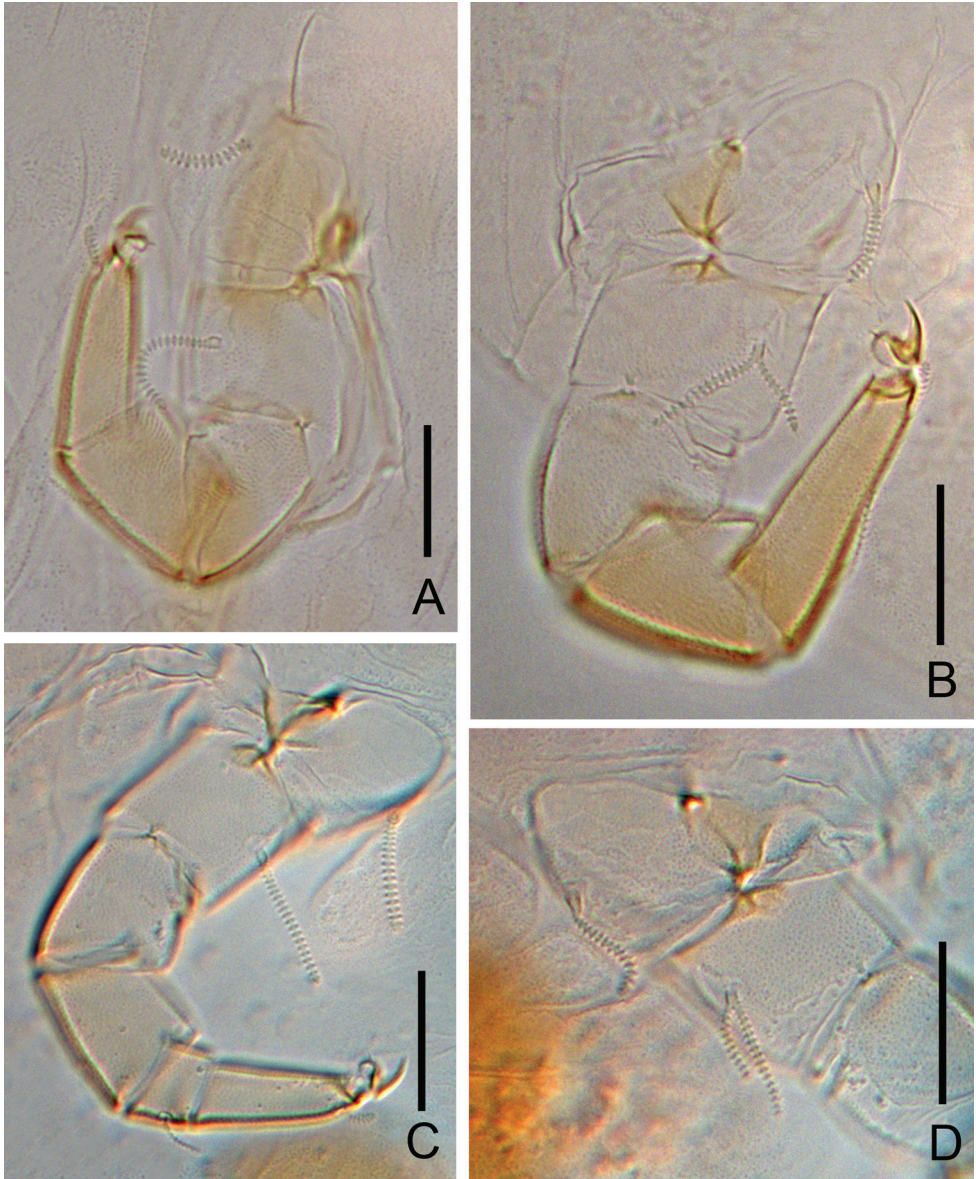


Figure 3. *Colinauropus chinensis* sp. nov. **A** leg 1 **B** leg 9 **C** leg 4 **D** coxa and trochanter of leg 9. Scale bars: 20 μ m.

***Colinauropus chongzhoui* sp. nov.**

<http://zoobank.org/9DB912C3-DB79-4AC1-8649-AAAC2985E274>

Figures 4–6

Material examined. *Holotype*, female adult with 9 pairs of legs (slide no. JS-WX-PA2018007), China, Jiangsu Province, Wuxi City, Daji Mountain, extracted from

soil samples in bamboo forest, elev. 5 m, 31°32'N, 120°12'E, 8-X-2018, coll. Y. Bu. Non-type specimens, 1 juvenile with 8 pairs of legs (slides no. JS-WX-PA2017034), 2 juveniles with 6 pairs of legs (slides no. JS-WX-PA2018008, JS-WX-PA2018009), same data as holotype.

Diagnosis. *Colinauropus chongzhoui* sp. nov. is characterized by the slender, annulate-striate setae on head, antennae and tergites; tergite I with 1 large sclerotized plate; tergite II with 6 small and 2 large sclerotized plates; tergites III–V each with 4 large and 4 small plates; tergite VI with 2 large plates; seta *st* on tergum of pygidium clavate; bothriotrichum T_3 brush-shaped, with branched pubescence distally.

Description. Adult body length 0.97 mm ($N = 1$); body white-yellow in alcohol, sclerotized plates on tergites brown (Fig. 5A).

Head (Figs 4A, 5C). Dorsal setae short, cylindrical, annulate-striate, except seta a_3 of second row which is slender and tapering. Relative lengths of setae, 1st row: $a_1 = 10$, $a_2 = 10$; 2nd row: $a_1 = 8$, $a_2 = 14$, $a_3 = 14$; 3rd row: $a_1 = 9$, $a_2 = 10$; 4th row: $a_1 = 12$, $a_2 = 14$, $a_3 = 21$, $a_4 = 12$; lateral group setae $l_1 = 23$, $l_2 = 21$, $l_3 = 19$; the ratio $a_1/a_1 - a_1$ in 1st row 1.5, 2nd row 0.6, 3rd row 0.9 and 4th row 0.7. Temporal organs oval in dorsal view, their length 1.1 times as long as their shortest distance apart. Pistil present. Head cuticle with dense granules.

Antennae (Figs 4E, 5B). Antennal segments 1–3 with 2, 2, 3 short, cylindrical, annulate setae respectively, and 1 rudimentary seta present on segment 3. Antennal segment 4 with 4 cylindrical setae and rudimentary seta *u*; relative lengths of setae: $p = 10$, $p' = 6$, $p'' = 6$, $r = 6$, $u = 1$; tergal seta *p* 1.1 times as long as tergal branch *t*; the latter cylindrical, 2.2 times as long as its greatest diameter and 0.9 of sternal branch *s*, which itself is 1.9 times as long as its greatest diameter. Seta *q* cylindrical, annulate, 1.3 times as long as *s*. Relative lengths of flagella (base segments included) and base segments: $F_1 = 100$, $bs_1 = 10$; $F_2 = 52$, $bs_2 = 5$; $F_3 = 88$, $bs_3 = 9$. F_1 6.4 times as long as *t*, F_2 and F_3 2.9 and 4.9 times as long as *s* respectively. Distal calyces spherical; apex of flagella fusiform, with a short lateral flap. Globulus *g* 1.7 times as long as wide; about 12 bracts, capsule spherical; width of *g* 0.5 of the greatest diameter of *t*. Antennal cuticle densely granulated.

Trunk. Setae on collum segment cylindrical, annulate; sublateral setae length 23 μ m, 2.1 times as long as submedian setae; sternite process triangular, furcate and granulated; appendages cylindrical and tapering (Fig. 5D). Tergite I with 4+4 cylindrical setae (12–13 μ m) and 1 large sclerotized plate (Fig. 5E) (2 plates in juveniles, Fig. 5F); Tergite II with 6+6 setae (12–23 μ m), 6 small anterior and 2 large posterior sclerotized plates (Figs 4B, 5G); Tergites III–V each with 6+6 setae (6–27 μ m), 4 large and 4 small sclerotized plates (Fig. 5H–J); Tergite VI with 4+2 setae and 2 large plates (Fig. 5K), posterior setae 23 μ m long, their mutual distance 18 μ m (Fig. 5K). Sclerotized plates with dense, brown granules, diameter 2–4 μ m, and each granule with one short straight apical hair (Fig. 4B). Other areas of cuticle on tergites with coarse granules.

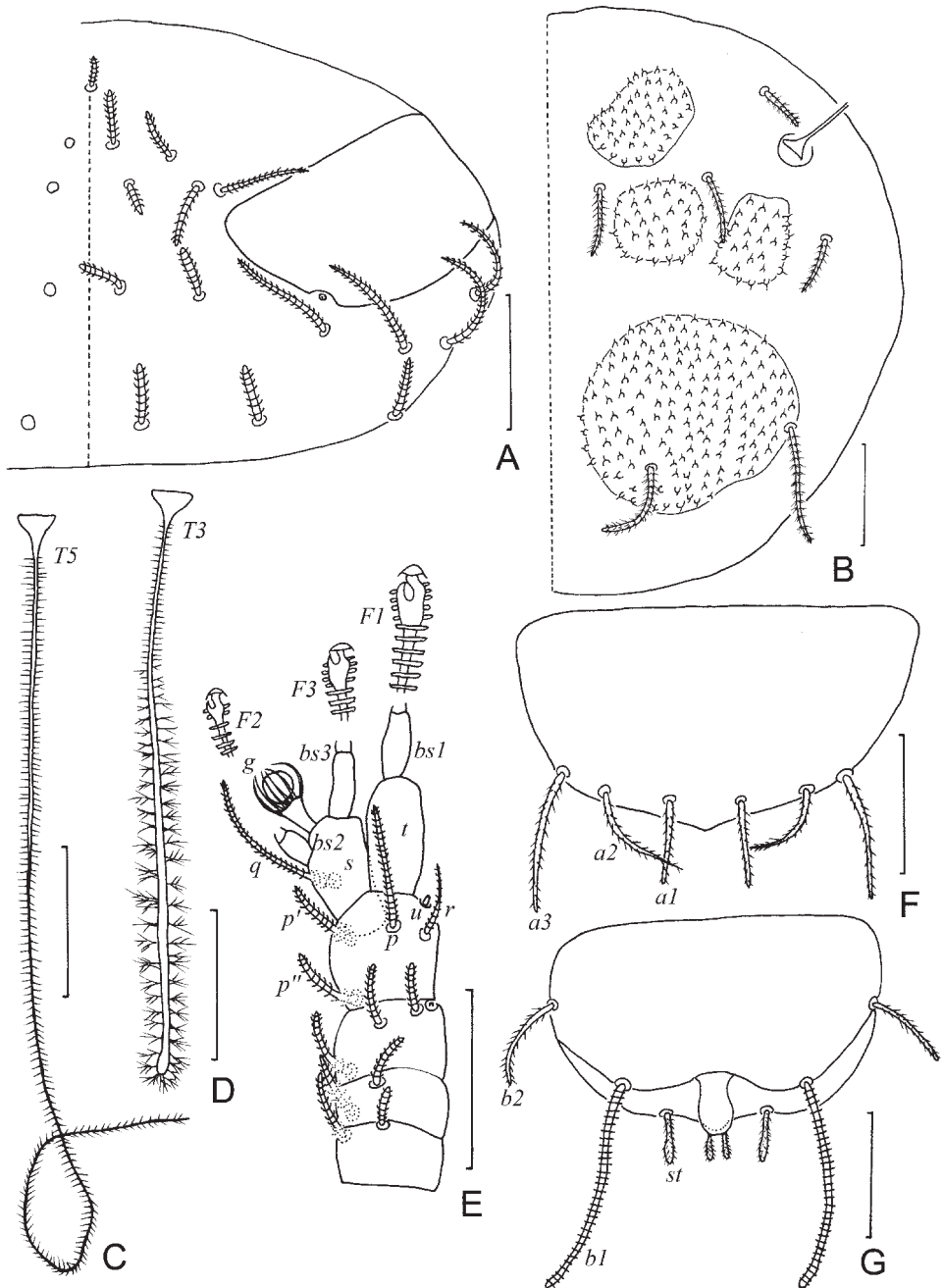


Figure 4. *Colinauropus chongzhoui* sp. nov. **A** head, dorsal view, right side **B** tergite II, right side **C** T₅, **D** T₃ **E** right antenna, tergal view **F** tergum of pygidium **G** sternum of pygidium and anal plate. Scale bars: 20 μm.

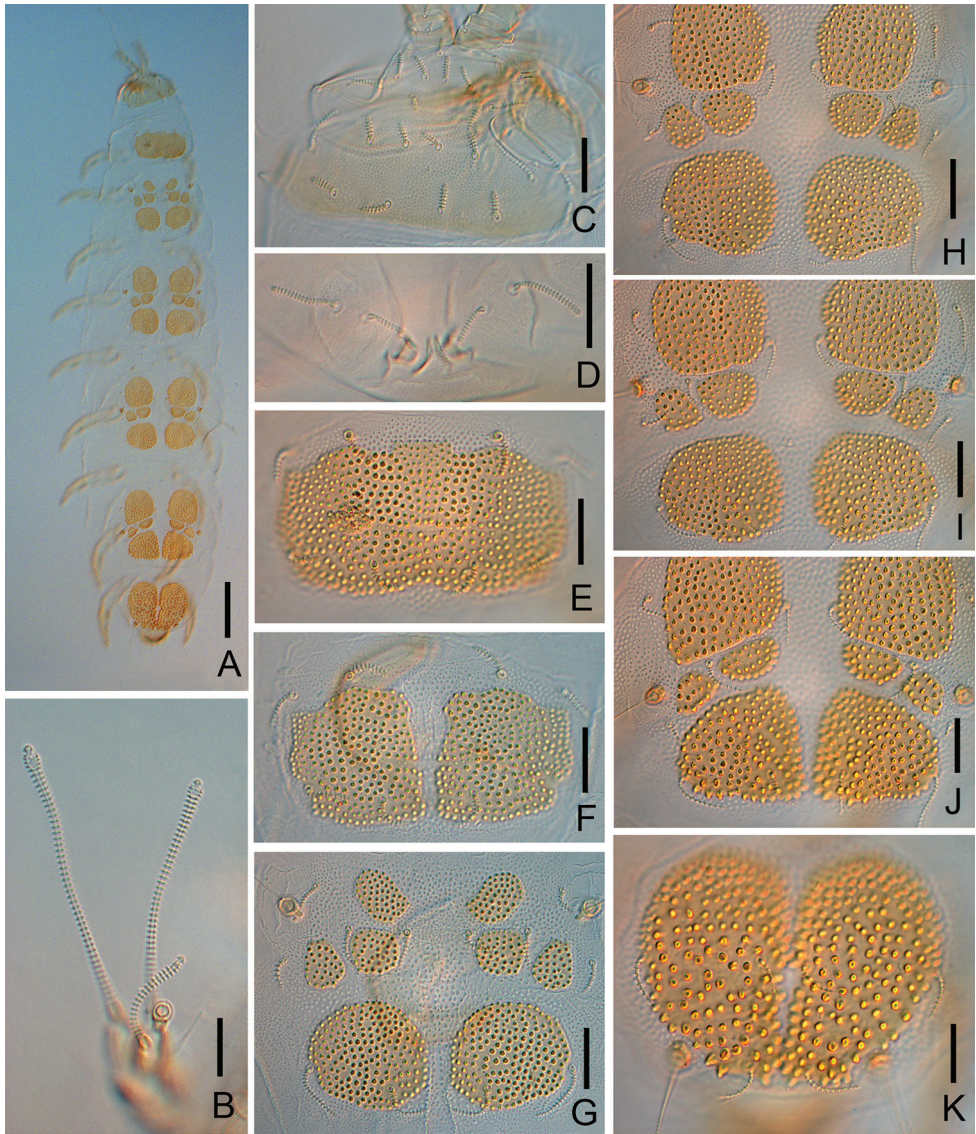


Figure 5. *Colinauropus chongzhoui* sp. nov. **A** habitus, tergal view **B** left antenna, sternal view **C** head, dorsal view **D** collum segment, sternal view **E** tergite I of adult **F** tergite I of juvenile **G** tergite II **H** tergite III **I** tergite IV **J** tergite V **K** tergite VI. Scale bars: 100 μm (**A**); 20 μm (**B–K**).

Bothriotricha. Relative lengths: $T_1 = 100$, $T_2 = 113$, $T_3 = 86$, $T_4 = 118$, $T_5 = 167$. T_1 , T_2 , T_4 and T_5 thin, long, with short erect or oblique pubescence on axis (Fig. 4C). T_3 brush-shaped, with thicker axis and branched pubescence in distal 2/3 (Figs 4D, 6E).

Legs. First and last pair of legs 5-segmented, others 6-segmented. Setae on coxa and trochanter of legs 1–8 cylindrical, annulate, length 13–15 μm and 16–20 μm respectively (Fig. 6D). Setae on coxa of leg 9 cylindrical, annulate, length 12 μm (Fig. 6C). Seta

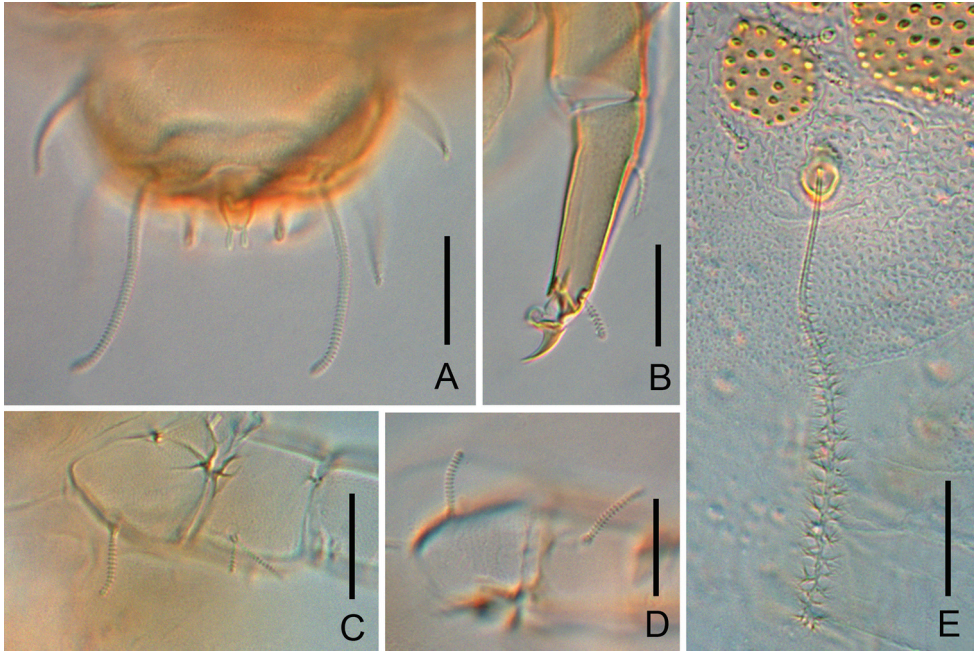


Figure 6. *Colinauropus chongzhoui* sp. nov. **A** sternum of pygidium and anal plate **B** tarsus of leg 9 **C** coxa and trochanter of leg 9 **D** coxa and trochanter of leg 1 **E** T_3 . Scale bars: 20 μm .

on trochanter of leg 9 furcate, with two subcylindrical, annulate, blunt branches, shorter one about 0.5 of longer one (Fig. 6C). Tarsi 1–8 with short annulate distal seta (8 μm) only. Tarsus of leg 9 tapering, 40 μm in length, 3.6 times as long as its greatest diameter (Fig. 6B), proximal seta slender, pointed, striate, 11 μm in length; distal one cylindrical, annulate, 9 μm in length, about 0.2 of the tarsal length. Cuticle of tarsus pubescent.

Pygidium. Tergum. Posterior margin blunt triangular. Relative lengths of setae: $a_1 = 10$, $a_2 = 12$, $a_3 = 16$, $st = 5$. Setae distinctly differentiated, a_1 cylindrical, pubescent; a_2 and a_3 slender, pubescent (Fig. 4F); st short, clavate, pubescent (Figs 4G, 6A). Distance $a_1 - a_1$ 0.7 of length of a_1 ; distance $a_1 - a_2$ 1.6 times as long as $a_2 - a_3$; distance $st - st$ 2.0 times as long as st and 1.5 times as long as distance $a_1 - a_1$.

Sternum (Figs 4G, 6A). Posterior margin with one lower indentation between b_1 . Relative lengths of setae ($a_1 = 10$): $b_1 = 28$, $b_2 = 12$. Seta b_1 cylindrical, thick, annulate; b_2 slender, short, pubescent. Distance $b_1 - b_1$ 0.8 of length of b_1 ; distance $b_1 - b_2$ 0.9 of b_2 .

Anal plate linguiform, 1.7 times longer than broad; a pair of clavate appendage inserted posteriorly, 0.4 of the length of plate, and with short pubescence (Figs 4G, 6A).

Etymology. The species is dedicated to the honor of the late Professor Chongzhou Zhang (1930–2014) who was an eminent zoologist from Institute of Zoology, Chinese Academy of Sciences, for his great contribution to the knowledge of Myriapoda of China (Stoev et al. 2014).

Distribution. China (Jiangsu). Only known from the type locality.

Remarks. *Colinauropus chongzhoui* sp. nov. is similar to *Colinauropus regis* Remy, 1956 in the shape of anal plate. They can be easily distinguished by the number of sclerotized plates on tergite I (1 large plate in *C. chongzhoui* sp. nov. vs. 2 in *C. regis*) and tergite II (8 in *C. chongzhoui* sp. nov., vs. 6 in *C. regis*), shape of setae on tergites (slender and striate in *C. chongzhoui* sp. nov. vs. clavate and pubescent in *C. regis*), and the shape of seta a_1 on pygidium (tapering in *C. chongzhoui* sp. nov. vs. clavate in *C. regis*).

***Colinauropus foliosus* sp. nov.**

<http://zoobank.org/867E5192-CE51-4339-947B-7C17D668C86E>

Figures 7–9

Material examined. *Holotype*, female adult with 9 pairs of legs (slide no. SC-PA2017002), China, Sichuan Province, Ganzi Tibetan Autonomous Region, Kangding City, Yala town, 30°06'N, 101°57'E, elev. 3100 m, soil samples from mixed forest, 11-VIII-2017, coll. C.W. Huang. *Paratypes*, 1 male adult with 9 pairs of legs (slides no. SC-PA2017001) and 1 female adult with 9 pairs of legs (slide no. SC-PA2017003), same data as holotype.

Diagnosis. *Colinauropus foliosus* sp. nov. is characterized by the leaf-shaped pubescent setae on head and tergites; tergite I with one large sclerotized plate; tergites II–IV each with 4 large and 4 small plates; tergite V with 4 large and 2 small middle sclerotized plates; tergite VI with 2 large plates; granules on plates ovoid, each inserted with one fine hair; seta *st* on tergum of pygidium clavate; bothriotrichum T_3 with thick axis and dense tufted pubescence distally.

Description. Adult body length 1.28 (–1.32) mm ($N = 3$); body white-yellow in alcohol, sclerotized plates on tergites brown (Fig. 8A).

Head (Figs 7A, 8D). Dorsal setae distinctly differentiated, on first and second rows cylindrical to tapering; on third and fourth rows leaf-shaped and with long pubescence; seta a_3 of second row slender and tapering. Relative lengths of setae, 1st row: $a_1 = 10$, $a_2 = 10$ (–12); 2nd row: $a_1 = 10$ (–11), $a_2 = (11–) 12$, $a_3 = 12$ (–13); 3rd row: $a_1 = (18–) 20$, $a_2 = 18$ (–20); 4th row: $a_1 = 13$ (–16), $a_2 = (15–) 17$, $a_3 = 20$ (–23), $a_4 = 16$ (–17); lateral group setae $l_1 = 18$ (–24), $l_2 = 18$ (–23), $l_3 = 25$ (–32); the ratio $a_1/a_1 - a_1$ in 1st row (1.6–) 1.7, 2nd row (0.7–) 0.8, 3rd row 1.0 (–1.1) and 4th row 0.7 (–0.8). Temporal organs oval in dorsal view, their length (0.8–) 0.9 of their shortest distance apart. Pistil present. Head cuticle with coarse granules.

Antennae (Figs 7C, 8B, C). Antennal segments 1–3 with 2, 2, 3 short cylindrical pubescent setae respectively, and 1 rudimentary seta present on segment 3. Antennal segment 4 with 4 tapering setae and a short, rudimentary *u*; relative lengths of setae: $p = 10$, $p' = 7$ (–8), $p'' = (6–) 7$, $r = 5$ (–6), $u = 1$; tergal seta *p* (0.9 of –) 1.0 times as long as tergal branch *t*; the latter cylindrical, 1.8 (–2.0) times as long as its greatest diameter and 0.7 (–0.9) of sternal branch *s*, which itself about 2.0 times as long as its greatest diameter. Seta *q* cylindrical, annulate, 0.8 (–1.0 times as long as) of *s*. Relative lengths of flagella (base segments included) and base segments: $F_1 = 100$, $bs_1 = 8$ (–11); $F_2 = (35–) 42$, $bs_2 = (4–) 5$; $F_3 = (78–) 93$, $bs_3 = 7$ (–9). F_1 (5.8–) 8.6 times as long as *t*, F_2

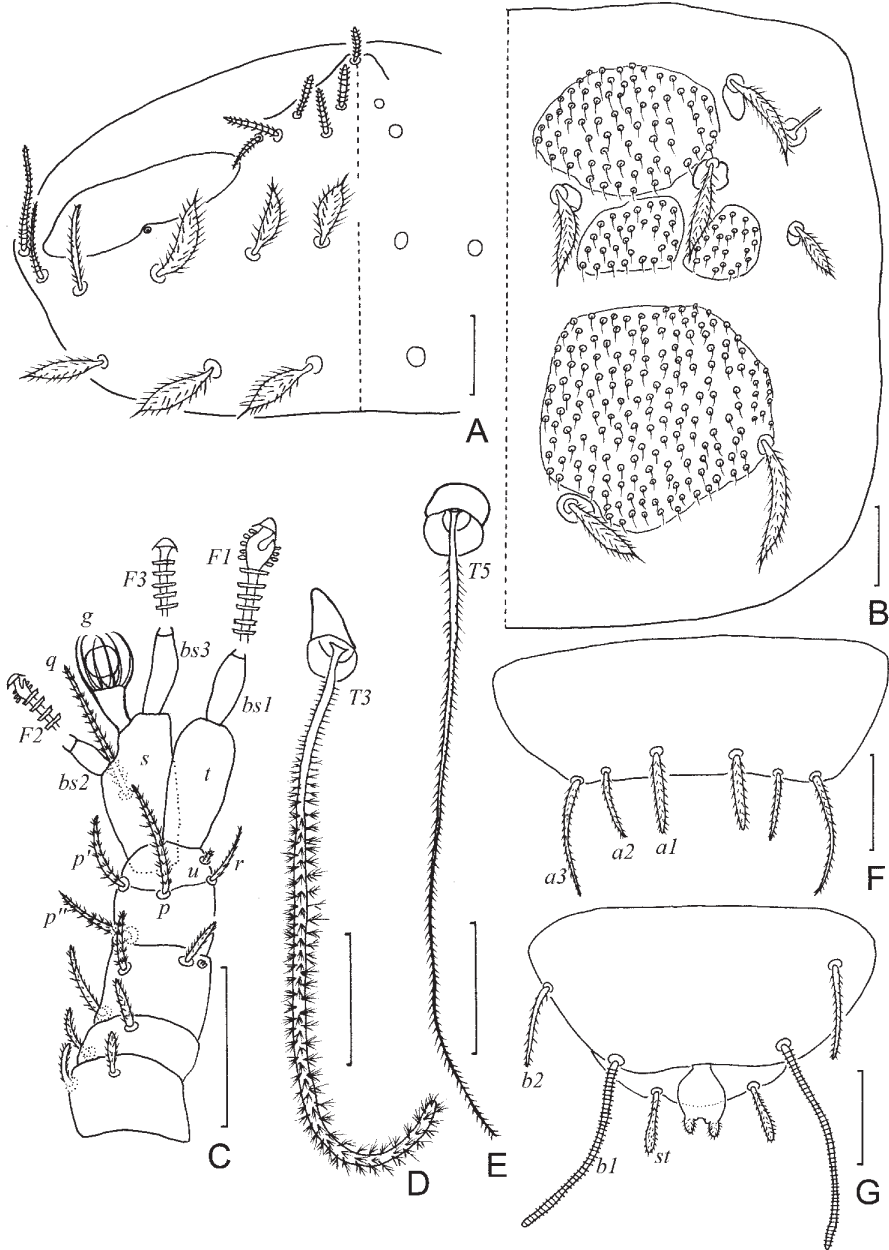


Figure 7. *Colinauropus foliosus* sp. nov. **A** head, dorsal view, left side **B** tergite II, right side **C** right antenna, tergal view **D** T_3 **E** T_5 **F** tergum of pygidium **G** sternum of pygidium and anal plate. Scale bars: 20 μ m.

and F_3 2.0 (-2.1) and 4.4 (-4.8) times as long as s respectively. Distal calyces spherical; apex of flagella fusiform, on F_1 and F_3 with a short lateral flap. Globulus g 1.7 times as long as wide; about 12 bracts, capsule spherical; width of g (0.4-) 0.6 of the greatest diameter of t . Antennal cuticle granulated.

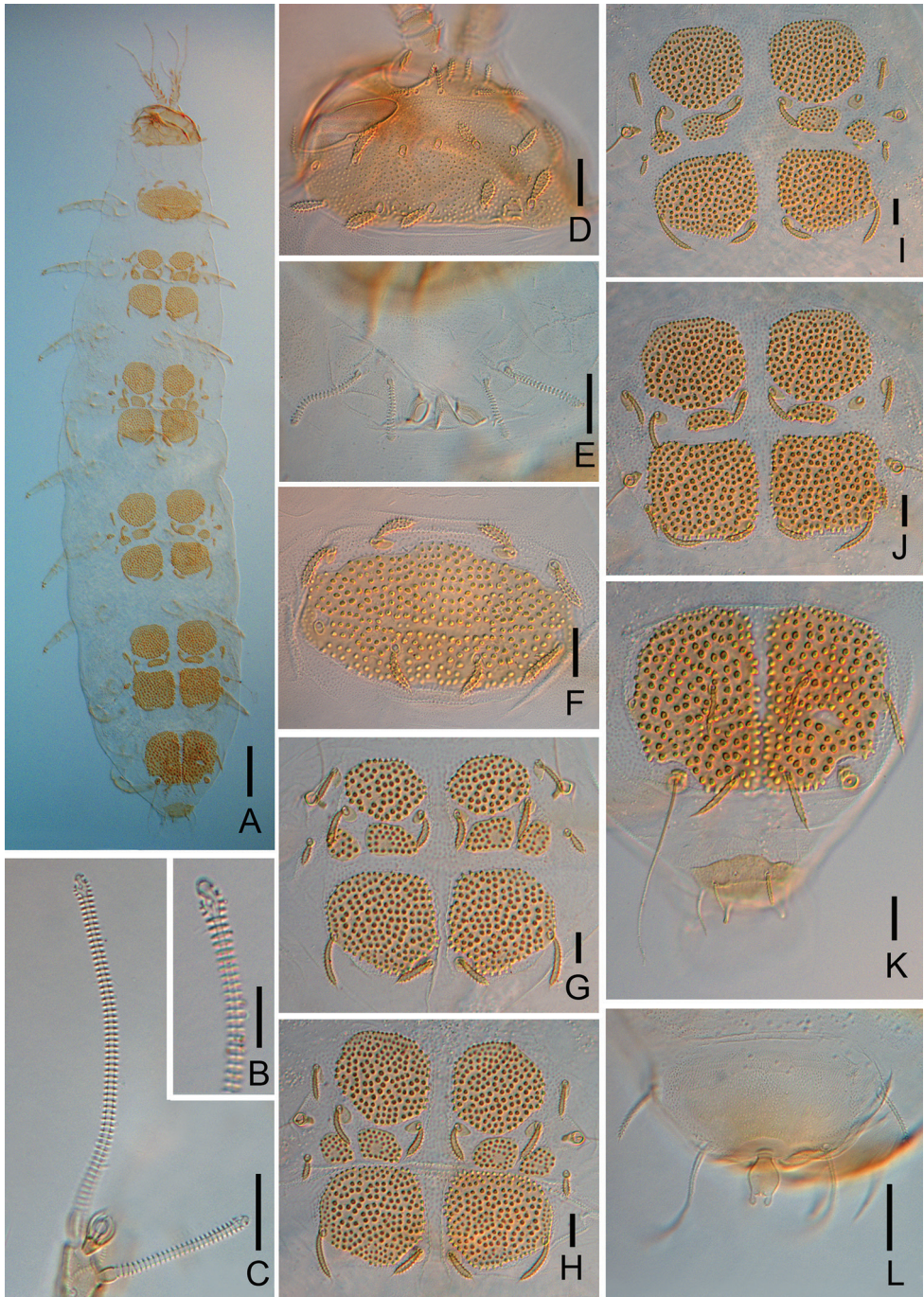


Figure 8. *Colinauropus foliosus* sp. nov. **A** habitus, tergal view **B** terminal part of F_1 **C** sternal branch of left antenna, show F_2 , F_3 and globulus **D** head, dorsal view **E** collum segment, sternal view **F** tergite I **G** tergite II **H** tergite III **I** tergite IV **J** tergite V **K** tergite VI and tergum of pygidium **L** sternum of pygidium and anal plate. Scale bars: 100 μm (**A**); 20 μm (**B–K**).

Trunk. Setae on collum segment cylindrical, annulate; sublateral setae length 22 (–34) μm , (1.4–) 1.7 times as long as submedian setae; sternite process triangular, furcate and granulated; appendages tapering (Fig. 8E). Tergite I with 4+4 leaf-shaped setae (22–27 μm) and 1 large sclerotized plate (Fig. 8F); Tergites II–IV each with 6+6 setae (18–40 μm), 4 large and 4 small sclerotized plates (Figs 7B, 8G–I); Tergite V with 6+6 slender setae (20–40 μm), 4 large and 2 small sclerotized plates, posterior plates square (Figs 8J, 9A); Tergite VI with 4+2 setae and 2 large plates (Fig. 8K), posterior setae 35 μm long, their mutual distance 24 (–26) μm (Fig. 8K). Sockets of some setae on tergites and bothriotricha with distinct thickened cuticle surrounded (Figs 7B, D, E, 8F–J). Sclerotized plates with ovoid, brown granules, diameter 1.5–5.0 μm and each with one long curved hair (Figs 7B, 9A). Cuticle granulated or pubescent.

Male genital papillae (Fig. 9E) glabrous, subuliform, 1.5 times as long as greatest diameter; seta 0.5 of the length of papilla. Seta on coxa of leg 2 in male with two adjacent setae (only 1 thick setae in female, 20–25 μm), both cylindrical and annulate, one thick and short, 17 μm in length, another slender and longer, 20 μm in length (Fig. 9E).

Bothriotricha. Relative lengths: $T_1 = 100$, $T_2 = (110\text{--}) 100$, $T_3 = (95\text{--}) 105$, $T_4 = 114$ (–120), $T_5 = (115\text{--}) 120$. T_1 , T_2 , T_4 and T_5 thin, long, with short erect pubescence on axes (Fig. 7E). T_3 cylindrical, with thicker axis and dense tufted pubescence in distal 2/3 part (Fig. 7D).

Legs. First and last pair of legs 5-segmented, others 6-segmented (Fig. 9C, D). Setae on coxa and trochanter of legs 1–8 cylindrical, annulate (Fig. 9B), length 23 (–26) μm and 23 (–27) μm respectively. Seta on coxa of leg 9 cylindrical, annulate, length 22 (–25) μm (Fig. 9D). Seta on trochanter of leg 9 furcate, with subcylindrical, annulate, blunt branches, shorter branch about 0.5 of longer one (Fig. 9D). Tarsi 1–8 with short, annulate distal seta (6–8 μm) only (Fig. 9C). Tarsus of leg 9 tapering, 48 (–55) μm in length, 3.7 (–4.2) times as long as its greatest diameter (Fig. 9F), proximal seta slender, pointed, pubescent, 12 (–15) μm in length; distal one cylindrical, annulate, 6 (–8) μm in length, about 0.1 of the tarsal length. Cuticle of tarsus pubescent.

Pygidium. Tergum. Posterior margin straight. Relative lengths of setae: $a_1 = 10$, $a_2 = (8\text{--}) 9$, $a_3 = (12\text{--}) 16$, $st = (7\text{--}) 9$. Setae a_1 cylindrical, pubescent; a_2 and a_3 slender and pubescent (Figs 7F, 8K); st clavate, pubescent (Fig. 7G). Distance $a_1\text{--}a_1$ (0.6–) 0.8 of a_1 ; distance $a_1\text{--}a_2$ 2.0 (–2.5) times as long as $a_2\text{--}a_3$; distance $st\text{--}st$ (1.5–) 1.6 times as long as st and (1.7–) 2.0 times as long as distance $a_1\text{--}a_1$.

Sternum (Figs 7G, 8L). Posterior margin straight between b_1 . Relative lengths of setae ($a_1 = 10$): $b_1 = (25\text{--}) 29$, $b_2 = 14$ (–15). Seta b_1 cylindrical, thick, annulate; b_2 tapering, short, pubescent. Distance $b_1\text{--}b_1$ (0.7–) 0.8 of length of b_1 ; distance $b_1\text{--}b_2$ (0.6–) 0.7 of b_2 .

Anal plate round, glabrous, 1.5 times longer than broad, lateral margins bulged in middle part, posterior part divided into two round, pubescent branches, two tiny lobes present at inner side (Figs 7G, 8L).

Etymology. The species name “*foliosus*” from the Latin “*foliose*”, leaf-shaped, referring to the leaf-shaped setae on head and tergites.

Distribution. China (Sichuan). Only known from the type locality.

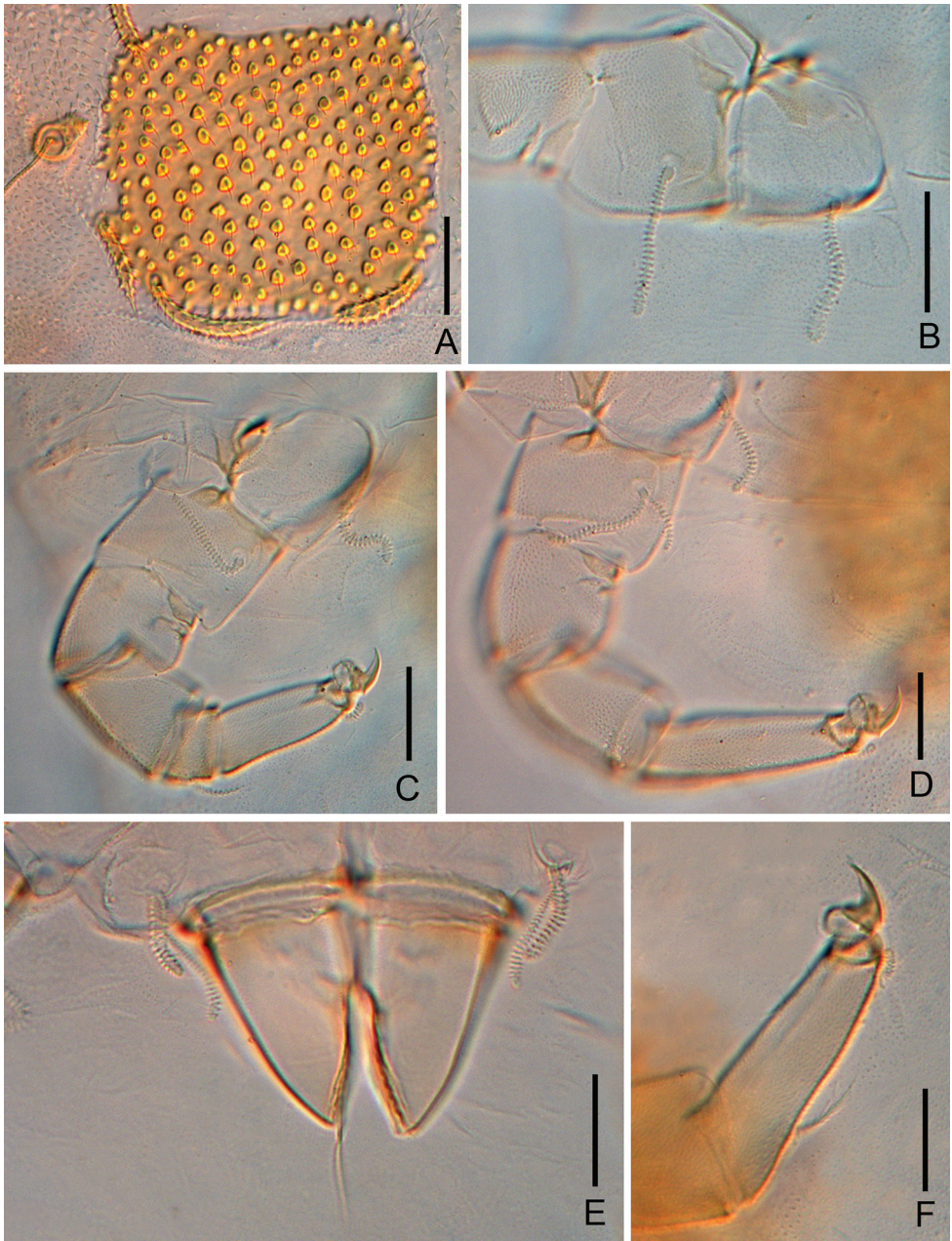


Figure 9. *Colinauropus foliosus* sp. nov. **A** posterior plate on tergite V, left side **B** coxa and trochanter of leg 2 **C** leg 8 **D** leg 9 **E** male genital papillae and coxa of leg 9 **F** tarsus of leg 9. Scale bars: 20 μ m.

Remarks. *Colinauropus foliosus* sp. nov. differs from all other congeners by having 6 sclerotized plates on tergite V, and the posterior two square-shaped, compared with 4 or 8 irregular plates in congeners. It is similar to *C. regis* Remy, 1956 in the leaf-shaped setae on tergites, but they can be easily distinguished by the number of sclerotized

plates on tergite I and II (1 and 8 in *C. foliosus* sp. nov. vs. 2 and 6 in *C. regis*), shape of the setae in the posterior two rows of the head (leaf-shaped in *C. foliosus* sp. nov. vs. cylindrical in *C. regis*), and the shape of anal plate (with two round posterior branches in *C. foliosus* sp. nov. vs. with two clavate appendages in *C. regis*).

Key to the species of the genus *Colinauropus* Remy, 1956

- 1 Tergite I without sclerotized plates, at most with two posterior thickened patches..... **2**
- Tergite I with distinct sclerotized plates..... **3**
- 2 Tergite II with 4 large and 4 small sclerotized plates, tergite VI with 4 plates..... ***C. haginoi* Scheller, 2009 (Philippines)**
- Tergite II with 2 large and 4 small sclerotized plates, tergite VI with 2 plates..... ***C. chinensis* sp. nov. (China)**
- 3 Tergite I with 1 large sclerotized plate **4**
- Tergite I with 2 sclerotized plates **5**
- 4 Setae on head and tergite cylindrical, tergite II with 2 large and 6 small sclerotized plates..... ***C. chongzhoui* sp. nov. (China)**
- Setae on head and tergite leaf-shaped, tergite II with 4 large and 4 small sclerotized plates..... ***C. foliosus* sp. nov. (China)**
- 5 Tergites II and V with 6 and 8 sclerotized plates respectively, anal plate rounded with 2 posterior appendages, setae on tergites II–V clavate..... ***C. regis* Remy, 1956 (Réunion, Mauritius)**
- Tergites II and V with 8 and 4 sclerotized plates respectively, anal plate indented mediodistally without appendages, setae on tergites II–V cylindrical...
..... ***C. schelleri* Hagino, 1991 (Japan)**

Discussion

The genus *Colinauropus* Remy, 1956 is well defined by the presence of sclerotized plates on the tergites. The number of plates on tergites I, II, V and VI, which varies from 1 to 8, are good characters for species identification, while tergites III and IV always have 8 plates in all species. The shape and arrangement of the plates are also taxonomically informative for species definition. On tergite I, the plates are absent or at most with small patches of thickened cuticle posteriorly (*C. haginoi*, *C. chinensis* sp. nov.), with 1 complete large plate (*C. chongzhoui* sp. nov., *C. foliosus* sp. nov.) or with 2 axially separated plates (*C. regis*, *C. schelleri*). On tergite II, 4 small anterior plus 2 large posterior plates are present in *C. regis* and *C. chinensis* sp. nov., 6 small anterior plus 2 large posterior plates are present in *C. chongzhoui* sp. nov., while there are 4 small plus 4 large plates in the remaining three species. On tergite V, the number of plates can be 4 in *C. schelleri*, 4 large plus 2 small middle plates in *C. foliosus* sp. nov., and 4 large plus 4 small plates in others. On tergite VI, all species have 2 large plates, except *C. haginoi* which has 4 plates. The shapes of plates are usually ovoid, round, sub-triangular, or irregular, while the two pos-

terior large plates on tergite V are nearly square-shaped in *C. foliosus* sp. nov. Variation of plates within a species has never been reported in former studies but is observed here in *C. chongzhoui* sp. nov., which exhibits 2 plates on tergite I in juveniles vs. 1 complete plate in adults. Thus, caution is advised when describing species of this genus, which should be based on fully mature specimens. As an additional taxonomic character, the bothriotrichum T_3 is also well differentiated and nicely separates species. The most informative characters are the shape and appendages of the anal plates. The six known species of the genus *Colinauropus* Remy, 1956 can be distinguished by the key provided above.

Acknowledgements

I thank Dr Osami Nakamura (Japan) and Prof. Claude Tautel (France) for their help in sending some reprints of references, Dr Chang-Yuan Qian also shared several references, Mr Chengwang Huang collected the specimens from Sichuan. I also cordially thank Dr Nikolaus Szucsich (Austria) and another anonymous referee for their valuable comments during the review of the manuscript. This research is supported by the National Natural Science Foundation of China (no. 31772509) and the Research Foundation of Shanghai Science and Technology Museum.

References

- Hagino Y (1991) New species of the family Pauropodidae (Pauropoda) from Central Japan. *The Canadian Entomologist* 123(5): 1009–1045. <https://doi.org/10.4039/Ent1231009-5>
- Hagino Y (2005) Contribution to the knowledge of the Japanese pauropod fauna I: A cumulative list of identified pauropod specimens from Japan during 1985–2003. *Natural History Research* 8(2): 15–51.
- Qian CY, Bu Y, Dong Y, Luan YX (2018) Study on the Pauropoda from Tibet, China. Part I. The genera *Decapauropus* and *Hemipauropus* (Myriapoda). *ZooKeys* 754: 33–46. <https://doi.org/10.3897/zookeys.754.24210>
- Remy PA (1956) Un nouveau Pauropode de l'île de la Réunion: *Colinauropus regis* n. g., n. sp. *Bulletin du Muséum national d'Histoire naturelle* 28(1): 119–123.
- Remy PA (1959) Pauropodes de l'île Maurice. *The Mauritius Institute Bulletin* 5(5): 149–194.
- Scheller U (1985) On the classification of the family Brachypauropodidae (Myriapoda; Pauropoda). *Bijdragen tot de Dierkunde* 55(1): 202–208.
- Scheller U (2009) Records of Pauropoda (Pauropodidae, Brachypauropodidae, Eurypauropodidae) from Indonesia and the Philippines with descriptions of a new genus and 26 new species. *International Journal of Myriapodology* 2: 69–148. <https://doi.org/10.1163/187525409X12577705044548>
- Scheller U (2011) Pauropoda. In: Minelli A (Ed.) *Treatise on Zoology-Anatomy, Taxonomy, Biology: the Myriapoda* (Vol. 1). Brill, Leiden, 467–508. https://doi.org/10.1163/9789004188266_022
- Stoev P, Li SQ, Meng K (2014) In memoriam Chong-zhou Zhang [1930–2014]. *Bulletin du Centre International de Myriapodologie* 47: 25–29.

Diversity and distribution of *Epeorus* (*Caucasiron*) (Ephemeroptera, Heptageniidae) in Iran, with descriptions of three new species

Luboš Hrivniak^{1,2}, Pavel Sroka¹, Jindřiška Bojková³, Roman J. Godunko^{1,4}, Javid Imanpour Namin⁵, Samereh Bagheri⁵, Farshad Nejat⁶, Ashgar Abdoli⁶, Arnold H. Staniczek⁷

1 Biology Centre of the Czech Academy of Sciences, Institute of Entomology, Branišovská 31, 37005 České Budějovice, Czech Republic **2** Faculty of Sciences, University of South Bohemia, Branišovská 31, 37005 České Budějovice, Czech Republic **3** Department of Botany and Zoology, Masaryk University, Kotlářská 2, 61137 Brno, Czech Republic **4** Department of Invertebrate Zoology and Hydrobiology, University of Łódź, Banacha 12/16, 90237 Łódź, Poland **5** Department of Fishery, Faculty of Natural Resources, University of Guilan, POB 1144, Sowmehsara-Rasht, Iran **6** Department of Biodiversity and Ecosystem Management, Environmental Sciences Research Institute, Shahid Beheshti University, Daneshjou Boulevard, 1983969411 Tehran, Iran **7** Department of Entomology, State Museum of Natural History Stuttgart, Rosenstein 1, 70191 Stuttgart, Germany

Corresponding author: Luboš Hrivniak (lubos.hrivniak@gmail.com)

Academic editor: B. Price | Received 18 February 2020 | Accepted 5 May 2020 | Published 8 July 2020

<http://zoobank.org/3297FBE4-111C-4849-9533-225A53F7DB3C>

Citation: Hrivniak L, Sroka P, Bojková J, Godunko RJ, Namin JI, Bagheri S, Nejat F, Abdoli A, Staniczek AH (2020) Diversity and distribution of *Epeorus* (*Caucasiron*) (Ephemeroptera, Heptageniidae) in Iran, with descriptions of three new species. ZooKeys 947: 71–102. <https://doi.org/10.3897/zookeys.947.51259>

Abstract

Combining morphological and molecular data in an integrative approach, three new mayfly species of *Epeorus* (*Caucasiron*) are described. These include *Epeorus* (*Caucasiron*) *alborzicus* Hrivniak & Sroka, **sp. nov.** and *Epeorus* (*Caucasiron*) *shargi* Hrivniak & Sroka, **sp. nov.** from northern Iran, and *Epeorus* (*Caucasiron*) *zagrosicus* Hrivniak & Sroka, **sp. nov.** from central Iran. They are unambiguously delimited using both distance-based and likelihood-based approaches in the analyses of barcode COI sequences. Each new species is compared with other species of the subgenus and morphological diagnostic characters are provided. Based on extensive sampling of streams throughout the country, the distribution and habitat preferences of all *Caucasiron* species in Iran are assessed. Altogether, there are now six species recorded, among them also *E. (C.) nigripilosus* Sinitshenkova, 1976 is reported for the first time in Iran. Five species are distributed in the Alborz Mts. in northern Iran, one species was found in the Zagros Mts. in central Iran.

Keywords

barcoding, Caucasus, diversity, mayflies, Middle East, taxonomy

Introduction

The genus *Epeorus* Eaton, 1881, subgenus *Caucasiron* Kluge, 1997 represents a group of mountainous mayflies distributed in Palaearctic region. Kluge (1997) defined *Caucasiron* based on a unique larval apomorphy, a projection on the costal margin of gill plates II–VII. Other larval diagnostic characters include the presence of medio-dorsally directed hair-like setae along anterior margin of head and gill plates forming a so-called "adhesive disc", consisting of enlarged gill plate I and overlapping gill plates II–VII. Gill plate VII has a longitudinal fold allowing to bend the plate ventrally under the abdominal segments. The systematic position of *Caucasiron* within *Epeorus*-related taxa was unclear for a long time (e.g., Braasch 2006, Kluge 2015). The recent study by Hrivniak et al. (2020) confirmed its monophyly and subgeneric position within *Epeorus* s.l. Moreover, the study pointed out its close phylogenetic relationship with the subgenus *Iron* Eaton, 1883 distributed in Central Asia and Nearctic realm.

Caucasiron occurs in the Eastern Mediterranean (Samos and Cyprus Island), Anatolia, Caucasus, and central and western Asia (Hrivniak et al. 2019, 2020). Their larvae inhabit riffle sections of montane and submontane streams with coarse bed substrate (Nguyen et al. 2004; Bauernfeind and Soldán 2012). At present there are 17 species described (Hrivniak et al. 2020), but apparently several Central Asian taxa described in the genus *Iron* rather belong to *Caucasiron* (Chen et al. 2010; Hrivniak et al. 2017). In any case, a taxonomic revision of these species is needed to clarify their systematic position.

The highest species richness of *Caucasiron* and a remarkable regional and local endemism was found in the Caucasus Mountains (Hrivniak et al. 2017; Hrivniak et al. 2020), which represent one of the world biodiversity hotspots (Myers et al. 2000). The 12 species known from the Caucasus and adjacent areas are as follows: *E. (C.) caucasicus* (Tshernova, 1938), *E. (C.) znojkoii* (Tshernova, 1938), *E. (C.) nigripilosus* (Sinitshenkova, 1976), *E. (C.) magnus* (Braasch, 1978), *E. (C.) alpestris* (Braasch, 1979), *E. (C.) soldani* (Braasch, 1979), *E. (C.) sinitshenkovae* (Braasch & Zimmermann, 1979), *E. (C.) longimaculatus* (Braasch, 1980), *E. (C.) bicolliculatus* Hrivniak, 2017, *E. (C.) turcicus* Hrivniak, Türkmen & Kazancı, 2019, *E. (C.) iranicus* (Braasch & Soldán, 1979), and *E. (C.) insularis* (Braasch, 1983). The latter two species for a long time were considered as subspecies of *E. (C.) caucasicus* and *E. (C.) znojkoii*, respectively. The recent molecular study of the Caucasian *Caucasiron* fauna, however, confirmed all morphologically defined species/subspecies as distinct evolutionary lineages and, consequently, both subspecies were raised to species level (Hrivniak et al. 2020). Moreover, the delimitation of several additional evolutionary lineages indicated that the diversity of *Caucasiron* in the Caucasus region could be even higher. However, these lineages have remained without formal description to date (Hrivniak et al. 2020).

Individual *Caucasiron* species exhibit different distribution patterns within the Caucasus region varying from an endemic distribution in the Greater Caucasus to a wide distribution covering distant regions in the Pontic Mountains, Lesser Caucasus, Zagros, and Alborz Mountains (Hrivniak et al. 2020). The highest species richness and endemism of *Caucasiron* is concentrated in the western and central part of the Greater Caucasus, the most prominent mountain range in the Caucasus region. However, the individual mountain ranges of the Caucasus have been studied to a different extent until now. Especially the Alborz Mountains, a southeast part of the Caucasus biodiversity hotspot, and the Zagros Mountains, a dominant part of the Irano-Anatolian biodiversity hotspot, have been left unattended without detailed investigation (Bojková et al. 2018). The only *Caucasiron* species described and known exclusively from Iran, *E. (C.) iranicus* (Braasch & Soldán, 1979), is distributed in the Alborz and most likely represents an endemic species of this mountain range. However, given the size and diversity of the Iranian territory and stream habitats, the diversity and endemism within *Caucasiron* can be expected to be much higher in Iran. Summarizing recent knowledge on the diversity and distribution of Iranian mayflies, Bojková et al. (2018) reported two species of *Caucasiron* from Iran, namely *E. (C.) iranicus* and *E. (C.) znojkoï*.

Based on morphology and molecular analyses, we describe in this integrative study, two new species of *Caucasiron* from the Alborz Mountains and one new species from the Zagros Mountains. We provide morphological diagnostic characters of the three new species and differential diagnoses between all species known from the Caucasus and adjacent areas, plus an analysis of respective COI sequences. Following recent studies on Iranian mayflies by Bojková et al. (2018), Sroka et al. (2019), and Staniczek et al. (2020), we also sum up all records of *Caucasiron* species from our recent Iranian field trips to further contribute to a systematic research of mayflies in Iran.

The main objectives of this study are to (i) describe the morphology of three new *Caucasiron* species and provide their differential diagnoses, (ii) apply the molecular species delimitation methods using analytical tools for the single-locus COI dataset, (iii) provide basic information about habitat requirements of the new species, and (iv) summarize the distribution of all *Caucasiron* species recently known from Iran.

Materials and methods

The material used for this study was collected by J. Bojková, T. Soldán, J. Imanpour Namin, and S. Bagheri in April and May 2016–2018, and A. Staniczek, M. Pallmann, R. J. Godunko, and F. Nejat in April and May 2017. All specimens were preserved in 75–96% EtOH and are deposited in the collections of the Biology Centre of the Czech Academy of Sciences, Institute of Entomology, České Budějovice, Czech Republic (IECA), State Museum of Natural History, Stuttgart, Germany (SMNS) and Natural History Museum and Genetic Resources, Department of Environment, Tehran, Iran (MMTT_DOE). Material of other *Caucasiron* species used for the morphological and molecular comparisons was obtained from the collection of IECA. This publica-

tion and the nomenclatural acts therein are registered with ZooBank under the LSID urn:lsid:zoobank.org:pub:3297FBE4-111C-4849-9533-225A53F7DB3C.

Morphological examination

Parts of specimens were mounted on microscopic slides using HydroMatrix (Micro-Tech Lab, Graz, Austria) mounting medium. In order to remove the muscle tissue for an investigation of the cuticular structures, specimens were left overnight in a 10% solution of NaOH prior to slide mounting. Drawings were made using a stereomicroscope Olympus SZX7 and a microscope Olympus BX41, both equipped with a drawing tube. Photographs were obtained using Leica DFC450 camera fitted with macroscope Leica Z16 APO and folded in Helicon Focus version 5.3 X64. All photographs were subsequently enhanced with Adobe Photoshop CS5. Diagnostic characters for the description of larva were chosen according to Braasch and Soldán (1979) and Braasch (2006). The terminology was used mostly according to Kluge and Novikova (2011) and Kluge (2004, 2015).

DNA extraction, PCR, sequencing and alignment

Total genomic DNA of the species (4–8 specimens/species) was extracted from legs using the DEP-25 DNA Extraction Kit (TopBio s.r.o., Prague, Czech Republic) according to the manufacturer's protocol. Mitochondrial cytochrome oxidase subunit I (COI) was sequenced according to Hrivniak et al. (2017). COI sequences of other *Caucasiron* species used for comparisons were obtained from Hrivniak et al. (2017) (GenBank accession nos KY865691–KY865725) and Hrivniak et al. (2019) (GenBank accession nos KY865691–KY865725). Three specimens of *E. (C.) iranicus* were additionally sequenced. The PCR amplification of COI and reaction volumes was carried out as described in Hrivniak et al. (2017). Sequences were assembled in Geneious 7.0.6 (<http://www.geneious.com>) and aligned in the same software using the Mafft 7.017 (Katoh et al. 2002) plugin with default settings. Newly obtained sequences are deposited in GenBank with accession numbers (GB) MN856180–MN856198.

Molecular species delimitation

Species were delimited using the single locus (COI) coalescence based General Mixed Yule Coalescent model (GMYC, Pons et al. 2006; Fusijawa and Barraclough 2013). We used the single-threshold GMYC model as it has been found to outperform the multi-threshold (Fusijawa and Barraclough 2013) and was found to be highly suitable for species delimitation within *Caucasiron* (Hrivniak et al. 2019). The GMYC model identifies independent evolutionary clusters by detecting a threshold value at the transition from interspecific to intraspecific branching patterns (Bryson et al. 2013). A maximum likelihood approach is used to optimize the shift in branching patterns. A likelihood ratio test assesses if the mixed model fits the data significantly better than a null model that

assumes a single coalescent process for the entire tree (Pons et al. 2006; Monaghan et al. 2009). Analyses were performed using the SPLITS package for R (<http://r-forge-project.org/projects/splits>). An ultrametric COI gene tree was reconstructed under relaxed molecular clock (uncorrelated lognormal distribution) using BEAST 2 (Bouckaert et al., 2014) on CIPRES Science Gateway 3.3 (Miller et al. 2010). An input file was generated in BEAUti 2. The substitution model was selected by bModelTest (Bouckaert and Drummond 2017) implemented in BEAUti 2 using a model averaging approach. A coalescent constant population tree prior was preferred, because the GMYC null model constitutes a single coalescent cluster (Monaghan et al. 2009; Zaldívar-Riverón et al. 2010; Vuataz et al. 2011). Other settings were default. Two analyses of MCMC chains were run for 50 million generations sampled every 5000 generations. Convergence and effective sample size (ESS > 200) were verified using Tracer 1.6. The first 10% of trees (1000) from each run were discarded as burn-in. The files from both independent runs were combined using LogCombiner 1.8.4. The maximum clade credibility tree was constructed from 18000 trees using TreeAnnotator 1.8.4 with default settings.

Inter- and intra-specific K2P pairwise genetic distances were calculated in MEGA 7 (Kumar et al. 2016). The distance matrix was analysed using Automatic Barcode Gap Discovery (ABGD) (Puillandre et al. 2012) (online version: <http://www.wabi.snv.jussieu.fr/public/abgd/>) with default settings. The method identifies so-called barcode gap that corresponds to threshold between intra- and inter-specific genetic distances and splits sequences to groups corresponding to putative species accordingly.

Results and discussion

Taxonomy

All of the species described below are attributed to the subgenus *Caucasiron* within the genus *Epeorus* based on the presence of projections on the costal rib of gill plates II–VII, and the presence of medio-dorsally directed hair-like setae located on the anterior margin of the head (see Kluge 2015 for a revision of the subgenus).

Epeorus (Caucasiron) alborzicus Hrivniak & Sroka, sp. nov.

<http://zoobank.org/F1721BB2-DC7C-4BBC-9AD2-8252A5D01EBF>

Figures 1, 2

Type material. Holotype: female mature larva: IRAN, Mazandaran Province, Panjab village, unnamed brook (LT of Haraz River); 36°05'52.8"N, 052°15'16.0"E (locality no. 152); 955 m a.s.l.; J. Bojková, T. Soldán, J. Imanpour Namin, S. Bagheri leg., 9.5.2018, SMNS_EPH_010056.

Paratypes: 38 female larvae (3 mounted on slide), 10 male larvae (2 mounted on slide): same data as holotype, SMNS_EPH_010056. DNA extracted from 1 fe-

male (code: IR11, stored in EtOH) and 2 males (codes: IR12 and IR14, both stored in EtOH).

33 female larvae, 24 male larvae: IRAN, Tehran Province, Zayegan village, Lalan River; 35°58'39.2"N, 051°34'56.5"E (locality no. 55); 2290 m a.s.l.; A. Staniczek, M. Pallmann, R. J. Godunko, F. Nejat leg., 8.5.2017, SMNS_EPH_007617.

1 female larva: IRAN, Golestan Province, above Chah-e Ja village, unnamed brook (RT of river flowing to Fazelabad); 36°40'22.8"N, 054°46'37.9"E (locality no. 104); 1450 m a.s.l.; J. Bojková, T. Soldán, J. Imanpour Namin leg., 27.4.2018. DNA extracted specimen (code: IR13, stored in EtOH).

17 female larvae (3 mounted on slide), 6 male larvae: IRAN, Alborz Province, 2.5 km W of Asara village, Karaj River; 36°01'52.1"N, 051°13'10.0"E (locality no. 58); 1890 m a.s.l.; A. Staniczek, M. Pallmann, F. Nejat leg., 10.5.2017, SMNS_EPH_007627.

The holotype and 50 paratypes are deposited in SMNS, 50 paratypes (including DNA extracted specimens) are deposited in IECA and 29 paratypes in MMTT_DOE.

Other material examined. 8 larvae: same data as holotype, SMNS_EPH_010056; young instars or damaged specimens.

13 larvae: IRAN, Mazandaran Province, NE of Kahrud village, unnamed brook (LT of Haraz River); 36°03'42.7"N, 052°15'24.8"E (locality no. 153); 1020 m a.s.l.; J. Bojková, T. Soldán, J. Imanpour Namin, S. Bagheri leg., 9.5.2018.

2 larvae: IRAN, Mazandaran Province, 3.5 km E of Polour village, Lasem Rud (RT of Haraz River); 35°50'09.4"N, 052°04'38.4"E (locality no. 73); 2100 m a.s.l.; A. Staniczek, M. Pallmann, F. Nejat leg., 14.5.2017, SMNS_EPH_007680; 17 larvae: S. Bagheri leg., 16.4.2018.

1 larva: IRAN, Mazandaran Province, 1.5 km S of Part Kola village, Shirin Rud (LT of Sefidrud); 36°9'04.3"N, 053°20'54.7"E (locality no. 63); 750 m a.s.l.; A. Staniczek, M. Pallmann, F. Nejat leg., 11.5.2017, SMNS_EPH_007641; 10 larvae: S. Bagheri leg., 5.4.2018.

7 larvae: IRAN, Mazandaran Province, 3.5 km W of Razan village, Baladeh River; 36°11'39.6"N, 052°8'34.6"E (locality no. 73); 1360 m a.s.l.; A. Staniczek, M. Pallmann, F. Nejat leg., 14.5.2017, SMNS_EPH_007677.

1 larva: IRAN, Tehran Province, Lalan village, Lalan River; 35°59'50.3"N, 051°34'51.0"E (locality no. 53); 2438 m a.s.l.; A. Staniczek, M. Pallmann, R. J. Godunko, F. Nejat leg., 8.5.2017, SMNS_EPH_007613.

17 larvae: IRAN, Tehran Province, Igol village, Fasham River; 35°55'11.2"N, 051°28'51.3"E (locality no. 56); 2020 m a.s.l.; A. Staniczek, M. Pallmann, R. J. Godunko, F. Nejat leg., 8.5.2017, SMNS_EPH_007618.

10 larvae: IRAN, Alborz Province, 4 km NW of Shahrestanak village, Shahrestanak River; 35°59'01.2"N, 051°19'09.6"E (locality no. 57); 2100 m a.s.l.; A. Staniczek, M. Pallmann, F. Nejat leg., 10.5.2017, SMNS_EPH_007622.

Etymology. The species name refers to the type locality and distribution of the species in the Alborz mountain range.

Localities and habitat preferences of larvae. Larvae inhabit small streams (2–8 m width, 20–50 cm depth) at high altitudes (six of eleven localities at approx. 2000 m

a.s.l.) in the central Alborz (Fig. 9). One larva was found in the eastern Alborz (Fig. 9). Larvae were found only in cold and clear streams where they dwelled on large stones in riffles with very fast flow. All localities were situated in deep valleys with rivers draining high mountains. They were mostly treeless, only sometimes with sparse solitary shrubs and trees at the banks (Fig. 10A, B). Streams had a very coarse bed substrate with prevailing boulders and stones and a low share of fine sediments, and turbulent to strongly turbulent flow. They were characteristic of high fluctuation of discharge, with sudden peaks of discharge after spates on the mountains (Fig. 10A).

Description of larva. General colouration of larvae yellowish brown with dark brown maculation. Body length of mature larvae: 13.3–15.8 mm (female), 10.3–11.3 mm (male). Length of cerci approximately 1.3× body length.

Head. Shape trapezoidal; anterior and lateral margin rounded, posterior margin rounded in female, slightly rounded or nearly straight in male (Fig. 1D, E). Anterior margin with shallow concavity medially. Head dimensions of mature larvae: length 2.8–3.1 mm, width 4.0–4.6 mm (female); length 2.2–2.7 mm, width 3.2–3.7 mm (male). Head width/length ratio: 1.4–1.5 (both male and female). Dorso-medial part with pair of stripes. Pair of maculae located between ocelli (sometimes fused into single macula). Rounded maculae ventrolateral of lateral ocelli and blurred maculae near in-

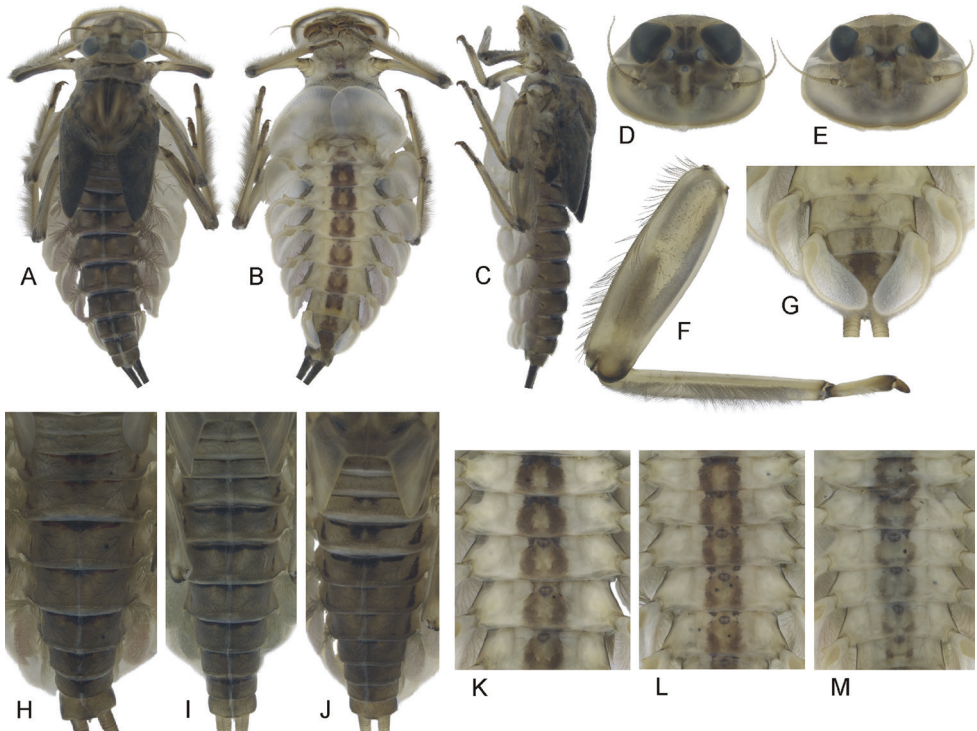


Figure 1. *Epeorus (Caucasiron) alborzicus* sp. nov., larva: **A** habitus in dorsal view **B** habitus in ventral view **C** habitus in lateral view **D** head of male in dorsal view **E** head of female in dorsal view **F** middle leg in dorsal view **G** distal part of abdomen in ventral view **H–J** colouration of abdominal terga **K–M** colouration of abdominal sterna.

ner edges of compound eyes. Pale stripes extending horizontally from lateral ocelli to lateral edges of head. Pair of elongated, curved maculae located along coronal suture. Compound eyes grey to black in female, brownish or greyish and basally black in male mature larva. Ocelli blackish, basally paler. Antennae yellowish brown, scapus and pedicellus darkened. Anterior margin of head densely covered with hair-like setae extending to lateral margins and directed medio-dorsally. Dorsal surface of head covered with fine hair-like setae and sparsely distributed stick-like setae. Sparse longer and fine hair-like setae located posteriorly to eyes.

Mouthparts. Labrum (Fig. 2A) widened anteriorly, with anterior margin slightly rounded or nearly straight (in dorsal view). Lateral angles rounded (shape of labrum may vary among individual specimens). Dorsal surface (Fig. 2A, right half) sparsely covered with setae of different size; 4–6 longer bristle-like setae located antero-medially and two bristles antero-laterally. Epipharynx with longer, slightly plumose bristles situated along lateral to anterior margin (Fig. 2A, left half, range of setation figured as large black dots), and cluster of fine, hair-like setae medially (not figured). Posterior margin of labrum irregularly concave; group of 6–17 setae of various size located on ventral surface close to posterior margin. Outer incisors of both mandibles (Fig. 2B, C) with three apical teeth; outer tooth blunt in both mandibles. Inner incisor of left mandible with three apical teeth, right inner incisor bifurcated.

Thorax. Pronotum anteriorly narrowed, lateral edges nearly straight. Metanotum with slight postero-medial projection. Dorsal surface covered with fine, hair-like setae (as on abdominal terga and head); sparse longer, hair-like setae along pro-, meso- and metanotal suture.

Legs. Colour pattern of femora as in Fig. 1F. Femora without medial hypodermal spot. Patella-tibial suture darkened; tarsi proximally and distally darkened. Coxal projections of fore- and hind legs pointed or bluntly pointed; in middle legs blunt. Trochanteres with spatulate setae as on dorsal surface of femora (Fig. 2D). Tibiae of forelegs 1.20–1.37× femur length, tibiae of middle legs 1.0–1.2× femur length, and tibiae of hind legs 0.92–1.08× femur length. Tarsi of all legs 0.26–0.34× tibia length. Dorsal surface of femora covered by short and sporadically elongated spatulate setae (Fig. 2D), hair-like setae, and sparsely distributed stick-like setae. Anterior margin of femora with short, pointed or bluntly pointed spine-like setae; posterior margin with row of long blade-like setae and sparse row of bluntly pointed, spine-like setae. Dorsal margin of tibiae and tarsi with row of long setae; ventral margin of both with irregular row of spine-like setae accumulated distally. Tarsal claws with 2–3 denticles.

Abdominal terga. Colour pattern of abdominal terga (Fig. 1A, H–J) consists of transversal stripe along anterior margin of terga I–IX (X), medially extending to single blurred macula or pair of rounded maculae on terga II–IV and short triangular or nearly rectangular macula on terga V–IX. Terga VIII and IX (X) medially darkened. Pattern of abdominal terga sometimes poorly expressed, only with medially thickened transversal stripe along anterior margin.

Lateral margins with oblique maculae on terga I–IX, sometimes dorso-posteriorly extended. Pair of sigilla sometimes coloured, in form of short stripes or spots located

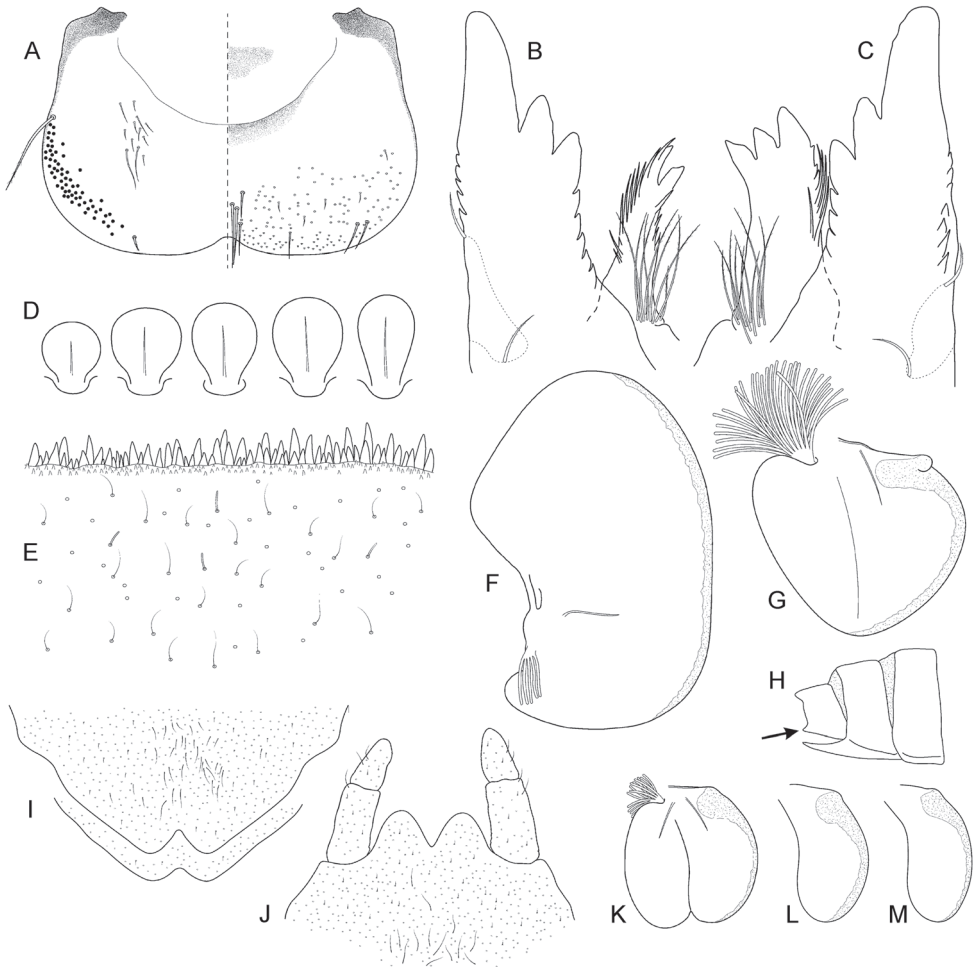


Figure 2. *Epeorus (Caucasiron) alborzicus* sp. nov., larva: **A** labrum (right half in dorsal view, left half in ventral view) **B** incisors of right mandible in ventral view **C** incisors of left mandible in ventral view (both flattened on slide) **D** setae on dorsal surface of femora **E** surface and posterior margin of abdominal tergum VII **F** gill I **G** gill III **H** abdominal segments VIII–X **I** sternum IX, female **J** sternum IX, male **K** gill VII (flattened on slide) **L–M** gill VII (in natural position from ventral view), variability in shape.

antero-laterally to medial macula. Denticles on posterior margin on terga of various size, irregular and pointed (Fig. 2E). Surface of terga covered with hair-like setae and sparsely with stick-like setae. Tergum X with distinct postero-lateral projections (Fig. 2H, arrow). Supra-tergalial projection (sensu Kluge 2004) short and blunt. Longitudinal row of hair-like setae along abdominal terga present medially.

Abdominal sterna. Yellowish, with distinct colour pattern in form of medial circular macula (Fig. 1B, G, K–M, best expressed on sterna II–VI). Medio-anterior sigilla partly pigmented, lateral sigilla not pigmented; medio-posterior sigilla in form of pale

spots in intensively pigmented specimens. Nerve ganglia occasionally darkened. Intensity of colouration varies among individuals (Fig. 1K–M). Sternum IX with V-shaped medial emargination; surface covered by irregularly distributed short hair-like setae, and medially accumulated longer hair-like setae (Fig. 2I, J).

Gills. Dorsal surface of gill plate I yellowish; of gill plates II–VII greyish on anterior half, brownish (sometimes reddish) on posterior half. Ventral margin of all gill plates yellowish. Projection of gill plate III well developed (Fig. 2G). Gill plate VII relatively wide (in natural position of ventral view, Figs 1G, 2L, M). Filaments of gills II–VI reaching 0.40–0.58× length of respective plate, filaments of gill VII reaching 0.18–0.24× (in late-instar larvae).

Cerci. Yellowish brown, basally darkened.

Subimago, imago and eggs. Unknown.

Morphological diagnostics of larvae. The main larval diagnostic characters of *E. (C.) alborzicus* sp. nov. are as follows: (i) colour pattern of abdominal terga (Fig. 1A, H–J) and sterna (Fig. 1B, K–M), (ii) presence of distinct postero-lateral projections on tergum X (Fig. 2H), (iii) absence of medial hypodermal femur spot (Fig. 1F), (iv) gill plate VII relatively wide (in natural position from ventral view; Figs 1G, 2L, M), and (v) fine hair-like setae on surface of abdominal terga (Fig. 2E).

Affinities. The combination of diagnostic characters mentioned above clearly distinguish larvae of *E. (C.) alborzicus* sp. nov. from all other *Caucasiron* species known so far. However, some of the diagnostic characters occur also in other *Caucasiron* species distributed in the Caucasus. The colour pattern of abdominal sterna in *E. (C.) alborzicus* sp. nov. is similar in *E. (C.) bicolliculatus* (Hrivniak et al. 2017: 356, fig. 8) and *E. (C.) alpestris* (Braasch 1979: 284, fig. 1d). Both species also lack a medial hypodermal femur spot. *Epeorus (C.) bicolliculatus* can be distinguished from *E. (C.) alborzicus* sp. nov. by (i) the presence of flattened setae on the surface of abdominal terga (Hrivniak et al. 2017: 359, fig. 23), (ii) the presence of paired postero-medial protuberances on terga II–IX (Hrivniak et al. 2017: 356, figs 10, 11; 360, figs 31, 32), and (iii) the absence of a postero-lateral projection on the tergum X.

Epeorus (C.) alpestris differs by the characteristic colour pattern of abdominal terga (Braasch 1979: 294, fig. 1c) and the absence of postero-lateral projections on the tergum X.

The presence of postero-lateral projections on the abdominal tergum X is characteristic for two species distributed in the Caucasus, *E. (C.) magnus*, *E. (C.) nigripilosus*, and sporadically also in *E. (C.) znojkoii*. *Epeorus (C.) magnus* differs from *E. (C.) alborzicus* sp. nov. in the absence of colouration of abdominal sterna and the characteristic setation on the dorsal margin of labrum (numerous thickened bristle-like setae, Hrivniak et al. in prep.). *Epeorus (C.) nigripilosus* can be separated from *E. (C.) alborzicus* sp. nov. by the presence of the distinct medial hypodermal femur spot and unique colour pattern of abdominal sterna (Sinitshenkova 1976: 89, fig. 28). *Epeorus (C.) znojkoii* can be clearly distinguished from *E. (C.) alborzicus* sp. nov. by the colour pattern of abdominal terga and conspicuous reddish colouration of abdominal sterna (Braasch 1980: 172, fig. 4b–c).

Two species, *E. (C.) soldani* and *E. (C.) sinitschenkova*, are lacking a medial hypodermal femur spot just like *E. (C.) alborzicus* sp. nov. Both can be separated from the latter by the absence of postero-lateral projections on tergum X, narrower gill plates VII (in natural position from ventral view), and the absence of a distinct colour pattern of abdominal sterna. Additionally, *E. (C.) soldani* differs from *E. (C.) alborzicus* sp. nov. by the presence of flattened setae on the surface of abdominal terga (Hrivniak et al. 2017: 359, fig. 25).

Other *Caucasiron* species distributed in the Caucasus and adjacent areas do not share important diagnostic characters with *E. (C.) alborzicus* sp. nov. All of these species can be easily distinguished by the following combination of characters: (i) absence of the colour pattern of abdominal sterna and presence of the medial hypodermal femur spot in *E. (C.) turcicus*, *E. (C.) longimaculatus*, *E. (C.) shargi* sp. nov. and (ii) colour pattern of abdominal terga and sterna in *E. (C.) caucasicus* (Braasch 1979: fig. 3a), *E. (C.) iranicus* (Braasch and Soldán 1979: fig. 12), and *E. (C.) zagrosicus* sp. nov. (Fig. 5A–C, G, H–K). The larva of *E. (C.) insularis* is currently not described.

***Epeorus (Caucasiron) shargi* Hrivniak & Sroka, sp. nov.**

<http://zoobank.org/6F5FE6F7-8710-416D-80DB-C202C71DE7FC>

Figures 3, 4

Type material. Holotype: female mature larva: IRAN, Golestan Province, Shirinabad village, unnamed river; 36°48'01.4"N, 055°01'05.8"E (locality no. 108); 740 m a.s.l.; J. Bojková, T. Soldán, J. Imanpour Namin leg., 27.4.2018, SMNS_EPH_010057.

Paratypes: 19 female, 11 male larvae: same data as holotype.

36 female (5 mounted on slide), 25 male (1 mounted on slide) larvae: IRAN, Golestan Province, above Chah-e Ja village, unnamed brook (RT of river flowing to Fazelabad); 36°40'22.8"N, 054°46'37.9"E (locality no. 104); 1450 m a.s.l.; J. Bojková, T. Soldán, J. Imanpour Namin leg., 27.4.2018. DNA extracted from 2 females (codes: IR23 and IR24, mounted on slides).

19 female (3 mounted on slide), 7 male (1 mounted on slide) larvae: IRAN, Golestan Province, below Chah-e Ja village (main valley), unnamed river flowing to Fazelabad, 36°41'46.3"N, 054°47'35.0"E (locality no. 105); 1240 m a.s.l.; J. Bojková, T. Soldán, J. Imanpour Namin leg., 27.4.2018. DNA extracted from 1 female (code: IR21, mounted on slide) and 1 male (code: IR22, stored in EtOH).

The holotype (SMNS_EPH_010057) and 50 paratypes (SMNS_EPH_010057) are deposited in SMNS, 50 paratypes (including DNA extracted specimens) are deposited in IECA, and 17 paratypes in MMTT_DOE.

Other material examined (not paratypes): 3 larvae: same data as holotype; young instars or damaged specimens.

Etymology. The species name derives from *shargi* (شَرَقِي), which means eastern in Farsi. It refers to the distributional range of the species in the eastern part of the Alborz mountain range.

Localities and habitat preferences of larvae. Larvae were found in three clear streams at middle altitude (740–1450 m a.s.l.) in the eastern Alborz (Fig. 9). Habitat conditions of these streams differed from each other. Larvae were abundant in a cold, alkaline brook (water conductivity 1320 $\mu\text{S}/\text{cm}$) with patches of precipitated calcium crusts on the bed and in the non-alkaline water (with water conductivity reaching the values of clear montane streams in the region, 433 $\mu\text{S}/\text{cm}$) of the type locality. Both localities were characterised by stony bed sediment with leaf litter debris and fine gravel along the banks, and by fast, turbulent flow (Fig. 10C, D). Lower abundance of larvae was found in a river with uniform coarse substrate flowing in a wide gravel river channel. All streams were surrounded by deciduous forests (Fig. 10C, D). The species was not found in urban and agricultural areas in this region where many localities were investigated.

Description of larva. General colouration of larvae yellowish brown with dark brown maculation. Body length of mature larvae 13.7–15.6 mm (female), 11.7–13.0 mm (male). Length of cerci approximately 1.1 \times body length.

Head. Shape trapezoidal; anterior and lateral margin rounded, posterior margin rounded in female, slightly rounded in male (Fig. 3D, E). Anterior margin with shal-

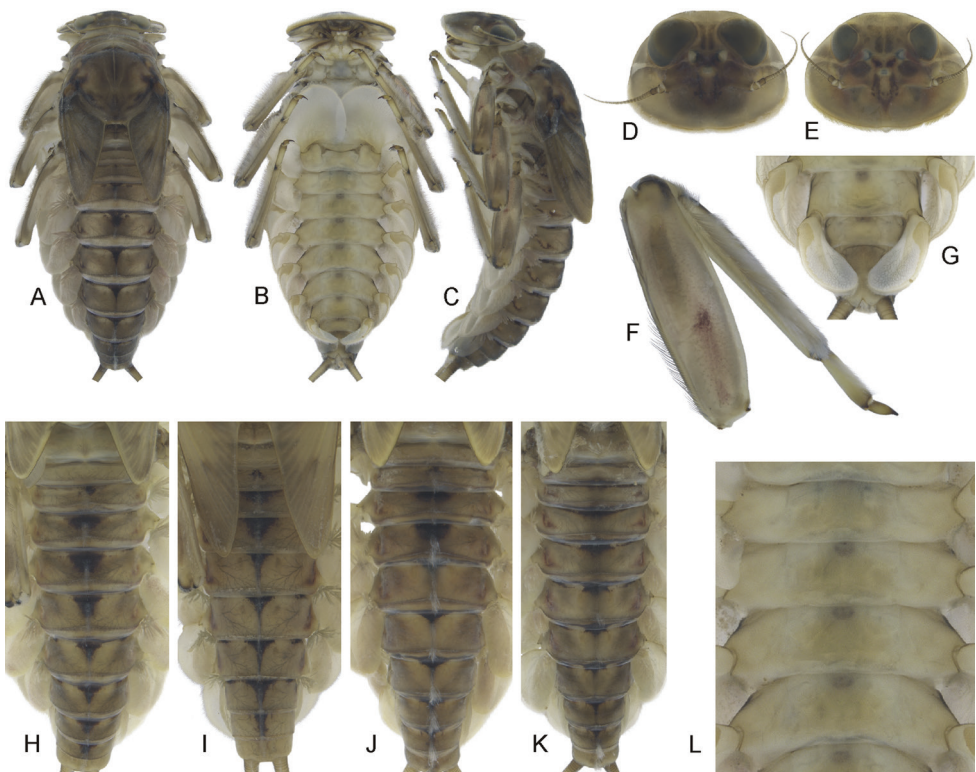


Figure 3. *Epeorus (Caucasiron) shargi* sp. nov., larva: **A** habitus in dorsal view **B** habitus in ventral view **C** habitus in lateral view **D** head of male in dorsal view **E** head of female in dorsal view **F** middle leg in dorsal view **G** distal part of abdomen in ventral view **H–K** colouration of abdominal terga **L** colouration of abdominal sterna.

low concavity medially. Head dimensions of mature larvae: length 3.0–3.2 mm, width 4.1–4.4 mm (female); length 2.70–2.95 mm, width 3.5–4.0 mm (male). Head width/length ratio: 1.33–1.40 (both male and female). Dorso-medial part with brown, rectangular or oval smudge, sometimes reduced to pair of stripes. Pair of maculae located between ocelli (sometimes fused into single macula). Rounded maculae lateroventral of lateral ocelli and blurred maculae near inner edges of compound eyes. Pair of pale stripes extending from lateral ocelli to lateral edges of head. Pair of maculae located along coronal suture. Compound eyes dark grey to black in female, brownish and basally blackish in male mature larva. Ocelli dark grey to black, basally paler. Antennae

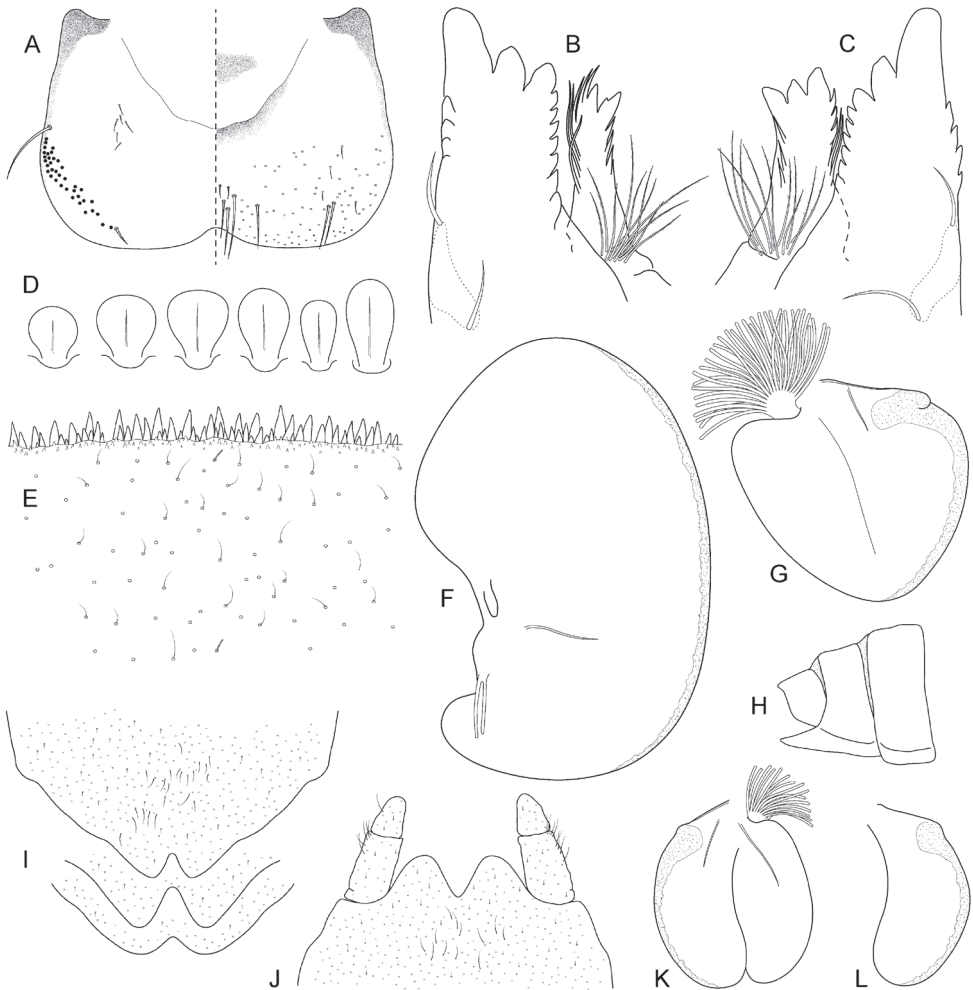


Figure 4. *Epeorus (Caucasiron) shargi* sp. nov., larva: **A** labrum (right half in dorsal view, left half in ventral view) **B** incisors of right mandible in ventral view **C** incisors of left mandible in ventral view (both flattened on slide) **D** setae on dorsal surface of femora **E** surface and posterior margin of abdominal tergum VII **F** gill I **G** gill III **H** abdominal segments VIII–X **I** sternum IX, female **J** sternum IX, male **K** gill VII (flattened on slide) **L** gill VII (in natural position from ventral view).

yellowish-brown, scapus and pedicellus darkened. Anterior margin of head densely covered with hair-like setae extending to lateral margins and directed medio-dorsally. Dorsal surface of head covered with fine hair-like setae and sparsely distributed stick-like setae. Sparse longer fine hair-like setae located posteriorly to eyes.

Mouthparts. Labrum (Fig. 4A) widened anteriorly, with anterior margin slightly rounded or nearly straight (in dorsal view). Lateral angles rounded (shape of labrum may vary among individual specimens). Dorsal surface (Fig. 4A, right half) sparsely covered with setae of different size; 4–6 longer bristle-like setae located antero-medially and two antero-laterally. Epipharynx with longer, shortly plumose bristles situated along lateral to anterior margin (Fig. 4A, left half), range of setation figured as large black dots), and brush of fine hair-like setae medially (not figured). Posterior margin of labrum irregularly concave; with group of 5–10 setae of various size located on ventral surface close to posterior margin. Outer incisors of both mandibles (Fig. 4B, C) with three apical teeth; outer tooth blunt in both mandibles. Inner incisor of left mandible with three apical teeth, right inner incisor bifurcated (inner side of right tooth usually with small denticle).

Thorax. Pronotum anteriorly narrowed, lateral edges nearly straight or slightly rounded. Metanotum with slight, blunt, postero-medial projection. Dorsal surface covered with fine hair-like setae (as on abdominal terga and head); sparse longer hair-like setae along pro-, meso- and metanotal suture.

Legs. Colour pattern of femora as in Fig. 3F. Femora with rounded or slightly elongated medial hypodermal femur spot. Patella-tibial suture darkened; tarsi proximally and distally darkened. Coxal projections of fore- and hind legs pointed or bluntly pointed; of middle legs blunt. Trochanteres with spatulate setae as on dorsal surface of femora (Fig. 4D). Tibiae of forelegs 1.23–1.28× femur length, tibiae of middle legs 1.03–1.50× femur length, and tibiae of hind legs 0.87–1.06× femur length. Tarsi of all legs 0.28–0.32× tibia length. Dorsal surface of femora covered by short, sporadically elongated spatulate setae (Fig. 4D), hair-like setae, and sparsely distributed stick-like setae. Anterior margin of femora with short, pointed and/or bluntly pointed spine-like setae; posterior margin with row of long blade-like setae and sparse row of bluntly pointed spine-like setae. Dorsal margin of tibiae and tarsi with row of long setae; ventral margin of both with irregular row of spine-like setae accumulated distally. Tarsal claws with 2–3 denticles.

Abdominal terga. Colour pattern of abdominal terga (Fig. 3A, H–K) consists of transversal stripe along anterior margin of terga I–IX (X) medially extending to i) triangular or blurred macula on terga (II) III–IV; ii) triangular or T-shaped macula on terga V–IX, reaching to half or stretching to posterior margin of corresponding tergum (medial macula of terga VIII and IX often widened). Transversal stripe along anterior margin of terga laterally extends to pair of short maculae. Medial maculae often surrounded by pale background. Tergum X without distinct maculation. Pair of sigilla sometimes coloured and forming pair of short stripes adjacent laterally to medial macula. Lateral margins of abdomen with oblique maculae on terga I–IX. Denticles along posterior margin on terga of various size, irregular and pointed (Fig. 4E). Surface

of terga covered with hair-like setae and sparsely with stick-like setae. Supra-tergalial projections short and blunt. Tergum X without distinct postero-lateral projections (Fig. 4H). Longitudinal row of hair-like setae along abdominal terga present medially.

Abdominal sterna. Yellowish, without distinct colour pattern. Nerve ganglia often dark brown pigmented (Fig. 3B, G, L). Sternum IX with V-shaped medial emargination; surface covered by irregularly distributed short hair-like setae and medially accumulated longer hair-like setae (Fig. 4I, J).

Gills. Dorsal surface of gill plate I yellowish, of gill plates II–VII greyish on anterior half and brownish to reddish on posterior half. Ventral margin of all gill plates yellowish. Projection of gill plate III well developed (Fig. 4G). Gill plate VII relatively wide (in natural position of ventral view, Figs 3G, 4L). Gill filaments reaching to 0.41–0.50× length of respective plate, filaments of gill VII to 0.24–0.28× (in late-instar larvae).

Cerci. Brownish, basally darkened.

Subimago, imago and eggs. Unknown

Morphological diagnostics of larvae. The main larval diagnostic characters of *E. (C.) shargi* sp. nov. are as follows: (i) colour pattern of abdominal terga (Fig. 3A, H–K) and no colouration of abdominal sterna (Fig. 3B, G, L), (ii) lack of distinct postero-lateral projections on tergum X (Fig. 4H), (iii) presence of medial hypodermal femur spot (Fig. 3F), (iv) relatively wide shape of gill plate VII (in natural position from ventral view; Figs 3G, 4L), and (v) fine hair-like setae on surface of abdominal terga (Fig. 4E).

Affinities. Based on the colour pattern of abdominal terga and sterna, *E. (C.) shargi* sp. nov. resembles several species distributed in the Caucasus and adjacent areas. At first glance, *E. (C.) soldani* and *E. (C.) turcicus* are most similar. Larvae of *E. (C.) soldani* possess triangular maculae on abdominal terga (Braasch 1979: 284, fig. 2b) and an indistinct, sometimes not expressed, colour pattern of abdominal sterna. It can be distinguished from *E. (C.) shargi* sp. nov. by a comparatively narrower gill plate VII (in natural position from ventral view), the presence of flattened setae on the surface of abdominal terga (Hrivniak et al. 2017: 359, fig. 25), and the absence of a medial hypodermal femur spot.

Epeorus (C.) turcicus shares with *E. (C.) shargi* sp. nov. the lack of colouration on abdominal sterna (Hrivniak et al. 2019: 61, fig. 2), the presence of a medial hypodermal femur spot (Hrivniak et al. 2019: 62, fig. 9), and fine hair-like setae on the dorsal surface of abdominal terga (Hrivniak et al. 2019: 63, fig. 11). Nevertheless, *E. (C.) turcicus* differs from *E. (C.) shargi* sp. nov. by the different colour pattern of abdominal terga, with anteriorly widened stripe stretching between anterior and posterior margins (Hrivniak et al. 2019: 61, fig. 1), in contrast to *E. (C.) shargi* sp. nov. with more or less triangular maculae on abdominal terga (Fig. 3A, H–K), and a distinctly narrower gill plate VII (in natural position from ventral view) (Hrivniak et al. 2019: 63, figs 15, 16).

Similar to *E. (C.) shargi* sp. nov., there is no colour pattern of abdominal sterna in several other species, namely *E. (C.) longimaculatus*, *E. (C.) sinitschenkova*, and *E. (C.) magnus*. *Epeorus (C.) longimaculatus* can be clearly separated from *E. (C.) shargi* sp. nov. by (i) a distinctly narrower gill plate VII (in natural position of ventral view),

(ii) flattened setae on the surface of abdominal terga (Hrivniak et al. 2017: 359, fig. 25), (iii) poorly developed projection on the costal margin of gill plate III (Braasch 1980: 172, fig. 6b), and (iv) elongated medial hypodermal femur spot (Braasch 1980: 172, fig. 11).

Epeorus (C.) sinitschenkova can be distinguished from *E. (C.) shargi* sp. nov. by the absence of a medial hypodermal femur spot, the characteristic colour pattern of femora (Braasch and Zimmerman 1979: 106, fig. 10), and the colour pattern of abdominal terga (Braasch 1979: 105, fig. 2).

Epeorus (C.) magnus can be reliably distinguished by the presence of distinct postero-lateral projections on abdominal tergum X and characteristic setation of labrum (numerous thickened bristle-like setae, Hrivniak et al. in prep.).

All other species distributed in the Caucasus and adjacent areas differ from *E. (C.) shargi* sp. nov. by the distinct colour pattern of abdominal sterna, namely *E. (C.) bicolliculatus* (Hrivniak et al. 2017: 356, figs 7–9), *E. (C.) alpestris* (Braasch, 1979: 284, fig. 1d), *E. (C.) alborzicus* sp. nov., (Fig. 1B, K–M), *E. (C.) caucasicus*, *E. (C.) iranicus* (Braasch 1979: 284, fig. 3b), *E. (C.) nigripilosus* (Sinitschenkova 1976: 89, fig. 28), *E. (C.) znojko*i (Braasch, 1980: 172, 4b), and *E. (C.) zagrosicus* sp. nov. (Fig. 5B, K).

***Epeorus (Caucasiron) zagrosicus* Hrivniak & Sroka, sp. nov.**

<http://zoobank.org/A49F6070-C918-4FA2-9287-D0B3D9BDBC01>

Figures 5, 6

Type material. Holotype: female larva: IRAN, Lorestan Province, 4.5 km SW of Varayeneh village, Sarab-e Gamasiab River, 34°2'46.2"N, 048°22'32.6"E (locality no. 9); 1842 m a.s.l.; A. Staniczek, M. Pallmann, A. Abdoli, F. Nejat leg., 25.4.2017, SMNS_EPH_007520.

Paratypes: 79 female larvae, 68 male larvae: same data as holotype, SMNS_EPH_007520. 6 female (2 mounted on slide), 5 male (2 mounted on slide) larvae: IRAN, Chaharmahal and Bakhtiari Province, Dimeh village, Chehme-Dimeh River, 32°30'11.6"N, 050°13'04.5"E (locality no. 45); 2220 m a.s.l.; A. Staniczek, M. Pallmann, R. J. Godunko, F. Nejat leg., 5.5.2017, SMNS_EPH_007707. DNA extracted from 3 females (code: IR32, stored in EtOH; codes: IR34 and IR35, mounted on slides) and 2 males (codes: IR33b and IR36, mounted on slides).

15 female (3 mounted on slide), 5 male larvae: IRAN, Kohgiluyeh and Boyer-Ahmad Province, 4 km E of Yasuj, Yasuj fall, 30°40'34.7"N, 051°37'35.6"E (locality no. 37); 2060 m a.s.l.; A. Staniczek, M. Pallmann, R. J. Godunko, F. Nejat leg., 4.5.2017, SMNS_EPH_007568. DNA extracted from 2 females (code: SP38, mounted on slide; code: IR33a, stored in EtOH) and 1 male (code: SP37, stored in EtOH).

2 female, 2 male larvae: IRAN, Chaharmahal and Bakhtiari Province, 5 km W of Chelgerd, Kouhrang River, 32°28'9.3"N, 050°5'26.2"E (locality no. 46); 2402 m a.s.l.; A. Staniczek, M. Pallmann, R. J. Godunko, F. Nejat leg., 5.5.2017, SMNS_EPH_007689.

The holotype and 100 paratypes are deposited in SMNS, 50 paratypes (including DNA extracted specimens) are deposited in IECA and 32 paratypes in MMTT_DOE.

Other material examined: 42 larvae: same data as holotype; young instars or damaged specimens.

1 male larva: IRAN, Chaharmahal and Bakhtiari Province, 4 km E. of Bajgiran, Dehno River, 31°54'26.2"N, 050°42'20.6"E (locality no. 50); 1721 m a.s.l.; A. Staniczek, M. Pallmann, R. J. Godunko, F. Nejat leg., 6.5.2017, SMNS_EPH_007606.

Etymology. The species name refers to its known records in the Zagros mountain range.

Localities and habitat preferences of larvae. Larvae were found in five streams of different size at high altitude, above 1700 m a.s.l. Three streams were strongly turbulent rivers with very coarse bed substrate flowing in high-mountain valleys (Fig. 10E). Larvae were found also in a shallow, slow-flowing brook with finer, gravel substrate flowing in the forest (locality near Yasuj fall, Fig. 10F), and in a small stream with moderate, slightly turbulent flow and stony bed substrate with fine gravel, silt, and macrophytes (Chehme-Dimeh River). The species was not found in streams that were polluted or seasonally drying out.

Description of larva. General colouration of larvae yellowish brown with dark brown maculation. Body length of mature larvae 13.5–14.5 mm (female), 10.0–11.0 mm (male). Length of cerci approximately 1.3× body length.

Head. Shape trapezoidal; anterior and lateral margin rounded, posterior margin slightly rounded or nearly straight (Fig. 5D, E). Anterior margin with shallow concavity medially.

Head dimensions of mature larvae: length 2.6–2.7 mm, width 3.6–4.0 mm (female); length 2.3–2.4 mm, width 3.3 mm (male). Head width/length ratio: 1.36–1.49 (both male and female).

Dorso-medial part with indistinct brown rectangular or oval macula, sometimes reduced to pair of stripes. Rounded maculae under lateral ocelli and blurred or triangular maculae near inner edges of compound eyes. Pair of pale stripes extending from lateral ocelli to lateral edges of head. Pair of maculae located along coronal suture. Compound eyes dark grey to black in female, brownish and basally blackish in male mature larva. Ocelli dark grey to black, basally paler. Antennae yellowish-brown, scapus and pedicellus darkened. Anterior margin densely covered with hair-like setae extending to lateral margins and directed medio-dorsally. Dorsal surface covered with fine hair-like setae and sparsely distributed stick-like setae. Sparse longer, fine, hair-like setae located posteriorly to eyes.

Mouthparts. Labrum (Fig. 6A) widened anteriorly, with anterior margin slightly rounded or nearly straight (in dorsal view). Lateral angles rounded (shape of labrum may vary among individual specimens). Dorsal surface (Fig. 6A, right half) sparsely covered with setae of different size; four longer, bristle-like setae located antero-medially and two antero-laterally. Epipharynx with longer, shortly plumose bristles situated along lateral to anterior margin (Fig. 6A, left half; range of setation figured as large black dots), and brush of fine hair-like setae medially (not figured). Posterior margin of

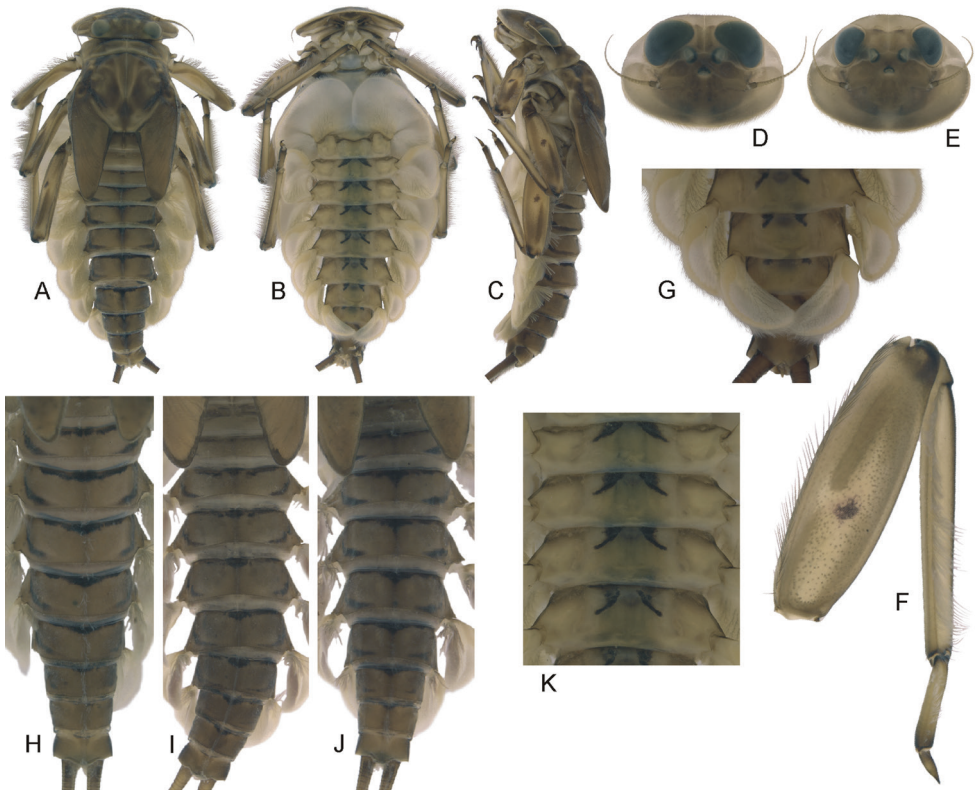


Figure 5. *Epeorus (Caucasiron) zagrosicus* sp. nov., larva: **A** habitus in dorsal view **B** habitus in ventral view **C** habitus in lateral view **D** head of male in dorsal view **E** head of female in dorsal view **F** middle leg in dorsal view **G** distal part of abdomen in ventral view **H–J** colouration of abdominal terga **K** colouration of abdominal sterna.

labrum irregularly concave; with group of 6–10 setae of various size located on ventral surface close to posterior margin. Outer incisors of both mandibles (Fig. 6B, C) with three apical teeth; outer tooth blunt in both mandibles. Inner incisor of left mandible with three apical teeth, right inner incisor bifurcated.

Thorax. Pronotum anteriorly narrowed, lateral edges nearly straight. Metanotum with slight postero-medial projection. Dorsal surface covered with fine hair-like setae (as on abdominal terga and head); sparse longer hair-like setae along pro, meso- and metanotal suture.

Legs. Colour pattern of femora as in Fig. 5F. Femora with rounded medial hypodermal femur spot. Patella-tibial suture darkened; tarsi proximally and distally darkened. Coxal projections of fore- and hind legs pointed or bluntly pointed; of middle legs blunt. Trochanters with spatulate setae as on dorsal surface of femora (Fig. 6D). Tibiae of forelegs 1.20–1.31× femur length, tibiae of middle legs 1.06–1.14× femur length, and tibiae of hind legs 0.90–1.04× femur length. Tarsi of all legs 0.25–0.34× tibia length. Dorsal surface of femora covered by elongated and sporadically short

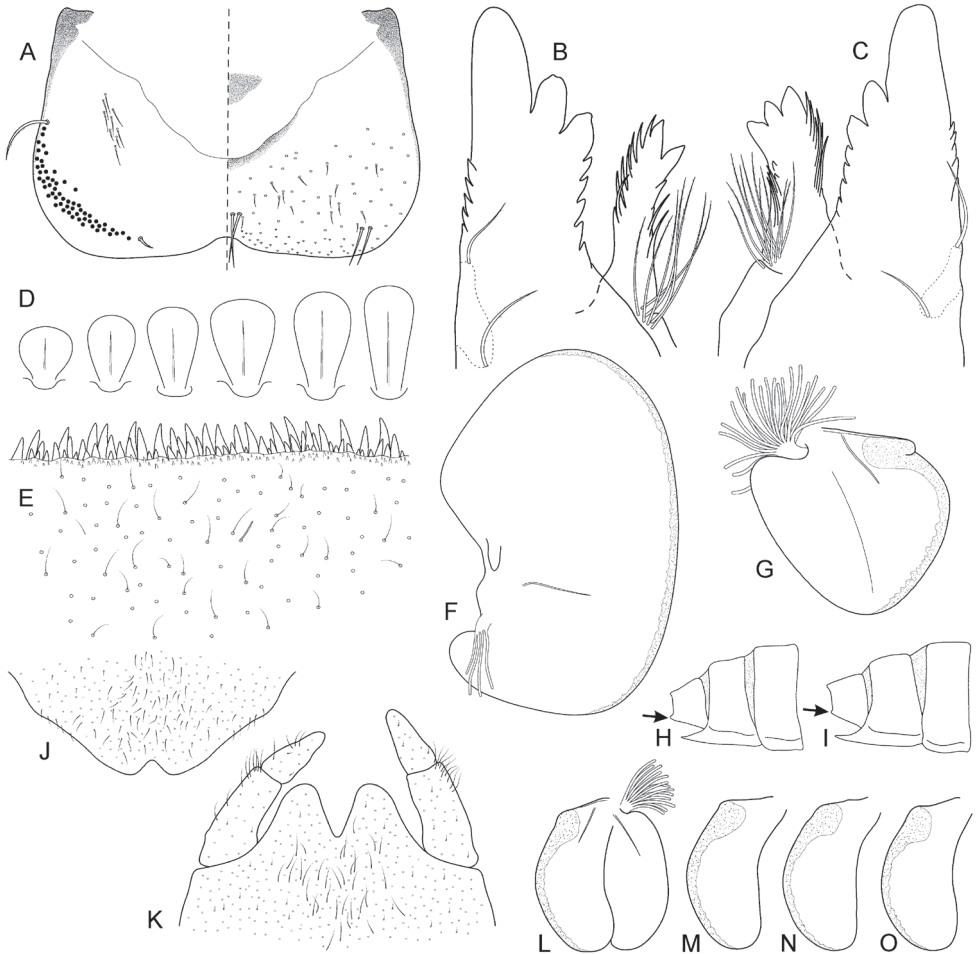


Figure 6. *Epeorus (Caucasiron) zagrosicus* sp. nov., larva: **A** labrum (right half in dorsal view, left half in ventral view) **B** incisors of right mandible in ventral view **C** incisors of left mandible in ventral view (both flattened on slide) **D** setae on dorsal surface of femora **E** surface and posterior margin of abdominal tergum VII **F** gill I **G** gill III **H-I** abdominal segments VIII-X **J** sternum IX, female **K** sternum IX, male **L** gill VII (flattened on slide) **M-O** gill VII (in natural position from ventral view), variability in shape.

rounded spatulate setae (Fig. 6D); hair-like setae and sparsely distributed stick-like setae. Anterior margin of femora with short, pointed and/or bluntly pointed spine-like setae; posterior margin with row of long blade-like setae and sparse row of bluntly pointed spine-like setae. Dorsal margin of tibiae and tarsi with row of long setae; ventral margin of both with irregular row of spine-like setae accumulated distally. Tarsal claws with two or three denticles.

Abdominal terga. Colour pattern of abdominal terga includes transversal stripe along anterior margin of terga I-IX (X) medially extending to triangular, short rectan-

gular or stripe-like medial macula on terga (III) IV–IX (transversal stripe sometimes not distinctly extended, for variability see Fig. 5A, H–J). Pair of sigilla sometimes coloured, in form of short stripes or spots located antero-laterally to medial macula. Tergum X without distinct maculation. Lateral margins of abdomen with oblique maculae on terga I–IX extending to dorso-posterior margin. Denticles along posterior margin on terga of various size, irregular and pointed, sometimes curved (Fig. 6E). Surface of terga covered with hair-like setae and sparsely with stick-like setae. Supra-tergalial projections short and blunt. Tergum X with more or less developed postero-lateral projections (Fig. 6H, I, arrows). Longitudinal row of hair-like setae medially along abdominal terga present.

Abdominal sterna. Yellowish, with distinct colouration pattern consisting of anteriorly widened pair of stripes (medio-anterior sigilla) on terga II–VIII (Fig. 5B, G, K). Sometimes only oblique stripes are present, without anterior widening (especially on sterna VI–VIII). Nerve ganglia occasionally darkened. Intensity of colouration varies among individuals. Sternum IX with V-shaped medial emargination; surface covered by irregularly distributed short hair-like setae, and medially accumulated longer hair-like setae (Fig. 6J, K).

Gills. Dorsal surface of gill plate I yellowish; of gill plates II–VII greyish on anterior half and brownish to reddish on posterior half. Ventral margin of all gill plates yellowish. Projection of gill plate III well developed (Fig. 6G). Shape of gill plate VII (in natural position from ventral view) varies from narrow to relatively wide (Figs 5G, 6M–O). Gill filaments reaching to 0.4–0.5× length of respective plate, filaments of gill VII to 0.24–0.30× (in late-instar larvae).

Cerci. Brownish, basally darkened.

Subimago, imago and eggs. Unknown

Morphological diagnostics of larvae. The main larval diagnostic characters of *E. (C.) zagrosicus* sp. nov. are as follows: (i) colour pattern of abdominal sterna (Fig. 5B, G, K) and abdominal terga (Fig. 5A, H–J), (ii) presence of postero-lateral projections on tergum X (Fig. 6H, I), (iii) presence of hypodermal medial femur spot (Fig. 5F), and (iv) fine hair-like setae on surface of abdominal terga (Fig. 6E).

Affinities. Based on the colour pattern of abdominal sterna, *E. (C.) zagrosicus* sp. nov. is most similar to *E. (C.) caucasicus* and *E. (C.) iranicus*. Both latter species possess pigmented medio-anterior sigilla forming a pair of oblique stripes on abdominal sterna II–VIII (e.g., Braasch 1979: 284, fig. 3b), and a medial hypodermal femur spot. However, *E. (C.) zagrosicus* sp. nov. differs by the distinct widening at the anterior margin of medio-anterior sigilla of abdominal sterna. If the sternal colour pattern is not fully developed (sporadically only stripes are present on all or several sterna), *E. (C.) zagrosicus* sp. nov. is distinguishable by the colour pattern of abdominal terga (Fig. 5A, H–J), which is different in *E. (C.) caucasicus* (Braasch 1979: 284, fig. 3a) and *E. (C.) iranicus* (Braasch and Soldán 1979: 264, fig. 12). In *E. (C.) zagrosicus* sp. nov., the postero-lateral projections on the tergum X are well-developed, whereas they are not significantly pronounced in either of the two species mentioned above (only small projections may be sporadically present).

Distinct postero-lateral projections on the tergum X are characteristic for *E. (C.) magnus*, *E. (C.) nigripilosus*, and *E. (C.) alborzicus* sp. nov. Small projections are also sporadically present in *E. (C.) znojkoii*. *E. (C.) magnus* can be easily distinguished from *E. (C.) zagrosicus* sp. nov. by the absence of colour pattern of abdominal sterna, the absence of a medial hypodermal femur spot, and setation on dorsal margin of labrum (numerous thickened bristle-like setae, Hrivniak et al., in prep.). *E. (C.) nigripilosus* and *E. (C.) alborzicus* sp. nov. differ by a typical colouration pattern of abdominal sterna (Sinitshenkova 1976: 89, fig. 28 for *E. (C.) nigripilosus* and Fig. 1B, G, K–M for *E. (C.) alborzicus* sp. nov.). *E. (C.) znojkoii* can be distinguished from *E. (C.) zagrosicus* sp. nov. by the colour pattern of abdominal terga and characteristic reddish colouration of abdominal sterna (Braasch 1980: 172, fig. 4b, c).

The presence of a medial hypodermal femur spot makes *E. (C.) zagrosicus* sp. nov. slightly similar to *E. (C.) turcicus* and *E. (C.) alborzicus* sp. nov. However, the presence of the characteristic pattern of abdominal sterna in *E. (C.) alborzicus* sp. nov. (Fig. 1B, G, K–M), and the absence of colouration pattern of abdominal sterna in *E. (C.) turcicus* reliably differentiate both species from *E. (C.) zagrosicus* sp. nov. Additionally, *E. (C.) turcicus* differs by the characteristic colour pattern of abdominal terga (Hrivniak et al. 2019: 61, fig. 1).

The other five species distributed in the Caucasus, namely *E. (C.) sinitshenkovae*, *E. (C.) alpestris*, *E. (C.) bicolliculatus*, *E. (C.) longimaculatus*, and *E. (C.) soldani*, do not share any important diagnostic characters with *E. (C.) zagrosicus* sp. nov. Nevertheless, *E. (C.) sinitshenkovae* and *E. (C.) alpestris* can be separated from *E. (C.) zagrosicus* sp. nov. by the absence of a medial hypodermal femur spot, overall colouration of the dorsal surface of femora (*E. (C.) sinitshenkovae*, Braasch and Zimmerman 1979: 106, fig. 10), and the different colouration of abdominal sterna (*E. (C.) alpestris*, Braasch 1979: 284, fig. 1d). Fine hair-like setae on the dorsal surface of abdominal terga clearly distinguish *E. (C.) zagrosicus* sp. nov. from *E. (C.) bicolliculatus*, *E. (C.) longimaculatus*, and *E. (C.) soldani*. All three species are characteristic by the presence of flattened setae on abdominal terga (Hrivniak et al. 2017: 359, figs 23–25).

Results from molecular species delimitation

The GMYC model provided significantly better fit to COI gene tree than the null model expecting uniform coalescent branching rates across entire tree (likelihood ratio test = $3.671927e-06^{***}$). The GMYC estimated 15 species (CI=13–19) consisting of 14 ML clusters and one singleton (CI = 12–16). All three newly described species were confirmed, and the overall number of delimited GMYC species corresponded well to morphologically defined species within *Caucasiron* (Fig. 7C). Monophyly of all species clusters were highly supported (PP = 1).

The ABGD analysis of the COI distance matrix recognized 15 stable groups within initial partition. All groups corresponded well to morphologically defined species and were congruent with GMYC analysis. All three newly proposed species were recognized as distinct groups (Fig. 7C). The mean pairwise genetic K2P distances between

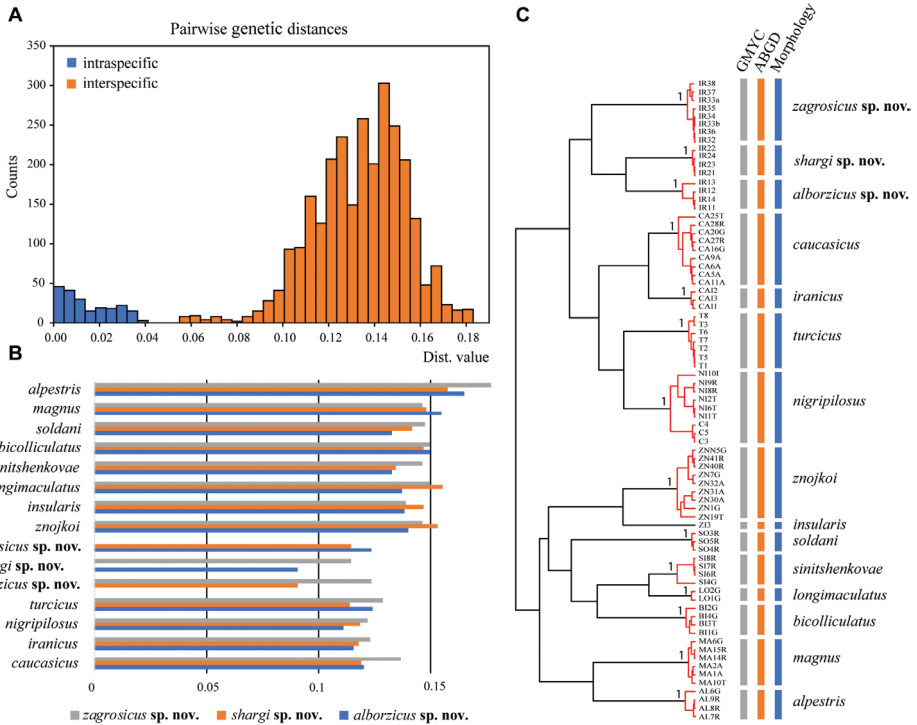


Figure 7. Results of the molecular species delimitation: **A** distribution of K2P pairwise genetic distances **B** mean pairwise genetic distances between new species and all Caucasian *Caucasion* species known **C** COI gene tree with the results of molecular species delimitation analyses and morphology (node supports for species are indicated).

all *Caucasion* species, including newly described, ranged between 6.71% (*E. (C.) caucasicus* / *E. (C.) iranicus*) and 17.68% (*E. (C.) alpestris* / *E. (C.) zagrosicus* sp. nov.). Maximum intraspecific and minimum interspecific distances were observed in *E. (C.) nigripilosus* (4.12%; Iran/Cyprus) and *E. (C.) caucasicus* / *E. (C.) iranicus* (5.48%), respectively. Overall distribution of K2P pairwise genetic distances is figured on Fig. 7A. Mean intraspecific genetic distances for all new species relative to individual *Caucasion* species are shown in Fig. 7B.

Distribution of *Caucasion* in Iran

Specimens of the genus *Epeorus* were found in 68 localities of all 254 localities investigated by us in 2016–2018 (Fig. 8) and in seven additional localities investigated by others (Braasch and Soldán 1979; Mousavi and Hakobyan 2017) (Table 1). Their occurrence was limited to streams with good water quality at altitudes between -4 and 2440 m a.s.l. (Table 1). They were neither found in polluted streams of agricultural and urban areas, nor in seasonally drying streams. Most of the species and



Figure 8. The map showing the occurrence of *Epeorus* (*Caucasiron*) spp. at all localities investigated in Iran. Colour of symbols shows the occurrence of species: green – *Epeorus* (*Caucasiron*) *zagrosicus* sp. nov., dark blue – *Epeorus* (*Epeorus*) *zaitzevi*, and violet – all other *Epeorus* (*Caucasiron*) species. Black symbols show collection points where no species of *Epeorus* was found. The letter H shows the locality of the respective holotype.

records were found in the Alborz in northern Iran (Fig. 9). These mountains host five species of the subgenus *Caucasiron* and one species of the subgenus *Epeorus* (*E. zaitzevi*). Except for the newly described species, *E. (C.) nigripilosus* found in five localities in the Alborz is new for Iran (its genetic data from the Alborz were used in phylogeographical analyses in Hrivniak et al. 2020). It is a widely distributed species ranging from Cyprus and Turkey to Georgia, Russia and Iraq (Sinitschenkova, 1976; Braasch 1979; Al-Zubaidi et al. 1987; Salur et al. 2016; Gabelashvili et al. 2018; Hrivniak et al. 2020). The identification of *E. (C.) nigripilosus* was confirmed by both morphological characters and molecular delimitation. The specimen from the

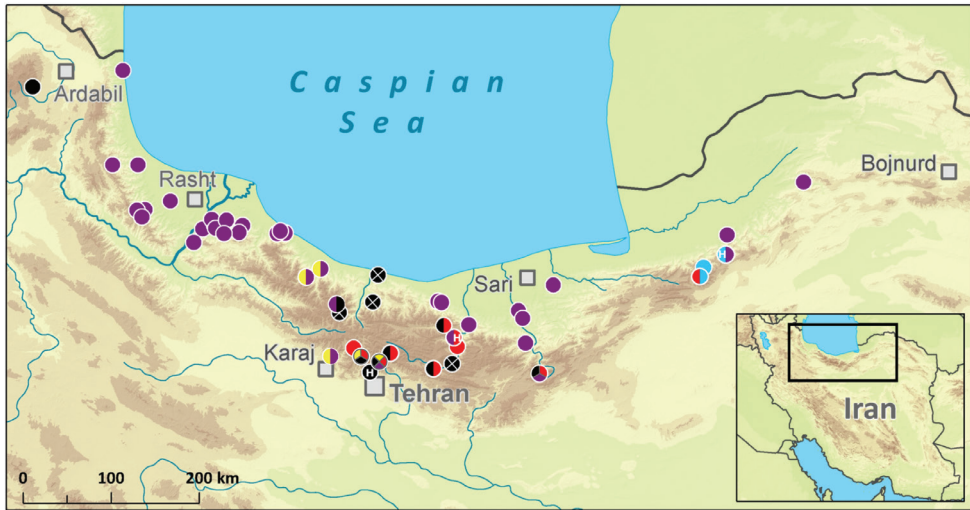


Figure 9. Distribution of *Epeorus* (*Caucasiron*) species in northern Iran. Colour of symbols shows the occurrence of species: red – *E. (C.) alborzicus* sp. nov., light blue – *E. (C.) shargi* sp. nov., violet – *E. (C.) cf. znojkoii*, black – *E. (C.) iranicus*, yellow – *E. (C.) nigripilosus*. The letter H shows the localities of holotypes. Black symbols with white cross show unrevised records of *E. (C.) iranicus*.

Alborz (coded as NI10I in Fig. 7C) clustered within the clade containing conspecific individuals from Russia and Turkey in the analysis of COI. It differed from these conspecifics in 2.8–3.6 % of K2P distance.

The most common *Caucasiron* species in the Alborz is *E. (C.) cf. znojkoii* distributed from the Talysh Mts. in the west to the Golestan NP in the east (Fig. 9). However, our study dealing with the molecular diversity of *Caucasiron* species in the Caucasus and adjacent regions (Hrivniak et al. 2020) indicated that *E. (C.) znojkoii* might represent a complex of cryptic species (only a subset of sequences included in the present study). The lineage *Caucasiron* sp. 4 (see Hrivniak et al. 2020) occurring in Iran (here called *E. (C.) cf. znojkoii*) differed from the Central Caucasian lineage. The delimitation of species within *E. (C.) znojkoii* s. l. requires further study. Nevertheless, the morphotype of *E. (C.) cf. znojkoii* has a wide geographical and ecological range, occurring at altitudes from -4 to 2290 m a.s.l. in northern Iran (Table 1). It was often found in shallow warm streams with good water quality flowing in humid broadleaved forests in the Caspian Sea lowland; approximately half of its localities was below 350 m a.s.l. At higher altitude, it may co-occur with *E. (C.) alborzicus* sp. nov., *E. (C.) shargi* sp. nov., *E. (C.) nigripilosus*, and *E. (C.) iranicus* (Fig. 9).

Three *Caucasiron* species, *E. (C.) iranicus*, *E. (C.) alborzicus* sp. nov., and *E. (C.) shargi* sp. nov., were described from the Alborz and are so far only known from there. *E. (C.) iranicus* is reliably reported from 12 localities, eight of them above 2000 m a.s.l. These include the Sabalan Mt. slopes in the western Alborz and the central Alborz, where it can co-occur with *E. (C.) alborzicus* sp. nov. (Fig. 9). It was found only in very cold streams fed by glaciers and melting snow from the highest mountains, with



Figure 10. Photos of the localities of the new *Epeorus* (*Caucasiron*) species described herein: **A** unnamed brook near Panjab village – type locality of *E. (C.) alborzicus* sp. nov. **B** unnamed brook near Kahrud-e Bala village – locality of *E. (C.) alborzicus* sp. nov. **C** unnamed river near Shirinabad village – type locality of *E. (C.) shargi* sp. nov. **D** unnamed brook near Chah-e Ja village – locality of *E. (C.) shargi* sp. nov. **E** Gamasiab River near Varayeneh village – type locality of *E. (C.) zagrosicus* sp. nov. **F** Yasuj fall near Yasuj village – locality of *E. (C.) zagrosicus* sp. nov.

Alborz (coded as NI10I in Fig. 7C) clustered within the clade containing conspecific individuals from Russia and Turkey in the analysis of COI. It differed from these conspecifics in 2.8–3.6 % of K2P distance.

The most common *Caucasiron* species in the Alborz is *E. (C.)* cf. *znojkoii* distributed from the Talysh Mts. in the west to the Golestan NP in the east (Fig. 9). However,

Alborz (coded as NI10I in Fig. 7C) clustered within the clade containing conspecific individuals from Russia and Turkey in the analysis of COI. It differed from these conspecifics in 2.8–3.6 % of K2P distance.

The most common *Caucasiron* species in the Alborz is *E. (C.) cf. znojkoii* distributed from the Talysh Mts. in the west to the Golestan NP in the east (Fig. 9). However, our study dealing with the molecular diversity of *Caucasiron* species in the Caucasus and adjacent regions (Hrivniak et al. 2020) indicated that *E. (C.) znojkoii* might represent a complex of cryptic species (only a subset of sequences included in the present study). The lineage *Caucasiron* sp. 4 (see Hrivniak et al. 2020) occurring in Iran (here called *E. (C.) cf. znojkoii*) differed from the Central Caucasian lineage. The delimitation of species within *E. (C.) znojkoii* s. l. requires further study. Nevertheless, the morphotype of *E. (C.) cf. znojkoii* has a wide geographical and ecological range, occurring at altitudes from -4 to 2290 m a.s.l. in northern Iran (Table 1). It was often found in shallow warm streams with good water quality flowing in humid broadleaved forests in the Caspian Sea lowland; approximately half of its localities was below 350 m a.s.l. At higher altitude, it can co-occur with *E. (C.) alborzicus* sp. nov., *E. (C.) shargi* sp. nov., *E. (C.) nigripilosus*, and *E. (C.) iranicus* (Fig. 9).

Three *Caucasiron* species, *E. (C.) iranicus*, *E. (C.) alborzicus* sp. nov., and *E. (C.) shargi* sp. nov., were described from the Alborz and are so far only known from there. *E. (C.) iranicus* is reliably reported from 12 localities, eight of them above 2000 m a.s.l. These include the Sabalan Mt. slopes in the western Alborz and the central Alborz, where it can co-occur with *E. (C.) alborzicus* sp. nov. (Fig. 9). It was found only in very cold streams fed by glaciers and melting snow from the highest mountains, with very rapid flow and strongly turbulent riffle sections. Four records of *E. (C.) iranicus* published by Mousavi and Hakobyan (2017) should be revised, because they included a wide range of altitude (20–2120 m a.s.l.) and were very close to our records of *E. (C.) alborzicus* sp. nov. and *E. (C.) cf. znojkoii*. The two new species from the Alborz seem to differ in habitat requirements. *Epeorus (C.) alborzicus* sp. nov. was only found in higher altitudes. These were all treeless localities in montane valleys with harsh climatic conditions, whereas *E. (C.) shargi* sp. nov. was found well below in submontane streams that were flowing in forests. The latter species was recorded only in the eastern Alborz near Gorgan (Fig. 9).

Other streams investigated in Iranian mountain ranges were dominated by Baetidae, and Heptageniidae were generally only scattered there. Larvae of *E. (C.) zagrosicus* sp. nov. and *E. (E.) zaitzevi* were found only in five and seven localities respectively, relatively distant to each other in the Zagros (Fig. 8). However, most of the streams explored in the Zagros were polluted or seasonally drying out due to the water storage in dams and water abstraction for irrigation of surrounding fields. Moreover, streams at higher altitude with presumably better water quality were almost inaccessible for us in April and May during our field trips. As *E. (C.) zagrosicus* sp. nov. was mostly found in natural streams in high-mountain valleys only with sparse villages, we expect that its distribution is limited to clear and cold mountain streams. However, a more detailed investigation of mayflies in high-mountain streams in Iran is needed.

Table 1. List of records of the *Caucasian* species found in Iran (three new species are not included). Abbreviations: RT – right tributary; LT – left tributary; JB – Jindriška Bojková; TS – Tomáš Soldán; IN – Javid Imanpour Namin; SB – Samereh Bagheri; AHS – Arnold H. Stancizek; MP – Milan Pallmann; RJG – Roman J. Godunko; FN – Farshad Nejati; AA – Ashgar Abdoli; HV – H. Válikhani; PT – P. Taban. Number of specimens includes larvae.

Species	Province	Stream	Locality	Nearest settlement	Altitude	Latitude (N) / Longitude (E)	Sampling date	Collector/reference	Number of specimens
<i>E. (C.) iranicus</i>	Alborz	Karaj R., Shahrestanak branch	SE of Shahrestanak	Chavar Chalun	2220	35°57'45.8"N, 051°21'59.7"E	1.9.2016	AA, HV, PT	4
	Ardabil	unnamed brook	in Alvaresi (below Alvares ski area)	Sarein	2235	38°09'38.0"N, 047°56'21.0"E	17.5.2016	JB, TS, IN; Bojková et al. 2018	2
	Mazandaran	Koshk Sara R.	in Kosh Sara	Chalus	18	36°37'57.7"N, 051°28'04.4"E	25.9.2013	Mousavi and Hakobyan 2017	2
	Mazandaran	Firuz Abad R.	near Dasht Nazir	Marzan Abad	929	36°24'33.8"N, 051°24'42.5"E	11.9.2014	Mousavi and Hakobyan 2017	80
	Mazandaran	Haraz R.	in Gazanak	Gazanak	1590	35°54'08.3"N, 052°13'30.0"E	10.7.2013	Mousavi and Hakobyan 2017	8
	Mazandaran	Dalir R.	above Dalir	Marzan Abad	2126	36°19'23.2"N, 051°04'27.5"E	26.7.2014	Mousavi and Hakobyan 2017	174
	Mazandaran	Lasem R.	E of Polour	Polour	2180	35°50'04.1"N, 052°05'07.6"E	14.5.2017	AHS, MP, FN	1
	Mazandaran	RT of Sardab Rud	SW of Kelardasht	Kelardasht	2020	36°26'06.5"N, 051°03'52.6"E	8.3.2018	SB	85
	Mazandaran	LT of Sardab Rud	NW of Vandarbon	Kelardasht	2250	36°25'53.7"N, 051°01'59.1"E	9.3.2018	SB	63
	Mazandaran	Sardab Rud	S of Vandarbon	Kelardasht	2290	36°25'23.0"N, 051°02'12.4"E	10.3.2018	SB	5
	Tehran	Darban valley (type locality)	N of Tehran	Tehran	2100	35°50'24.0"N, 051°25'19.9"E	18.7.1970	Braasch and Soldán 1979	14
	<i>E. (C.) nigripilosus</i>	Tehran	Lalan R.	above Zayegan	Fasham	2290	35°58'39.2"N, 051°34'56.5"E	8.5.2017	AHS, MP, RJG, FN
Tehran		Lalan R.	in Lalan	Lalan	2440	35°59'50.3"N, 051°34'51.0"E	8.5.2017	AHS, MP, RJG, FN	87
Tehran		Ahar R.	near Igol	Fasham	2020	35°55'11.2"N, 051°28'51.3"E	8.5.2017	AHS, MP, RJG, FN	1
Tehran		Shahrestanak R.	NW of Shahrestanak	Asara	2100	35°59'01.2"N, 051°19'09.6"E	10.5.2017	AHS, MP, FN	1
Alborz		Kordan R.	N of Kordan	Kordan	1430	36°57'15.6"N, 050°50'25.3"E	10.5.2017	AHS, MP, FN	4
Mazandaran		RT of Dohezar R.	N of Holu Kaleh	Tonkaboon	880	36°37'37.5"N, 050°44'30.2"E	16.6.2018	SB	1
Mazandaran		Dohezar R.	SW of Parde Sar	Tonkaboon	450	36°40'07.0"N, 050°49'20.0"E	16.6.2018	SB	1
Tehran		Ahar R.	near Igol	Fasham	2020	35°55'11.2"N, 051°28'51.3"E	8.5.2017	AHS, MP, RJG, FN	5
Tehran		Shahrestanak R.	NW of Shahrestanak	Asara	2100	35°59'01.2"N, 051°19'09.6"E	10.5.2017	AHS, MP, FN	1

Species	Province	Stream	Locality	Nearest settlement	Altitude	Latitude (N) / Longitude (E)	Sampling date	Collector/reference	Number of specimens
<i>E. (C.) cf. znojtkoi</i>	Alborz	Kordan R.	N of Kordan	Kordan	1430	35°57'15.6"N, 050°50'25.3"E	10.5.2017	AHS, MP, FN	4
	Gilan	RT of Khara Rud	S of Paerin Khara Rud (S of Pashaki)	Sangar	210	37°02'29.0"N, 049°47'52.0"E	12.5.2016	JB, TS, IN	71
	Gilan	left fork of Khara Rud	in Madarsara (S of Pashaki)	Sangar	105	37°04'12.0"N, 049°46'36.0"E	12.5.2016	JB, TS, IN	27
	Gilan	right fork of Khara Rud	in Golestansara (S of Pashaki)	Sangar	201	37°02'20.0"N, 049°47'27.0"E	12.5.2016	JB, TS, IN	2
	Gilan	Zilaki River (RT of Sefid Rud)	in Mush Bijar (E of Shahr-e Bijar)	Shahr-e Bijar	120	37°00'28.0"N, 049°40'24.0"E	13.5.2016	JB, TS, IN	1
	Gilan	Sefidab (RT of Siah Rud)	in Divarsh (NE of Shirkuh)	Tutkabon	280	36°53'59.0"N, 049°35'06.0"E	13.5.2016	JB, TS, IN	149
	Gilan	Sangdeh (LT of Shafa Rud)	W of Punel	Punel	240	37°31'47.0"N, 049°00'52.0"E	15.5.2016	JB, TS, IN	10
	Gilan	Shafa Rud	W of Punel	Punel	240	37°31'47.0"N, 049°00'52.0"E	15.5.2016	JB, TS, IN	6
	Gilan	LT of Shafa Rud	NW of Sangdeh	Sangdeh	1345	37°31'46.0"N, 048°45'19.0"E	15.5.2016	JB, TS, IN	50
	Gilan	Shakhzar R.	NE of Fuman	Fuman	6	37°14'13.0"N, 049°20'43.0"E	15.5.2016	JB, TS, IN	1
	Gilan	LT of Bala Rud	S of Siahkal	Siahkal	490	37°00'31.0"N, 049°51'51.0"E	16.5.2016	JB, TS, IN	16
	Gilan	Lanak waterfalls	S of Siahkal	Siahkal	510	37°00'31.0"N, 049°51'49.0"E	16.5.2016	JB, TS, IN	5
	Gilan	Shamrud (RT of Sefid Rud)	S of Tushi (S of Siahkal)	Siahkal	315	37°03'00.0"N, 049°55'54.0"E	16.5.2016	JB, TS, IN	37
	Gilan	Chelavand R.	W of Chelvand	Lavandvil	-4	38°17'20.0"N, 048°51'35.0"E	19.5.2016	JB, TS, IN	2
	Gilan	unnamed brook	N of Chaldasht	Amlash	1255	36°59'33.0"N, 050°05'19.0"E	21.5.2016	JB, TS, IN	3
	Gilan	RT of Shalman Rud	in Bolurdekan	Amlash	345	37°01'09.0"N, 050°03'51.0"E	21.5.2016	JB, TS, IN	2
	Gilan	LT of Ghale Rudkhan	NE of Masuleh	Fuman	885	37°09'47.0"N, 049°00'17.0"E	22.5.2016	JB, TS, IN	66
	Gilan	RT of Ghale Rudkhan	NE of Masuleh	Fuman	705	37°09'42.0"N, 049°01'17.0"E	22.5.2016	JB, TS, IN	6
	Gilan	Ghale Rudkhan R.	E of Masuleh	Fuman	370	37°10'02.0"N, 049°05'03.0"E	22.5.2016	JB, TS, IN	4
Golestan	unnamed river	in Shirinabad	Aliabad-e Katul	740	36°48'01.0"N, 055°01'05.0"E	27.4.2018	JB, TS, IN	50	
Golestan	Shirabad waterfalls	above Shirabad	Shirabad	140	36°57'33.0"N, 055°01'57.0"E	28.4.2018	JB, TS, IN	48	
Golestan	RT of Madarsu R.	E of Tangrah	Tangrah	495	37°23'27.0"N, 055°48'51.0"E	30.4.2018	JB, TS, IN	1	

Species	Province	Stream	Locality	Nearest settlement	Altitude	Latitude (N) / Longitude (E)	Sampling date	Collector/reference	Number of specimens
<i>E. (C.) cf. znojtkoi</i>	Mazandaran	Shirinrud	S of Part Kola	Farim	770	36°09'02.5"N, 05°3'20'58.1"E	11.5.2017	AHS, MP, FN	203
	Mazandaran	trib. Kaspel R.	SW of Chamestan	Chamestan	400	36°25'31.4"N, 05°2'03'38.4"E	13.5.2017	AHS, MP, FN	17
	Mazandaran	Chelav R.	N of Pasha Kola	Pasha Kola	820	36°12'24.7"N, 05°2'25'51.9"E	14.5.2017	AHS, MP, FN	63
	Mazandaran	Chelav R.	NW of Pasha Kola	Pasha Kola	570	36°13'28.9"N, 05°2'23'35.4"E	14.5.2017	AHS, MP, FN	2
	Mazandaran	Baladeh R.	W of Razan	Razan	1360	36°11'39.6"N, 05°2'08'34.6"E	14.5.2017	AHS, MP, FN	9
	Mazandaran	Chat Bagh R.	E of Andar Koli	Ghaem Shahr	200	36°20'30.0"N, 05°2'54'03.0"E	8.5.2018	JB, TS, IN, SB	27
	Mazandaran	RT of Haraz R.	NW of Pasha Kola	Amol	570	36°13'27.0"N, 05°2'23'36.0"E	9.5.2018	JB, TS, IN, SB	5
	Mazandaran	LT of Haraz R.	in Panjab	Amol	955	36°05'52.0"N, 05°2'15'15.0"E	9.5.2018	JB, TS, IN, SB	1
	Mazandaran	unnamed brook	above Darab Kola	Neka	135	36°33'10.0"N, 05°3'15'32.0"E	10.5.2018	JB, TS, SB	2
	Mazandaran	unnamed brook	in Momey Khal	Ghaem Shahr	760	36°04'24.0"N, 05°2'58'19.0"E	11.5.2018	JB, TS, SB	1
	Mazandaran	Palang Darreh R.	SE of Shirgah	Shirgah	320	36°16'31.0"N, 05°2'56'54.0"E	11.5.2018	JB, TS, SB	2
	Mazandaran	LT of Palang Darreh R.	SE of Shirgah	Shirgah	345	36°16'30.0"N, 05°2'56'51.0"E	11.5.2018	JB, TS, SB	1
	Mazandaran	RT of Sardab Rud	SW of Kelardasht	Kelardasht	2020	36°26'06.5"N, 05°1'03'52.6"E	9.3.2018	SB	9
	Mazandaran	Sardab Rud	S of Vandarboon	Kelardasht	2290	36°25'23.0"N, 05°1'02'12.4"E	16.6.2018	SB	57
	Mazandaran	RT of Dohezar R.	N Holu Kaleh	Tonkabon	880	36°37'37.5"N, 05°0'44'30.2"E	16.6.2018	SB	83
	Mazandaran	Dohezar R.	SW Parde Sar	Tonkabon	450	36°40'07.0"N, 05°0'49'20.0"E	16.6.2018	SB	46
	Mazandaran	RT of Sehezar R.	S Parde Sar	Tonkabon	570	36°38'41.5"N, 05°0'50'11.1"E	16.6.2018	SB	20
	Mazandaran	Sehezar R.	S Parde Sar	Tonkabon	540	36°39'01.0"N, 05°0'50'00.0"E	24.8.2018	SB	21
	Mazandaran	Lavij Rud	SE of Kiakola	Noor	820	36°21'33.1"N, 05°2'03'11.0"E	24.8.2018	SB	8
	Mazandaran	Vaz Rud	E of Vaz Oliya	Noor	1140	36°19'08.0"N, 05°2'08'24.1"E	15.6.2018	SB	33
	Mazandaran	Safarud	SW of Ramsar	Ramsar	490	36°52'55.8"N, 05°0'33'56.1"E	15.6.2018	SB	1
	Mazandaran	LT of Safarud	SW of Ramsar	Ramsar	610	36°53'24.4"N, 05°0'33'56.1"E	15.6.2018	SB	2
	Mazandaran	LT of Safarud	SW of Ramsar	Ramsar	330	36°54'06.1"N, 05°0'35'12.1"E	15.6.2018	SB	11
Mazandaran	Chalak Rud	SW of Galeshmahalleh	Ramsar	100	36°49'13.0"N, 05°0'43'23.8"E	15.6.2018	SB	3	
Mazandaran	LT of Chalak Rud	NW of Taleh Sara	Ramsar	180	36°50'46.9"N, 05°0'40'25.9"E	8.3.2018	SB	8	
Tehran	Ahar R.	near Igol	Fasham	2020	35°55'11.2"N, 05°1'28'51.3"E	8.5.2017	AHS, MP, RJG, FN	4	

Acknowledgements

We thank the Faculty of Natural Resources of the University of Gilan, the Department of Biodiversity and Ecosystem Management, Environmental Sciences Research Institute, Shahid Beheshti University, Tehran, and the Department of Environment, Natural History Museum and Genetic Resources, Tehran, for collaboration, support, sampling and export permits, and accompanying the authors during field trips. This research was part of the SMNS Research Incentive 2016 to AHS and conducted with support from the Grant Agency of University of South Bohemia: GAJU 152/2016/P provided for LH and institutional support of Institute of Entomology (Biology Centre of the Czech Academy of Sciences): RVO: 60077344 for LH, PS and RJG.

References

- Al-Zubaidi F, Braasch D, Al-Kayatt A (1987) Mayflies from Iraq (Insecta, Ephemeroptera). Faunistische Abhandlungen. Staatliches Museum für Tierkunde. Dresden 14: 179–184.
- Bauernfeind E, Soldán T (2012) The mayflies of Europe (Ephemeroptera). Apollo Books, Olerup, 781 pp.
- Bojková J, Sroka P, Soldán T, Imanpour Namin J, Staniczek AH, Polášek M, Hrivniak L, Abdoli A, Godunko RJ (2018) Initial commented checklist of Iranian mayflies (Insecta: Ephemeroptera), with new area records and description of *Procloeon caspicum* sp. n. (Baetidae). ZooKeys 749: 87–123. <https://doi.org/10.3897/zookeys.749.24104>
- Bouckaert R, Heled J, Kühnert D, Vaughan T, Wu CH, Xie D, Suchard MA, Rambaut A, Drummond AJ (2014) BEAST 2: A Software Platform for Bayesian Evolutionary Analysis. PLoS Comput Biol. 10, e1003537. <https://doi.org/10.1371/journal.pcbi.1003537>
- Bouckaert R, Drummond AJ (2017) bModelTest: Bayesian phylogenetic site model averaging and model comparison. BMC Evol. Biol. 17, 42. <https://doi.org/10.1186/s12862-017-0890-6>
- Braasch D (1979) Beitrag zur Kenntnis der Gattung *Iron* Eaton im Kaukasus (UdSSR) (III) (Ephemeroptera, Heptageniidae). Reichenbachia 17: 283–294.
- Braasch D (1980) Beitrag zur Kenntnis der Gattung *Iron* Eaton (Heptageniidae, Ephemeroptera) im Kaukasus (UdSSR), 2. Entomologische Nachrichten 24: 166–173.
- Braasch D (2006) Neue Eintagsfliegen der Gattungen *Epeorus* und *Iron* aus dem Himalaja (Ephemeroptera, Heptageniidae). Entomologische Nachrichten und Berichte 50: 79–88.
- Braasch D, Soldán T (1979) Neue Heptageniidae aus Asien (Ephemeroptera). Reichenbachia 17: 261–272.
- Braasch D, Zimmermann W (1979) *Iron sinitschenkova* sp.n. – eine neue Heptageniide (Ephemeroptera) aus dem Kaukasus. Entomologische Nachrichten 23: 103–107.
- Bryson RW, Warren E, Savary WE, Prendini L (2013) Biogeography of scorpions in the *Pseudouroctonus minimus* complex (Vaejovidae) from south-western North America: implications of ecological specialization for pre-Quaternary diversification. Journal of Biogeography 40, 1850–1860. <https://doi.org/10.1111/jbi.12134>

- Chen P, Wang Y, Zhou C-F (2010) A New Mayfly Species of *Epeorus* (*Caucasiron*) from Southwestern China (Ephemeroptera: Heptageniidae). *Zootaxa* 2527: 61–68. <https://doi.org/10.11646/zootaxa.2527.1.4>
- Fujisawa T, Barraclough TG (2013) Delimiting Species Using Single-Locus Data and the Generalized Mixed Yule Coalescent Approach: A Revised Method and Evaluation on Simulated Data Sets. *Systematic Biology* 62: 707–724. <https://doi.org/10.1093/sysbio/syt033>
- Gabelashvili S, Mumladze L, Bikashvili A, Sroka P, Godunko RJ, Japoshvili B (2018) The first annotated checklist of mayflies (Ephemeroptera: Insecta) of Georgia with new distribution data and a new record for the country. *Turkish Journal of Zoology* 42: 252–262. <https://doi.org/10.3906/zoo-1709-4>
- Hrivniak L, Sroka P, Bojková J, Godunko RJ, Soldán T, Staniczek AH (2020) The impact of Miocene orogeny for the diversification of Caucasian *Epeorus* (*Caucasiron*) mayflies (Ephemeroptera: Heptageniidae). *Molecular Phylogenetics and Evolution*. <https://doi.org/10.1016/j.ympev.2020.106735>
- Hrivniak L, Sroka P, Godunko RJ, Žurovcová M (2017) Mayflies of the genus *Epeorus* Eaton, 1881 s.l. (Ephemeroptera: Heptageniidae) from the Caucasus Mountains: a new species of *Caucasiron* Kluge, 1997 from Georgia and Turkey. *Zootaxa* 4341: 353–374. <https://doi.org/10.11646/zootaxa.4341.3.2>
- Hrivniak L, Sroka P, Türkmen G, Godunko RJ, Kazancı N (2019) A new *Epeorus* (*Caucasiron*) (Ephemeroptera: Heptageniidae) species from Turkey based on molecular and morphological evidence. *Zootaxa* 4550: 58–70. <https://doi.org/10.11646/zootaxa.4550.1.2>
- Katoh K, Misawa K, Kuma K, Miyata T (2002) MAFFT: a novel method for rapid multiple sequence alignment based on fast Fourier transform. *Nucleic Acids Research* 30: 3059–3066. <https://doi.org/10.1093/nar/gkf436>
- Kluge NJ (1997) New subgenera of Holarctic mayflies (Ephemeroptera: Heptageniidae, Leptophlebiidae, Ephemerellidae). *Zoosystematica Rossica* 5: 233–235.
- Kluge NJ (2004) *The phylogenetic system of Ephemeroptera*. Springer, Dordrecht, 456 pp. <https://doi.org/10.1007/978-94-007-0872-3>
- Kluge NJ (2015) Central Asian mountain Rhithrogenini (Ephemeroptera: Heptageniidae) with pointed and ephemeropteroid claws in the winged stages. *Zootaxa* 3994: 301–353. <https://doi.org/10.11646/zootaxa.3994.3.1>
- Kluge NJ, Novikova EA (2011) Systematics of the mayfly taxon *Acentrella* (Ephemeroptera, Baetidae), with description of new Asian and African species. *Russian Entomological Journal* 20: 1–56. <https://doi.org/10.15298/rusentj.20.1.01>
- Kumar S, Stecher G, Tamura K (2016) MEGA7: Molecular Evolutionary Genetics Analysis Version 7.0 for Bigger Datasets. *Molecular Biology and Evolution* 33: 1870–1874. <https://doi.org/10.1093/molbev/msw054>
- Miller MA, Pfeiffer W, Schwartz T (2010) Creating the CIPRES Science Gateway for inference of large phylogenetic trees. *Gateway Computing Environments Workshop, 2010*, 1–8. <https://doi.org/10.1109/GCE.2010.5676129>
- Monaghan MT, Wild R, Elliot M, Fujisawa T, Balke M, Inward DJG, Lees DC, Ranaivosolo R, Eggleton P, Barraclough TG, Vogler AP (2009) Accelerated species inventory on Madagas-

- car using coalescent-based models of species delineation. *Systematic Biology* 58: 298–311. <https://doi.org/10.1093/sysbio/syp027>
- Mousavi A, Hakobyan S (2017) Materials on the fauna of mayflies (Ephemeroptera), stoneflies (Plecoptera) and caddisflies (Trichoptera) of Mazandaran Province of Iran (Insecta). *National Academy of Sciences of RA, Electronic Journal of Natural Sciences* 1: 28.
- Nguyen VV, Bae YJ (2004) Larvae of the heptageniid mayfly genus *Epeorus* (Ephemeroptera: Heptageniidae) from Vietnam. *Journal of Asia-Pacific Entomology* 7: 19–28. [https://doi.org/10.1016/S1226-8615\(08\)60197-1](https://doi.org/10.1016/S1226-8615(08)60197-1)
- Myers N, Mittermeier RA, Mittermeier CG, Da Fonseca GAB, Kent J (2000) Biodiversity hotspots for conservation priorities. *Nature* 403: 853–858. <https://doi.org/10.1038/35002501>
- Pons J, Barraclough TG, Gomez-Zurita J, Cardoso A, Duran DP, Hazell S, Kamoun S, Sumlin WD, Vogler AP (2006) Sequence-based species delimitation for the DNA taxonomy of undescribed insects. *Systematic Biology* 55: 595–609. <https://doi.org/10.1080/10635150600852011>
- Puillandre N, Lambert A, Brouillet S, Achaz G (2012) ABGD, Automatic Barcode Gap Discovery for primary species delimitation. *Molecular Ecology* 21: 1864–77. <https://doi.org/10.1111/j.1365-294X.2011.05239.x>
- Salur A, Darilmaz MC, Bauernfeind E (2016) An annotated catalogue of the mayfly fauna of Turkey (Insecta, Ephemeroptera). *ZooKeys* 620: 67–118. <https://doi.org/10.3897/zookeys.620.9405>
- Sinitshenkova ND (1976) Mayflies of the Genus *Iron* Eaton (Ephemeroptera, Heptageniidae) in the Fauna of the Caucasus. *Entomologicheskoye obozreniye* 55: 853–862.
- Sroka P, Bojková J, Godunko RJ, Soldán T, Namin JI, Nejat F, Abdoli A, Staniczek AH (2019) New Oligoneuriidae (Insecta, Ephemeroptera) from Iran. *ZooKeys* 872: 101–126. <https://doi.org/10.3897/zookeys.872.36098>
- Staniczek AH, Malzacher P, Bojková J, Sroka P, Soldán T, Imanpour Namin J, Nejat F, Abdoli A, Godunko RJ (2020) Caenidae (Insecta: Ephemeroptera) of Iran, with new records and re-description of the nymph of *Caenis kopetdagi* Kluge, 1985. *Aquatic Insects* 41(2): 106–130. <https://doi.org/10.1080/01650424.2020.1735449>
- Vuataz L, Sartori M, Wagner A, Monaghan MT (2011) Toward a DNA taxonomy of Alpine *Rhithrogena* (Ephemeroptera: Heptageniidae) using a mixed Yule-coalescent analysis of mitochondrial and nuclear DNA. *PLoS ONE* 6, e19728. <https://doi.org/10.1371/journal.pone.0019728>
- Zaldívar-Riverón A, Martínez JJ, Ceccarelli SF, De Jesús-Bonilla VS, Rodríguez-Pérez AC, Reséndiz-Flores A, Smith MA (2010) DNA barcoding a highly diverse group of parasitoid wasps (Braconidae: Doryctinae) from a Mexican nature reserve. *Mitochondrial DNA* 21 (Supplement 1): 18–23. <https://doi.org/10.3109/19401736.2010.523701>

Two new species of the genus *Xya* Latreille, 1809 (Orthoptera, Tridactyloidea, Tridactylidae) from Yunnan with a key to all *Xya* species in China

Chengquan Cao¹, Hua Rong¹, Hassan Naveed¹

¹ College of Life Science, Leshan Normal University, Leshan, Sichuan 614004, China

Corresponding author: Chengquan Cao (chqcao1314@163.com)

Academic editor: T. Robillard | Received 12 February 2020 | Accepted 28 May 2020 | Published 8 July 2020

<http://zoobank.org/E648CEFB-A673-45A6-B41E-DF7CA673D1F0>

Citation: Cao C, Rong H, Naveed H (2020) Two new species of the genus *Xya* Latreille, 1809 (Orthoptera, Tridactyloidea, Tridactylidae) from Yunnan with a key to all *Xya* species in China. *ZooKeys* 947: 103–112. <https://doi.org/10.3897/zookeys.947.51067>

Abstract

This contribution to the taxonomy of *Xya* Latreille, 1809 (Orthoptera, Tridactyloidea, Tridactylidae) adds descriptions and photographic illustrations of two new species: *Xya xishangbanna* **sp. nov.** and *Xya yunnanensis* **sp. nov.** from Xishuangbanna, Yunnan Province, China. *Xya xishangbanna* **sp. nov.** can be diagnosed by the shiny dark brown hind femora, and the epiproct with a shallow bottom of the middle “v-shaped” crack in the upper part and straight sides; *Xya yunnanensis* **sp. nov.** can be diagnosed by the compound eye bearing no narrow band along the inner margin, and the epiproct with the bottom of the side edge with a sharply angled protrusion and a narrow lower anchor-shaped base less than 1/2 the width of the upper one. Distributional information and bionomics for these two new species and photos for the habitat are given. A key to all Chinese species of *Xya* is provided.

Keywords

key, new species, Orthoptera, pygmy mole cricket, taxonomy, Tridactylidae, *Xya*

Introduction

The pygmy mole cricket genus *Xya* (Orthoptera, Tridactyloidea, Tridactylidae) was established by Latreille in 1809 with *Tridactylus variegatus* as its type species. The genus *Xya* Latreille, 1809 contains 59 described species worldwide, of which about 19 species are known to occur in Asia. According to the online Orthoptera Species File (<http://orthoptera.speciesfile.org/HomePage/Orthoptera/HomePage.aspx>, accessed 6 April 2018) the nine species that have been reported in China are: *Xya japonica* (Haan, 1844); *Xya nitobei* (Shiraki, 1911); *Xya manchurei* Shiraki, 1936; *Xya apicicornis* (Chopard, 1928); *Xya riparia* (Saussure, 1877); *Xya leshanensis* Cao, Shi & Hu, 2017; *Xya shandongensis* Zhang, Yin & Yin, 2018; *Xya sichuanensis* Cao, Shi & Yin, 2018 and *Xya fujianensis* Cao, Chen & Yin, 2020 (Latreille 1809; Haan 1844; Walker 1871; Saussure 1877, 1896; Brunner von Wattenwyl 1893; Bolívar 1900 (1899); Shiraki 1911; Chopard 1928, 1936, 1968; Bey-Bienko 1967; Günther 1974, 1980, 1995; Ingrisch 1987; Yin et al. 1996; Murai 2005; Yin et al. 2013; Heads and Hollier 2016; Kuravova and Kocarek 2016; Cao et al. 2017; Zhang et al. 2017; Cigliano et al. 2018; Cao et al. 2018 and Cao et al. 2020)

During an ongoing study of pygmy mole crickets, we collected a series of specimens belonging to the genus *Xya*, described two new species, namely *Xya xishangbanna* sp. nov. and *Xya yunnanensis* sp. nov., and provide a key to all the Chinese *Xya* species.

Material and methods

All the jumping pygmy mole cricket specimens examined in the present study were collected by a small patented appliance (Cao et al. 2015) with high collection efficiency. Photos of the habitat were taken by a Canon camera (EOS 100D). After killed in a poison bottle with diethyl ether and the body postures arranged, specimens were examined using an Olympus SZX9 stereomicroscope, and habitus photographs and measurements were taken using a microscopic LY-WN system. All pictures were then processed using Photoshop CS6 software.

All examined specimens are deposited in the Leshan Normal University, Leshan, Sichuan Province, China.

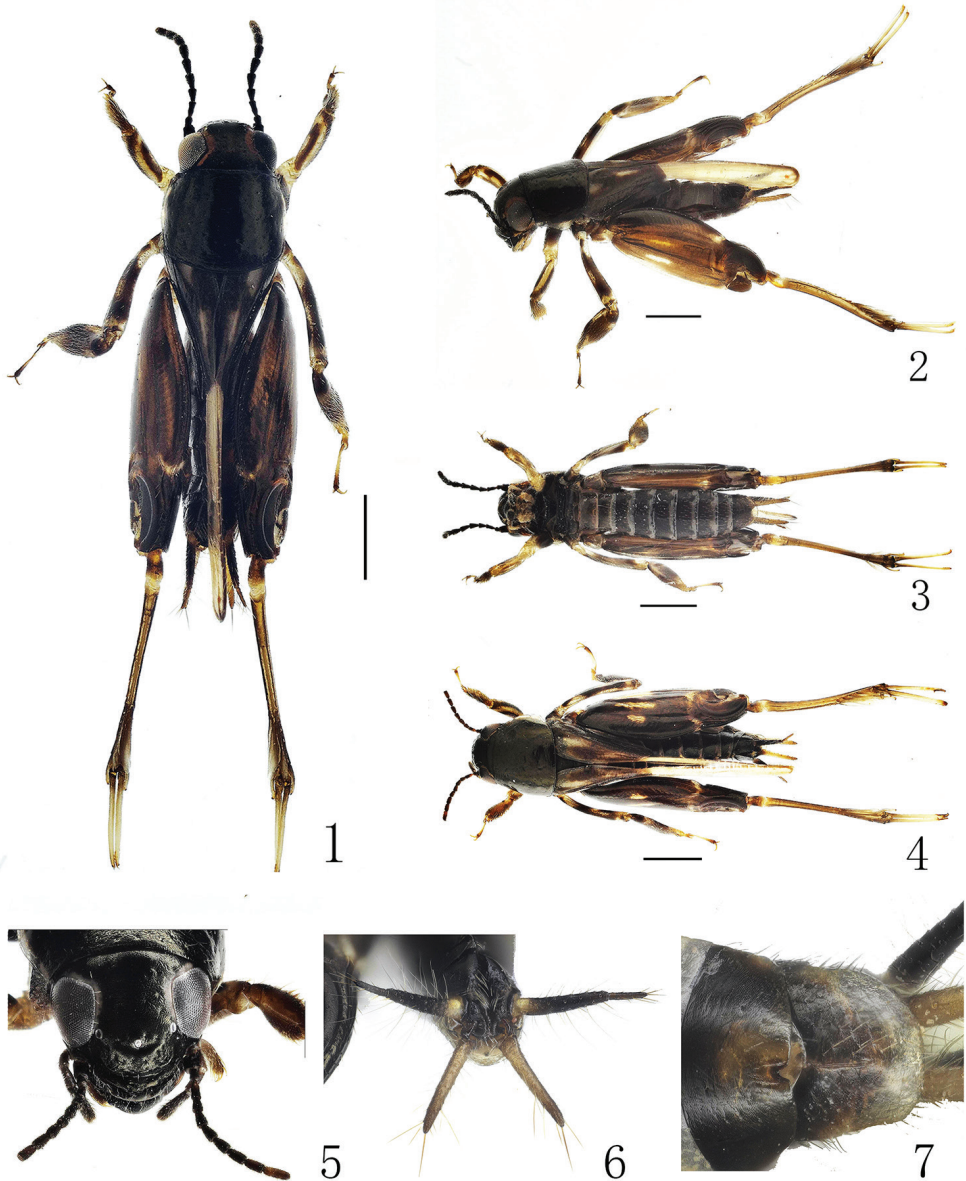
Taxonomy

Xya xishangbanna sp. nov.

<http://zoobank.org/2BA1572A-C865-4DFE-81DF-91CE1E936591>

Figures 1–7

Type material. *Holotype*: CHINA • ♂; Yunnan Province, Xishuangbanna, Mengla County, Wuxiangguangchang; 21.92N, 101.11E; 21–24 Mar. 2019; leg. Chao Tong and Shenchi Chen.



Figures 1–7. *Xya xishangbanna* sp. nov. **1** body in dorsal view ♂ **2** body in lateral view ♂ **3** body in ventral view ♂ **4** body in dorsal view ♀ **5** head in frontal view ♀ **6** end of abdomen in posterior view ♂ **7** gonopore in ventral view ♀. Scale bars: 1.0 mm.

Paratype. CHINA • 1♀, same data as holotype.

Description. Male. Habitus with bright or shiny surface. Head black with brown band along inner margin of compound eyes. Antennae moniliform, black, 10 segments, length of each antennomere almost equal to width. Compound eyes dark brown to black, 2 times broader than longer, rounded in front. Ocelli grayish white. Gena black.

Thorax. Pronotum black, width about 1.25 times length, yellow on ventral margin. Forewings blackish-brown, with pair of basal and medial brown spots. Hindwings yellowish-white, extending beyond the end of abdomen distinctly. Fore and mid legs dark brown with yellow spots. Hind legs with femora dark brown, dorsal margin black, with yellowish-white spots; hind tibiae yellowish-brown, with three (inside) and four (outside) pairs of articulated lamellae.

Abdomen. Abdomen black, gray along posterior margin of each segment. Apex of every sternite with distinct transverse white stripe. Cerci black, paraproctal lobe slightly lighter in coloration than cerci. Epiproct with bottom of the middle “v-shaped” crack in the upper part shallow, and sides straight (Fig. 13A). **Female.** Body larger than male in size. Abdominal segments black with posterior margin gray for each segment. Epiproct rounded. Subgenital plate margin with a notch. Others same as male.

Measurement (mm). Length of body: ♂ 5.63, ♀ 7.16. Length of fore wing: ♂ 1.59, ♀ 2.37. Length of hind wing: ♂ 4.84, ♀ 6.28. Length of hind femur: ♂ 3.76, ♀ 4.50.

Distribution. China (Yunnan).

Diagnosis. This species can be diagnosed by the shiny dark brown hind femora. It is most similar to *X. leshanensis* Cao et al. in the compound eyes with a narrow band along the inner margin. It can be distinguished from the latter by the body with dorsal surface not rough, but more shiny; the compound eyes with a prominent brown band along their inner margin on both sides; the hind femora dark brown, with a pair of white and yellow longitudinal spots; forewings with a pair of basal and apical brownish spots; the length of hind wing more than 4.0 mm; and the epiproct with shallow bottom of the middle “v-shaped” crack in the upper part, and straight sides. In *X. leshanensis*, the body surface is rough; the compound eyes bear a yellowish-white band along the inner margin; the hind femora are black, bearing four yellowish-white spots near the middle; the forewings have no spot; the length of hind wings is less than 4.0 mm; and the epiproct has deep “v-shaped” crack in the upper part with the sides curved (Fig. 13B). Major differences are listed in Table 1.

Etymology. The specific epithet is named after Xishuangbanna, the type locality.

Table 1. Comparison of *Xya xishuangbanna* sp. nov. and *Xya leshanensis* Cao et al.

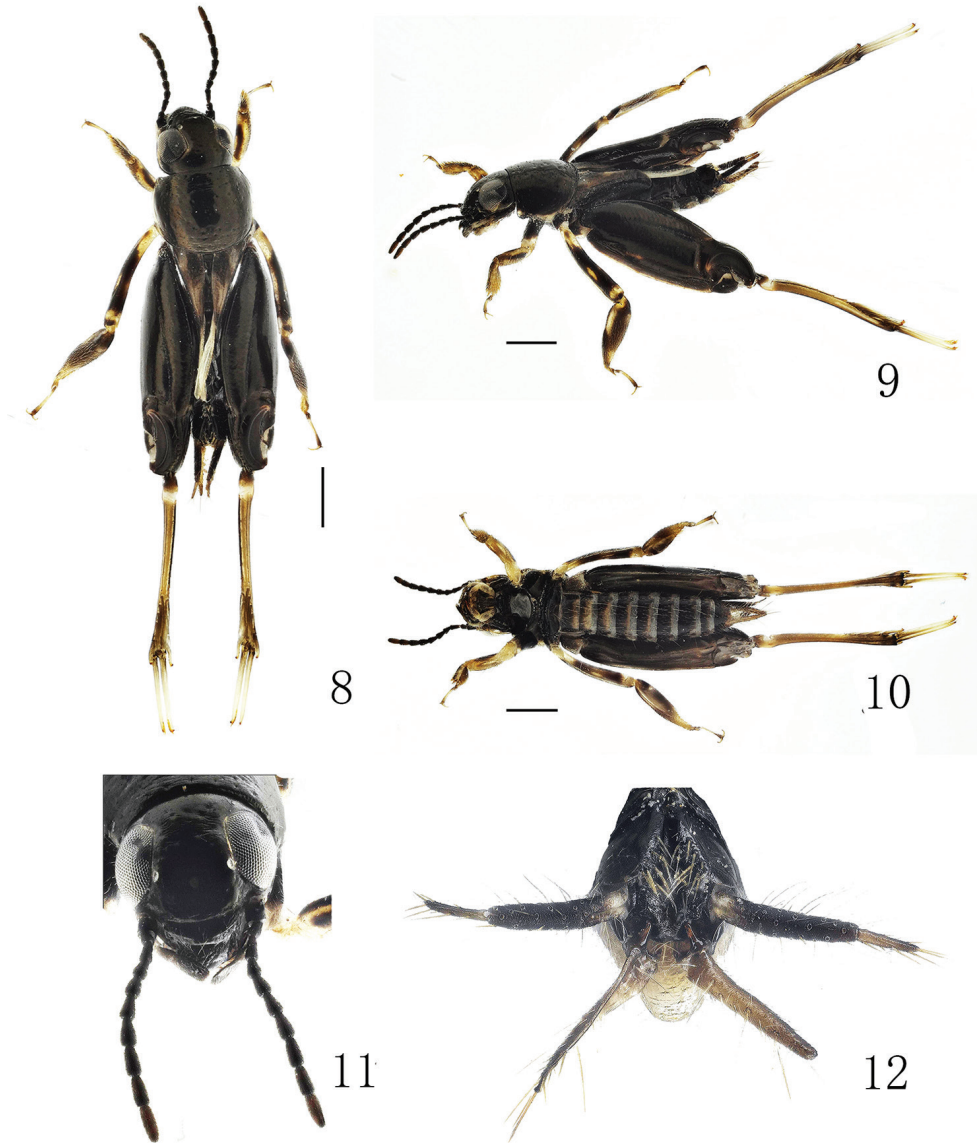
Characters	<i>Xya xishuangbanna</i> sp. nov.	<i>X. leshanensis</i>
Body surface	Not rough, more shiny	Rough, without shiny appearance
Antennomere of antennae	Apical part narrower than basal part in width	Apical part almost same as basal part in width
Compound eyes	With brown band along inner margin	With yellowish-white band along inner margin
Hind femora	Dark brown, with pair of white and yellow longitudinal spots	Black, with four yellowish-white spots near the middle
Forewings	Blackish-brown with a pair of basal and apical brownish spots, more than 1.4 mm long	Blackish-brown without spots, less than 1.4 mm long
Hindwings	More than 4.0 mm long	Less than 4.0 mm long
Epiproct	Bottom of the middle “v-shaped” crack in the upper part is shallow, and the sides straight.	Bottom of the middle “v-shaped” crack in the upper part is deep, and the sides curved.

Xya yunnanensis sp. nov.

<http://zoobank.org/0D105287-AD35-420C-A732-F982405D669E>

Figures 8–12

Type material. *Holotype*: CHINA • ♂; Yunnan Province, Xishuangbanna, Mengla County, ♂, Wujiazhai; 22.05N, 100.89E; 21–24 Mar. 2019; leg. Chao Tong and Shenzi Chen.



Figures 8–12. *Xya yunnanensis* sp. nov. **8** Body in dorsal view ♂ **9** Body in lateral view ♂ **10** Body in ventral view ♂ **11** Head in frontal view ♂ **12** End of abdomen in posterior view ♂. Scale bars: 1.0 mm.

Description. Male. Head black, without band along inner margin of compound eye. Labial palpi black. Antennae filiform, black, 10 segmented, 10th segment dark fuscous, each segment widens from base to apex. Compound eyes grayish black. Three white ocelli. Gena below the compound eye black.

Thorax. Pronotum black, width about 1.2 times length, with reddish brown luster, white on lateral margin intermittently. Forewings black, with two obscure dirty white sub-rectangular patches at base and apex respectively. Hindwings white, black along posterior margin, about 5/6 length of abdomen. Fore legs yellowish-white; femora with black longitudinal stripe; tarsi with three yellowish-white distal spines. Mid legs black, with yellowish-white irregular markings on femora and tibiae. Hind legs with femora black, with a narrow yellowish-brown marking on basal 1/3 ventrally; semi-lunar process black, yellowish-brown at base; tibia yellowish-brown, darkens toward apex, with three (inside) and four (outside) pairs of articulated lamellae.

Abdomen. Abdomen black, white along posterior margin of each segment. Cerci with two segments, 1st segment black, white at base; 2nd segment pale fuscous, with sparse long white setae. Stylus black on outer side, pale fuscous on inner side, shorter than cerci. Epiproct with shallow “v-shaped” crack in the upper part, bottom of the side edge has a sharply angled protrusion, and width of the narrow lower anchor-shaped base is less than 1/2 the width of the upper one (Fig. 13C).

Female. Unknown.

Measurement (mm). Length of body: ♂ 5.43. Length of fore wing: ♂ 1.28. Length of hind wing: ♂ 2.47. Length of hind femur: ♂ 3.72.

Distribution. China (Yunnan).

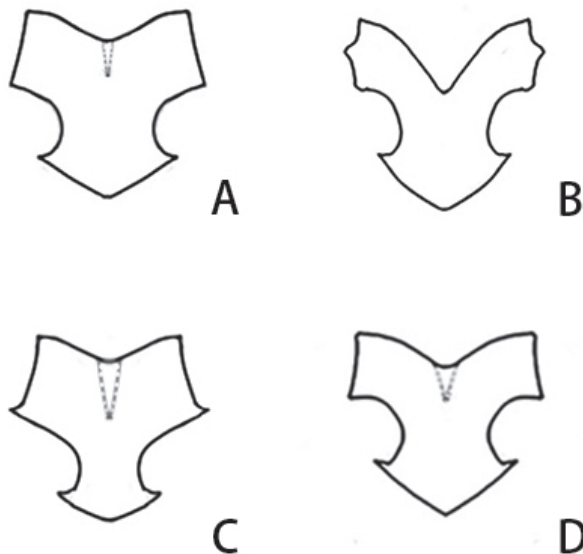


Figure 13. The line diagrams for male epiproct of four *Xya* species. **A** *Xya xishangbanna* sp. nov. **B** *Xya leshanensis* **C** *X. yunnanensis* sp. nov. **D** *X. sichuanensis*.

Diagnosis. This species can be diagnosed by the compound eye bearing no narrow band along the inner margin. It is most similar to *X. sichuanensis* Cao et al. in having four markings on the forewing, and lacking a patch on the pronotum dorsally. It can be distinguished from the latter by the compound eyes without a narrow band along the inner margin; with no ring around the median ocelli; the black gena below the compound eye; the forewing with obscure dirty white sub-rectangular patches, the length of fore wing about 1.28 mm; the white hindwing; and the epiproct with bottom of the side edge with a sharply angled protrusion and the narrow lower anchor-shaped base less than 1/2 the width of the upper one. In *X. sichuanensis*, the compound eyes bear a narrow yellow band along inner margin; bears a yellow ring around the median ocelli; the gena below the compound eye is yellow; the forewings have yellow triangular patches, the length of fore wing is about 0.9–1.1 mm; the hindwings are yellow; the epiproct with bottom of the side edge without a sharply angled protrusion and the large lower anchor base about 4/5 the width of the upper one (Fig. 13D). Major differences are listed in Table 2.

Etymology. The specific epithet is named after Yunnan, the type locality.

Biology. These two new species are found along waterways and under mud and stones amidst many different plants and shrubs (Fig. 14). They seem to be living near humid sand with water nearby. The adults were collected during the month of August. They can jump from both the ground and water.



Figure 14. Landscape of habitat in Wuxiangguangchang (A, B) and in Wujiazhai (C, D) in Xishuangbanna, Yunnan, China.

Table 2. Comparison of *X. yunnanensis* sp. nov. and *X. sichuanensis* Cao et al.

Characters	<i>X. yunnanensis</i> sp. nov.	<i>X. sichuanensis</i>
Compound eyes	Without narrow band along inner margin	With a narrow yellow band along inner margin
Median ocelli	Without ring around	With a yellow ring around
Gena below the compound eye	Yellow	Black
Forewings	With obscure dirty white sub-rectangular patches, about 1.28 mm	With yellow triangular patches, about 0.9-1.1 mm
Hindwings	White	Yellow
Hind femora	With a narrow yellowish-brown marking on basal 1/3 ventrally	Without marking on basal 1/3 ventrally
Epiproct	Bottom of the side edge with a sharply angled protrusion and the narrow lower anchor-shaped base less than 1/2 the width of the upper one	Bottom of the side edge without a sharply angled protrusion and the large lower anchor base about 4/5 the width of the upper one

Key to all *Xya* species in China based on the male superficial characters

- 1 Hind femur with marking..... 2
- Hind femur without marking 8
- 2 Hindwing white..... 3
- Hindwing black or dark..... 7
- 3 Antenna with apical 2 or 3 segments white *X. apicicornis*
- Antenna with apical 2 or 3 segments black 4
- 4 Forewing with marking..... 5
- Forewing without marking *X. lesbanensis*
- 5 Hind femur with pair of longitudinal spots..... 6
- Hind femur with four spots *X. riparia*
- 6 Pronotum with two yellow spots near anterior margin *X. fujianensis*
- Pronotum without spots near anterior margin
..... *X. xishangbanna* sp. nov.
- 7 Hind femur with a yellowish-white sub-ovate spot..... *X. shandongensis*
- Hind femur with a white triangular spot..... *X. nitobei*
- 8 Forewing with marking..... 9
- Forewing without marking 10
- 9 Compound eye with narrow band along inner margin.....
..... *X. sichuanensis*
- Compound eye without narrow band along inner margin.....
..... *X. yunnanensis* sp. nov.
- 10 Hindwing black..... *X. japonica*
- Hindwing pale yellowish-brown *X. manchurei*

Acknowledgements

We sincerely thank Prof. John Richard Schrock (Emporia State University, USA) for reviewing this manuscript with valuable comments. We express our cordial thanks to

Shenzhi Chen, Chao Tong, Kun Xie and Yinchong Ma who participated in the field collection, and also to Jiahui Luo and Kaiyan Yang who took the photographs and finished the drawings. This study was supported by the Scientific Research Foundation of Leshan Normal University (No. LZD009; No. XJR18005) and Cooperative Research Projects between University and Enterprises (No. LHX191201).

References

- Bey-Bienko GY (1967) Some Orthopteroid insects of the orders Blattoptera, Orthoptera and Dermaptera from Afghanistan. *Acta Entomologica Bohemoslovaca* 64: 407–438.
- Bolívar I (1900[1899]) Les Orthopteres de St. Joseph's College a Trichonopoly (Sud de l'Inde), 2 e partie. *Annals Society Entomology France* 68: 761–812.
- Brunner von Wattenwyl K (1893) Révision du Système des Orthoptères et description des espèces rapportées par M. Leonardo Fea de Birmanie. *Annali di Museo Civico di Storia Naturale di Genova, Series 2*, 13:1–230, pls i–vi. <https://doi.org/10.5962/bhl.title.5121>
- Cao CQ, Hu, YL, Tong C (2015) A kind of collecting equipment for small and jumping insects. Patent ZL 201520689069.X
- Cao C Q, Shi JP, Hu YL (2017) A new species of the genus *Xya* Latreille, 1809 (Orthoptera, Tridactyloidea, Tridactylidae) from Sichuan, China. *Zootaxa* 4247(2): 185–188. <https://doi.org/10.11646/zootaxa.4247.2.11>
- Cao CQ, Shi JP, Yin Z (2018) A new species of the genus *Xya* Latreille, 1809 from China (Orthoptera, Tridactyloidea, Tridactylidae). *Zootaxa* 4413(2): 397–400. <https://doi.org/10.11646/zootaxa.4413.2.13>
- Cao CQ, Chen SZ, Yin Z (2020) A new species of the genus *Xya* Latreille, 1809 from Fujian, China (Orthoptera, Tridactyloidea, Tridactylidae). *Zootaxa* 4731(3): 447–450. <https://doi.org/10.11646/zootaxa.4731.3.13>
- Chopard L (1928) Revision of the Indian Gryllidae. *Records of the India Museum* 30: 2–3.
- Chopard L (1936) The Tridactylidae and Gryllidae of Ceylon. *Ceylon Science Journal, Biology Science* 20: 9–87.
- Chopard L (1968) Beitrage zur Kenntnis der Fauna Afghanistans. (Sammelergebnisse con O Jakes [1963–64], D Povolny [1965], D Povolny, Fr Tenora [1966], J Simek [1965–66], D Povolny, J Geisler, Z Sebek, Fr Tenora [1967]). *Gryllodea et Tridactyloidea. Acta Musei Moraviae* 53 (Supplement): 275–286.
- Cigliano MM, Braun H, Eades DC, Otte D (2018) Orthoptera Species File. Version 5.0/5.0. (20-2-2018). <http://Orthoptera.SpeciesFile.org> [accessed 6 April 2018]
- Günther KK (1974) Über die Tridactyloidea (Saltatoria, Insecta) in den Sammlungen des Museums für Naturgeschichte der Stadt Genf. *Revue Suisse de Zoologie* 81(4): 1024–1076. <https://doi.org/10.5962/bhl.part.76059>
- Günther KK (1980) Catalogue der Caelifera. *Deutsche Entomologische Zeitschrift* 27(1–3): 149–178. <https://doi.org/10.1002/mmnd.4810270114>
- Günther KK (1995) Die Tridactyloidea des südlichen Afrika (Orthoptera, Caelifera). *Deutsche Entomologische Zeitschrift* 42: 213–286. <https://doi.org/10.1002/mmnd.19950420202>

- Haan W de (1844) Bijdragen tot de kennis der Orthoptera. In: Temminck (Ed.) Verhandelingen over de Natuurlijke Geschiedenis der Nederlansche Overzeesche Bezittingen 24 (Zoology 10): 238.
- Heads SW, Hollier J (2016) The type specimen and generic placement of *Tridactylus galla* Saussure, 1895 (Orthoptera: Caelifera: Tridactylidae). *Zootaxa* 4193(1): 195–196. <https://doi.org/10.11646/zootaxa.4193.1.12>
- Ingrisch S (1987) Zur Orthopterenfauna Nepals. *Deutsche Entomologische Zeitschrift* 34(1–3): 113–139. <https://doi.org/10.1002/mmnd.4800340108>
- Kuravova K, Kocarek P (2016) Mandibular morphology and dietary preferences in two pygmy mole crickets of the genus *Xya* (Orthoptera: Tridactylidae). *Turkish Journal of Zoology* 40: 1–9. <https://doi.org/10.3906/zoo-1510-19>
- Latreille PA (1809) Histoire naturelle, generale et particuliere des Crustaces et des Insects, Band 4. Dufart; Paris.
- Murai T (2005) The family Tridactylidae (Orthoptera) from Japan. *Tettigonia* 7: 9–22.
- Saussure H de (1877) Mélanges orthoptérologiques. v fascicule: gryllides. *Mémoires de la Société de Physique et d'histoire naturelle de Genève* 25(1): 1–352.
- Saussure H de (1896) Révision du genre *Tridactylus*. *Revue suisse de Zoologie*, 4: 407–420. <https://doi.org/10.5962/bhl.part.75143>
- Shiraki T (1911) Monographie der Grylliden von Formosa, mit der Uebersicht der japanischen Arten. *Gouvernement-Entomology, Taihoku (=Taipei), Formosa*: 129 pp.
- Shiraki T (1936) Insects of Johol Order Orthoptera Family Tridactylidae. Report of the First Scientific Expedition to Manchoukuo (5): 1, Pt 6, 4.
- Walker F (1871) Supplement. Catalogue of the Specimens of Dermaptera Saltatoria in the Collection of the British Museum, 1871: 1–17.
- Yin H, Wang PX, Liu H X, Xu Q, Zhang DC (2013) The complete mitochondrial genome of *Xya japonica* (Haan, 1842) (Orthoptera: Tridactyloidea). *Mitochondrial DNA* 1–2. <https://doi.org/10.3109/19401736.2013.825778>
- Yin XC, Shi JP, Yin Z (1996) A Synonymic Catalogue of Grasshoppers and Their Allies of the World. China Forestry Publishing House, Beijing: 1266 pp.
- Zhang X H, Hao J F, Xia Y, Chang Y, Zhang DC, Yin H (2017) Molecular phylogenetic analysis of the Orthoptera (Arthropoda, Insecta) based on Hexamerin sequences. *Zootaxa* 4232(4): 523–534. <https://doi.org/10.11646/zootaxa.4232.4.4>
- Zhang DP, Yin HX, Yin Z (2018) A new species of the genus *Xya* Latreille, 1809 from Shandong, China (Orthoptera, Tridactyloidea, Tridactylidae). *Zootaxa* 4455(3): 593–596. <https://doi.org/10.11646/zootaxa.4455.3.17>

The family Oestridae in Egypt and Saudi Arabia (Diptera, Oestroidea)

Magdi S. A. El-Hawagry¹, Mahmoud S. Abdel-Dayem², Hathal M. Al Dhafer²

1 Department of Entomology, Faculty of Science, Cairo University, Egypt **2** College of Food and Agricultural Sciences, King Saud University, Riyadh, the Kingdom of Saudi Arabia

Corresponding author: Magdi S. A. El-Hawagry (elhawagry@gmail.com)

Academic editor: Torsten Dikow | Received 22 March 2020 | Accepted 29 May 2020 | Published 8 July 2020

<http://zoobank.org/8B4DBA4E-3E83-46D3-B587-EE6CA7378EAD>

Citation: El-Hawagry MSA, Abdel-Dayem MS, Al Dhafer HM (2020) The family Oestridae in Egypt and Saudi Arabia (Diptera, Oestroidea). ZooKeys 947: 113–142. <https://doi.org/10.3897/zookeys.947.52317>

Abstract

All known taxa of the family Oestridae (superfamily Oestroidea) in both Egypt and Saudi Arabia are systematically catalogued herein. Three oestrid subfamilies have been recorded in Saudi Arabia and/or Egypt by six genera: *Gasterophilus* (Gasterophilinae), *Hypoderma*, *Przhevalskiana* (Hypodermatinae), *Cephalopina*, *Oestrus*, and *Rhinoestrus* (Oestrinae). Five *Gasterophilus* spp. have been recorded in Egypt, namely, *G. haemorrhoidalis* (Linnaeus), *G. intestinalis* (De Geer), *G. nasalis* (Linnaeus), *G. nigricornis* (Loew), and *G. pecorum* (Fabricius). Only two of these species have also been recorded in Saudi Arabia, namely: *G. intestinalis* (De Geer) and *G. nasalis* (Linnaeus). The subfamily Hypodermatinae is represented in the two countries by only four species in two genera, namely, *H. bovis* (Linnaeus) and *H. desertorum* Brauer (in Egypt only), and *H. lineatum* (Villers) (in Saudi Arabia only) and *Przhevalskiana silenus* (Brauer) (in both countries). The subfamily Oestrinae is represented by two widely distributed species in both countries, namely, *C. titillator* (Clark) and *O. ovis* (L.), in addition to another species represented in Egypt only, *R. purpureus* (Brauer). For each species, synonymies, type localities, distribution, Egyptian and Saudi Arabian localities with coordinates, and collection dates are presented.

Keywords

Activity periods, bot flies, distribution, gad flies, heel flies, hosts, localities, parasites, warble flies

Introduction

The Oestridae are a family within the superfamily Oestroidea, together with the families Calliphoridae, Rhiniidae, Sarcophagidae, Mystacinobiidae, Tachinidae, and Rhizophoridae (Pape et al. 2011). These families, except for Calliphoridae, are monophyletic, and the concept of Oestridae as a monophyletic family within the Oestroidea has been clearly established (Pape 1992; Pape 2001; Pape and Arnaud Jr 2001; Marinho et al. 2012).

Flies of the family Oestridae are large robust flies, with hair-like setae or soft setulae, without stout setae, mostly bee- or wasp-like, without vibrissae, and with reduced mouthparts (Marshall et al. 2017). They are commonly known as bot flies, warble flies, heel flies, and gad flies (Mote 1928; Saini and Sankhala 2015). Several species of these flies have significant medical and veterinary importance because of their mammal-parasitizing habits; thus, they receive substantial attention from applied entomologists, wildlife ecologists, and assuredly from taxonomists (Pape 2001).

Bot flies were formerly classified into four families: Cuterebridae, Gasterophilidae, Hypodermatidae, and Oestridae. However, they are conveniently treated now as a single family, Oestridae, including the former families as subfamilies, namely: Cuterebrinae, Gasterophilinae, Hypodermatinae, and Oestrinae (Wood 1987; Pape 1992; Pape 2001). All these subfamilies, except the first, are represented in Saudi Arabia and/or Egypt by six genera (Table 1): *Gasterophilus* (Gasterophilinae), *Hypoderma*, *Przhevalskiana* (Hypodermatinae), *Cephalopina*, *Oestrus* and *Rhinoestrus* (Oestrinae) (Steyskal and El-Bialy 1967; Büttiker and Zumpt 1982).

Larvae of the genus *Gasterophilus* are common obligatory endoparasites of the alimentary tract of equines (*Equus* spp.) including horses, donkeys, and zebras in the family Equidae (Abdel Rahman et al. 2018). They can also affect other animals, such as rhinoceroses, lions, cows, sheep, goats, and even were recorded in a human infant (Royce et al. 1999). These larvae cause gastrointestinal myiasis leading to gastrointestinal ulcerations, gut obstructions or volvulus, rectal prolapses, anemia, diarrhea, and other digestive disorders (Hoseini et al. 2017). Species of the genus *Gasterophilus* have become near cosmopolitan because their distribution coincides with that of their domesticated hosts (Li et al. 2019a). Six *Gasterophilus* spp. have been recorded from the Old World (Zumpt 1965; Soós and Minar 1986a). Five of these have been recorded in Egypt, namely, *G. haemorrhoidalis* (Linnaeus), *G. intestinalis* (De Geer), *G. nasalis* (Linnaeus), *G. nigricornis* (Loew), and *G. pecorum* (Fabricius) (Steyskal and El-Bialy 1967, Soós and Minar 1986a). Only two have also been recorded from Saudi Arabia, namely: *G. intestinalis* and *G. nasalis* (Abu-Thuraya 1982; Büttiker and Zumpt 1982; Abu-Zoherah et al. 1993; Al-Ahamdi and Salem 1999).

The subfamily Hypodermatinae is represented in both Egypt and Saudi Arabia by only four species in two genera, namely, *H. bovis* (Linnaeus) and *H. desertorum* Brauer (in Egypt only), and *H. lineatum* (Villers) and *P. silenus* (Brauer) (in both Egypt and Saudi Arabia) (Steyskal and El-Bialy 1967; Büttiker and Zumpt 1982; Soós and Minar 1986b; El-Azzazy 1997; Morsy et al. 1998). The common and best

Table 1. Oestrid species recorded from Egypt and Saudi Arabia (* = recorded, x = not recorded).

Species	Egypt	Saudi Arabia
Subfamily Gasterophilinae		
<i>Gasterophilus haemorrhoidalis</i> (Linnaeus, 1758)	*	x
<i>Gasterophilus intestinalis</i> (De Geer, 1776)	*	*
<i>Gasterophilus nasalis</i> (Linnaeus, 1758)	*	*
<i>Gasterophilus nigricornis</i> (Loew, 1863)	*	x
<i>Gasterophilus pecorum</i> (Fabricius, 1794)	*	x
Subfamily Hypodermatinae		
<i>Hypoderma bovis</i> (Linnaeus, 1758)	*	x
<i>Hypoderma desertorum</i> Brauer, 1897	*	x
<i>Hypoderma lineatum</i> (Villers, 1789)	x	*
<i>Przhevalskiana silenus</i> (Brauer, 1858)	*	*
Subfamily Oestrinae		
<i>Cephalopina titillator</i> (Clark, 1816)	*	*
<i>Oestrus ovis</i> (Linnaeus, 1758)	*	*
<i>Rhinoestrus purpureus</i> (Brauer, 1858)	*	x

known subcutaneous myiasis in domesticated and wild ruminants called bovine hypodermosis is caused by larvae of *Hypoderma* species across the Old World (Boulard 2002). This disease is endemic in livestock, including cattle, buffaloes, goats, sheep, and deer. Hypodermosis results in a severe decline in the production of meat and milk and depreciation in hide quality from holes and other flaws caused by *Hypoderma* larvae (Hall and Wall 1995). The larvae of *P. silenus* (goat warble fly) are known to cause subcutaneous myiasis distinguished by nodules on the back of goats and sheep. This myiasis causes severe economic problems to the livestock industry, including abortion and reduction in the body weight, fertility, and dairy production of the infested animals, in addition to a reduction in the quality of the hides and wool of the animal (Liakos 1986; El-Azzazy 1997).

Flies in the subfamily Oestrinae are known as nasopharyngeal bot flies; they are host specific and cause obligatory myiasis in many animal species. Their obligatory parasitic larvae are known to cause nasopharyngeal myiasis giving rise to respiratory problems, rhinitis, irritation, purulent mucous exudates, and nasal discharge (Catts and Mullen 2002; Otranto et al. 2003). Two oestrine species are widely distributed in both Egypt and Saudi Arabia, namely, *O. ovis* (sheep nasal bot fly) and *C. titillator* (camel nasal bot fly), which cause economic damage in the animal husbandry industry (Abu-Thuraya 1982; Büttiker and Zumpt 1982; Zayed 1998; Alahmed 2002). Another oestrine species, *R. purpureus* (equine nasal bot fly), is represented in Egypt and causes a parasitic disease in horses and donkeys called rhinoestrosis, which is characterized by clinical signs ranging from inflammation to coughing, sneezing, and dyspnea (Otranto 2004; Hilali et al. 2015).

Egypt and Saudi Arabia are two neighboring Middle Eastern countries separated by the Red Sea and the Gulf of Aqaba (Fig. 1). They are biogeographically comparable being located at the junction of the Palearctic and the Afrotropical Realms (Wallace 1876; Hölzel 1998; El-Hawagry and Gilbert 2014).



Figure 1. A satellite map of Egypt and Saudi Arabia.

An arid desert climate prevails in both countries, with the exception of small strip of the Mediterranean coastline in Egypt and the Asir Highlands along the Red Sea coast of Saudi Arabia. The climate in both countries is characterized by hot summer and a mild winter. From north to south across Egypt, three general climatic zones may be distinguished (Ullrich 1996): The Mediterranean coast zone with 70–200 mm annual precipitation and mean temperature ranging from 9.4 °C in January to 29.7 °C in July; the middle zone with 29N as its latitudinal boundary, with less than 1 mm (Siwa Oasis) to 35 mm (Cairo) annual precipitation, and has only slightly higher temperature than the Mediterranean coast zone and the third zone is the upper Egypt, where rainfall is scant and capricious, ranging from 3 mm (Aswan) to none, with mean temperature (at Aswan) ranging from 9.3 °C in January to 41.8 °C in July. In general, the rainfall is low in the most Egyptian areas and deserts (<80 mm annually). Only the Mediterranean coastal strip from Salloum to Alexandria, Gebel Elba in the extreme southeast, and the mountains of southern Sinai receive higher and less erratic rainfall (ca 200 mm annually). In Saudi Arabia, the average annual temperature is 25.2 °C, the average high temperature is about 37.8 °C during summer (June to August) and is about 11.1 °C during winter (December to February). It is cool, with frost and snow may occur in the Asir Highlands during winter. The precipitation is also low throughout the country (<100 mm). It is more than 480 mm in the highlands of Asir; however, a decade may pass with no precipitation at all in the Rub' al Khali (Empty Quarter) in the southeastern Saudi Arabia (Almazroui 2011).

Efflatoun Bey, often called the “father of Egyptian entomology”, comprehensively surveyed the Diptera of Egypt and established big collections of flies pinned and pre-

served in three Egyptian museums in Cairo University, Ministry of Agriculture, and Entomological Society of Egypt. The oestrid specimens in these collections are considered in the present study.

During the nineteenth century, two species of subfamily Oestrinae, *Oestrus maculatus* Wiedemann, 1830 and *O. libycus* Clark, 1843, originally described from Egypt have been later synonymized with *Cephalopina titillator*. Then Brauer (1897) has described *Hypoderma desertorum* from Helwan (Cairo), Egypt.

No systematic studies on bot flies have been previously conducted in Egypt. Only a list of species of dipterous families in Egypt was published by Steyskal and El-Bialy (1967), where 1,339 species have been listed, including 10 oestrid species (treated as Gasterophilidae and Oestridae). The list involved only family names with a list of species within each family, without any other taxonomic or faunistic data. Subsequently, between 1987 and 2018, the species prevalence and infestation by oestrids have been received attention by entomologists and veterinarians, but no study has been carried out to explore the national prevalence of this group. The infestation of donkeys by *Gastrophilus* and *Rhinoestrus* species has been investigated in the slaughterhouse of the National Cairo Circus and in Giza Zoo abattoir by Hilali et al. (2015) and Attia et al. (2018). In sheep, the infestation by maggots of *Oestrus ovis* in Cairo and *Przhevalskiana silenus* in Sinai has been studied by Amin et al. (1997) and Morsy et al. (1998), respectively. Two studies have been conducted to illustrate the morphological characterization of larval stage of *Gastrophilus* species infest stomach of donkeys (El-Bakry and Fadly 2014, Abdel Rahman et al. 2018).

Although documentation of biological diversity in Saudi Arabia began in the second half of the 1960s, the first traces of the Saudi Arabian oestrid flies are found in a work dated 1982, as five species, *Cephalopina titillator*, *Gastrophilus intestinalis*, *G. nasalis*, *Hypoderma lineatum*, and *Oestrus ovis* have been mentioned from Riyadh Region (Büttiker and Zumpt 1982). In the same year, a book on the agricultural pests in the Kingdom of Saudi Arabia has been published (Abu Thuraya 1982). This book has documented four species *C. titillator*, *G. intestinalis*, *G. nasalis*, and *O. ovis*. El-Azzazy (1997) reported the larvae of the goat warble fly, *Przhevalskiana silenus*, on the backs of goat carcasses at the Jeddah abattoir (Makkah Region) for the first time. Between 1988–2018, entomological, medical and veterinary works have been published, but most of these studies were carried out at provincial scale. The ocular myiasis in man caused by the sheep bot fly *O. ovis* has been firstly reported in Saudi Arabia from Abha (Asir Region) by Omar et al. (1988). The prevalence variation of *C. titillator* infesting dromedary camels has been studied in the Eastern Province (Fatani and Hilali 1994), Jeddah (Gadallah and Bosly 2006) and Riyadh (Alahmed 2002). Also, the prevalence of *O. ovis* infesting sheep has been investigated in Asir (Kenawy et al. 2014), Jazan (Bosly 2013), Jeddah (Alikhan et al. 2018) and Riyadh (Alahmed 2000). Akhter et al. (2000) report two cases of cutaneous infestation in a man and a woman caused by *Dermatobia hominis* in Taif, Saudi Arabia. This record is doubtful as *D. hominis* is native to the Americas, and the species was identified only from larvae.

This study is one in a series of studies planned to catalogue the superfamily Oestroidea in Egypt and Saudi Arabia. Two papers in this series have already been published (El-Hawagry 2018; El-Hawagry and El-Azab 2019).

Materials and methods

The present data were gathered from some adult specimens collected and pinned by the authors from different Egyptian and Saudi Arabian localities, in addition to adult specimens pinned and preserved in Efflatoun Bey's collection, Department of Entomology, Faculty of Science, Cairo University, Egypt (EFC); the Ministry of Agriculture Collection, Plant Protection Research Institute, Dokki, Giza, Egypt (PPDD), and the King Saud University Museum of Arthropods, Riyadh, Saudi Arabia (KSMA). A great deal of biological, faunistic, and taxonomic information, including synonymies, distribution, collection localities, and dates were also obtained from relevant literature.

This study catalogues all known taxa of the family Oestridae recorded from Egypt and Saudi Arabia. Subfamilies are arranged phylogenetically according to Pape (2001). Genera and species within subfamilies are arranged alphabetically. Synonyms comprised all available and unavailable names of genera and species are listed chronologically.

Family-group and genus-group names are written in bold uppercase letters and left-justified, with the genus-group names italicized. The genus-group names are listed again and left-justified under the headings, and written in bold italicized letters, with the first letter in uppercase and the remaining letters in lowercase, followed by the author, year, journal, and pages. Type species for each genus is given at the end, followed by the method by which it was fixed. Species names are left-justified as well, and written in bold italicized letters. Names of taxonomically valid species (senior synonyms) are listed again, combined with their original genera and left-justified under the headings followed by the author, year, journal, and pages. Synonyms of genera and species are listed in chronological order and written in regular italicized letters, followed by the author, year, journal, and pages as in senior taxa. The type locality for each species, including both senior and junior synonyms, is provided from the original descriptions. World distribution of each species based on relevant literature is listed alphabetically. The concept of Kirk-Spriggs and Sinclair (2017) regarding the boundaries between the Palearctic and Afrotropical realms is considered herein. Exceptions are the southwestern part of Saudi Arabia, south to the Tropic of Cancer and Gebel Elba, the southeastern triangle of Egypt, which are considered herein as Afrotropical (Sclater 1858; Wallace 1876; Ghazanfar and Fisher 1998; El-Hawagry and Gilbert 2014; Al Dhafer and El-Hawagry 2016; El-Hawagry 2017; El-Hawagry et al. 2018). The collection localities and dates in both Egypt and Saudi Arabia are given in tables to provide the local distribution and activity periods of oestrid flies. Localities within each Egyptian ecological zone and Saudi Arabian region are arranged in alphabetical order. The recording method, e.g., literature, museum material, and collected material are provided. Coordinates of each locality are mostly given, and distribution maps for species are provided using ArcMap 10.4.

Abbreviations used:

AF	Afrotropical Realm
AU	Australasian Realm
EFC	Collection of the Department of Entomology, Faculty of Science, Cairo University, Egypt (Eflatoun's collection)
KSA	Kingdom of Saudi Arabia
KSMA	King Saud University Museum of Arthropods, Riyadh, Saudi Arabia
Is	Island
MCCB	Museum of Community College, Al-Baha University, KSA
MSHC	Personal collection M. El-Hawagry
NE	Nearctic Realm
NEO	Neotropical Realm
OR	Oriental Realm
PA	Palaearctic Realm
PPDD	Collection of the Plant Protection Research Institute, Ministry of Agriculture, Dokki, Giza, Egypt
St.	Saint
USA	United States of America

Catalogue of the family Oestridae in Egypt and Saudi Arabia

Order: Diptera

Suborder: Cyclorrhapha

Superfamily: Oestroidea

Family Oestridae

Subfamily Gasterophilinae

Genus *Gasterophilus* Leach, 1817

Gasterophilus Leach, 1817: 2. Type species: *Oestrus equi* Clark, 1797 (= *Oestrus intestinalis* De Geer, 1776), by subsequent designation of Curtis, 1826: 146.

Gastrus Meigen, 1824: 174. Type species: *Oestrus intestinalis* De Geer, 1776, by subsequent designation of Coquillett, 1910: 546.

Gastrophilus Agassiz, 1846: 160. Invalid emendation of *Gasterophilus*.

Enteromyza Rondani, 1857: 20. Unnecessary replacement name for *Gasterophilus*.

Rhinogastrophilus Townsend, 1918: 152. Type species: *Oestrus nasalis* Linnaeus, 1758, by original designation.

Enteromyza Enderlein, 1934: 425. Type species: *Oestrus haemorrhoidalis* Linnaeus, 1758, by original designation.

Stomachobia Enderlein, 1934: 425. Type species: *Oestrus pecorum* Fabricius, 1794, by original designation.

Haemorrhoestrus Townsend, 1934: 406. Type species: *Oestrus haemorrhoidalis* Linnaeus, 1758, by original designation.

Progastrophilus Townsend, 1934: 406. Type species: *Oestrus pecorum* Fabricius, 1794, by original designation.

***Gasterophilus haemorrhoidalis* (Linnaeus, 1758)**

Oestrus haemorrhoidalis Linnaeus, 1758: 584. Type localities: Probably Sweden, Germany, and France (see Li et al. 2019b).

Oestrus salutiferus Clark, 1816: 3. Type locality: England.

Oestrus duodenalis Schwab, 1840: 35. Type locality: Europe.

Gastrophilus pallens Bigot, 1884: 4. Type locality: Sudan (Suakin).

Gasterophilus pseudohaemorrhoidalis Gedoelst, 1923: 272. Type localities: Eritrea (Asmara); Republic of the Congo, Katanga Province (Biano), and Zambia.

Oestrus hemorrhoidalis Clark, 1815: 71. Incorrect subsequent spelling of *haemorrhoidalis* Linnaeus, 1758.

Oestrus hemorroidalis Guérin-Méneville, 1827: 96. Incorrect subsequent spelling of *haemorrhoidalis* Linnaeus, 1758.

Oestrus aemorrhoidalis Rondani, 1857: 21. Incorrect subsequent spelling of *haemorrhoidalis* Linnaeus, 1758.

Common name. Nose bot fly or Lip bot fly.

Distribution. AF: Burkina Faso, Democratic Republic of the Congo, Eritrea, Ethiopia, Kenya, Namibia, Republic of the Congo, Senegal, South Africa, Sudan, Tanzania, Zambia. AU: Australia, Hawaii, New Zealand, Tasmania. NE: Canada (Alberta, British Columbia, Manitoba, Saskatchewan), Mexico, USA (widespread). NEO: Argentina, Venezuela. OR: India. PA: Widespread. (see Soós and Minar 1986a; Kettle 1995; Li et al. 2019b).

Localities, hosts, and dates of collection. See Table 2 and Figure 3.

***Gasterophilus intestinalis* (De Geer, 1776)**

Fig. 2a

Oestrus intestinalis De Geer, 1776: 292. Type locality: Sweden.

Oestrus equi Clark, 1797: 298. Preoccupied by Fabricius, 1787. Type locality: England.

Oestrus gastricus major Schwab, 1840: 31. Unavailable name.

Oestrus bengalensis Macquart, 1843: 182. Type localities: Bangladesh and India.

Oestrus gastrophilus Gistel, 1848: 153. Type locality: Probably Germany.

Oestrus schuabianus Gistel, 1848: 153. Type locality: Probably Germany (Bavaria).

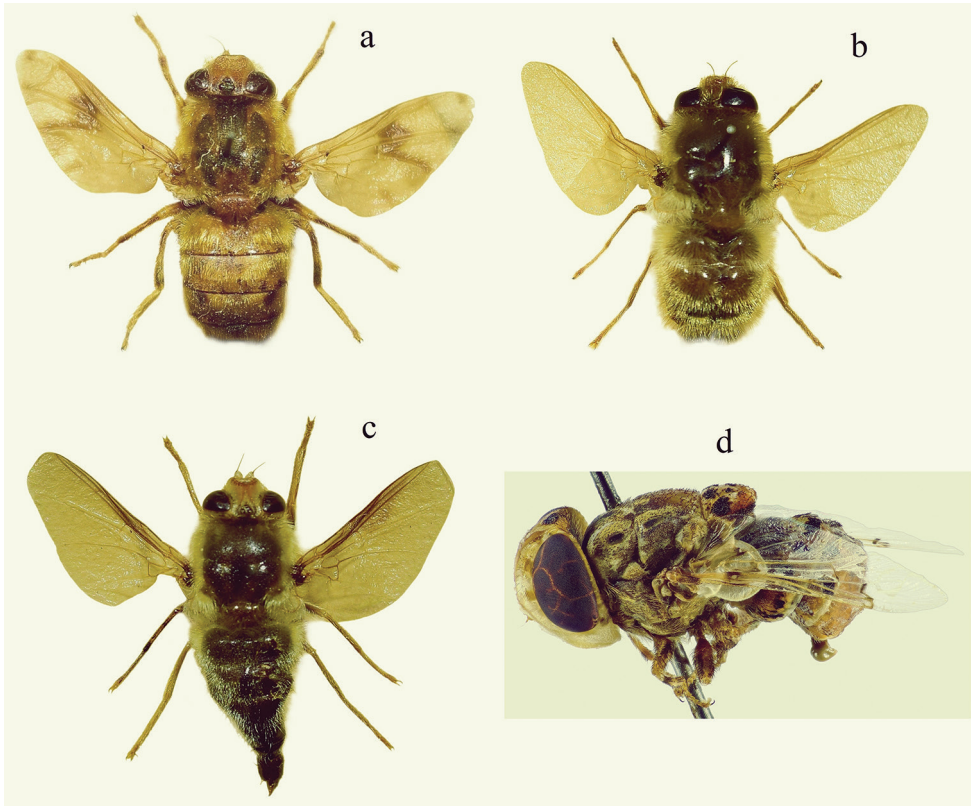
Gastrophilus equi var. *asininus* Brauer, 1863: 71. Type localities: Egypt and Sudan (“Egypten” & “Nubien”).

Gastrophilus aequi: Brauer 1863: 28. Incorrect subsequent spelling of *equi* Clark, 1797.

Gasterophilus magnicornis Bezzi, 1916: 29. Type locality: Eritrea.

Table 2. Localities, hosts, and dates of collection of *G. haemorrhoidalis*.

Country	Zone or Region	Locality	Coordinates	Host/s	Months of collection	Reference
Egypt	Coastal Strip	Alexandria	31.203358N, 29.917285E	mules and donkeys (from stomachs)	from October to April	El-Bakry and Fadly (2014)

**Figure 2.** **a** *Gasterophilus intestinalis* (habitus, dorsal) **b** *G. nasalis* (habitus, dorsal) **c** *G. nigricornis* (habitus, dorsal) **d** *Cephalopina titillator* (habitus, lateral).

Common name. Horse bot fly.

Distribution. AF: Burkina Faso, Chad, Eritrea, Ethiopia, Ghana, Kenya, Morocco, Nigeria, Republic of the Congo, Senegal, South Africa, St. Helena, Sudan, Tanzania, United Arab Emirates. AU: Australia (New South Wales, Norfolk Is, Tasmania), Hawaii, New Zealand. NE: Canada (Alberta, British Columbia, Manitoba, New Brunswick, Ontario, Quebec, Saskatchewan), Mexico (Aguascalientes, Chiapas), USA (widespread). NEO: Argentina, Brazil (Rio Grande do Sul), Chile (Bío Bío Region), Jamaica, Venezuela. OR: India. PA: Widespread. (see Soós and Minar 1986a; Kettle 1995; Li et al. 2019b).

Localities, hosts, and dates of collection. See Table 3 and Figure 3.

Table 3. Localities, hosts, and dates of collection of *G. Intestinalis*.

Country	Zone or Region	Locality	Coordinates	Host/s	Months of collection	Reference
Egypt	Coastal Strip	Alexandria	31.203358N, 29.917285E	mules and donkeys (from stomachs)	from October to April	El-Bakry and Fadly (2014)
	Lower Nile Valley & Delta	Cairo (at slaughterhouse of the National Cairo Circus)	30.122446N, 31.360598E	donkeys	throughout the year	Hilali et al. (1987)
		Cairo (at Cairo Manure Co.)	30.102160N, 31.253994E	mules and donkeys (from stomachs)	April to December	museum material (see material examined)
		Cairo (abattoir)	30.040022N, 31.244248E	donkeys (from stomachs)	June	museum material (see material examined)
		Giza (Giza Zoo)	30.027973N, 31.215963E	donkeys (from stomachs)	throughout the year	Abdel Rahman et al. (2018); Attia et al. (2018)
KSA	widespread in all regions, especially abundant in Al-Ehsaa, El-Kharj and Riyadh	Al-Ehsaa	25.388528N, 49.596223E	donkeys and horses (from stomachs)	March to September	Abu-Thuraya (1982)
		El-Kharj	24.148402N, 47.305011E	donkeys and horses (from stomachs)	March to September	
		Riyadh (near slaughterhouse)	24.578977N, 46.736175E	from dead domestic horse	March	Büttiker and Zumpt (1982)

**Figure 3.** Distribution map of *G. haemorrhoidalis* and *G. intestinalis*.

Material examined. EGYPT • 1 male; Cairo Manure Co.; 30.102160N, 31.253994E; 13.Nov.1924; from the stomach of a donkey; EFC • 1 male; same data as for preceding; 22.Apr.1930 • 1 male; same data as for preceding; 23.Nov.1930 • 1 female; same data as for preceding; 29.Oct.1924; PPDD • 1 ?male; same data as for preceding; Cairo abattoir; 30.040022N, 31.244248E; 7.Jun.1924.

***Gasterophilus nasalis* (Linnaeus, 1758)**

Fig. 2b

Oestrus nasalis Linnaeus, 1758: 584. Type locality: Sweden.

Oestrus equi Fabricius, 1787: 321. Type locality: Probably Europe.

Oestrus veterinus Clark, 1797: 312. New replacement name for *Oestrus nasalis* Linnaeus, 1758.

Oestrus salutaris Clark, 1815: pl. 1. *Nomen nudum*.

Gasterophilus clarkii Leach, 1817: 2. Type locality: England (Bantham).

Gastrus jumentarum Meigen, 1824: 179. Type locality: Probably Denmark.

Oestrus gastricus minor Schwab, 1840: 40. Unavailable name.

Gastrus subjacens Walker, 1849: 687. Type locality: Canada (Nova Scotia).

Oestrus stomachinus Gistel, 1848: 153. Type locality: Probably Germany (Bavaria).

Gasterophilus crossi Patton, 1924: 963. Type locality: India (Punjab).

Gastrophilus albescens Pleske, 1926: 228. Type locality: Egypt (Cairo).

Gastrophilus nasalis var. *nudicollis* Dinulescu, 1932: 28, 32. Type locality: Unknown.

Gastrophilus veterinus var. *aureus* Dinulescu, 1938: 315. Type locality: Unknown.

Gastrus jumentorum: Brauer, 1863: 87, 280. Incorrect subsequent spelling of *jumentarum* Meigen, 1824.

Oestrus nasulis: Fabricius, 1787: 321. Incorrect subsequent spelling of *nasalis* Linnaeus, 1758.

Common name. Throat bot fly or Horse nasal bot fly.

Distribution. Cosmopolitan.

Localities, hosts, and dates of collection. see Table 4 and Figure 4.

Material examined. EGYPT • 1 male; Abu-Rawash; 30.045837N, 31.091406E; 18.May.1935; EFC • 1 female; Cairo Manure Co.; 30.102160N, 31.253994E; 11.Jun.1924; from the stomach of a mule; EFC • 1 male; Helwan; 29.839022N, 31.300160E; 18.May.1934 • 1 female; Maadi; 29.961203N, 31.266910E; 9.Apr.1916; EFC.

***Gasterophilus nigricornis* (Loew, 1863)**

Fig. 2c

Gastrus nigricornis Loew, 1863: 38. Type locality: Moldova (Bessarabia).

Table 4. Localities, hosts, and dates of collection of *G. nasalis*.

Country	Zone or Region	Locality	Coordinates	Host/s	Months of collection	Reference
Egypt	Coastal Strip	Alexandria	31.203358N, 29.917285E	mules and donkeys (from stomachs)	from October to April	El-Bakry and Fadly (2014)
	Lower Nile Valley & Delta	Abu-Rawash	30.045837N, 31.091406E	not given	May	museum material (see material examined)
		Cairo (at slaughter house of the National Cairo Circus)	30.122446N, 31.360598E	donkeys	throughout the year	Hilali et al. (1987)
		Cairo (no further data)	–	–	–	Li et al. (2019b)
		Cairo (at Cairo Manure Co.)	30.102160N, 31.253994E	mules (from stomachs)	June	museum material (see material examined)
		Helwan	29.839022N, 31.300160E	not given	April and December	museum material (see material examined)
		Maadi	29.961203N, 31.266910E	not given	April	museum material (see material examined)
KSA	Widespread in all regions, especially abundant in Al-Ehsaa, El-Kharj and Riyadh	Al-Ehsaa	25.388528N, 49.596223E	donkeys and horses (from stomachs)	March to September	Abu-Thuraya (1982)
		El-Kharj	24.148402N, 47.305011E	donkeys and horses (from stomachs)	March to September	
		Riyadh (near slaughterhouse)	24.578977N, 46.736175E	from dead domestic horse	March	Büttiker and Zumpt (1982)

Gastrophilus viridis Sultanov, 1951: 41. Type locality: Kazakhstan.

Gasterophilus migricornis: Colwell, 2006: 291. Incorrect subsequent spelling of *nigricornis* Loew, 1863.

Common name. Horse stomach bot fly.

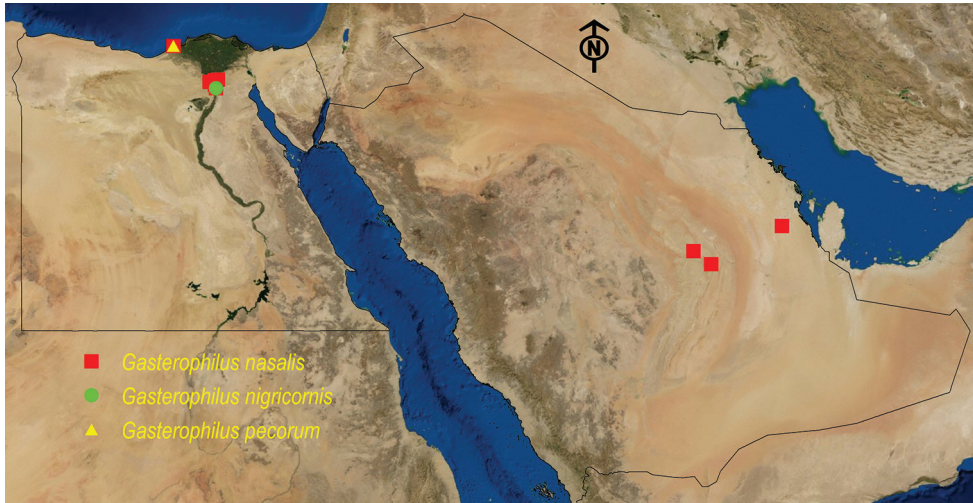
Distribution. PA: China, Egypt, Kazakhstan, Kyrgyzstan, Moldova, Mongolia, Russia, Tajikistan, Turkmenistan, Ukraine, Uzbekistan (see Soós and Minar 1986a; Kettle 1995; Li et al. 2019b).

Localities, hosts, and dates of collection. See Table 5 and Figure 4.

Material examined. EGYPT • 1 female; Helwan; 29.839022N, 31.300160E; 13.Apr.1935; EFC.

Table 5. Localities, hosts, and dates of collection of *G. nigricornis*.

Country	Zone or Region	Locality	Coordinates	Host/s	Months of collection	Reference
Egypt	Lower Nile Valley & Delta	Helwan	29.839022N, 31.300160E	not given	April	museum material (see material examined)

**Figure 4.** Distribution map of *G. nasalis*, *G. nigricornis*, and *G. pecorum*.

Gasterophilus pecorum (Fabricius, 1794)

Oestrus pecorum Fabricius, 1794: 230. Type locality: Probably Europe.

Oestrus vituli Fabricius, 1794: 231. Type locality: Not given, probably Sweden and France.

Gastrus jubarum Meigen, 1824: 179, 180. Type locality: Austria.

Gastrus lativentris Brauer, 1858b: 465. Type locality: Latvia (Curland).

Gastrus ferruginatus Zetterstedt, 1844: 978. Type locality: Sweden (Skåne, Tranås socken, Esperöd).

Gasterophilus pecorum var. *zebrae* Rodhain & Bequaert, 1920: 181. Type localities: Kenya and Tanzania.

Gastrophilus vulpecula Pleske, 1926: 227. Type locality: China (Inner Mongolia, Alxa League).

Gastrophilus gammeli Szilády, 1935: 140. Type locality: Hungary.

Gastrophilus hammeli: Paramonov, 1940: 34, 46. Incorrect subsequent spelling of *gammeli* Szilády, 1935.

Gastrus selysi Walker, 1849: 687. *Nomen nudum*.

Common name. Dark-winged horse bot fly.

Table 6. Localities, hosts, and dates of collection of *G. pecorum*.

Country	Zone or Region	Locality	Coordinates	Host/s	Months of collection	Reference
Egypt	Coastal Strip	Alexandria	31.203358N, 29.917285E	mules and donkeys (from stomachs)	from October to April	El-Bakry and Fadly (2014)

Distribution. AF: Burkina Faso, Kenya, Namibia, Senegal, South Africa, Tanzania, Uganda, Zambia. OR: India. PA: Belgium, China (Heilongjiang, Inner Mongolia, Xinjiang), Czech Republic, Denmark, Egypt, France, Germany, Hungary, Iran, Italy, Latvia, Lithuania, Mongolia, Poland, Romania, Sweden, Switzerland, The Netherlands, Turkey, Ukraine, United Kingdom (see Soós and Minar 1986a; Kettle 1995; Li et al. 2019b).

Localities, hosts, and dates of collection. See Table 6 and Figure 4.

Subfamily Hypodermatinae

Genus *Hypoderma* Latreille, 1818

Hypoderma Latreille, 1818: 272. Type species: *Oestrus bovis* Linnaeus, 1758, by monotypy.

Marmaryga Gistel, 1848: 9. Unjustified name for *Hypoderma*.

Atelecephala Townsend, 1916: 617. Type species: *Hypoderma diana* Brauer, 1858a, by monotypy.

Hypoderma bovis (Linnaeus, 1758)

Oestrus bovis Linnaeus, 1758: 584. Type locality: Not given (? Sweden).

Oestrus ericetorum Clark, 1815. *Nomen dubium*.

Oestrus subcutaneus Greve, 1818: 2. Type locality: Not given.

Oestrus bovinus Schwab, 1840: 43. Type locality: Not given.

Hypoderma heteroptera Macquart, 1843: 181. Type locality: Algeria (Oran).

Hypoderma bellieri Bigot, 1862: 113. Type locality: France (Corsica).

Common name. Ox warble fly.

Distribution. AU: Hawaii, New Zealand. NE: Widespread. PA: Widespread.

Localities, hosts, and dates of collection. Unknown.

Notes. This species is known to be recorded in Egypt only from the list of Steyskal and El-Bialy (1967), but no specimens of this species were collected or found in the Egyptian museums.

Hypoderma desertorum Brauer, 1897

Hypoderma desertorum Brauer, 1897: 377. Type locality: Egypt (Helwan).

Table 7. Localities, hosts, and dates of collection of *H. desertorum*.

Country	Zone or Region	Locality	Coordinates	Host/s	Months of collection	Reference
Egypt	Lower Nile Valley & Delta	Helwan	29.839022N, 31.300160E	not given	April	Brauer (1897)

**Figure 5.** Distribution map of *C. titillator*, *H. desertorum*, and *H. lineatum*.

Common name. No specific common name.

Distribution. PA: Egypt.

Localities, hosts, and dates of collection. See Table 7 and Figure 5.

Notes. Steyskal and El-Bialy (1967) listed this species as a junior synonym of *Hypoderma bovis* (Linnaeus, 1758); however, Soós and Minar (1986b) catalogued it as a valid species. No specimens are available to confirm its validity. Grunin (1965) keyed the *Hypoderma* spp. in the Palearctic Region and used the colour of hairs on mesonotum, shape of antennal segments and body length to differentiate between *H. desertorum* and *H. bovis*. Holotype is deposited in Naturhistorisches Museum Wien, Wien, Austria (NMW).

Hypoderma lineatum (Villers, 1789)

Oestrus lineatum Villers, 1789: 349. Type locality: Not given (Europe).

Hypoderma bonassi Brauer, 1875: 75. Type locality: USA (Colorado).

Oestrus supplens Walker, 1849: 685. Type locality: Canada (Nova Scotia).

Common name. Lesser cattle warble fly.

Distribution. Cosmopolitan.

Localities, hosts, and dates of collection. See Table 8 and Figure 5.

Table 8. Localities, hosts, and dates of collection of *H. lineatum*.

Country	Zone or Region	Locality	Coordinates	Host/s	Months of collection	Reference
KSA	Riyadh	Dhurma	24.613516N, 46.151759E	a dairy cow air-shipped from Canada	unknown	Büttiker and Zumpt (1982)
	Makkah	Wadi Qatan	22.200883N, 41.556635E	domestic goat	November	Büttiker and Zumpt (1982)

Genus *Przhevalskiana* Grunin, 1948

Przhevalskiana Grunin, 1948: 469 (as subgenus of *Hypoderma* Latreille, 1818). Type species: *Hypoderma orongonis* Grunin, 1948, by monotypy.

Crivellia Grunin, 1956: 716. Type species: *Hypoderma corinnae* Crivelli, 1862, by original designation.

Przhevalskiana silenus (Brauer, 1858)

Hypoderma silenus Brauer, 1858b: 460. Type localities: Italy (Sicily, Palermo); Egypt (Sinai).

Hypoderma aegagri Brauer, 1863: 134, 281. Type locality: Greece (Crete).

Hypoderma gazellae Gedoelst, 1916: 263. Type locality: Tanzania (Massai).

Hypoderma crossi Patton, 1922: 573. Type locality: India (Punjab).

Hypoderma aeratum Austen, 1931: 423. Type locality: Cyprus (Tillyria, Kyrenia).

Hypoderma capreum Gauser, 1940: 38. Type locality: Azerbaijan.

Common name. Goat warble fly.

Distribution. AF: East Africa, Saudi Arabia [as “South western part”]. OR: India. PA: Central Asia, Middle East, North Africa, southern Europe.

Localities, hosts, and dates of collection. See Table 9 and Figure 6.

Material examined. SAUDI ARABIA • 1 female; Al-Mekhwah; 19.759526N, 41.428219E; 3.Feb.2009; El-Hawagry leg.; sweeping net; MCCB.

Subfamily Oestrinae

Genus *Cephalopina* Strand, 1928

Cephalopina Strand, 1928: 48 (replacement name for *Cephalopsis*).

Cephalopsis Townsend, 1912: 53. Type species: *Oestrus maculatus* Wiedemann, 1830 (= *Oestrus titillator* Clark, 1816), by original designation. Preoccupied by Fitzinger, 1873 in Pisces.

Table 9. Localities, hosts, and dates of collection of *P. silenus*.

Country	Zone or Region	Locality	Coordinates	Hosts and/or methods of collection	Months of collection	Reference
Egypt	Sinai	Al Arish (abattoir)	31.131795N, 33.795749E	goats (larvae from slaughtered goats, and adults by baited traps)	throughout the year	Morsy et al. (1998)
		Bir Al Abd	31.005486N, 33.111721E	goats (larvae from slaughtered goats, and adults by baited traps)	throughout the year	Morsy et al. (1998)
		Hasanah	30.800220N, 33.815971E	goats (larvae from slaughtered goats, and adults by baited traps)	throughout the year	Morsy et al. (1998)
KSA	Al-Baha	Al-Mekhwa	19.759526N, 41.428219E	sweeping net by El-Hawagry	February	collected specimen (see material examined)
	Makkah	Jeddah (Jeddah Abattoir)	21.483464N, 39.201734E	goats (nodules caused by larvae are noticed on the backs of goat carcasses)	December to April	El-Azzazy (1997)

**Figure 6.** Distribution map of *O. ovis*, *P. silenus*, and *R. purpureus*.***Cephalopina titillator* (Clark, 1816)**

Fig. 2d

Oestrus titillator Clark, 1816: 4. Type locality: Syria.*Oestrus maculatus* Wiedemann, 1830: 256. Type locality: Egypt.*Oestrus libycus* Clark, 1841: 100. *Nomen nudum*.*Oestrus libycus* Clark, 1843: 93. Type locality: Egypt.*Pharyngobalbus cameli* Steel, 1887: 27. Type localities: Sudan, ?Afghanistan.

Common name. Camel nasal bot fly.

Distribution. AF: East Africa, Saudi Arabia [as “South western part”]. AU: Australia. OR: India. PA: Widespread in association with camels, particularly, Afghanistan, Middle East, Mongolia, North Africa, South Europe.

Localities, hosts, and dates of collection. See Table 10 and Figure 5.

Material examined. EGYPT • 1 male; Cairo abattoir; 30.040022N, 31.244248E; 6.Jun.1924; Efflatoun leg.; from nose of camel; EFC • 1 male; same data as for preceding; 2.Jul.1924 • 1 female; same data as for preceding; 19.Nov.1929 • 1 male; Kerdassa;

Table 10. Localities, hosts, and dates of collection of *C. titillator*.

Country	Zone or Region	Locality	Coordinates	Hosts and/or methods of collection	Months of collection	Reference
Egypt	Lower Nile Valley & Delta	Abu-Rawash	30.045837N, 31.091406E	dromedary camels (from the nasal cavities)	May	museum material (see material examined)
		Birqash	30.162842N, 31.039242E	sweeping, by El-Hawagry	June	collected specimens (see material examined)
		Cairo (Cairo abattoir)	30.040022N, 31.244248E	dromedary camels (from the nasal cavities)	throughout the year	museum material (see material examined)
		El-Bassatin (abattoir)	29.995917N, 31.276171E	camels	not given	Hendawy et al. (2012)
		El-Warrak (abattoir)	30.110544N, 31.210915E	camels	not given	Hendawy et al. (2012)
		Kerdassa	30.025663N, 31.113349E	dromedary camels (from the nasal cavities)	May	museum material (see material examined)
	Sinai	W. El-Sheikh	28.56568N, 33.96525E	not given	April	museum material (see material examined)
KSA	all regions	widespread	–	dromedary camels (nasal cavities)	throughout the year	Abu-Thuraya (1982); Alahmed (2002)
	Riyadh	Riyadh (slaughterhouse)	24.578977N, 46.736175E	dromedary camels	March to May	Büttiker and Zumpt (1982)
	Makkah	Jeddah (Jeddah abattoir)	21.483464N, 39.201734E	dromedary camels	throughout the year	Gadallah and Bosly (2006)

30.02566N, 31.11335E; 19.May.1924; R.M. leg.; from nose of camel; EFC • 1 male, 1 female; Sinai, W. El-Sheikh; 28.56568N, 33.96525E; 21–27.Apr.1939; B.C.E. leg.; EFC • 1 female; Cairo abattoir; 30.040022N, 31.244248E; 20.Jan.1924; H.C.E. leg.; from the nose of a camel; PPDD • 1 female, 1 male; Birqash; 30.162842N, 31.039242E; 21.Jun.1999; El-Hawagry leg.; sweeping net; MSHC.

SAUDI ARABIA • 2 females; Riyadh, slaughterhouse; 24.578977N, 46.736175E; 30.Oct.1999; Azzam Alahmed leg.; from dromedary camels; KSMA.

Genus *Oestrus* Linnaeus, 1758

Oestrus Linnaeus, 1758: 584. Type species: *Oestrus ovis* Linnaeus, 1758, by original designation of Curtis, 1826: 106.

Cephalemyia Latreille, 1818: 273. Type species: *Oestrus ovis* Linnaeus, 1758, by monotypy. *Cephalomyia* Agassiz, 1846: 71. Unjustified emendation of *Cephalemyia*.

***Oestrus ovis* (Linnaeus, 1758)**

Oestrus ovis Linnaeus, 1758: 585. Type locality: Not given (? Sweden).

Oestrus argalis Pallas, 1776: 29. Type locality: Not given (? Middle Asia).

Oestrus perplexus Hudson, 1892: 63. Type locality: New Zealand. *Nomen nudum*.

Common name. Sheep nasal bot fly.

Distribution. Cosmopolitan (introduced with sheep in most parts of the world, see Papavero (1977)).

Localities, hosts, and dates of collection. See Table 11 and Figure 6.

Material examined. EGYPT • 1 male; Burg; 30.916760N, 29.533268E; 16.Mar.1935; H.C.E & M.T leg.; EFC • 3 males, 3 females; Cairo, Cairo abattoir; 30.040022N, 31.244248E; 5.Jun.1929; Efflatoun leg.; from sheep's nose; EFC • 1 male, 1 female; same data as for preceding; 23.Dec.1929 • 2 males; same data as for preceding; 26.Nov.1929 • 1 male, same data as for preceding; 2.Jul.1924 • 1 male, same data as for preceding; 2. Apr.1924 • 1 female, same data as for preceding; 5. Apr.1924 • 1 female; Kerdassa; 30.025663N, 31.113349E; 18.Mar.1924; from the nose of sheep; EFC • 1 female; same data as for preceding; 22.May.1924; R. M. leg. • 1 female; Wadi Hoff; 29.880357N, 31.312991E; 14.Apr.1921; Efflatoun leg.; EFC • 1 female; Wadi Rishrash; 29.41666N, 31.51666E; 16.Apr.1932; ET & R leg.; EFC • 1 female; Wadi Rishrash; 29.41666N, 31.51666E; 29.Mar.1935; H.C.E. & M.T. leg.; EFC • 1 male; Ashmoun Gereiss; 30.325046N, 30.925513E; Wardan; 30.321045N, 30.905128E; 23.Mar.1924; H.C.E. leg.; reared from larvae from the nose of sheep; PPDD • 1 female; El-Mallah, East of Helwan; 3.May.1926; Farag leg.; PPDD • 1 female; El-Katta; 30.225859N, 30.970563E; 20.Sep.1924; PPDD • 1 male; Kerdassa; 30.025663N, 31.113349E; 15.May.1938; Mabrouk leg.; PPDD.

Table 11. Localities, hosts, and dates of collection of *O. ovis*.

Country	Zone or Region	Locality	Coordinates	Hosts and/or methods of collection	Months of collection	Reference	
Egypt	Coastal Strip	Burg	30.916760N, 29.533268E	not given	March	material (see material examined)	
	Eastern Desert	Wadi El-Mallah	–	not given	May	material (see material examined)	
		Wadi Hoff	29.880357N, 31.312991E	not given	April	material (see material examined)	
		Wadi Rishrash	29.41666N, 31.51666E	not given	November to April	material (see material examined)	
	Lower Nile Valley & Delta	Ashmoun Gereiss	30.325046N, 30.925513E	sheep (reared from larvae from nose)	March	material (see material examined)	
		Cairo, Cairo (abattoir)	30.040022N, 31.244248E	sheep (from nose)	April to December	museum material (see material examined) and Amin et al. (1997)	
		El-Hager	30.282066N, 30.913711E	sweeping net by El-Hawagry	April	collected specimens (see material examined)	
		El-Katta	30.225859N, 30.970563E	not given	September	museum material (see material examined)	
		Kerdassa	30.025663N, 31.113349E	sheep (from nose)	March and April	museum material (see material examined)	
		Wardan	30.321045N, 30.905128E	sheep (reared from larvae from nose)	March	material (see material examined)	
	KSA	all regions	widespread	–	sheep and goats (from the nasal cavities and head sinuses)	March to June	Abu-Thuraya (1982)
		Asir	widespread (slaughterhouses)	–	not given	throughout the year	Kenawy et al. (2014)
		Jazan	Abu Arish	16.9595N, 42.8348E	Sheep (heads)	throughout the year	Bosly (2013)
Riyadh		Riyadh (slaughterhouse)	24.578977N, 46.736175E	sheep and goats	May	Büttiker and Zumpt (1982)	

Genus *Rhinoestrus* Brauer, 1886

Rhinoestrus Brauer, 1886: 300. Type species: *Cephalomyia purpurea* Brauer, 1858, by monotypy.

Hippoestrus Townsend, 1933: 447. Type species: *Rhinoestrus hippopotami* Grünberg, 1904, by original designation.

Table 12. Localities, hosts, and dates of collection of *R. purpureus*.

Country	Zone or Region	Locality	Coordinates	Hosts and/or methods of collection	Months of collection	Reference
Egypt	Lower Nile Valley & Delta	Cairo	29.999896N, 31.270483E	Donkey (from head)	May	museum material (see material examined)
		El-Magadlah	–	not given	April	museum material (see material examined)
		Giza	30.015432N, 31.207837E	not given	May	museum material (see material examined)
		Giza, Giza zoo abattoir (donkeys originally obtained from four governorates: Giza, Monofia, Fayoum, and Bani Sweif)	30.027973N, 31.215963E	donkeys	throughout the year	Hilali et al. (2015)

Rhinoestrus purpureus (Brauer, 1858)

Cephalomyia purpurea Brauer, 1858b: 457. Type locality: Austria (Bisamberg).
Rhinoestrus nasalis: Brumpt, 1913: 700. Misidentification.

Common name. Equine nasal bot fly.

Distribution. AF, OR: Widespread (introduced with horses, see Papavero (1977)).
 PA: Widespread.

Localities, hosts, and dates of collection. See Table 12 and Figure 6.

Material examined. EGYPT • 1 male; Cairo; 29.999896N, 31.270483E; 10.May.1922; Efflatoun leg.; from donkey's head; EFC • 1 male; El-Magadlah; 27.Apr.1924; R. Mabrouk leg.; EFC • 1 female; Giza; 30.015432N, 31.207837E; 2.May.1907; EFC.

Discussion

Egypt and Saudi Arabia are biogeographically comparable being located at the junction of the Palearctic and the Afrotropical Realms. In Egypt, the Afrotropical Realm is thought to involve the southeastern triangle of the country, which known as the Gebel Elba ecological zone. This is the only ecological zone in Egypt, which has an Afrotropical faunal affiliation. However, the faunal affiliation of the other seven ecological zones is mostly Palearctic, namely, the Coastal Strip, Eastern Desert, Western Desert, Fayoum, Lower Nile Valley, and Delta, Sinai, and Upper Nile Valley (Fig. 1) (El-Hawagry and Gilbert 2014; El-Hawagry 2017; El-Hawagry et al. 2018; El-Hawagry et al. 2020). In Saudi Arabia, many biogeographers agree that the border of the Afrotropical Realm should be extended up to Taif City, i.e., up to the Tropic of Cancer, covering the

southwestern part of the country (Wallace 1876; Hölzel 1998; El-Hawagry et al. 2017; El-Hawagry and Al Dhafer 2019; El-Hawagry et al. 2019). All these biogeographic facts undoubtedly reflect on the distribution of oestrid species treated in the present study as all reported species, except three, are of both Palaearctic and Afrotropical affinities. Only *Gasterophilus nigricornis* and *Hypoderma bovis* are Palaearctic, and *Hypoderma desertorum* is endemic to Egypt. Some of the reported species are also known as cosmopolitan and should be widespread in both Egypt and Saudi Arabia; however, the majority of species were reported only from some restricted regions. Surprisingly, no records of oestrid flies were reported from Upper Nile Valley, Western Desert and Gebel Elba in Egypt. This is most likely due to the fact that most collections were focused predominantly in Alexandria, Greater Cairo (slaughterhouses, circus, Giza Zoo, Manure Co., near pyramids and wadies southwestern to Cairo) and Sinai Peninsula. The same situation is in Saudi Arabia as few records were reported especially from Al-Baha, Eastern Province, Makkah, and Riyadh regions (Abu-Thuraya 1982).

Oestrid flies in Egypt and Saudi Arabia, as far as is known, infest domesticated animals and in some cases humans. Infections with *Cephalopina titillator* larvae have been reported in the dromedary camel (Family Camelidae) (Abu-Thuraya 1982, Büttiker and Zumpt 1982, Hussein et al. 1982, Fatani and Hilali 1994, Alahmed 2002, Hendawy et al. 2012). Attacks by larvae of different *Gasterophilus* species have been reported in donkeys and horses (family Equidae) (Abu-Thuraya 1982, Büttiker and Zumpt 1982, Hilali et al. 1987, El-Bakry and Fadly 2014, Abdel Rahman et al. 2018, Attia et al. 2018) and *Rhinoestrus purpureus* (Hilali et al. 2015). The goats and sheep (Family Bovidae) have been reported as hosts for the larvae of *Hypoderma lineatum* (Büttiker and Zumpt 1982), *Oestrus ovis* (Abu-Thuraya 1982, Büttiker and Zumpt 1982, Amin et al. 1997, Bosly 2013), and *Przhevalskiana silenus* (El-Azzazy 1997, Morsy et al. 1998). Ophthalmomyiasis infestation of human eye with larvae of *O. ovis* was documented from Saudi Arabia (Omer et al. 1988). Two cases of gastric myiasis with larvae of unidentified *Oestrus* sp. were reported from Egypt, Minia Governorate (Ahmad et al. 2011).

The low abundance and diversity of species in both Egypt and Saudi Arabia should be taken with caution, since the family seems to lack sampling efforts in both countries. We think that the distributional data of these economically important flies within Egypt and Saudi Arabia is still scanty, and more efforts would be highly desirable in the future. Nevertheless, the present catalogue presented some new locality records especially for *Gasterophilus intestinalis*, *Gasterophilus nasalis*, *Gasterophilus nigricornis*, *Przhevalskiana silenus*, *Cephalopina titillator*, *Oestrus ovis* and *Rhinoestrus purpureus*. This catalogue undoubtedly will act as a baseline for further study in both countries.

Acknowledgements

The authors would like to extend their sincere appreciation to the Deanship of Scientific Research at King Saud University for funding this study [research group: RGP-1438-082].

We are grateful to Editage, a division of cactus communications (www.editage.com) for English language editing. We are also grateful to Dr. Babak Gharali, the Research Centre for Agriculture and Natural Resources, Iran, and Dr Adrian Pont, Oxford University Museum of Natural History, Oxford, UK for supplying us with some relevant papers.

References

- Abdel Rahman MM, Hassanen EA, Abdel Mageed MA (2018) Light and scanning electron microscopy of *Gasterophilus intestinalis* (larvae and adult fly) infesting donkeys with emphasis on histopathology of the induced lesions. *Egyptian Veterinary Medical Society of Parasitology Journal* 14: 15–31. <https://doi.org/10.21608/evmspj.2018.33951>
- Abu-Thuraya NH (1982) General survey, agricultural pests in Saudi Arabia. Ministry of Agriculture and Water, Agriculture Research Department of Plant Protection: Kingdom of Saudi Arabia, 326 pp.
- Abu-Zoherah R, Al-Taher K, Tilkian S (1993) List of insects recorded from Saudi Arabia. Ministry of Agriculture and Water, National Agriculture and Water Research Centre, Riyadh, Kingdom of Saudi Arabia, 394 pp.
- Alahmed AM (2000) Seasonal infestation of *Oestrus ovis* larvae in sheep heads in central region of Saudi Arabia. *Journal of the Egyptian Society of Parasitology* 30(3): 895–901.
- Alahmed AMI (2002) Seasonal Prevalence of *Cephalopina titillator* Larvae in camels in Riyadh Region, Saudi Arabia. *Arab Gulf Journal of Scientific Research* 20(3): 161–164.
- Al-Ahmadi AZ, Salem MM (1999) Entomofauna of Saudi Arabia, Part 1: Checklist of insects. Academic Publishing & Press, King Saud University, Kingdom of Saudi Arabia, 240 pp.
- Al Dhafer HM, El-Hawagry MS (2016) Records for the Family Ulidiidae (Diptera, Tephritoidea) in Saudi Arabia. *African Entomology* 24(1): 225–232. <https://doi.org/10.4001/003.024.0225>
- Agassiz JLR (1846) *Nomenclatoris zoologici index universalis: continens nomina systematica classium, ordinum, familiarum, et generum animalium omnium, tam viventium quam fossilium*. Jent & Gassmann: Switzerland, 393 pp.
- Ahmad AK, Abdel-Hafeez EH, Makhloof M, Abdel-Raheem EM (2011) Gastrointestinal Myiasis by Larvae of *Sarcophaga* sp. and *Oestrus* sp. in Egypt: Report of Cases, and Endoscopic and Morphological Studies. *Korean Journal of Parasitology* 49: 51–57. <https://doi.org/10.3347/kjp.2011.49.1.51>
- Akhter J, Qadri SM, Imam AM (2000) Cutaneous myiasis due to *Dermatobia hominis* in Saudi. *Saudi Medical Journal* 21(7): 689–691.
- Alikhan M, Al-Ghamdi K, Al-Zahrani FS, Khater EI, Allam AM (2018) Prevalence and salient morphological features of myiasis causing Dipteran flies in Jeddah, Saudi Arabia. *Biosciences, Biotechnology Research Asia* 15: 101–9. <https://doi.org/10.13005/bbra/2612>
- Amin AR, Morsy TA, Shoukry A, Mazyad SA (1997) Oestrid head maggots in slaughtered sheep in Cairo abattoir. *Journal of the Egyptian Society of Parasitology* 27: 855–861.

- Attia MM, Khalifa MM, Mahdy OA (2018) The prevalence of *Gasterophilus intestinalis* (Diptera: Oestridae) in donkeys (*Equus asinus*) in Egypt with special reference to larvicidal effects of neem seed oil extract (*Azadirachta indica*) on third stage larvae. Open Veterinary Journal 8(4): 423–431. <https://doi.org/10.4314/ovj.v8i4.12>
- Austen EE (1931) A new species of warble-fly (Diptera – Family Tachinidae, Subfamily Hypoderminae, Genus Hypoderma), which attacks goats in Cyprus. Bulletin of Entomological Research 22: 423–429. <https://doi.org/10.1017/S0007485300029941>
- Bezzi M (1916) Un nuova specie di Estride dell'Eritrea. Bollettino del Laboratorio di zoologia generale e agraria della R. Scuola superiore d'agricoltura in Portici 10: 27–32.
- Bigot JMF (1884) Descriptions de Diptères nouveaux récoltés par M. le professeur Magretti dans le Soudan oriental. Annales de la Société entomologique de France, 6 4(2): 57–59.
- Bosly AH (2013) Seasonal prevalence of *Oestrus ovis* L. (Diptera: Oestridae) larvae in infested sheep in Jazan Region, Saudi Arabia. Journal of Parasitology and Vector Biology 5(5): 66–71.
- Boulard C (2002) Durably controlling bovine hypodermosis. Veterinary Research 33: 455–464. <https://doi.org/10.1051/vetres:2002032>
- Brauer F (1858a) Die Oestriden (Dasselfliegen) des Hochwildes, nebst einer Tabelle zur Bestimmung aller europäischen Arten dieser Familie. Verhandlungen der Zoologisch-Botanischen Gesellschaft in Wien 8: 385–414.
- Brauer F (1858b) Neue Beiträge zur Kenntniss der europäischen Oestriden. Verhandlungen der Kaiserlich-Königliche Zoologisch-Botanischen Gesellschaft in Wien 8: 449–470.
- Brauer F (1863) Monographie der Oestriden. C. Ueberreuter, Vienna, 291 pp. <https://doi.org/10.5962/bhl.title.57896>
- Brauer F (1875) Beschreibung neuer und ungenugend bekannter Phryganiden und Oestriden. Verhandlungen der Zoologisch - Botanische Gesellschaft in Wien 25: 69–78.
- Brauer F (1886) Nachträge zur Monographie der Oestriden. I. Ueber die von Frau A. Zugmayer und Herrn F. Wolf entdeckte Lebensweise des *Oestrus purpureus*. Wiener Entomologische Zeitung 5: 289–304. <https://doi.org/10.5962/bhl.part.20610>
- Brauer F (1897) Beiträge zur Kenntniss der Muscaria schizometopa und Beschreibung von zwei *Hypoderma*-Arten. I. Bemerkungen zu den Original Exemplaren der von Bigot, Macquart und Robineau-Desvoidy beschriebenen Muscaria schizometopa aus der Sammlung des Herrn G.H. Verrall. Sitzungsberichte der Kaiserlichen Akademie der Wissenschaften in Wien, Mathematisch-Naturwissenschaftliche Classe 106: 329–382.
- Brumpt E (1913) Précis de Parasitologie. 2nd ed., Masson et Cie, Paris, 1215 pp.
- Büttiker W, Zumpt F (1982) Veterinary and applied zoology in KSA: Myiasis in domestic animals. Fauna of Saudi Arabia 4: 520–524.
- Causar E (1940) Hypodermatids of goats in Azerbaidzhán. Publishing House of Azerbaijan branch of the USSR Academy of Sciences, Baku, 44 pp.
- Catts EP, Mullen GR (2002) Myiasis (Muscoidea, Oestroidea) In: Mullen G, Durden L (Eds) Medical and veterinary entomology. San Diego, Elsevier Science Academic Press, 317–348. <https://doi.org/10.1016/B978-012510451-7/50018-9>
- Clark B (1797) Observations on the genus *Oestrus*. Transactions of the Linnean Society of London 3: 289–329. <https://doi.org/10.1111/j.1096-3642.1797.tb00570.x>
- Clark B (1815) An essay on the bots of horses and other animals. Old Bailey, London, 72 pp. <https://doi.org/10.5962/bhl.title.159664>

- Clark B (1816) Supplementary sheet. Discovery of the fly of the white bot. Published by the author, London, 4 pp.
- Clark B (1841) An appendix or supplement to a treatise on the Oestri and Cuterebrae of various animals. Proceedings of the Linnean Society of London 1: 99–100.
- Clark B (1843) An appendix or supplement to a treatise on the Oestri and Cuterebrae of various animals. Transactions of the Linnean Society of London (Zoology) 19(2): 81–94. <https://doi.org/10.1111/j.1096-3642.1842.tb00353.x>
- Colwell DD (2006) Life cycle strategies. In: Colwell DD, Hall MJR, Scholl PJ (Eds) The Oestrid flies: Biology, host-parasite relationships, impact and management. Wallingford, CABI, 67–77. <https://doi.org/10.1079/9780851996844.0067>
- Coquillett DW (1910) The type-species of the North American genera of Diptera. Proceedings of the United States National Museum, Washington 37: 499–647. <https://doi.org/10.5479/si.00963801.37-1719.499>
- Curtis J (1826) British entomology: being illustrations and descriptions of the genera of insects found in Great Britain and Ireland: Containing coloured figures from nature of the most rare and beautiful species, and in many instances of the plants upon which they are found. Printed for the author, London, 146 pp.
- De Geer C (1776) Mémoires pour servir à l'histoire des insectes. Tome sixième. P. Hesselberg, Stockholm, 523 pp.
- Dinulescu G (1932) Recherches sur la biologie des gastrophiles, anatomie, physiologie, cycle évolutif. Annales des Sciences Naturelles Zoologie 10: 1–183.
- Dinulescu G (1938) *Gastrophilus veterinus* var. *aureus*. Archives Roumaines de Pathologie Expérimentale et de Microbiologie (Bucuresti) 11: 315–335.
- El-Azzazy OME (1997) Goat warble fly, *Przhevalskiana silenus* (Brauer) (Diptera: Oestridae) in Saudi Arabia. Small Ruminant research 24(1): 65–67. [https://doi.org/10.1016/S0921-4488\(96\)00918-2](https://doi.org/10.1016/S0921-4488(96)00918-2)
- El-Bakry KM, Fadly S (2014) Differential identification of *Gasterophilus* larval spp. in donkeys by electron microscope. Assiut Veterinary Medical Journal 60(142): 144–155.
- El-Hawagry MS (2017) Catalogue of Egyptian Tephritoidea (Diptera: Schizophora: Acalypterae). Zootaxa 4299(2): 151–190. <https://doi.org/10.11646/zootaxa.4299.2.1>
- El-Hawagry MS (2018) Catalogue of the Tachinidae of Egypt (Diptera: Oestroidea). Egyptian Journal of Biological Pest Control 28: 46. <https://doi.org/10.1186/s41938-018-0042-3>
- El-Hawagry MS, Abdel-Dayem MS, Al Dhafer HM (2019) On the taxonomy of the genus *Thyridanthrax* Osten Sacken in Egypt and the Kingdom of Saudi Arabia, with description of a new species (Diptera: Bombyliidae). Zootaxa 4701(6): 501–519. <https://doi.org/10.11646/zootaxa.4701.6.1>
- El-Hawagry MS, Al Dhafer HM (2019) The family Bombyliidae in the Kingdom of Saudi Arabia (Diptera: Brachycera: Asiloidea). Zootaxa 4590(1): 059–094. <https://doi.org/10.11646/zootaxa.4590.1.3>
- El-Hawagry MS, El-Azab SA (2019) Catalog of the Calliphoridae, Rhiniidae, and Sarcophagidae of Egypt (Diptera: Oestroidea). Egyptian Journal of Biological Pest Control 29: 15. <https://doi.org/10.1186/s41938-019-0118-8>
- El-Hawagry MS, Abdel-Dayem MS, El-Sonbati SA, Al dhafer HM (2017) A preliminary account of the fly fauna in Garf Raydah Nature Reserve, Kingdom of Saudi Arabia, with new

- records and biogeographical remarks (Diptera: Insecta). *Journal of Natural History* 51: 1499–1530. <https://doi.org/10.1080/00222933.2017.1347299>
- El-Hawagry MS, El-Azab SE-DA, Abdel-Dayem MS, Al Dhafer HM (2020) Biting midges of Egypt (Diptera: Ceratopogonidae). *Biodiversity Data Journal* 8: e52357. <https://doi.org/10.3897/BDJ.8.e52357>
- El-Hawagry MS, Zatwarnicki T, Ebrahim AM (2018) Catalogue of the Egyptian Ephydroidea (Diptera: Schizophora: Acalyptratae). *Zootaxa* 4444(3): 201–246. <https://doi.org/10.11646/zootaxa.4444.3.1>
- Enderlein G (1934) *Dipterologica*. Sitzungsberichte der Gesellschaft naturforschender Freunde zu Berlin 1933: 416–429.
- Fabricius JC (1787) *Mantissa insectorum sistens eorum species nuper detectas adiectis characteribus genericis, differentiis specificis, emendationibus, observationibus*. Impensis Christiani Gottlob Proft, Copenhagen, 382 pp. <https://doi.org/10.5962/bhl.title.36471>
- Fabricius JC (1794) *Entomologia systematica emendata et aucta*, Vol. 4: Secundum classes, ordines, genera, species. Impensis Christi Gottl Proft, Copenhagen, 472 pp.
- Fatani A, Hilali M (1994) Prevalence and monthly variations of the second and third instars of *Cephalopina titillator* (Diptera: Oestridae) infesting camels (*Camelus dromedarius*) in the Eastern Province of Saudi Arabia. *Veterinary Parasitology* 53: 145–151. [https://doi.org/10.1016/0304-4017\(94\)90026-4](https://doi.org/10.1016/0304-4017(94)90026-4)
- Fitzinger LJFJ (1873) Die Gattungen der europäischen Cyprinen nach ihren äusseren Merkmalen. Sitzungsberichte der Kaiserlichen Akademie der Wissenschaften. Mathematisch-Naturwissenschaftliche Classe 68: 145–170.
- Gadallah NS, Bosly HA (2006) Diptera associated with camels in the Jeddah region, western Saudi Arabia. *Fauna of Arabia* 21: 339–350.
- Gedoelst LM (1916) Notes sur les Oestrides. *Revue Zoologique Africaine* 4: 259–264.
- Gedoelst LM (1923) Note sur la larve du *Gasterophilus haemorrhoidalis* et description de la larve d'une nouvelle espèce africaine. *Annales de Parasitologie* 1: 269–275. <https://doi.org/10.1051/parasite/1923013269>
- Ghazanfar SA, Fisher M (1998) Vegetation of the Arabian peninsula. *Geobotany* 25: 1–362. https://doi.org/10.1007/978-94-017-3637-4_1
- Gistel J (1848) *Naturgeschichte des Thierreichs für höheren Schulen*. R. Hoffmann, Stuttgart, 216 pp.
- Grunberg K (1904) Ueber eine neue Oestridenlarve (*Rhinoestrus hippopotami* n. sp.) aus der Stirnhöhle des Nilpferdes. *Der Gesellschaft Naturforschender Freunde zu Berlin* 1904: 35–39.
- Grunin KJ (1948) A new species of botfly from under the skin of the *Orongo antelope* (*Pantholops hodgsoni* Abel). *Doklady Akademii Nauk SSSR* 63(4): 469–472.
- Grunin KJ (1956) Ueber die in *Gazella subgutterosa* Gueld. schmarotzenden Dasselfliegen (Diptera, Hypodermatidae). *Revue d'Entomologie de l'URSS* 35: 716–723.
- Grunin KJ (1965) 64b. Hypodermatidae. In: Lindner E (Ed.) *Die Fliegen der Paläarktischen Region* 8. Schweizerbart'sche, Stuttgart, 153 pp.
- Guérin-Méneville FÉ (1827) *Dictionnaire classique d'histoire naturelle*. Paris, Rey et Gravier, Libraires-Editeurs, Auai des Augustins, no. 55; Baudouin FrèreS, Libraires-Editeurs, Imprimeurs de la société D'Histoire Naturelle, Rue de Vaugirard, no. 36, Paris, 634 pp.

- Hall M, Wall R (1995) Myiasis of humans and domestic animals. *Advances in Parasitology* 35: 257–334. [https://doi.org/10.1016/S0065-308X\(08\)60073-1](https://doi.org/10.1016/S0065-308X(08)60073-1)
- Hendawy SHM, Allam NAT, Kandil OM, Zayed AA, Desouky ARAY, El-Rafey MA (2012) Partial COI and 16S rRNA genes sequences of *Cephalopina titillator* mitochondrial DNA: Evidence for variation in evolutionary rates within myiasis-causing species. *Global Veterinaria* 9(6): 769–778.
- Hilali M, Derhali FS, Baraka A (1987) Incidence and monthly prevalence of *Gasterophilus* spp. larvae (Diptera: Gastrophilidae) in the stomach of donkeys (*Equus asinus*) in Egypt. *Veterinary Parasitology* 23: 297–30. [https://doi.org/10.1016/0304-4017\(87\)90015-X](https://doi.org/10.1016/0304-4017(87)90015-X)
- Hilali MA, Mahdy OA, Attia MM (2015) Monthly variations of *Rhinoestrus* spp. (Diptera: Oestridae) larvae infesting donkeys in Egypt: Morphological and molecular identification of third stage larvae. *Journal of Advanced Research* 6(6): 1015–1021. <https://doi.org/10.1016/j.jare.2014.12.003>
- Hölzel H (1998) Zoogeographical features of Neuroptera of the Arabian Peninsula. *Acta Zoologica Fennica* 209: 129–140.
- Hoseini SM, Zaheri BA, Adibi MA, Ronaghi H, Moshrefi AH (2017) Histopathological study of esophageal infection with *Gasterophilus pecorum* (Diptera: Oestridae) in Persian onager (*Equus hemionus onager*). *Journal of Arthropod-Borne Diseases* 11(3): 441–445.
- Hudson GV (1892) *An elementary manual of New Zealand entomology. Being an introduction of our native insects.* West, Newman, & Co., London, 128 pp. <https://doi.org/10.5962/bhl.title.8441>
- Hussein MF, El-Amin FM, El-Taib NT, Basmaeil SM (1982) The pathology of nasopharyngeal myiasis in Saudi Arabian camels (*Camelus dromedarius*). *Veterinary Parasitology* 9: 253–160. [https://doi.org/10.1016/0304-4017\(82\)90060-7](https://doi.org/10.1016/0304-4017(82)90060-7)
- Kenawy MA, Al Ashry HA, Shobrak M (2014) Synanthropic flies of Asir Province, southwest of Saudi Arabia. *Journal of Entomological and Acarological Research* 46: 4623. <https://doi.org/10.4081/jear.2014.4623>
- Kettle DS (1995). *Medical and Veterinary Entomology.* 2nd ed., C.A.B. international, U.K. at the University press, Cambridge, 725 pp.
- Kirk-Spriggs AH, Sinclair BJ (2017) *Manual of Afrotropical Diptera.* Vol. 1. Introductory chapters and keys to Diptera families. South African National Biodiversity Institute, Pretoria, 425 pp.
- Latreille PA (1818) *Oestre, Nouveau dictionnaire d'histoire naturelle, appliquée aux arts, à l'agriculture, à l'économie rurale et domestique, à la médecine, etc. Par une société de naturalistes et d'agriculteurs.* Nouvelle Edition 23, 264–274.
- Leach WE (1817) On the arrangement of oestrideous insects. In *On the genera and species of epoboscideous insects, and on the arrangement of oestrideous insects.* Neill & Co., Edinburg, 1–20.
- Li X-Y, Pape T, Zhang D (2019a) *Gasterophilus flavipes* (Oestridae: Gasterophilinae): A horse stomach bot fly brought back from oblivion with morphological and molecular evidence. *PLoS ONE* 14 (8): e0220820. <https://doi.org/10.1371/journal.pone.0220820>
- Li X-Y, Pape T, Zhang D (2019b) Taxonomic review of *Gasterophilus* (Oestridae, Gasterophilinae) of the world, with updated nomenclature, keys, biological notes, and distributions. *ZooKeys* 891: 119–156. <https://doi.org/10.3897/zookeys.891.38560>

- Liakos BD (1986) Effect of hypodermatosis on the body weight of young goats. Bulletin of the Hellenic Veterinary Medical Society 37: 8–12.
- Linnaeus C (1758) Systema naturae per regna tria naturae :secundum classes, ordines, genera, species, cum characteribus, differentiis, synonymis, locis. Salvii, Stockholm, 824 pp. <https://doi.org/10.5962/bhl.title.542>
- Loew H (1863) Zwei neue europäische Dipterengattungen. Wiener Entomologische Monatschrift 7: 38–40.
- Macquart PJM (1843) Diptères exotiques nouveaux ou peu connus. Tome deuxième, 3eme partie. Roret, Paris, 460 pp.
- Marshall SA, Kirk-Spriggs AH, Muller BS, Paiero SM, Yau T, Jackson MD (2017) [Chapter] 12. key to Diptera families. In: Kirk-Spriggs AH, Sinclair BJ (Eds) Manual of Afrotropical Diptera. Volume 1. Introductory chapters and keys to Diptera families. Suricata 4, South African National Biodiversity Institute, Pretoria, 267–355.
- Meigen JW (1824) Systematische Beschreibung der bekannten europäischen zweiflügeligen Insekten. Vierter Theil. Schulz-Wundermann'sche Buchhandlung, Hamm, 428 pp.
- Morsy TA, Shoukry A, Mazyad SA, Abou Gamra MM (1998) The goat warble fly, *Przhevalskiana silenus* Brauer) in north Sinai, Egypt. Journal of the Egyptian Society of Parasitology 28: 373–378.
- Mote DC (1928) The ox warble flies. Ohio Agricultural Experiment Station Bulletin, 428, 45 pp.
- Omar MS, Das AB, Osman NI (1988) External ophthalmomyiasis due to the sheep nostril botfly larva *Oestrus ovis* in Saudi Arabia, Annals of Tropical Medicine and Parasitology 82(2) 221–223. <https://doi.org/10.1080/00034983.1988.11812235>
- Otranto D, Traversa D, Guida B, Tarsitano E, Fiorente P, Stevens J (2003) Molecular characterization of the mitochondrial cytochrome oxidase I gene of Oestridae species causing obligate myiasis. Medical and Veterinary Entomology 17(3): 307–315. <https://doi.org/10.1046/j.1365-2915.2003.00442.x>
- Otranto D, Colwell D, Milillo P, Di Marco V, Paradies P, Napoli C (2004) Report in Europe of nasal myiasis by *Rhinoestrus* spp. in horses and donkeys: seasonal patterns and taxonomical consideration. Veterinary Entomology 122: 79–88. <https://doi.org/10.1016/j.vetpar.2004.03.015>
- Pallas PS (1776) Spicilegia zoologica quibus novae imprimis et obscurae animalium species iconibus, descriptionibus atque commentariis illustrantur. Fasciculus undecimus, Berlin, 86 pp.
- Papavero N (1977) The world Oestridae (Diptera), mammals and continental drift. Dr. W.Junk bv Publishers-The Hague, 240 pp. <https://doi.org/10.1007/978-94-010-1306-2>
- Pape T (1992) Phylogeny of the Tachinidae family-group (Diptera: Calypttratae). Tijdschrift voor Entomologie 135: 43–86.
- Pape T (2001) Phylogeny of Oestridae (Insecta: Diptera). Systematic Entomology 26: 133–171. <https://doi.org/10.1046/j.1365-3113.2001.00143.x>
- Pape T, Blagoderov V, Mostovski MB (2011) Order Diptera Linnaeus, 1758. In: Zhang ZQ (Ed.) Animal biodiversity: an outline of higher-level classification and survey of taxonomic richness. Zootaxa 3148: 222–229. <https://doi.org/10.11646/zootaxa.3148.1.42>

- Paramonov SJ (1940) *Gastrophilidae und ihre Bekämpfungen*. Kiew-Lwow, 128 pp.
- Patton WS (1922) *Hypoderma crossii* sp. n. parasitic in its larval stages in cattle and goats in the Punjab. *Indian Journal of Medical Research* 10: 573–578.
- Patton WS (1924) *Gasterophilus crossi* sp. nov., parasitic in its larval stage in the stomach of the horse in the Punjab. *Indian Journal of Medical Research* 11: 963.
- Pleske T (1926) *Revue des espèces paléarctiques des Oestrides et catalogue raisonné de leur collection au Musée Zoologique de l'Académie des Sciences. Annuaire du Musée Zoologique de l'Académie Impériale des Sciences de Saint Pétersbourg* 26: 215–230.
- Rodhain J, Bequaert J (1920) Oestrides d'antilopes et de zèbres recueillis en Afrique orientale avec un conspectus du genre *Gasterophilus*. *Revue Zoologique Africaine* 8: 169–228. <https://doi.org/10.5962/bhl.part.22396>
- Rondani C (1857) *Dipterologiae Italicae prodromus. Vol. 2. Species Italicae ordinis dipteriorum in genera characteribus definita, ordinatim collectae, methodo analitica distinctae, et novis vel minus cognitis descriptis. Pars prima: Oestridae, Syrphidae, Conopidae*. Stocchi, Parmae, 264 pp. <https://doi.org/10.5962/bhl.title.8160>
- Royce LA, Rossignol PA, Kubitz ML, Burton FR (1999) Recovery of a second instar *Gasterophilus* larva in a human infant: A case report. *The American Journal of Tropical Medicine and Hygiene* 60(3): 403–404. <https://doi.org/10.4269/ajtmh.1999.60.403>
- Saini RK, Sankhala LN (2015) A case report of bovine hypodermosis. *International Journal of Science, Environment and Technology* 4(3): 725–726.
- Schwab KC (1840) *Die Oestraciden – Bremsen – der Pferde, Rinder und Schafe*. Matthäus Pössenbacher, München, 83 pp.
- Slater PL (1858) On the general geographical distribution of the members of the class Aves. *Journal of the Proceedings of the Linnean Society of London. Zoology* 2: 130–145. <https://doi.org/10.1111/j.1096-3642.1858.tb02549.x>
- Soós A, Minar J (1986a) Family *Gasterophilidae*. In: Soos A, Papp L (Eds) *Catalogue of Palaearctic Diptera. Volume 11. Scathophagidae–Hypodermatidae*. Akadémiai Kiado, Budapest, 237–240.
- Soós A, Minar J (1986b) Family *Oestridae*. In: Soos A, Papp L (Eds) *Catalogue of Palaearctic Diptera. Volume 11. Scathophagidae–Hypodermatidae*. Akadémiai Kiado, Budapest, 240–244.
- Steel JH (1887) On bots (Larval Oestridae) of the horse and camel. *Journal of the Bombay Natural History Society* 2: 27–30.
- Steyskal GC, El-Bialy S (1967) A list of Egyptian Diptera with a bibliography and key to families. *Ministry of Agriculture Technical Bulletin* 3: 32–37.
- Strand E (1928) *Miscellaneae nomenclaturica zoologica et palaeontologica*. *Archiv für Naturgeschichte* 92A(8): 30–75.
- Sultanov MA (1951) A new species of botflies from horse – *Gasterophilus viridis* sultanov sp. nov. *Doklady Akademii Nauk Uzbekskoi SSR* 1951: 41–44.
- Szilády Z (1935) Die ungarischen Dasselfliegen. *Állattani Közlemények* 32: 136–140.
- Townsend CHT (1912) A readjustment of muscoid names. *Proceedings of the Entomological Society of Washington* 14: 45–53.

- Townsend CHT (1916) Diagnoses of new genera of muscoid flies founded on old species. Proceedings of the United States National Museum 49: 617–633. <https://doi.org/10.5479/si.00963801.2128.617>
- Townsend CHT (1918) New muscoid genera, species and synonymy (Diptera). Insecutor Inscitiae Menstruus 6: 157–182.
- Townsend CHT (1933) New genera and species of Old World oestromuscoid flies. Journal of the New York Entomological Society 40: 439–479.
- Townsend CHT (1934) New Neotropical oestromuscoid flies. Revista de Entomologia 4: 201–212.
- Villers CJ (1789) Caroli Linnaei entomologia, faunae Suecicae descriptionibus aucta; DD. Scopoli, Geoffroy, de Geer, Fabricii, Schrank, &c. speciebus vel in systemate non enumeratis, vel nuperrime detectis, vel speciebus Galliae australis locupletata, generum specierumque rariorum iconibus ornata; curante & augente Carolo de Villers, Acad. Lugd. Massil. Villa-Fr. Rhotom. necnon Geometriae Regio Professore. Tomus tertius. Piestre et Delamolliere, Lyon, xxiv + 657 pp.
- Walker F (1849) List of the specimens of dipterous insects in the collection of the British Museum. Part III. British Museum (Natural History), London, 485–687.
- Wallace AR (1876) The geographical distribution of animals, vVols 1, 2. Macmillan, London, 574 pp + 650 pp.
- Wiedemann CRW (1830) Aussereuropäische zweiflügelige Insekten. Als Fortsetzung des Meigenschen Werkes, zweiter Theil. Schulz, Hamm, xii + 684 pp.
- Wood DM (1987) Chapter 107. Oestridae. In: McAlpine JF, et al. (Eds) Manual of Nearctic Diptera, vol. 2. Agriculture Canada Monograph, 1147–1158.
- Zayed AA (1998) Localization and migration route of *Cephalopina titillator* (Diptera: Oestridae) larvae in the head of infested camels (*Camelus dromedarius*). Veterinary Parasitology 80(1): 65–70. [https://doi.org/10.1016/S0304-4017\(98\)00182-4](https://doi.org/10.1016/S0304-4017(98)00182-4)
- Zetterstedt JW (1844) Diptera Scandinaviæ disposita et descripta. Tomus 3. Officina Lundbergiana, Lundae [= Lund], 895–1280.
- Zumpt F (1965) Myiasis of Man and Animals in the Old World. Butterworths, London, 267 pp.

GPS tracking data of Western marsh harriers breeding in Belgium and the Netherlands

Tanja Milotić¹, Peter Desmet¹, Anny Anselin¹, Luc De Bruyn^{1,2}, Nico De Regge¹, Kjell Janssens¹, Raymond Klaassen^{3,4}, Ben Koks³, Tonio Schaub^{3,4}, Almut Schlaich³, Geert Spanoghe¹, Filiep T’Jollyn¹, Joost Vanoverbeke¹, Willem Bouten⁵

1 Research Institute for Nature and Forest (INBO), Havenlaan 88/73, 1000, Brussels, Belgium **2** Evolutionary Ecology, University of Antwerp, Universiteitsplein 1, 2610, Wilrijk, Belgium **3** Dutch Montagu’s Harrier Foundation, Postbus 46, 9679, ZG Scheemda, The Netherlands **4** Conservation Ecology Group, Groningen Institute of Evolutionary Life Sciences, University of Groningen, Postbus 11103, 9700, CC Groningen, The Netherlands **5** Institute for Biodiversity and Ecosystem Dynamics (IBED), University of Amsterdam, Science Park 904, 1098, XH, Amsterdam, The Netherlands

Corresponding author: Tanja Milotić (tanja.milotic@inbo.be)

Academic editor: Knud Jønsson | Received 26 March 2020 | Accepted 19 May 2020 | Published 8 July 2020

<http://zoobank.org/A9C5EEBC-88DE-495B-BED2-28D1B2699939>

Citation: Milotić T, Desmet P, Anselin A, De Bruyn L, De Regge N, Janssens K, Klaassen R, Koks B, Schaub T, Schlaich A, Spanoghe G, T’Jollyn F, Vanoverbeke J, Bouten W (2020) GPS tracking data of Western marsh harriers breeding in Belgium and the Netherlands. ZooKeys 947: 143–155. <https://doi.org/10.3897/zookeys.947.52570>

Abstract

In this data paper three datasets are described containing GPS tracking and acceleration data of Western marsh harriers (*Circus aeruginosus*) breeding in Belgium and the Netherlands. The Western marsh harrier is included as a threatened bird species in Annex I of the European Bird Directive due to the steep decline in population densities. In order to collect data of habitat use and migration behaviour, Western marsh harriers were equipped with light-weight solar powered GPS trackers developed by the Institute for Biodiversity and Ecosystem Dynamics (IBED) at the University of Amsterdam (University of Amsterdam Bird Tracking System, UvA-BiTS). These trackers automatically collect and store data on the bird’s activity and 3D position in time and transmit these data to ground stations.

The datasets were collected by the Research Institute for Nature and Forest (INBO) and the Dutch Montagu’s Harrier Foundation. Tracked Western marsh harriers were breeding in the northeast of the Dutch province of Groningen and on the opposite side of the river Ems in Germany (H_GRONINGEN), in the region of Waterland-Oudeman near the Belgian-Dutch border (MH_WATERLAND), and at the left bank of the Scheldt estuary, close to the Belgian-Dutch border and north of the city of Antwerp (MH_ANT-

WERPEN). Most individuals remained within 10 km from their nesting sites during the breeding season and wintered in West Africa. H_GRONINGEN contains 987,493 GPS fixes and 3,853,859 acceleration records of four individuals since 2012. MH_WATERLAND contains 377,910 GPS fixes of seven individuals. Sampling in this region began in 2013. Three more Western marsh harriers were tagged in the Scheldt estuary near Antwerp more recently in 2018 (one individual) and 2019 (two individuals) for the MH_ANTWERPEN study, which contains 47,917 GPS fixes and 227,746 acceleration records.

The three Western marsh harrier datasets were published as separate studies in Movebank (<https://www.movebank.org>) and archived as data packages in Zenodo (<https://www.zenodo.org>) to ensure long-term preservation and versioning of the data.

Keywords

Animal movement, bird tracking, biologging, *Circus aeruginosus*, GPS tracking, habitat use, LifeWatch, machine observation, migration data, Movebank, UvA-BiTS

Data published through

Koks B, Schlaich A, Schaub T, Klaassen R, Anselin A, Desmet P, Milotic T, Janssens K, Bouten W (2019) H_GRONINGEN – Western marsh harriers (*Circus aeruginosus*, Accipitridae) breeding in Groningen (the Netherlands). Dataset. <https://doi.org/10.5281/zenodo.3552507>

Anselin A, Desmet P, Milotic T, Janssens K, T’Jollyn F, De Bruyn L, Bouten W (2019) MH_WATERLAND – Western marsh harriers (*Circus aeruginosus*, Accipitridae) breeding near the Belgium-Netherlands border. Dataset. <https://doi.org/10.5281/zenodo.3532940>

Spanoghe G, Desmet P, Milotic T, Janssens K, De Regge N, Vanoverbeke J, Bouten W (2019) MH_ANTWERPEN – Western marsh harriers (*Circus aeruginosus*, Accipitridae) breeding near Antwerp (Belgium). Dataset. <https://doi.org/10.5281/zenodo.3550093>

Rationale

The Western marsh harrier (*Circus aeruginosus* Linnaeus, 1758) is a large harrier species native to temperate and subtropical Eurasia and Africa. Due to the steep population decline observed in Europe since the 1970s, the species has been included as a threatened species in annex I of the European Birds Directive in 1979. In Flanders, the Western marsh harrier appears as an endangered species on the red list of breeding bird species (Devos et al. 2016). In the Netherlands, the Western marsh harrier is not listed as a red list species (van Kleunen et al. 2017), but breeding populations are in decline since 1990 due to similar pressures as in Flanders (changed land-use, agricultural practices etc.) (van Bruggen et al. 2011).

In 2012, the Dutch Montagu’s Harrier Foundation (GKA) initiated a GPS tracking study in the northeastern part of the Netherlands (Groningen) using lightweight, solar powered GPS tags. The research objectives for this monitoring study were to de-

termine habitat use of Western marsh harriers in agricultural landscapes, to reveal their migration behaviour, and to study flying behaviour in the vicinity of wind turbines for estimating collision risks.

The Research Institute for Nature and Forest (INBO) started studying the ecology of the Western marsh harrier in Belgium in 2011. One of the aims was to study detailed habitat use and migration patterns. In 2013, the INBO started a GPS sensor network for birds as part of the Belgian contribution to the LifeWatch observatory, using the same technology as GKA. In this network, individuals of a breeding population of Western marsh harriers in the northern part of Flanders (Waterland-Oudeman region) were equipped with GPS trackers in collaboration with GKA. In 2018, a third population was tagged with GPS trackers in the Scheldt estuary north of the city of Antwerp. The research objectives of these projects were to study the trade-off between migratory behaviour, reproductive performance and survival, and to study the home-range area, habitat preference, and foraging behaviour of Western marsh harriers in agricultural areas. To allow greater use of the data beyond our research questions, all data are now published as open data.

Taxonomic coverage

The dataset contains data from four individuals breeding in Groningen (The Netherlands) (H_GRONINGEN), seven individuals breeding near the Belgian-Dutch border (MH_WATERLAND), and three individuals breeding near Antwerp (Belgium) (MH_ANTWERPEN) (Figure 1).

Taxonomic ranks

Kingdom: Animalia

Phylum: Chordata

Class: Aves

Order: Accipitriformes

Family: Accipitridae

Genus: *Circus*

Species: *Circus aeruginosus* (Linnaeus, 1758)

Geographic coverage

The tracked birds were breeding in the northeast of the Dutch province of Groningen and on the opposite side of the river Ems in Germany (H_GRONINGEN), in the region of Waterland-Oudeman near the Belgian-Dutch border (MH_WATERLAND), and at the left bank of the Scheldt estuary close to the Belgian-Dutch border and north of the city of Antwerp (MH_ANTWERPEN). All individuals from which data from the non-breeding period were available wintered in West Africa (Figure 2).



Figure 1. INBO researcher Anny Anselin holding Peter (animal ID L143457), one of the tagged Western marsh harriers in the MH_WATERLAND dataset (tag ID 623).

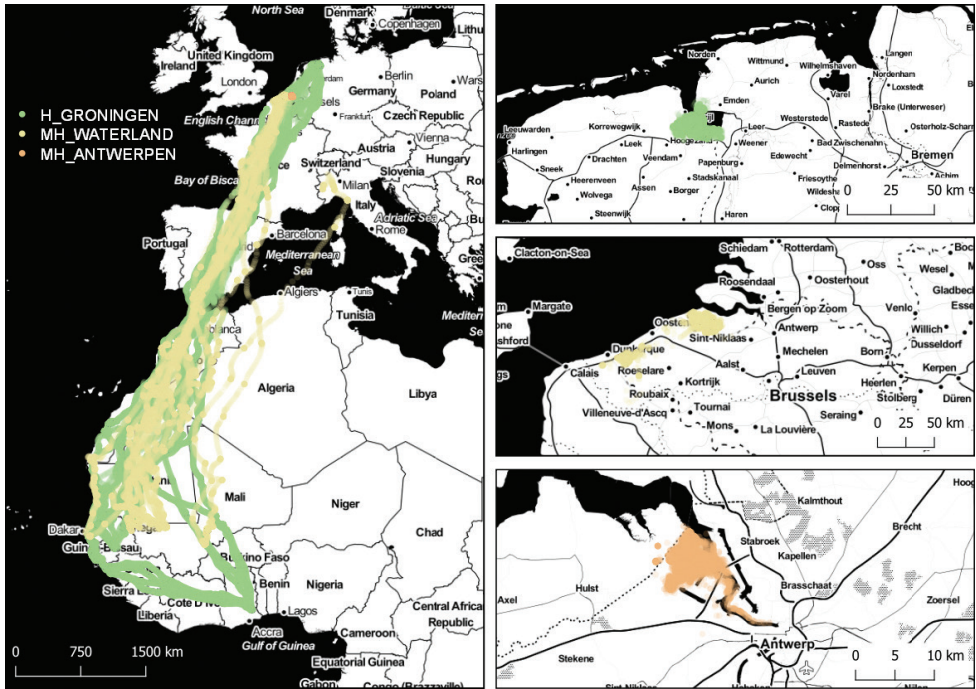


Figure 2. Left: Map giving an overview of the extent of the three datasets including the winter migration tracks; top right: summering data in H_GRONINGEN; middle right: summering data of MH_WATERLAND; and bottom right: summering data in MH_ANTWERPEN.

Bounding box

H_GRONINGEN: 6.65N to 53.40N; 16.92W to 7.32E

MH_WATERLAND: 13.38N to 51.47N; 17.13W to 10.01E

MH_ANTWERPEN: 51.23N to 51.35N; 4.18E to 4.39E

Temporal coverage

H_GRONINGEN: 2012-05-10 – 2018-07-11

MH_WATERLAND: 2013-05-16 – ongoing

MH_ANTWERPEN: 2018-07-18 – ongoing

Methodology

Study extent description

The studied Western marsh harrier populations breed in agricultural landscapes in the northeast of the Dutch province of Groningen (H_GRONINGEN; 53.278N,

6.981E), the polder area in the north-western part of Belgium (MH_WATERLAND; 51.276N, 3.595E), and in the polder area at the left bank of the Scheldt estuary in the northern part of Belgium (MH_ANTWERPEN; 51.312N, 4.285E). The tracked birds nested on the ground in small reed beds and cereal fields.

The harriers were trapped using a noose-trap on a sitting pole (Gartshore 1978) in the vicinity of their nesting place (H_GRONINGEN and MH_WATERLAND) or a bal-chatri (Berger and Mueller 1959) with live birds (MH_ANTWERPEN). As trapping proved very difficult, only a few individuals could be tagged per breeding season (Table 1). Once captured, biometrics were taken from all captured harriers: tarsus length, wing length, body mass and moulting stage following the methods of Bijlsma 1997 (H_GRONINGEN and MH_WATERLAND) and Ginn and Melville 1983 (MH_ANTWERPEN). Sex was determined on sight. UvA-BiTS GPS-trackers (Bouten et al. 2013) were attached to the birds with the body loop attachment method using a harness of Teflon tape (Figure 1).

In total, 14 Western marsh harriers were tracked (Table 1). All four individuals in the H_GRONINGEN study are assumed dead as they were not observed anymore during one or more years. In 2018, one of the tagged harriers (Roelof) came back to his breeding grounds, but the tracker got broken and he has not been spotted again in 2019 (status unknown). In the MH_ANTWERP study, two individuals were tagged in 2019, while one animal (Suzanna) was tagged in 2018 but did not come back after the migration in 2019 (status unknown). One of the individuals (Raymond) in MH_WATERLAND was found dead in the Italian Alps in spring 2016. His tracker was reused for another male (Ben). Another individual in the MH_WATERLAND dataset (Jozef)

Table 1. Overview of the tracked individuals per project, their status in 2019, total number of tracking days, number of GPS fixes and biometric data.

Project	Animal id	Animal name	Sex	Date first observation	Date last observation	Status in 2019	Tracking days	GPS fixes	Body mass (g)	Tarsus length (mm)	Wing length (mm)	Moult score
H_GRONINGEN	5327085	Job	male	2016-06-18	2016-09-03	assumed dead	78	21,337	513	70	383	0000000000
H_GRONINGEN	5336455	Kjell	male	2014-06-04	2014-06-23	assumed dead	20	5,420	540	74	406	5200000000
H_GRONINGEN	5325667	Roelof	male	2014-07-04	2018-07-11	unknown; tracker broken	1,469	781,906	504	69	418	0000000000
H_GRONINGEN	5446465	William	male	2012-05-10	2016-08-11	assumed dead	1,380	178,830	524	72	397	
MH_WATERLAND	H185298	Almut	female	2016-06-03	2016-06-13	assumed dead	11	475	656		420	
MH_WATERLAND	L143472	Ben	male	2016-05-02	2017-07-15	assumed dead	440	85,924	571		404	
MH_WATERLAND	L143451	Jozef	male	2013-06-25	2018-07-28	unknown	1,854	183,985	512	64	402	
MH_WATERLAND	H173481	Mia	female	2013-05-16	2013-08-02	assumed dead	78	13,209	785	77	430	
MH_WATERLAND	L143457	Peter	male	2013-07-22	2014-09-01	assumed dead	407	62,297	482	65	392	
MH_WATERLAND	L143467	Raymond	male	2015-05-26	2016-03-25	found dead in March 2016	305	31,070	472	71	385	
MH_WATERLAND	L143473	Walter	male	2016-06-01	2016-06-08	assumed dead	8	950	485		395	
MH_ANTWERPEN	H197169	Lilla	female	2019-04-18	2019-07-30	alive	104	28,181	810	80	426	0
MH_ANTWERPEN	L177801	Lillo	male	2019-05-16	2019-05-19	alive	4	17,046	520	72	410	0
MH_ANTWERPEN	H171693	Zuzanna	female	2018-07-18	2018-07-27	unknown	10	2,690	674	77	410	29

was tagged in 2013 in his breeding area in the Waterland-Oudeman region but moved to another breeding area at the Moeren close to Veurne at 70 km from his previous breeding ground in 2016, 2017 and 2018. The other individuals in this dataset have not been seen in their original breeding grounds in the past few years and are assumed dead.

Sampling description

Harriers in the three studies were equipped with the University of Amsterdam Bird Tracking System (UvA-BiTS) developed by the Institute for Biodiversity and Ecosystem Dynamics (IBED) at the University of Amsterdam. These lightweight, solar powered GPS trackers automatically record 3D position and air temperature. The built-in tri-axial accelerometer can be configured to collect body movements and bird behaviour and was deployed in the H_GRONINGEN and MH_ANTWERPEN studies. Each individual tri-axial accelerometer measurement consists of x (acceleration-raw- x), y (acceleration-raw- y) and z data points (acceleration-raw- z). Tilt values (tilt- x , tilt- y and tilt- z) are derived from the raw acceleration measurements (M), the calibration factors offset (O) and sensitivity (S). Thus acceleration for heave (tilt- z), surge (tilt- x) and sway (tilt- y) is calculated as: $A_z = (M_z - O_z) / S_z$; $A_x = (M_x - O_x) / S_x$; $A_y = (M_y - O_y) / S_y$ (UvA-BiTS 2018). Tilt data are expressed in g. Both raw acceleration data and derived tilt data are collected in groups of 20 samples. These samples should be analysed as a group because these multiple data recordings are collected in a rapid sequence (up to 20 tri-axial measurements per second) to produce a complete picture of bird behaviour.

Data are stored in the tracker's 4 MB built-in flash drive. Depending on the settings, up to 60,000 GPS records can be stored in the internal memory (Bouten et al. 2013). Trackers are equipped with a ZigBee transceiver and a whip antenna for transmitting data to a base station and for receiving new measurement settings. Unlike other bird tracking studies using similar technology (e.g., Stienen et al. 2016), base stations were not set up on fixed locations as breeding sites varied between years. Once the tagged harriers were spotted in their breeding locations, mobile base stations were used to read out data. This implies that data from birds that do not return to their previous breeding grounds cannot be retrieved unless they are spotted in a new breeding location (as happened with Jozef who moved to another breeding location in spring 2016).

Different intervals between successive GPS fixes were applied, ranging from 3 s to 30 min during the day, and 4 s to 2 h at night. In the H_GRONINGEN study, "high-resolution" GPS data with an interval of 3 s were collected during parts of the day using hourly blocks or virtual geographic fences in order to increase the positional accuracy of the GPS fixes (Bouten et al. 2013).

Data received by the base stations are automatically harvested, post-processed, and stored in a central PostgreSQL database at UvA-BiTS (<http://www.uva-bits.nl/virtual-lab>), which is accessible to the involved researchers only. In order to make our data available to the whole scientific community, all tracking data are eventually published as open data. We decided to upload the data to Movebank (<https://www.movebank.org>) as it is a specific repository for this type of data and it is well adopted by the scientific community (Mrozewski 2018). The Movebank data model enables the de-

scription of animals, tags, deployments, detections, and other measurements, such as acceleration data (Kranstauber et al. 2011).

Both reference, GPS data and acceleration data of our Western marsh harrier studies were downloaded from the UvA-BiTS database using SQL queries and then transformed into the Movebank data format (Movebank 2019) using R scripts (<https://github.com/inbo/bird-tracking>). This allows us to repeat the process when new data become available for active studies. These data were then uploaded to the Movebank database, with one study for each dataset (Table 2). As the Movebank data repository (<https://www.datarepository.movebank.org/>, offered as a service to archive movement data) currently does not support versioning and version-agnostic DOIs, we opted to archive our studies in the Zenodo data repository (<https://www.zenodo.org>). For each Movebank study, one Zenodo data package has been created (Table 2). These data packages consist of four different file types: a readme file with the terms of use and attributes of the data files, a reference data file about animals, tags and deployments, GPS data files, and files containing acceleration data. GPS and acceleration data are split into separate csv files per year, which makes it easier to download data in manageable chunks and to update these data packages with observations from an extra year. For this reason, the MH_ANTWERPEN dataset contains more GPS data records in the Movebank study compared to the Zenodo archive as data from 2019 are incomplete and will be archived on Zenodo in the course of 2020 after birds have returned from their wintering area. No GPS data are available for 2019 from birds in the H_GRONINGEN and MH_WATERLAND studies, as none of the tagged individuals were observed in 2019 (Figure 3).

Quality control description

GPS fixes that are likely incorrect (i.e., outliers) are marked in two ways: manually by the researcher in the UvA-BiTS database (indicated as TRUE in manually-marked-outlier) and automatically before uploading to Movebank for GPS-fixes with speeds above 30 m/s (indicated as TRUE in import-marked-outlier). Using this approach, 376, 97 and 16 observations were marked as outliers in H_GRONINGEN, MH_WATERLAND and MH_ANTWERPEN respectively. The workflow and scripts for querying data from the UvA-BiTS database and transforming these into the Movebank data format are publicly documented on GitHub (<https://github.com/inbo/bird-tracking>).

Table 2. Datasets and the respective links to the Movebank studies and Zenodo data packages.

Title	Movebank study ID	Zenodo
H_GRONINGEN – Western marsh harriers (<i>Circus aeruginosus</i> , Accipitridae) breeding in Groningen (the Netherlands)	922263102	https://doi.org/10.5281/zenodo.3552507
MH_WATERLAND – Western marsh harriers (<i>Circus aeruginosus</i> , Accipitridae) breeding near the Belgium-Netherlands border	604806671	https://doi.org/10.5281/zenodo.3532940
MH_ANTWERPEN – Western marsh harriers (<i>Circus aeruginosus</i> , Accipitridae) breeding near Antwerp (Belgium)	938783961	https://doi.org/10.5281/zenodo.3550093

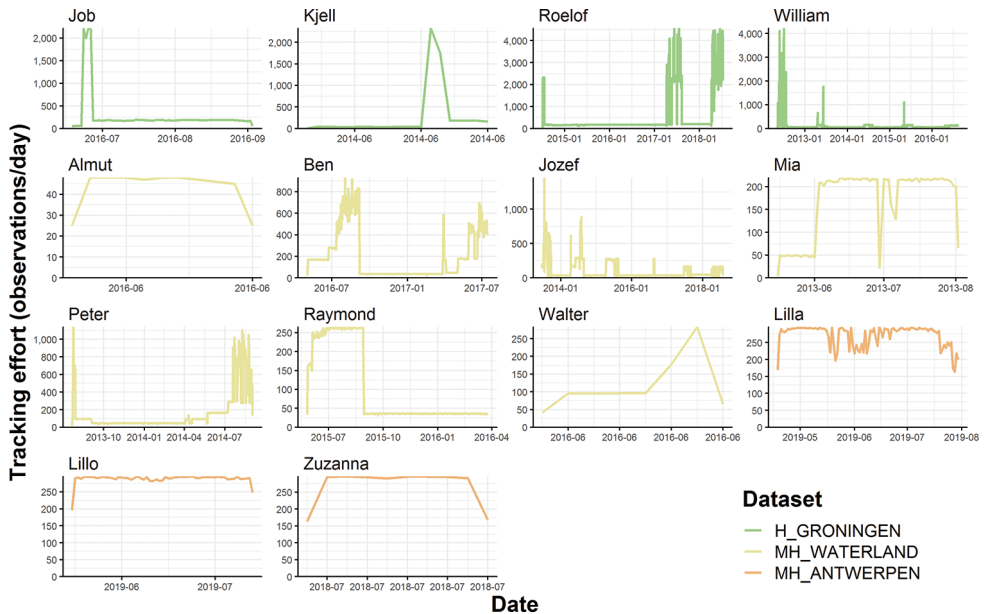


Figure 3. Tracking effort: number of observations per day and per individual.

Method step description

Data recording

1. Researcher captures bird, takes biometrics, attaches GPS tracker, and releases bird.
2. Researcher records or updates metadata about bird, GPS tracker and deployment.
3. Researcher sets a measurement scheme, which can be updated anytime.
4. GPS tracker records data.
5. GPS tracker automatically receives new measurement settings and transmits recorded data when a connection can be established with the mobile base station.
6. Recorded data are automatically harvested, post-processed, and stored in a central PostgreSQL database at UvA-BiTS.
7. Data stream stops when birds no longer return to the nesting site or if GPS trackers no longer function.

Data publication

1. Data (reference, GPS and acceleration) are periodically exported from UvA-BiTS in the Movebank data format.
2. GPS outliers are marked.
3. Data are uploaded to the appropriate study on Movebank and made publicly available.
4. Data are exported from Movebank and archived on Zenodo, where each update is a version with a DOI.

Datasets

Dataset description

Our data are grouped in three datasets (one dataset per study area). H_GRONINGEN is the largest dataset containing 987,493 GPS fixes in the period 2012–2018, while the MH_WATERLAND study started in 2013 with 377,910 GPS fixes until 2018, and MH_ANTWERPEN started in 2018 and contains 47,917 GPS fixes in the Movebank study for the period 2018–2019 (Figure 4). In the H_GRONINGEN and MH_ANTWERPEN studies acceleration data were collected as well, with respectively 3,853,859 and 227,746 acceleration records (Figure 5).

H_GRONINGEN dataset

- **Object name:** H_GRONINGEN – Western marsh harriers (*Circus aeruginosus*, Accipitridae) breeding in Groningen (the Netherlands)
- **Format name:** Movebank data format
- **Format version:** 2 (<http://vocab.nerc.ac.uk/collection/MVB/2/>)
- **Language:** English
- **License:** <http://creativecommons.org/publicdomain/zero/1.0/>
- **Usage norms:** <http://www.inbo.be/en/norms-for-data-use>
- **Publication date:** 2019-11-26
- **Derived from:** https://www.movebank.org/cms/webapp?gwt_fragment=page=studies,path=study922263102
- **DOI of version described in this paper:** <https://doi.org/10.5281/zenodo.3828298>
- **DOI for all versions:** <https://doi.org/10.5281/zenodo.3552507>

MH_WATERLAND dataset

- **Object name:** MH_WATERLAND – Western marsh harriers (*Circus aeruginosus*, Accipitridae) breeding near the Belgium-Netherlands border
- **Format name:** Movebank data format
- **Format version:** 2 (<http://vocab.nerc.ac.uk/collection/MVB/2/>)
- **Language:** English
- **License:** <http://creativecommons.org/publicdomain/zero/1.0/>
- **Usage norms:** <http://www.inbo.be/en/norms-for-data-use>
- **Publication date:** 2019-11-12
- **Derived from:** https://www.movebank.org/cms/webapp?gwt_fragment=page=studies,path=study604806671
- **Source of:** <https://doi.org/10.15468/rbguhj> (earlier version of dataset published to the Global Biodiversity Information Facility in the Darwin Core format)

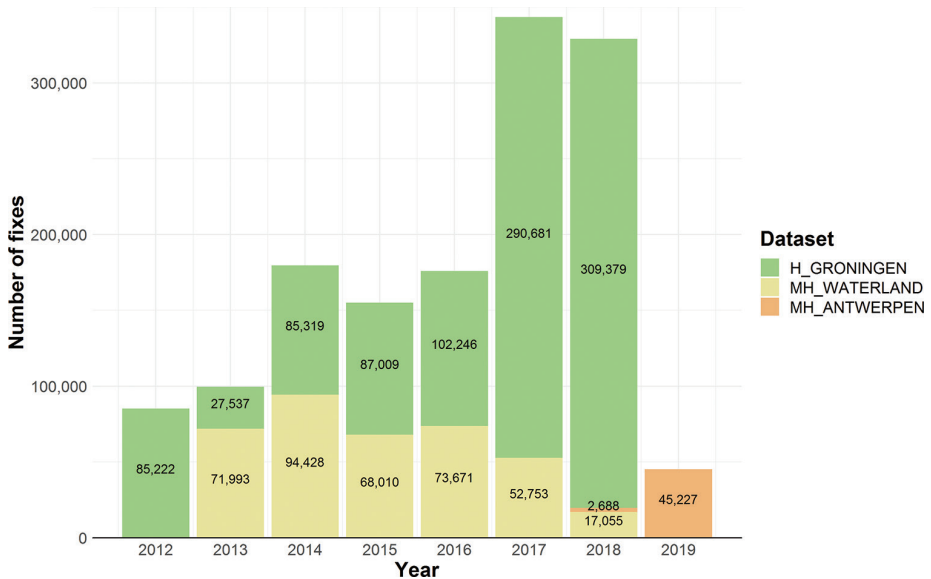


Figure 4. Number of GPS fixes per year and per dataset.

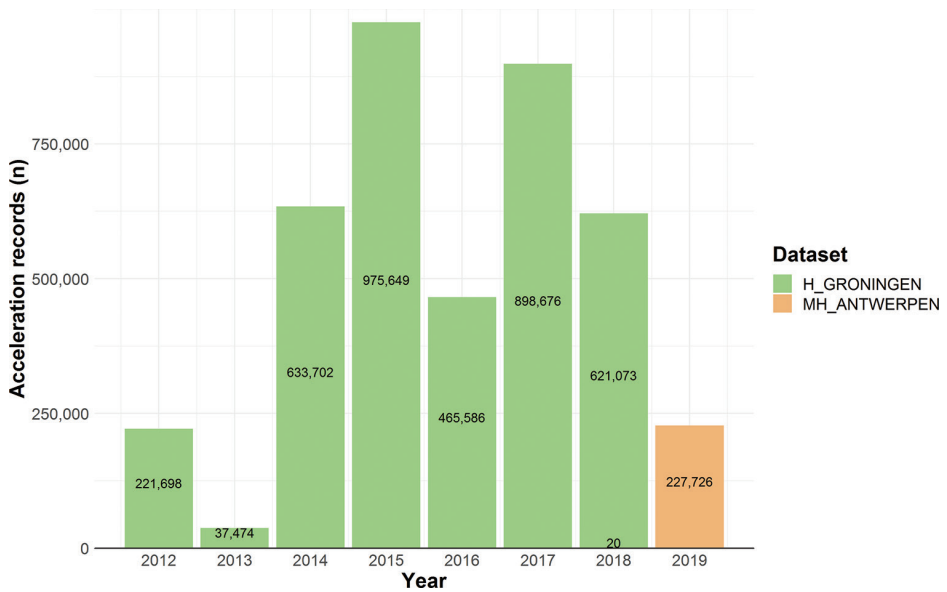


Figure 5. Number of acceleration records per year and per dataset.

- **DOI of version described in this paper:** <https://doi.org/10.5281/zenodo.3826591>
- **DOI for all versions:** <https://doi.org/10.5281/zenodo.3532940>

MH_ANTWERPEN dataset

- **Object name:** MH_ANTWERPEN – Western marsh harriers (*Circus aeruginosus*, Accipitridae) breeding near Antwerp (Belgium)
- **Format name:** Movebank data format
- **Format version:** 2 (<http://vocab.nerc.ac.uk/collection/MVB/2/>)
- **Language:** English
- **License:** <http://creativecommons.org/publicdomain/zero/1.0/>
- **Usage norms:** <http://www.inbo.be/en/norms-for-data-use>
- **Publication date:** 2019-11-21
- **Derived from:** https://www.movebank.org/cms/webapp?gwt_fragment=page=studied,path=study938783961
- **DOI of version described in this paper:** <https://doi.org/10.5281/zenodo.3827918>
- **DOI for all versions:** <https://doi.org/10.5281/zenodo.3550093>

Usage norms

To allow anyone to use these datasets, we have released the data to the public domain under a Creative Commons Zero waiver (<http://creativecommons.org/publicdomain/zero/1.0/>). We would appreciate however, if you read and follow these norms for data use (<http://www.inbo.be/en/norms-for-data-use>) and provide a link to the original dataset using the DOI whenever possible. If you use these data for a scientific paper, please cite the dataset(s) following the applicable citation norms and/or consider us for co-authorship. We are always interested to know how you have used or visualized the data, or to provide more information, so please contact us via the contact information provided in the metadata or opendata@inbo.be.

Acknowledgements

This work makes use of data and infrastructure provided by VLIZ and INBO funded by the Research Foundation – Flanders (FWO) as part of the Belgian contribution to LifeWatch.

Code to create the graphs in this paper: <https://gist.github.com/milotictanja/cb-c48b9aa5fcccd54dcd3754557ca8e0>

Code to process data for Movebank: <https://github.com/inbo/bird-tracking>

References

Berger DD, Mueller HC (1959) The bal-chatri: a trap for the birds of prey. *Bird-banding*, 30(1): 18–26. <https://doi.org/10.2307/4510726>

- Bijlsma RG (1997) Handleiding veldonderzoek Roofvogels. KNNV Uitgeverij, 160 pp. ISBN: 9789050115476 [in Dutch]
- Bouten W, Baaij EW, Shamoun-Baranes J, Camphuysen KC (2013) A flexible GPS tracking system for studying bird behaviour at multiple scales. *Journal of Ornithology* 154(2): 571–580. <https://doi.org/10.1007/s10336-012-0908-1>
- Devos K, Anselin A, Driessens G, Herremans M, Onkelinx T, Spanoghe G, Stienen E, T'Jollyn F, Vermeersch G, Maes D (2016) The IUCN red list of breeding birds in Flanders, northern Belgium (2016). Rapporten van het Instituut voor Natuur- en Bosonderzoek, INBO.R.2016.11485739, Instituut voor Natuur- en Bosonderzoek. [in Dutch] <https://doi.org/10.21436/inbor.11485739>
- Gartshore ME (1978) A noose trap for catching nesting birds. *North American Bird Bander* 3(1): 1–2.
- Ginn HB, Melville DS (1983) *Moult in Birds*. BTO Guide 19. The British Trust for Ornithology, Beech Grove, Tring, Hertfordshire, England, 112 pp. ISBN 0 903793 02 4
- Kranstauber B, Cameron A, Weinzerl R, Fountain T, Tilak S, Wikelski M, Kays R (2011) The Movebank data model for animal tracking. *Environmental Modelling & Software* 26(6): 834–835. <https://doi.org/10.1016/j.envsoft.2010.12.005>
- Movebank (2019) Movebank attribute dictionary. World Wide Web electronic publication. <http://vocab.nerc.ac.uk/collection/MVB/current/> [accessed in December 2019]
- Mrozewski T (2018) Movebank. *Bulletin-Association of Canadian Map Libraries and Archives (ACMLA)* 158: 24–27. <https://doi.org/10.15353/acmla.n158.220>
- Stienen EWM, Desmet P, Aelterman B, Courtens W, Feys S, Vanermen N, Verstraete H, Van de walle M, Deneudt K, Hernandez F, Houthoofd R, Vanhoorne B, Bouten W, Buijs RJ, Kavelaars MM, Müller W, Herman D, Matheve H, Sotillo A, Lens L (2016) GPS tracking data of Lesser Black-backed Gulls and Herring Gulls breeding at the southern North Sea coast. *ZooKeys* 555: 115–124. <https://doi.org/10.3897/zookeys.555.6173>
- UvA-BiTS (2018) UvA-BiTS tracking data. World Wide Web page. https://wiki.pubserv.e-ecology.nl/wiki/index.php/DB_Views_2015#Accelerometer_calibration [accessed in May 2020]
- van Bruggen J, van Kleunen A, van den Bremer L, Castelijns H (2011) 2010: Jaar van de Bruine Kiekendief. *Limosa* 84: 135–140. [in Dutch]
- van Kleunen A, Foppen R, van Turnhout C (2017) Basisrapport voor de Rode Lijst Vogels 2016 volgens Nederlandse en IUCN-criteria. Sovon-rapport 2017/34. Sovon Vogelonderzoek Nederland, Nijmegen. [in Dutch]

